Draft Final Report

Evaluating the Longevity and Hydraulic Performance of Permeable Reactive Barriers at Department of Defense Sites

Prepared for

Project Officer: Charles Reeter

Naval Facilities Engineering Service Center
Port Hueneme, California

by

Arun Gavaskar, Bruce Sass, Neeraj Gupta, Eric Drescher, Woong-Sang Yoon, Joel Sminchak, and James Hicks

Battelle
. . . Putting Technology To Work

Battelle
Columbus, Ohio

October 31, 2001

Project funded by

ESTCP

SERDP
Strategic Environmental Research and Development Program
Improving Mission Readiness through Environmental Research

The vendors and products, including the equipment, system components, and other materials identified in this report, are primarily for information purposes only. Although Battelle may have used some of these vendors and products in the past, mention in this report does not constitute Battelle's recommendation for using these vendors or products.

ACKNOWLEDGMENTS

The project team would like to acknowledge members of ESTCP and SERDP for providing the funds and review support for this project. The DoD project officer for this evaluation was Charles Reeter from the Naval Facilities Engineering Service Center (NFESC). Battelle, under a contract with the Navy, conducted the technical activities associated with the project. Battelle staff that contributed to this project include Arun Gavaskar (Project Manager), Bruce Sass, Neeraj Gupta, Eric Drescher, Woong-Sang Yoon, Joel Sminchak, and James Hicks. A significant achievement of this project was the broad participation and support received by the project team from various government agencies and local contractors, who are recognized as follows:

- Steve White, U.S. Army Corps of Engineers provided significant field guidance and support, especially at the Seneca Army Depot site, where he personally conducted several of the field measurements.

- Matt Turner, New Jersey Department of Environmental Protection, coordinated the Interstate Technologies Regulatory Cooperation (ITRC) participation in this project. The ITRC was instrumental in reviewing critical work plans and reports. Several ITRC members also participated in an important survey that was conducted to determine regulatory concerns and monitoring approach for this technology. The results of this survey helped to refocus the efforts of the project team during the project.

- Timothy McHale, Air Force Research Laboratory, and Robert Edwards (the designated Air Force Center for Environmental Excellence representative) provided guidance and review support.

- Gary Munekawa (Navy-Southwest Division) and Tim Mower (TetraTech Environmental Management Inc.) coordinated the local field support at former Naval Air Station Moffett Field.

- Bill Gallant and Trent Watne from Versar, Inc. provided local field support at Lowry AFB.

- Steve Absolom, Seneca Army Depot, and Eliza Schact, Parsons Engineering Science, Inc., coordinated the local field support at Seneca Army Depot.

- Greg Jackson and Bob Wickso, Dover AFB, coordinated the local field support at Dover AFB.

- Robert Puls and Rick Wilkin, U.S. EPA, for coordinating the EPA's and RTDF Permeable Barriers Work Group's review and participation through the Tri-Agency PRB Initiative.

- Libby West, Liyuan Liang, and Nic Korte with Oak Ridge National Laboratory for coordinating the U.S. Department of Energy's review and participation in the project through the Tri-Agency PRB Initiative.

- Incheol Pang from NFESC for his support and participation.

- Cathy Vogel, SERDP, and Scott Dockum, Hydrogeologic, Inc. for coordinating SERDP and ESTCP feedback and review.

CONTENTS

ACKNOWLEDGMENTS iii
FIGURES ix
TABLES xiii
ABBREVIATIONS AND ACRONYMS xiv
EXECUTIVE SUMMARY xvii

1.0 Introduction 1
1.1 Project Background 1
1.2 Interagency Cooperation 1
1.3 Project Objectives 2
1.4 Regulatory Issues 3
1.5 Previous and Other Ongoing Assessments of the Technology 3

2.0 Technology Description 5
2.1 Permeable Barrier Technology Description 5
2.2 Advantages and Limitation 6
2.3 Factors Influencing Cost and Performance 7

3.0 Description of DoD Sites with PRBs 9
3.1 Site Selection Background 9
3.2 Characteristics of Sites Selected for Detailed Evaluation 11
3.2.1 Former NAS Moffett Field 11
3.2.2 Former Lowry AFB 12
3.2.3 Seneca Army Depot 14
3.2.4 Dover AFB 14
3.2.5 Former NAS Alameda 16

4.0 Performance Assessment Approach 19
4.1 Performance Assessment Objectives 19
4.2 Performance Assessment Strategy 19
4.2.1 Longevity Evaluation Strategy 19
4.3 Sampling and Analysis Procedures 22
4.3.1 Longevity Evaluation 22
4.3.1.1 Groundwater Sampling 22
4.3.1.2 Iron Core Collection at Former NAS Moffett Field 23
4.3.1.3 Iron Core Sampling at Former Lowry AFB 23
4.3.1.4 Iron Core Processing 30
4.3.1.5 Iron Core Analysis Methods 31
4.3.1.6 Silt Sampling from Monitoring Wells 33
4.3.1.7 Accelerated Column Test Setup and Sampling 34
4.3.2 Hydraulic Performance Evaluation 38
4.3.2.1 Water-Level Measurements 39

4.3.2.2 Slug Tests 39
4.3.2.3 In-Situ Flow Sensors 39
4.3.2.4 Colloidal Borescope 40
4.4 Characterization Tools Considered but Not Used 41
4.4.1 Down-Hole Velocity Probes (Heat Sensors) 41
4.4.2 Diffusion Samplers 42

5.0 Performance Assessment for Longevity of PRBs 43
5.1 Field Evaluation of Longevity at Former NAS Moffett Field 43
5.1.1 Groundwater Sampling at Moffett Field 43
5.1.1.1 TCE Degradation 45
5.1.1.2 cis-DCE Degradation 47
5.1.1.3 PCE Degradation 47
5.1.1.4 Vinyl Chloride 47
5.1.1.5 Results of Field Parameter Measurements 48
5.1.1.6 Results of Inorganic Chemical Measurements 49
5.1.2 Iron Coring at Former NAS Moffett Field 53
5.1.2.1 XRF Analysis of Cores 53
5.1.2.2 XRD Analysis 55
5.1.3 Silt Collection from Monitoring Wells at Moffett Field 56
5.1.4 Microbiological Evaluation of the PRB at Former NAS Moffett Field 65
5.2 Field Evaluation of Longevity at Former Lowry AFB 66
5.2.1 Groundwater Sampling at Lowry 66
5.2.2 Iron Coring at Lowry 69
5.2.2.1 Carbon Analysis 69
5.2.2.2 XRD 70
5.2.2.3 Raman Spectroscopy 72
5.2.2.4 FTIR 73
5.2.3 Silt Coring at Lowry 73
5.2.4 Microbiological Evaluation of the PRB at Former Lowry AFB 74
5.3 Accelerated Column Tests 74
5.3.1 Former NAS Moffett Field Column Simulation 74
5.3.1.1 ORP and pH in the Moffett Field Column 76
5.3.1.2 TCE Degradation 76
5.3.1.3 Inorganic Measurements 81
5.3.2 Former Lowry AFB Column Simulation 87
5.3.2.1 ORP and pH in the Lowry Column 87
5.3.2.2 TCE Degradation 87
5.3.2.3 Inorganic Measurements 90
5.3.2.4 Analysis of Iron Cores from the Lowry AFB Column Test 94
5.4 Geochemical Modeling 95
5.4.1 Geochemical Modeling Approach 96
5.4.2 Geochemical Simulation Results 102
5.4.3 Comparison of Results with Estimated Corrosion Rates 106

5.5 Summary of Results and Conclusions from the Longevity Evaluation 109

6.0 Hydraulic Evaluation of PRBs at DoD Sites 117
6.1 Field Evaluations of Hydraulic Performance at DoD Sites 118
6.1.1 Water Level Surveys 120
6.1.2 Hydraulic Conductivity Measurements 128
6.1.3 Measurement of Velocity with Hydrotechnics Sensors and Colloidal Borescope 131
6.2 Groundwater Modeling for Performance Assessment 135
6.2.1 Capture Zones and Residence Times 138
6.2.1.1 Capture Zone 138
6.2.1.2 Residence Time 138
6.2.2 Seneca Army Depot CRB Modeling 140
6.2.3 Modeling the Hydraulic Aspects of PRBs 141
6.2.3.1 Effect of Hydraulic Parameters 144
6.2.3.2 Hanging Wall Configurations 144
6.2.4 Angled Flow into the PRB 146
6.3 Implications for Hydraulic Performance 155
6.3.1 Interpreting Groundwater Flow Patterns and Capture Zones 155
6.3.2 Evaluating Plume Bypass 156
6.3.3 Direct Measurement of Velocity 156
6.3.4 Tracer Tests 157
6.3.5 Residence Time and Flow Volume 157
6.3.6 Role of Groundwater Models 157

7.0 Update on PRB Construction and Costs 161
7.1 Advances in PRB Construction Methods 161
7.1.1 PRB Configurations 161
7.1.2 PRB Construction Techniques 165
7.1.2.1 Backhoe and Clamshell Trenching Methods 165
7.1.2.2 Caisson Excavation Method 166
7.1.2.3 Continuous Trenching Method 167
7.1.2.4 Biodegradable Slurry (Biopolymer) Trenching Method 168
7.1.2.5 Jetting Method 169
7.1.2.6 Hydraulic Fracturing Method 170
7.1.2.7 Vibrated Beam/Mandrel Methods 172
7.1.2.8 Deep Soil Mixing Methods 172
7.2 Update on New and Existing PRBs and Cost of PRB Applications 173

8.0 Regulatory Issues 195
8.1 Regulatory Issues with Permeable Barriers 195
8.1.1 Applications Received for Installation of New PRBs 195
8.1.2 Contingency Plans in Case of PRB Failure 196
8.1.3 Monitoring of a PRB after Installation 197

8.2 Future Regulatory Direction on PRBs 198

9.0 Technology Implementation 201
9.1 DoD Need 201
9.2 Transition 201

10.0 Summary of Results and Lessons Learned 203
10.1 Longevity Evaluation 203
10.2 Hydraulic Performance Evaluation 210
10.3 Summary of Recommendations 213

11.0 References 217

Appendix A: Points of Contact A-1
Appendix B: Data Archiving and Demonstration Plan B-1
Appendix C: Geochemical Data C-1
Appendix D: Supporting Information for Cost and Longevity Scenarios D-1
Appendix E: Supporting Information for the Hydraulic Performance Evaluation Results E-1

FIGURES

Figure 2-1. Schematic Illustrations of Some PRB Configurations 5
Figure 3-1. PRB at Former NAS Moffett Field Relative to Lithologic Variations in the Surrounding Aquifer 12
Figure 3-2. Design and Hydraulic Conductivity (ft/day) Distribution at Former Lowry AFB PRB 13
Figure 3-3. Hydraulic Conductivity Values (ft/d) from Slug Tests at the Seneca Army Depot CRB Showing Variations in Hydraulic Conductivity at the Site 14
Figure 3-4. Lithology at the Dover AFB PRB 15
Figure 3-5. Schematic View of PRB and Upgradient Contamination Profile at Former NAS Alameda Site 17
Figure 4-1. Coring Locations in Moffett Field Permeable Reactive Barrier (Plan View) 24
Figure 4-2. Coring Locations in Moffett Field Permeable Reactive Barrier (Vertical Profile) 25
Figure 4-3. Rig Used to Collect Iron Core Samples from the Moffett Field PRB 26
Figure 4-4. Rig Showing Sand Catcher Inside Core Barrel 26
Figure 4-5. Pea Gravel Being Removed from Drive Casing 27
Figure 4-6. Closed Stainless Steel Sample Sleeve and Excess Iron on Core Table 27
Figure 4-7. Coring Rig 28
Figure 4-8. Close-Up View of Coring Rig 28
Figure 4-9. Location of Cores Collected in the PRB at Former Lowry AFB 29
Figure 4-10. Preservation of Core Samples in the Field 31
Figure 4-11. Collecting Deposits from Silt Traps in Monitoring Wells 33
Figure 4-12. Photograph of Silt Sampler Ready to be Lowered Into a Monitoring Well 34
Figure 4-13. Schematic of Accelerated Column Test Setup 35
Figure 4-14. Picture of Accelerated Column Tests 36
Figure 4-15. HydroTechnics™ Flow Sensor 40
Figure 4-16. Colloidal Borescope Used at Former Lowry AFB 41
Figure 4-17. Diffusion Sampler 42
Figure 5-1. Plot Showing the Distribution of Dissolved Silica in the Moffett Field PRB in October 1998 52
Figure 5-2. SEM Micrograph of Silt from Well WW-12 Showing Ettringite (Needles) Adjacent to Calcite (Plates 59
Figure 5-3. Plot of Aluminum and Silicon in Moffett Field Silt 61
Figure 5-4. Plot of Potassium and Aluminum in Moffett Field Silt 62
Figure 5-5. Plot of Sulfur and Aluminum in Moffett Field Silt 62
Figure 5-6. Plot of Aluminum and Silicon in Moffett Field Silt 63
Figure 5-7. Silt Sample From WW-12 64
Figure 5-8. Comparison of the Relative Percentages of Total PLFA Structural Groups 67
Figure 5-9. Sampling Well Locations in the PRB and Vicinity at Former Lowry AFB 68
Figure 5-10. Plot Showing Stability of pH and ORP After 15 Pore Volumes of Groundwater 75

Figure 5-11. pH and ORP Values in the Moffett Field Column at Different Pore Volumes (Ages of Iron) 77
Figure 5-12. Plot of TCE Degradation Rates for Moffett Field Column at Different Cumulative Pore Volumes 80
Figure 5-13. Plot of TCE Half-Lives for Moffett Field Column at Different Cumulative Pore Volumes 80
Figure 5-14. Bar Graphs for Moffett Field Column Showing Input and Output Concentrations of Inorganic Analytes (Filtered) 84
Figure 5-15. pH and ORP Values in the Lowry Column at Different Pore Volumes Ages 87
Figure 5-16. Plot of TCE Degradation Rates for Lowry Column at Different Cumulative Pore Volumes 89
Figure 5-17. Plot of TCE Half-Lives for Lowry Column at Different Cumulative Pore Volumes 89
Figure 5-18. Bar Graphs Showing Input and Output Concentrations of Inorganic Analytes (Filtered) 93
Figure 5-19. pH and Eh Profile Based on Case 1 103
Figure 5-20. Profiles of Alkalinity, Ca, and Sulfate Based on Case 1 103
Figure 5-21. Profiles of Silica, Fe(II), and Mg Based on Case 1 103
Figure 5-22. Masses of Precipitates Based on Case 1 104
Figure 5-23. Masses of Minor Precipitates Based on Case 1 104
Figure 6-1. May 2001 Water Levels and Flow Patterns in the Vicinity of Former NAS Moffett Field PRB 122
Figure 6-2. Water Levels and Flow Patterns at Dover AFB PRB Site for February 1998 (Battelle, 2000a) 123
Figure 6-3. December 1999 Water Levels and other Hydraulic Measurements for Dover AFB PRB 124
Figure 6-4. November 1999 Water Levels and Other Hydraulic Measurements at Lowry AFB PRB 126
Figure 6-5. April 2001 Water Levels at Seneca Army Depot PRB 127
Figure 6-6. July 2001 Water Levels at Seneca Army Depot PRB 127
Figure 6-7. Example of Continuous Water Level Monitoring Data from Dover AFB PRB 129
Figure 6-8. Hydrotechnics Results for Lowry PRB Site Showing Groundwater Flow Velocity, Groundwater Flow Direction (Azimuth), and Precipitation Over Time at the Site 133
Figure 6-9. Example of Colloidal Borescope Results for Well U-7 at Former Lowry AFB PRB 136
Figure 6-10. Modeling Methods Used to Illustrate Capture Zone of PRBs 139
Figure 6-11. Example of Particle Tracking Used to Determine Residence Time Within a PRB 140
Figure 6-12. Model Setup and Permeability Zones at Seneca Army Depot PRB 142
Figure 6-13. Simulated Water Levels at Seneca Army Depot PRB 142
Figure 6-14. Simulated Flow Vectors at Seneca Army Depot PRB 143

Figure 6-15. Simulated Water Levels at Seneca Army Depot CRB with a Low Permeability Zone Upgradient of the PRB 143
Figure 6-16. Transport Modeling of a Slug of Contamination Through a Funnel-and-Gate PRB for a Range Hydraulic Conductivity in the PRB 145
Figure 6-17. Simulated Hydraulic Gradient Through a PRB for a Range of PRB Conductivity....146
Figure 6-18. Particle Tracking Through a Hanging Wall PRB Configuration....147
Figure 6-19. Graph of the Angle of Groundwater Flow to the PRB Versus the Angle of Refraction in a PRB for Various Ratios of Hydraulic Conductivity in the PRB and Aquifer....149
Figure 6-20. Transport Modeling of Plume Migration for a PRB Oriented at 70° to the Predominant Direction of Groundwater Flow Illustrating How Contamination is Diverted Around Portions of the PRB....150
Figure 6-21. Diagram Illustrating Correction Factor for Seasonal Fluctuations in the Direction of Gradient....151
Figure 6-22. Base Case Model and Groundwater Flow at an Angle to the CRB....152
Figure 6-23. Model with Trench and Groundwater Flow at an Angle to the CRB....152
Figure 6-24. Model With Downgradient Drain and Groundwater Flow at an Angle to the CRB....153
Figure 6-25. Model With Downgradient Barrier and Groundwater Flow at an Angle to the CRB....153
Figure 6-26. Model with Upgradient Trench and Groundwater Flow at Angle to the CRB....154
Figure 6-27. Model with Additional Reactive Barrier and Groundwater Flow at an Angle to the CRB....154
Figure 7-1. Summary of PRB Construction Methods 162
Figure 7-2. Depth of PRB Installations for all Construction Methods....162
Figure 7-3. Summary of PRB Configurations 164

TABLES

Table 4-1. Selected Core Samples for Solid Phase Characterization 32
Table 4-2. Characterization Techniques for Core Samples 32
Table 4-3. Locations of Sampling Points in the Column Tests 35
Table 4-4. Summary of Groundwater Flowrates used in Moffett Field Column Test 37
Table 4-5. Summary of Groundwater Flow 38
Table 5-1. Concentrations of CVOCs in the Upgradient A1 Aquifer Zone Groundwater for the Five Monitoring Events 44
Table 5-2. Target CVOC Concentrations During Quarterly Monitoring (October, 1997) 45
Table 5-3. Target CVOC Concentrations After Five Years of Operation (May 2001) 46
Table 5-4. Selected Results of Field Parameter Measurements for April 1997 48
Table 5-5. Selected Results of Field Parameter Measurements for May 2001 49
Table 5-6. Selected Results of Inorganic Chemical Measurements for April 1997 Sampling Event 50
Table 5-7. Selected Results of Inorganic Chemical Measurements for May 2001 50
Table 5-8. Silica Concentrations in Groundwater from October 1998 51
Table 5-9. Time Series Measurements in Upgradient and Downgradient Aquifer Wells at Former NAS Moffett Field 54
Table 5-10. Results of XRF Analysis of Five Iron Core Samples from the Moffett Field PRB 55
Table 5-11. Results of XRD Analysis Iron Core Samples from the Moffett Field PRB 56
Table 5-12. Recoverable Material from Silt Traps at Moffett Field Monitoring Wells 57
Table 5-13. Results of Chemical Analysis from Moffett Field Silt Traps 58
Table 5-14. Results of XRD Analysis from Moffett Field Silt Traps 58
Table 5-15. Results of EDS Analysis from Moffett Field Silt Traps 60
Table 5-16. Samples for Microbiological Evaluation in May 2001 65
Table 5-17. Summary of Microbiological Results 66
Table 5-18. CVOC Distribution in the Groundwater in the PRB and Vicinity at Former Lowry AFB (September 1999) 69
Table 5-19. Field Parameter Measurements in Groundwater in the PRB and Vicinity at Former Lowry AFB (September 1999) 70
Table 5-20. Inorganic Analysis of Groundwater in the PRB and Vicinity at Former Lowry AFB (September 1999) 71
Table 5-21. Carbon Composition (Weight Percent) of Iron from Lowry PRB 72
Table 5-22. Results of Core Sample Analysis of the PRB at Former Lowry AFB 72
Table 5-23. Material Sampled from Silt Traps at Lowry Monitoring Wells 73
Table 5-24. Results of XRD Analysis of Silt from Lowry AFB Monitoring Wells 74
Table 5-25. Results of TCE Measurements (mg/L) in Moffett Field Column Test 78
Table 5-26. Relative TCE Concentrations (C/C_0) in Moffett Field Column Test 78
Table 5-27. Results of Regression Calculation on Moffett Field Column Test 79
Table 5-28. Inorganic Analysis of Filtered Water Samples From Moffett Field Column 82

Table 5-29. Inorganic Analysis of Unfiltered Water Samples From Moffett Field Column 83
Table 5-30. Results of TCE Measurements (mg/L) in Lowry Column Test 87
Table 5-31. Relative TCE Concentrations (C/C_0) in Lowry Column Test 88
Table 5-32. Results of Regression Calculation for Lowry Column Test 90
Table 5-33. Inorganic Analysis of Filtered Water Samples from Lowry Column 91
Table 5-34. Inorganic Analysis of Unfiltered Water Samples from Lowry Column 92
Table 5-35. Dimensions of Iron Sections from Lowry AFB Column Test 94
Table 5-36. Results of XRF Analysis of Five Iron Samples from the Lowry Column Test 95
Table 5-37. Results of XRD Analysis from Lowry Column Simulation 95
Table 5-38. Comparison of Typical Analytes for Moffett Field Groundwater and Madison Tap Water 98
Table 5-39. Input Parameters for Moffett Field Groundwater after Pre-equilibration 100
Table 5-40. Formulas for Mineral Phases with Favorable Precipitation Kinetics 101
Table 5-41. Minerals Considered in Modeling Cases 101
Table 5-42. Residence Times and Iron Dissolution in Moffett Field Column Test 107
Table 5-43. Residence Times and Iron Dissolution Encountered in the PRB at Former NAS Moffett Field 107
Table 5-44. Comparison of Simulation Results for the Moffett Field PRB with Initial Conditions and Field Measurements 108
Table 5-45. Calculated Mass of Precipitate at 1 ft Inside Moffett Field PRB 108
Table 6-1. Representative Hydraulic Parameters Measured for Aquifers at the DoD PRB Sites Evaluated 119
Table 6-2. Summary of Hydraulic Gradients Through PRBs* 120
Table 6-3. Comparison of Slug Test Data in Aquifer Sediments and PRB Material 131
Table 6-4. Power Supply for HydroTechnics™ Sensors 132
Table 6-5. Colloidal Borescope Measurement Results in the Dover PRB (December 1999) 134
Table 6-6. Colloidal Borescope Measurement Results in the Vicinity of Former Lowry AFB PRB (October 1999) 135
Table 6-7. Summary of Groundwater Modeling at DoD PRB Sites 137
Table 6-8. Summary of Modeling to Increase Capture for Groundwater Flow at an Angle to the PRB 150
Table 7-1. Summary of Reactive Barrier Construction Techniques 165
Table 7-2. Update on Design, Construction, and Cost of PRBs 176
Table 7-3. Update on PRB Site Characteristics and Monitoring 183
Table 7-4. Present Value Estimates for PRBs Versus Pump-and-Treat Systems at Dover AFB and Former NAS Moffett Field 193

ABBREVIATIONS AND ACRONYMS

2-D	two-dimensional
3-D	three-dimensional
AFB	Air Force Base
AFCEE	Air Force Center for Environmental Excellence
AFRL	Air Force Research Laboratory
ATR	attenuated total reflectance
BEI	backscatter electron image
bgs	below ground surface
CCD	charge coupled device
CFC	chlorofluorocarbon
CPT	cone penetrometer testing
CRB	continuous reactive barriers
CVOC	chlorinated volatile organic compound
DCA	dichloroethane
DCE	dichloroethene
DO	dissolved oxygen
DoD	United States Department of Defense
DOE	United Stated Department of Energy
EDS	energy dispersive spectrometer/spectroscopy
ESTCP	Environmental Security Technology Certification Program
FTIR	Fourier Transform Infrared
FY	fiscal year
gpm	gallons per minute
HDPE	high-density polyethylene
ICP/MS	inductively-coupled plasma/mass spectroscopy
ITRC	Interstate Technology and Regulatory Cooperation
JAG	jet-assisted grouting
LCAAP	Lake City Army Ammunition Plant
LLNL	Lawrence Livermore National Laboratory

MCL	maximum contamination level
MTBE	methyl-*tert*-butyl ether
N/A	not available
NA	not analyzed
NAS	Naval Air Station
ND	not detected
NFESC	National Facilities Engineering Service Center
O&M	operations and maintenance
ORP	oxidation-reduction potential
ORNL	Oak Ridge National Laboratory
P&T	pump and treat
PCE	perchloroethylene
PLFA	phospholipid fatty acid
POC	point of contact
PRB	permeable reactive barrier
PV	present value
PVC	polyvinyl chloride
RACER	Remedial Action Cost Engineering and Requirements (System)
RIM	radio-wave imaging method
RPM	Remedial Program Manager
RTDF	Remediation Technologies Development Forum
SEM	scanning electron microscopy
SERDP	Strategic Environmental Research and Development Program
TCA	trichloroethane
TCE	trichloroethene
TDS	total dissolved solids
TIO	Technology Innovation Office
TPI	Tri-Agency PRB Initiative
U.S. EPA	United States Environmental Protection Agency
USACE	United States Army Corps of Engineers
VC	vinyl chloride
VOA	volatile organic analysis
VOC	volatile organic compound
WPI	Worldwide Performance Innovation

XRD	x-ray diffraction
XRF	x-ray fluorescence

EXECUTIVE SUMMARY

The purpose of this project is to evaluate short- and long-term performance issues associated with permeable reactive barriers (PRBs) installed at several United States Department of Defense (DoD) sites. The general technical approach consisted of the following elements:

- Reviewing existing field data from the DoD PRBs
- Identifying the challenges facing technology implementation
- Conducting additional monitoring and modeling at selected PRB sites to fill in any data gaps
- Recommend suitable long-term design/monitoring strategies for existing and new permeable barriers.

This project is being implemented by the DoD and is sponsored by the Strategic Environmental Research and Development Program (SERDP) and Environmental Security Technology Certification Program (ESTCP). The United States Environmental Protection Agency (U.S. EPA) and United States Department of Energy (DOE) also are implementing complementary projects with separate sources of funding. The combined effort of these three agencies is expected to span the PRBs at several government sites. The three agencies are planning to summarize their findings in a combined tri-agency report that contains the main results and conclusions from the evaluations conducted by the three agencies. The Remediation Technologies Development Forum (RTDF) Permeable Barriers Work Group and the Interstate Technology and Regulatory Corporation (ITRC) Permeable Reactive Barriers Team are providing document review support for the project.

The United States Naval Facilities Engineering Service Center (NFESC) is the lead agency on this DoD SERDP/ESTCP project. Battelle Memorial Institute, under contract to NFESC, is planning and implementing the technical scope and has prepared this interim modeling report to summarize the design challenges and recommendations following the field activities conducted in calendar year 1999. In addition to SERDP/ESTCP and NFESC, the Air Force Research Laboratory (AFRL), Air Force Center for Environmental Excellence (AFCEE), and United States Army Corps of Engineers (USACE) are participating in the DoD project.

This DoD project was conducted over a duration of three fiscal years (FY99 to FY01). The final product of the DoD project is this report that summarizes the outcome of the field investigations, and contains the objectives, technical approach, results, and design/monitoring recommendations.

The two primary objectives of the current project were:

- Assessing the longevity of PRBs made from iron, the most common reactive medium used so far. Longevity refers to the ability of a PRB to maintain its reactivity and hydraulic performance (residence time and capture zone) in the years following its field installation.

- Assessing the hydraulic performance of various PRBs in terms of their ability to provide the influent groundwater with the desired residence time in the reactive medium and to capture the desired portion of the upgradient plume.

Although field data from PRBs at several DoD sites initially were examined, the project subsequently focused on those sites that afforded the necessary range of site characteristics and PRB designs. The longevity evaluation focused primarily on two sites:

- Former NAS Moffett Field
- Former Lowry AFB

These two sites were selected because the PRBs there were installed at least three years before the current project started (that is, they had sufficient history of field operation) and because the groundwater at these sites was relatively high in total dissolved solids (TDS), an important factor in accelerating the determination of precipitation potential and longevity. The hydraulic performance evaluation focused primarily on four sites:

- Former NAS Moffett Field (funnel and gate)
- Former Lowry AFB (funnel and gate)
- Seneca Army Depot (continuous reactive barrier)
- Dover AFB (funnel with two gates)

These sites provided a range of PRB designs and hydrogeologic characteristics that could be studied so that appropriate guidance could be provided for future applications. In addition to these primary focus sites, PRBs at other sites, such as Cape Canaveral Air Station (Hangar K) and former NAS Alameda, initially were examined, but were de-emphasized as resources were focused on field investigations at sites that appeared to offer the most features of interest for the current project.

The longevity evaluation was conducted at former NAS Moffett Field and former Lowry AFB and consisted of the following elements:

- Groundwater geochemistry monitoring
- Iron core collection and analysis
- Geochemical modeling
- Accelerated column tests.

Although groundwater monitoring, iron core analysis, and geochemical modeling provided valuable information on the types and possible quantities of precipitates, during the middle of the current project, it was recognized that none of these tools would provide the critical link between the types and quantities of precipitates formed and any consequent loss of reactivity. Therefore, despite some limitations in simulating long periods of flow through the PRB, accelerated column tests were conducted to determine how the reactivity (or contaminant half-life) would change during long exposures to groundwater flow. The same groundwater and same iron medium at former NAS Moffett Field and former Lowry AFB were used in the column tests.

The column tests showed that the reactivity of the iron declined with long-term exposure to groundwater. The rate of decline in reactivity was higher for the Lowry AFB groundwater, which contained higher levels of dissolved solids than the NAS Moffett Field groundwater. The decline in reactivity occurred even though the pH and ORP distributions in the columns remained constant. Therefore, simple field measurements, such as pH and ORP, may not be indicative of the reactivity of the iron in field PRBs, in the long term.

The hydraulic performance evaluation was conducted at former NAS Moffett Field, former Lowry AFB, Seneca Army Depot, and Dover AFB. The PRB at Seneca Army Depot is a continuous reactive barrier, whereas the other sites have funnel-and-gate systems. The following tools were used in this evaluation:

- Water level measurements
- HydroTechnics™ in-situ flow sensors
- Colloidal borescope (down-hole instrument).

Careful and periodic water level measurements gave the best results at all these sites, and may be the best tool at future sites. The direct flow measurements with flow sensors and the borescope sometimes provided groundwater flow velocities and directions that contrasted sharply with the results of water level measurements. The direct flow measurements are point estimates; the sensors measure very localized flow in the immediate vicinity of the sensor, whereas the borescope measures preferential flow at specific depths in monitoring wells. The bulk flow estimates provided by water levels are probably more indicative of the flow regime around the PRB. The sensors or the borescope may be useful for further delineation of flow at highly heterogeneous sites, or at sites where groundwater chemistry or water level measurements have indicated sub-optimal hydraulic performance.

The former NAS Moffett Field site provided the most definitive indication that flow was progressing as designed. The relative success of the monitoring tools at this site may be due to the fact that flow was somewhat constrained by the site geology; a sand channel directs most of the targeted flow through the gate. At other sites, variability in hydraulic measurements led to more uncertainty in understanding groundwater flow. The results of the hydraulic performance evaluation can be summarized as follows:

- At former NAS Moffett Field, the capture zone was 30 ft wide and the best estimate of residence time in the reactive medium was 9 days. Although there was no clear evidence of a clean groundwater front emerging from the PRB in the downgradient aquifer, there are signs that such a front may appear in the future. The persistence of the downgradient contamination could be due to a variety of site- and PRB-specific factors.

- At former Lowry AFB, the capture zone appeared to be approximately 20 ft wide and the best guess of the residence time was 25 days. There was more uncertainty in the residence time estimate at this site. Groundwater capture was affected by an adjacent flowing stream, and most of the groundwater upgradient of the eastern funnel wall appeared to be flowing towards this stream.

- At Seneca Army Depot, the PRB was very thin (1-foot thickness) and created minimal disturbance in the flow regime. The upgradient flow divide was difficult to identify at this site, but appeared to be near the end of the PRB, on the northern end. Anthropogenic heterogeneities appeared to influence flow through the PRB. The southern end of the long PRB was not studied, as most of the new monitoring wells were focused on the northern end.

- At Dover AFB, an extremely low hydraulic gradient made water level measurements difficult. However, during certain monitoring events signs of groundwater capture could be identified. The capture zone appeared to be asymmetrical around each of the two gates.

The important recommendations from the evaluation are as follows:

- Because the PRB is a fixed installation, and future modifications, may be difficult and/or expensive, understanding the groundwater geochemistry and flow characteristics before construction is more important than addressing these factors during post-construction monitoring.

- Adequate site characterization, modeling of several flow and longevity-cost scenarios, and incorporation of appropriate safety factors are three main ways of addressing longevity and ensuring hydraulic performance.

- Post-construction monitoring can be done at lower frequencies, given the time it takes for changes to develop in the PRB. However, common and inexpensive measurements, such as pH and ORP, may not be good early-warning indicators of declining performance.

- There is a tradeoff between higher safety factors in the dimensions of the PRB and future risk of sub-optimal reactive and hydraulic performance. In other words, there is a tradeoff between current costs and the risk of incurring future costs, that should be taken into account when designing a PRB application.

In addition to the field and bench-scale evaluation, the report contains updates on construction techniques and costs at PRB sites in the United States, and the results of a survey of the PRB application review approach of several State regulatory agencies.

1.0 Introduction

1.1 Project Background

The purpose of this project is to address short- and long-term performance issues associated with permeable reactive barriers (PRBs) installed at several United States Department of Defense (DoD) sites. The technical approach is to review existing field data from the DoD PRBs, identify the challenges facing technology implementation, conduct additional monitoring to fill in any data gaps, and recommend suitable long-term design/monitoring strategies for existing and new permeable barriers.

This project is being implemented by the DoD and is sponsored by the Strategic Environmental Research and Development Program (SERDP) and Environmental Security Technology Certification Program (ESTCP). The United States Environmental Protection Agency (U.S. EPA) and United States Department of Energy (DOE) also are implementing complementary projects with separate sources of funding. The combined effort of these three agencies is expected to span the PRBs at several government sites. The Remediation Technologies Development Forum (RTDF) Permeable Barriers Group and the Interstate Technology and Regulatory Cooperation (ITRC) Permeable Barriers Subgroup are providing document review support for the project.

The United States Naval Facilities Engineering Service Center (NFESC) is the lead agency on this DoD SERDP/ESTCP project. Battelle Memorial Institute, under contract to NFESC, is planning and implementing the technical scope and has prepared this report to describe the design and monitoring challenges and recommendations following the field activities conducted during 1999-2001. In addition to SERDP/ESTCP and NFESC, the Air Force Research Laboratory (AFRL), Air Force Center for Environmental Excellence (AFCEE), and United States Army Corps of Engineers (USACE) are participating in the DoD project. Each agency has assigned a point of contact (POC) for this project (Appendix A).

This project was conducted over a duration of three fiscal years (FY99 to FY01). Appendix B contains information on the data archiving and demonstration plan (Battelle, 2000d). The final product of the project is this report that summarizes the outcome of the field investigations, and contains the objectives, technical approach, results, and design/monitoring recommendations.

1.2 Interagency Cooperation

To investigate the experience at as many PRB sites as possible, DoD, DOE, and U.S. EPA are cooperating in this effort to study the challenges facing the technology. This tri-agency cooperation allows the agencies to leverage each other's funding in order to assimilate the experience both at a large number of different sites and for different PRB designs. These three agencies are coordinating their efforts through the formation of the Tri-Agency PRB Initiative (TPI). The TPI members (DoD, DOE, and U.S. EPA) meet periodically and conduct regular conference calls to discuss objectives and progress of their respective field investigations. An Internet site describing the efforts of the three agencies has been set up to disseminate relevant

information (http://www.frtr.gov/prb/). This site will be updated periodically. The three agencies also have agreed to review each other's reports. The three agencies are considering a final product outlining the combined results and recommendations arising out of the three agencies' efforts.

In addition to cooperating in these areas of broad cooperation, the participating government agencies, and their representatives, also are cooperating at the field level. At former Lowry Air Force Base (AFB) and Dover AFB, Battelle (DoD representative) and Oak Ridge National Laboratory (ORNL) (DOE representative) conducted joint testing of the hydraulic flow characteristics of a PRB. The colloidal borescope, an instrument developed by ORNL, was tested as an indicator of flow velocity and direction.

1.3 Project Objectives

The two primary objectives of the current project are:

- Assessing the longevity of PRBs made from iron, the most common reactive medium used so far. Longevity refers to the ability of a PRB to maintain its reactivity and hydraulic performance (residence time and capture zone) in the years following its field installation.

- Assessing the hydraulic performance of various PRBs in terms of the ability of each to provide the influent groundwater with the desired residence time in the reactive medium and to capture the desired portion of the upgradient plume.

Although field data from PRBs at several DoD sites initially were examined, the project subsequently focused on those sites that afforded the necessary range of site characteristics and PRB designs. The longevity evaluation focused primarily on two sites:

- Former Naval Air Station (NAS) Moffett Field
- Former Lowry AFB.

These two sites were selected because the PRBs there were installed at least three years before the current project started (that is, they had sufficient history of field operation) and because the groundwater at these sites was relatively high in total dissolved solids (TDS), an important factor in accelerating the determination of precipitation potential and longevity. The hydraulic performance evaluation focused primarily on four sites:

- Former NAS Moffett Field (funnel-and-gate)
- Former Lowry AFB (funnel-and-gate)
- Seneca Army Depot (continuous reactive barrier)
- Dover AFB (funnel with two gates).

These sites provided a range of PRB designs and hydrogeologic characteristics that could be studied so that appropriate guidance could be provided for future applications. In addition to these primary focus sites, PRBs at other sites, such as Cape Canaveral Air Station (Hangar K) and former NAS Alameda, initially were examined, but were de-emphasized as resources were focused on field investigations at sites that appeared to offer the most features of interest for the current project. Also, a separate detailed study at former NAS Alameda (Einarson et al., 2000) provided sufficient information for this evaluation.

1.4 Regulatory Issues

Although regulatory agencies have shown general interest in the PRB technology, implementation of the technology has not been as widespread as anticipated. The two major concerns with the technology from a regulatory perspective have been longevity and hydraulic performance, resulting mainly from the short history of this technology. The uncertainty over the longevity of a field PRB has led to regulatory agencies requesting that site owners develop a contingency plan (such as implementation of a pump-and-treat system) in case of PRB failure. Regulatory agencies have tried to address uncertainties in hydraulic performance by requesting monitoring for plume breakthrough (insufficient residence time) and bypass (inadequate capture). The ITRC has been the main regulatory vehicle that has made considerable progress in defining the challenges facing the technology and preparing implementation and monitoring guidance for member states.

The current project supplements the efforts of various regulatory agencies by evaluating the longevity of the reactive medium (iron), defining the range of hydraulic performance of PRBs, and defining the capabilities and limitations of the characterization tools available to evaluate hydraulic performance on a site-specific basis.

1.5 Previous and Other Ongoing Assessments of the Technology

SERDP and ESTCP have sponsored one previous assessment of the PRB technology that involved installing a field pilot-scale PRB at Dover AFB and using the results of this demonstration and other PRB implementations to develop a design guidance for PRBs (Gavaskar et al., 2000). In the Dover AFB project, a funnel-and-gate system with two gates was installed to evaluate the performance of iron and an innovative reactive medium (iron and pyrite); an innovative installation technique using caissons was used to install the PRB to a maximum depth of 40 ft below ground surface (bgs). Other notable assessment projects that have involved relatively detailed evaluations of PRB performance are:

- Performance evaluation of a PRB at former NAS Moffett Field (Battelle, 1998)
- Performance evaluation of a PRB at the Coast Guard Site in Elizabeth City, North Carolina (Puls et al., 1995)

The current project seeks to further define the challenges identified during previous assessments and determine ways of addressing them during PRB design, construction, and monitoring.

In addition, SERDP has funded John Hopkins University to conduct column tests to determine the effect of individual groundwater constituents on precipitation and, concomitantly, the reactivity of the iron. These column tests are being conducted with artificial water, constituted by spiking deionized water with the component of interest (e.g., carbonate or silicate). The effect of each component is isolated by testing it in a separate column filled with granular iron. Recent reports (Arnold and Roberts, 2000; Totten et al., 2001) have indicated that some of the natural groundwater components can precipitate and saturate the reactive surfaces of the iron after a period of constant exposure. The results of this study are expected to provide new insights into the mechanisms through which different groundwater constituents affect the reactivity of the iron.

2.0 Technology Description

2.1 Permeable Barrier Technology Description

In its simplest form, a PRB is a trench in the path of contaminant plume (see Figure 2-1). The trench is filled with a medium that treats the contamination through processes such as chemical reduction, aerobic or anaerobic degradation, or adsorption. The primary advantage of the PRB technology is its passive nature; the plume is carried to the treatment zone by the natural groundwater flow.

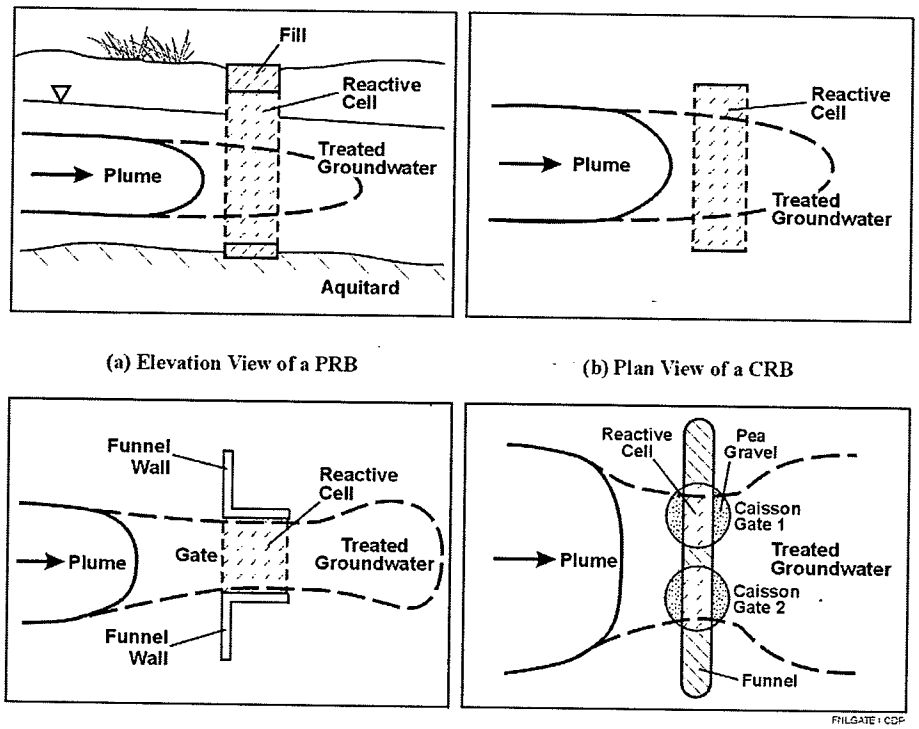

Figure 2-1. Schematic Illustrations of Some PRB Configurations

The two main PRB configurations are the continuous reactive barrier (CRB) and the funnel-and-gate system. A continuous reactive barrier has only a permeable section (filled with reactive medium), whereas a funnel-and-gate system has both permeable (gate) and impermeable (funnel) sections. The funnel directs more groundwater towards the gate and was devised early on as a means of capturing more groundwater while conserving relatively expensive reactive medium. However, because the price of granular iron dropped from $650/ton to about $350/ton, many sites have been using the less complex CRB configuration. Funnel-and-gate systems may still be

considered at some sites with special needs (for or example, sites with underground utilities or sites that need to retrieve and replace the reactive medium frequently).

This current project focused on the most common type of PRBs, namely, trench-type PRBs containing granular iron medium. Granular iron has been the most common reactive medium used in PRBs so far. The reasons for its popularity are easy availability, reasonable cost, and demonstrated ability to treat a variety of organic and inorganic dissolved contaminants. The passive nature of its operation makes this technology potentially cost-effective for environmentally persistent contaminants, such as chlorinated solvents, in groundwater. Chlorinated solvent plumes are expected to persist for several decades or centuries at many sites and a passive technology offers obvious long-term advantages. Examples of other groundwater contaminants amenable to treatment by various barrier media are chromium, uranium, and nitrates.

Trench-type barriers are common because they are relatively easy to install, quality control issues (e.g., continuity of the reactive medium in the treatment zone) are easier to address, and commonly available equipment can be used for their construction. In addition, with improvements in trenching techniques, relatively long (1,100 ft long at the Tonolli; Superfund Site) and deep (60 ft bgs at Lake City Army Ammunitions Plant) PRBs have become feasible with trenching. Other construction methods, such as jetting, hydraulic fracturing, and vibratory beam, have been demonstrated at some sites, as they offer some cost advantages at deep sites; however, their application is relatively more difficult and their performance has so far been difficult to evaluate.

2.2 Advantages and Limitation

The PRB technology offers the following potential advantages, especially in comparison to the conventional plume control remedy of pump and treat:

- The passive nature of PRB operation can lead to lower labor and energy requirements and costs in the long term.
- The absence of aboveground structures facilitates property transfers and the land surface is available for more diverse uses.
- The ability of PRBs to treat a variety of dissolved contaminants with a variety of commonly available reactive and adsorptive media has been proven to meet most applicable groundwater cleanup targets, as long as adequate capture and residence time can be achieved.

Potential limitations of the PRB technology are:

- PRB design and construction involves a greater capital investment than for an equivalent pump-and-treat system. Also, at many sites, pump-and-treat systems may already exist as part of an interim remedy.

- Post-construction modifications and changes, if required, may be more difficult and expensive than for a pump-and-treat system. It is more important to understand the groundwater flow regime and get the PRB installation and operation right the first time.

- The plume possibly may outlive the useful life of the PRB. The results of this current project show that granular iron PRBs, when designed with appropriate safety factors, probably can retain sufficient performance for many years, but may have to be regenerated or replaced at some point.

2.3 Factors Influencing Cost and Performance

A variety of factors affect the technical performance and cost of the PRB technology; these factors can often be evaluated in the early stages of implementation, namely, during feasibility evaluation or site conceptual model development. These factors include:

- Depth of the affected aquifer. This is the single most important factor that governs the type and cost of PRB construction.

- Amenability of the contaminants for treatment with commonly available barrier media.

- Degree of heterogeneity in the site geology and groundwater flow regime.

- Groundwater geochemistry and its effect on the longevity of the PRB.

- Underground and aboveground features (e.g., utility lines, buildings, and/or dense clays) that may impede construction.

3.0 Description of DoD Sites with PRBs

3.1 Site Selection Background

All existing PRBs at DoD sites were considered for more detailed performance evaluation. The preliminary field information obtained from these sites was summarized in a survey report prepared at the beginning of the current project (Battelle, 1999). As additional PRBs were installed at various sites during the progress of the current project, information on the new sites also was obtained. The updated list of 15 DoD sites where PRBs have been applied is as follows:

1. Former NAS Moffett Field
2. Former Lowry AFB
3. Seneca Army Depot
4. Dover AFB
5. Former NAS Alameda
6. Cape Canaveral Air Station (Hangar K)
7. Watervliet Arsenal
8. Massachusetts Military Reservation
9. Warren AFB
10. Pease AFB
11. Travis AFB
12. Maxwell AFB
13. Lake City Army Ammunition Plant
14. Vandenberg AFB
15. Naval Weapons Industrial Reserve Plant.

Initially, the current project focused on studying the first seven sites on this list in more detail, as these seven sites had the PRBs with the longest field history; the other sites are relatively new installations. Subsequently, resource limitations necessitated increased focus on about four sites. At this point, Watervliet Arsenal was dropped from further evaluation because in many ways it is similar to the PRB at Seneca Army Depot, where local logistical support was established more rapidly. Cape Canaveral Air Station (Hangar K) had some features of interest, especially the innovative construction techniques used. Also, iron cores previously collected from one of the PRBs at Hangar K were analyzed in the current project to evaluate degree of precipitate formation. However, the pilot-scale PRBs at the Cape site were only a few inches thick and a few feet long, and did not lend themselves to a detailed evaluation of longevity and hydraulic performance objectives with limited resources. Former NAS Alameda did present some features of interest (inadequate residence time in the reactive cell), especially for the hydraulic performance evaluation; however, a separate detailed study (Einarson et al., 2000) was completed during the second year of the current project and provided enough information for drawing the required conclusions and for comparing it with other sites on the list.

Eventually, the field evaluation focused on the first four sites on the list; these sites provided a suitable combination of PRB configurations, site characteristics, local logistical support, and alignment with the current project objectives. The longevity evaluation focused on the following two sites:

- Former NAS Moffett Field (permeable barrier installed in 1996). The groundwater at this site has moderate levels of dissolved solids, including moderate levels of alkalinity and sulfate.

- Former Lowry AFB (permeable barrier installed in 1995). This site presented another data point for longevity. The groundwater has a high level of dissolved solids, including high alkalinity and sulfate levels.

Higher levels of dissolved solids cause more precipitation in iron barriers and reduce the longevity of a PRB. In addition, faster precipitate formation generates more noticeable effects that can be studied in field cores of the iron and in long-term column tests. The hydraulic performance evaluation focused on the following four sites:

- Former NAS Moffett Field. A funnel-and-gate system installed in a sand channel. This relatively complex site offers considerable horizontal and vertical geologic heterogeneity, factors whose effects can be studied more easily.

- Seneca Army Depot (permeable barrier installed in 1998). A continuous reactive barrier located in a moderately heterogeneous aquifer. This site presents an opportunity to study the hydraulic performance of a PRB configuration that is becoming increasingly common.

- Former Lowry AFB. A funnel-and-gate system located near a surface water body (stream) in a relatively homogeneous aquifer. Extraneous site features, such as surface water bodies or operating pump-and-treat systems can affect interpretation of site characterization information and the functioning of the PRB.

- Dover AFB (permeable barrier installed in 1997). A funnel-and-gate system with two gates in a relatively homogeneous aquifer. This site provides a good example of the challenges involved in evaluating the hydrogeologic flow regime at a site with a very low hydraulic gradient and relatively large seasonal fluctuations in flow velocity and direction.

The sites selected were all variations of trench-type barriers. As described in Section 7.1, trenching is still the most widely used construction method at PRB sites. The primary advantage of trenching is that the continuity of the PRB is more or less assured. Installation is easier and quality control is fairly straightforward. As long as the orientation and dimensions of the PRB are properly designed, trench-type PRBs have a fair chance of meeting capture and residence

time requirements, assuming that the flow regime around the PRB is well understood. Although innovative installation techniques, such as jetting or hydraulic fracturing, have been tested for deeper aquifers at some sites and hold some promise, the performance of the resulting PRBs is difficult to evaluate. First, these innovative barriers have been installed fairly recently; some of them were installed even while the current project was underway. Second, many of these barriers are limited by the innovative construction techniques to a flow-through thickness of just a few inches, so their performance and their effect on the flow regime is more difficult to determine, as they have a minimal physical impact on the aquifer.

In addition, the trenching technique itself has been refined in the past few years so that PRBs as deep as 80 ft bgs have been installed economically at some sites. Therefore, the current project focused its limited resources on the trench-type barriers. One variation of the trenching technique that is highlighted in Section 7.1.2.4 is the bioslurry method, in which the walls of the trench are kept open with a biodegradable slurry, instead of with sheet piles or trench box. This variation has the potential to address some important construction issues related to trenching and is considered a significant advance in the implementation of the technique.

The characteristics of the four sites evaluated in detail in the current project are provided in Section 3.2. This section also contains a description of the former NAS Alameda site, a site that was studied under a separate project funded by NFESC. Appendix D contains descriptions of the other nine DoD sites with PRBs.

3.2 Characteristics of Sites Selected for Detailed Evaluation

The characteristics of the sites selected for detailed evaluation under the current project are described in this section. In addition, a description of the former NAS Alameda site is included, as this was one site where the PRB performance was tracked, although the fieldwork there was funded separately from the current project.

3.2.1 Former NAS Moffett Field. The funnel-and-gate PRB at the former NAS Moffett Field PRB site has been monitored and evaluated in significant details as part of a previous ESTCP project (Battelle, 1998). Water-level measurements were taken at this site during May 2001. These combined with the findings of the previous assessment provide valuable insights into the PRB technology. The surficial aquifer at this site is divided into two aquifer zones–a shallow zone (A1) and a deep zone (A2). The barrier is installed in the A1 zone of the surficial semi-confined aquifer at the site. The A1 aquifer zone is approximately 25 ft deep. Borings at the site suggest that several sand channels exist in the otherwise silty sand aquifer. The barrier was installed in a funnel-and-gate configuration through a major sand channel (Figure 3-1) within the lower conductivity silty and clayey layers. Hydraulic conductivity of the sand channel deposits is approximately 30 ft/day, porosity is 0.30, and the aquifer gradient was 0.007. Based on these parameters, groundwater flow velocity is 0.7 ft/day. Modeling of the system showed asymmetric capture of the plume and groundwater. In general, the site reflects channeled groundwater flow in a multi-aquifer system.

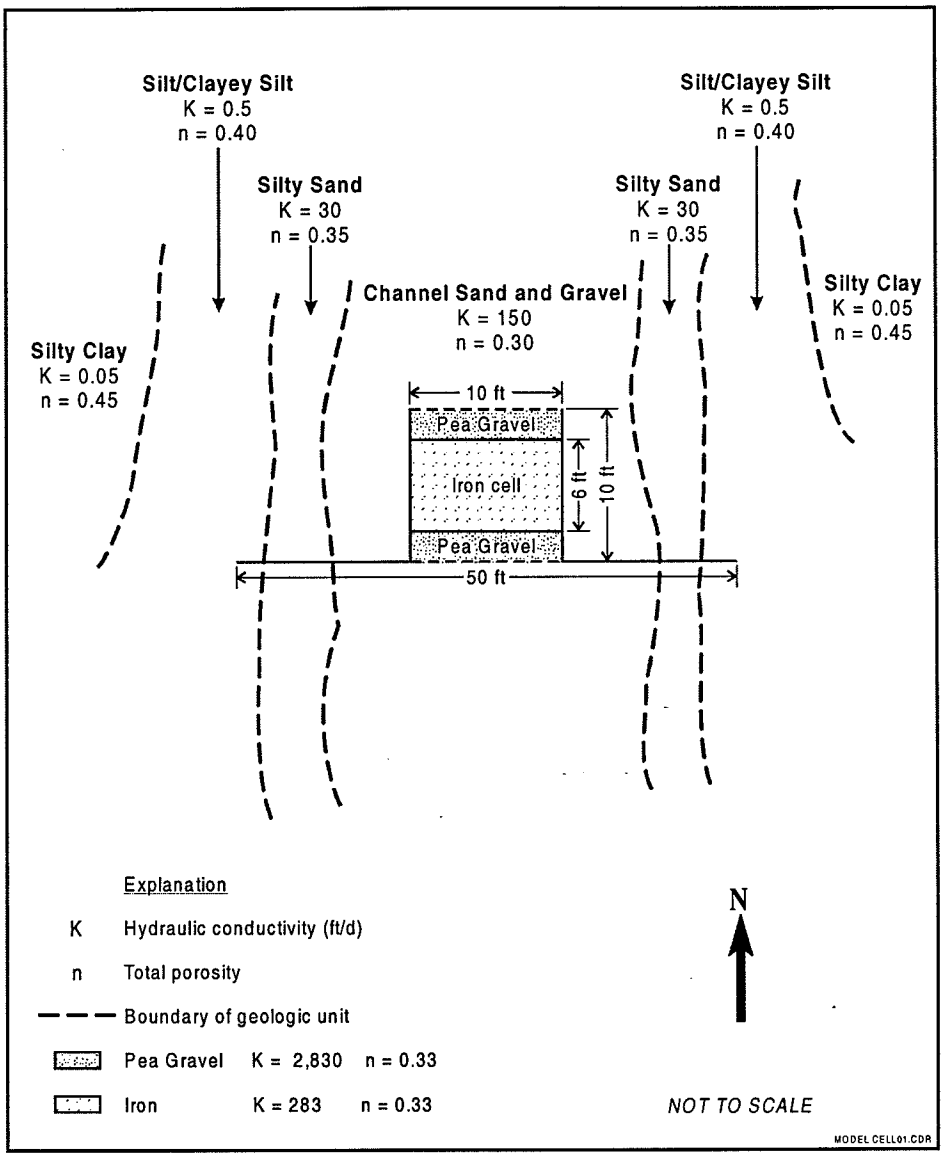

Figure 3-1. PRB at Former NAS Moffett Field Relative to Lithologic Variations in the Surrounding Aquifer

3.2.2 Former Lowry AFB. The aquifer at former Lowry AFB is comprised of 11 ft of silty-sand to sand and gravel in an unconfined aquifer which overlies weathered claystone bedrock 23-30 ft bgs (Versar, Inc., 1997). Hydraulic gradient through the barrier site is approximately 0.035. Representative aquifer permeability is 1.7 ft/day. Flow through the site is around 0.2 ft/day.

Some degree of heterogeneity is present in the form of sand and clay lenses. The barrier was set up in a funnel-and-gate arrangement with funnel walls at an angle to the reactive cell (Figure 3-2). Monitoring indicates plume capture, persistent mounding upgradient of the barrier, and

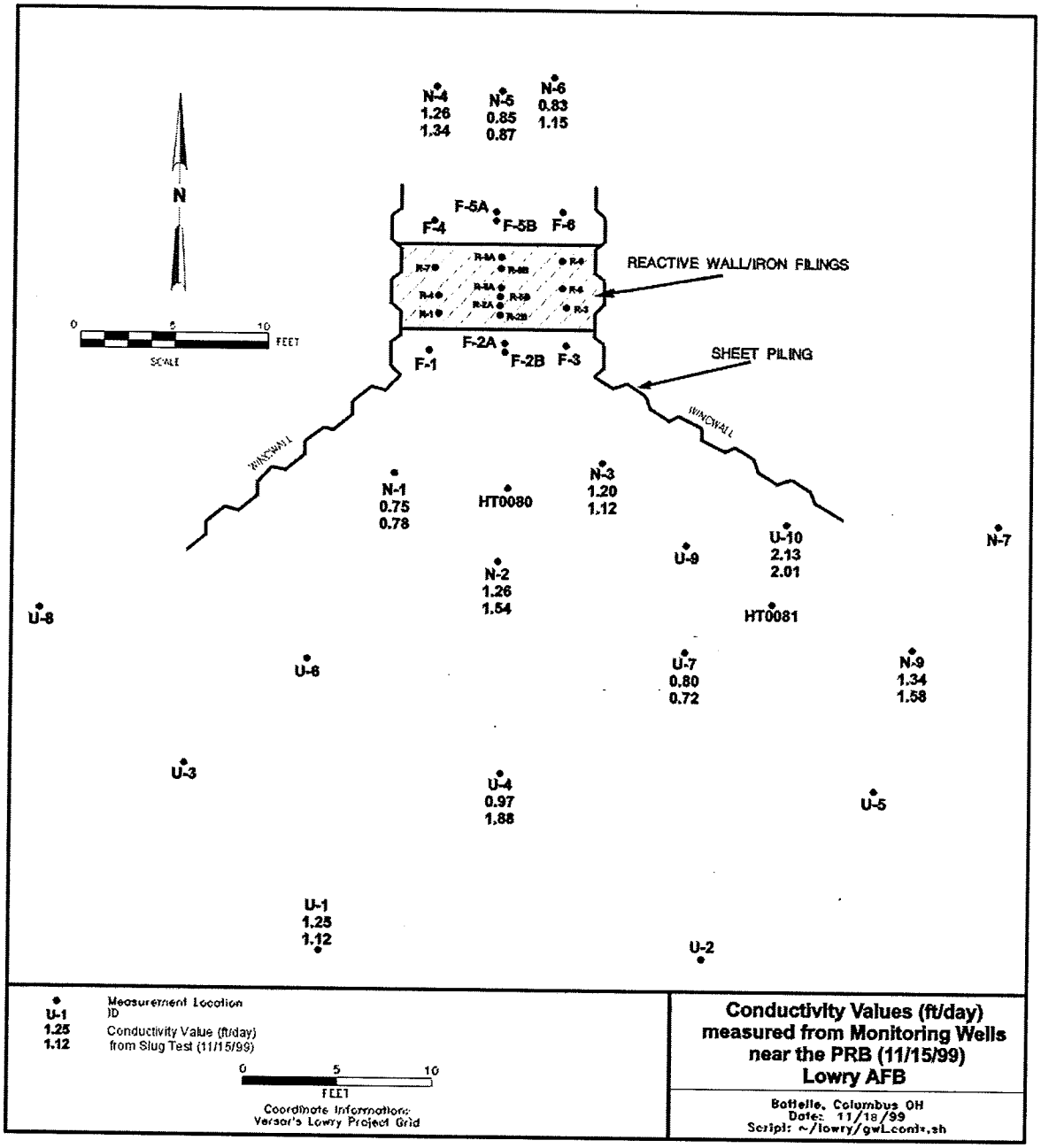

Figure 3-2. Design and Hydraulic Conductivity (ft/day) Distribution at Former Lowry AFB PRB

potential variations in flow velocities through the barrier. The monitoring activities at this site during the current project included installation of new monitoring wells and HydroTechnics™ sensors, monitoring of water levels, slug testing, and colloidal borescope measurements.

3.2.3 Seneca Army Depot. Groundwater flows through fractured shale and overlying glacial till at Seneca Army Depot (Parsons Engineering Services, Inc., 2000). The aquifer is unconfined. The PRB at Seneca is a 600-ft-long continuous trench, approximately 1 ft wide and keyed into competent shale bedrock 5-10 ft bgs (Figure 3-3). The barrier consists of a 50/50 mixture of sand and iron. Water flows through the PRB at a gradient of approximately 0.006.

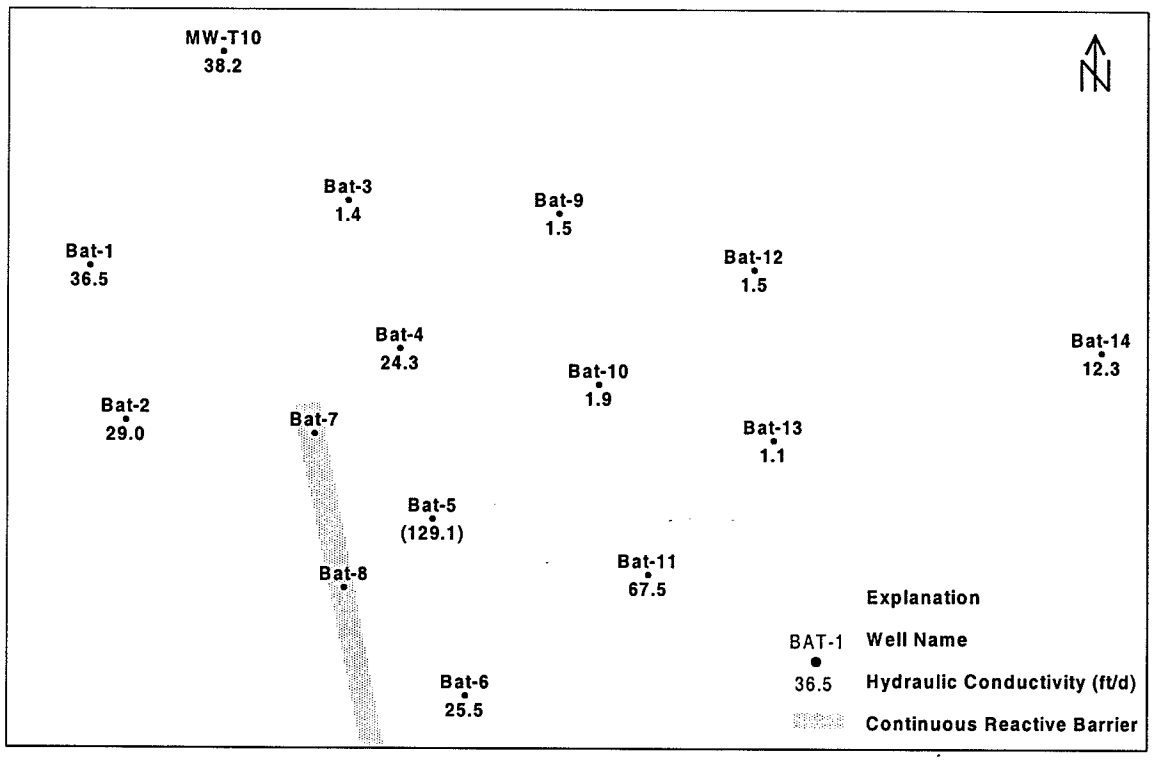

Figure 3-3. Hydraulic Conductivity Values (ft/d) from Slug Tests at the Seneca Army Depot CRB Showing Variations in Hydraulic Conductivity at the Site

Representative permeability of the sediments is approximately 25 ft/day. Some degree of deflection is discernible around the northern end of the barrier, where flow conditions are affected by the PRB. The hydraulic gradient upgradient of the barrier appears to be fairly flat. Overall, the Seneca Army Depot site reflects a shallow glacial till aquifer with a long, thin PRB designed to treat a diffuse plume spread over a large area. During the current project, 14 new 2-inch monitoring wells were installed (two inside the PRB and 12 in the surrounding aquifer, near the northern end of the PRB) to determine the flow divide and the capture zone.

3.2.4 Dover AFB. The funnel-and-gate PRB at Dover AFB was designed, installed, and monitored as part of a SERDP-funded project by Battelle (Battelle, 1997; 2000a). As shown in Figure 3-4, the aquifer at the Dover AFB site consists of unconfined silty sand deposits overlying a thick clayey confining layer. The aquifer is approximately 20-25 ft thick and fairly homogenous, except for several silty-clay lenses in the upper portion of the aquifer. The

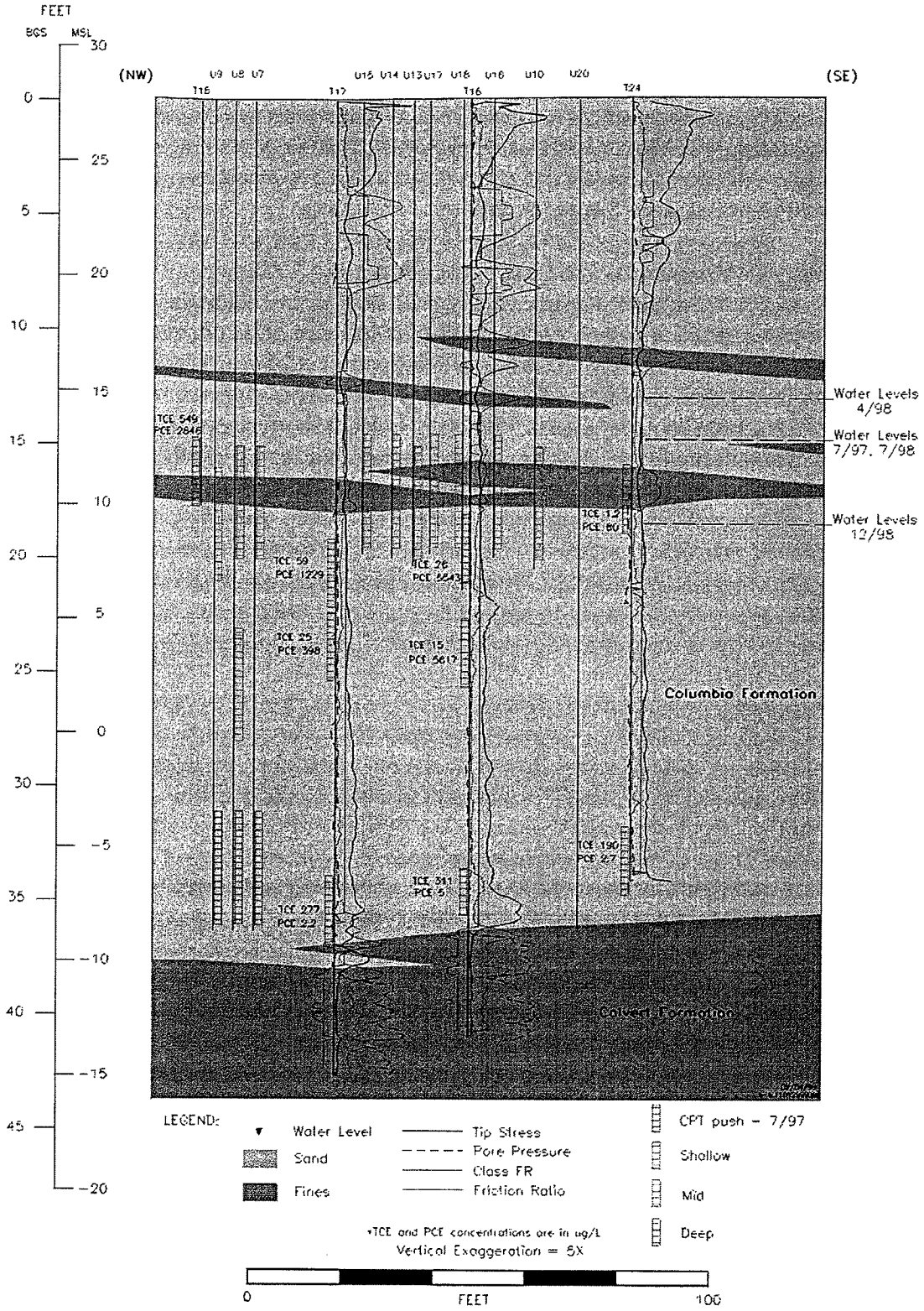

Figure 3-4. Lithology at the Dover AFB PRB

hydraulic gradient in the area is fairly low (0.002) and variable, with noticeable seasonal fluctuations. Based on the site conditions, the estimated groundwater flow is slow, at 0.04 ft/day. The PRB consists of a funnel-and-gate system with two gates. Interlocking sheet piles (Waterloo Barrier™) constitute the funnel and caisson excavations filled with reactive media (iron) constitute the two gates. The Dover AFB site represents a low-flow velocity setting in a thick, homogenous aquifer. As part of the current project, water level measurements and colloidal borescope measurements were performed at this site.

3.2.5 Former NAS Alameda. The aquifer at Former NAS Alameda is unconfined and composed of fill material placed on top of estuarine deposits to extend and stabilize the land at the northwest tip of Alameda Island (Einarson et al., 2000). The fill is comprised of silty sand to sandy materials and is approximately 20 ft thick. The aquifer is approximately 14 ft thick in the area of the PRB with a gradient of 0.007 ft. The site is hydraulically connected to San Francisco Bay, so diurnal fluctuations in groundwater levels are evident in the water table. Permeameter tests on wells screened in the fill materials suggest a representative hydraulic conductivity of 221 ft/day, with a fair amount of variation. As shown in Figure 3-5, the PRB was installed in a funnel-and-gate arrangement, with a relief gate on one side of the barrier wings and two extraction wells in the upgradient portion of the barrier to control residence times in the barrier. Modeling of the site suggested that tidal influences of the water table, leaky drains, and/or irrigation practices may have affected the groundwater flow directions and plume capture. Overall, the Alameda site is representative of an artificial fill aquifer that is subject to various hydrologic influences.

This site was not monitored as part of the current project. However, a detailed monitoring and performance assessment was funded separately by the Navy and is presented in Einarson et al. (2000). This report was the outcome of a detailed evaluation of the hydraulic performance of the Alameda PRB during 1999 following the appearance of higher-than-expected concentrations of *cis*-1,2-dichloroethene (*cis*-1,2-DCE) and vinyl chloride (VC) in the effluent from the iron reactive cell. These studies found that the chlorinated volatile organic compound (CVOC) plume had a thin, highly concentrated core that was passing through the iron without sufficient residence time. It is possible that there are multiple sources and multiple overlapping plumes at the site. During that a fairly comprehensive initial site characterization, longer-screen wells tended to average the CVOC concentrations, and the spacing between wells was probably insufficient to capture this extremely thin core. In the Einarson et al. (2000) study, shorter-screen wells that were spaced closer to each other were used, in what is probably the most intensive spatial characterization of a CVOC plume and aquifer conducted at a PRB site. The Alameda Study indicates that even after a relatively comprehensive site characterization, unusual contaminant or aquifer features may affect the expected contaminant loading on the reactive cell. The PRB at former NAS Alameda is a pilot installation and has been used to study a number of different PRB features and variations. However, the performance issues encountered at this site underscore the need for using suitable safety factors in the design of a PRB to account for potential uncertainties, such as uncertainties in future contaminant loading or groundwater flow velocity and direction.

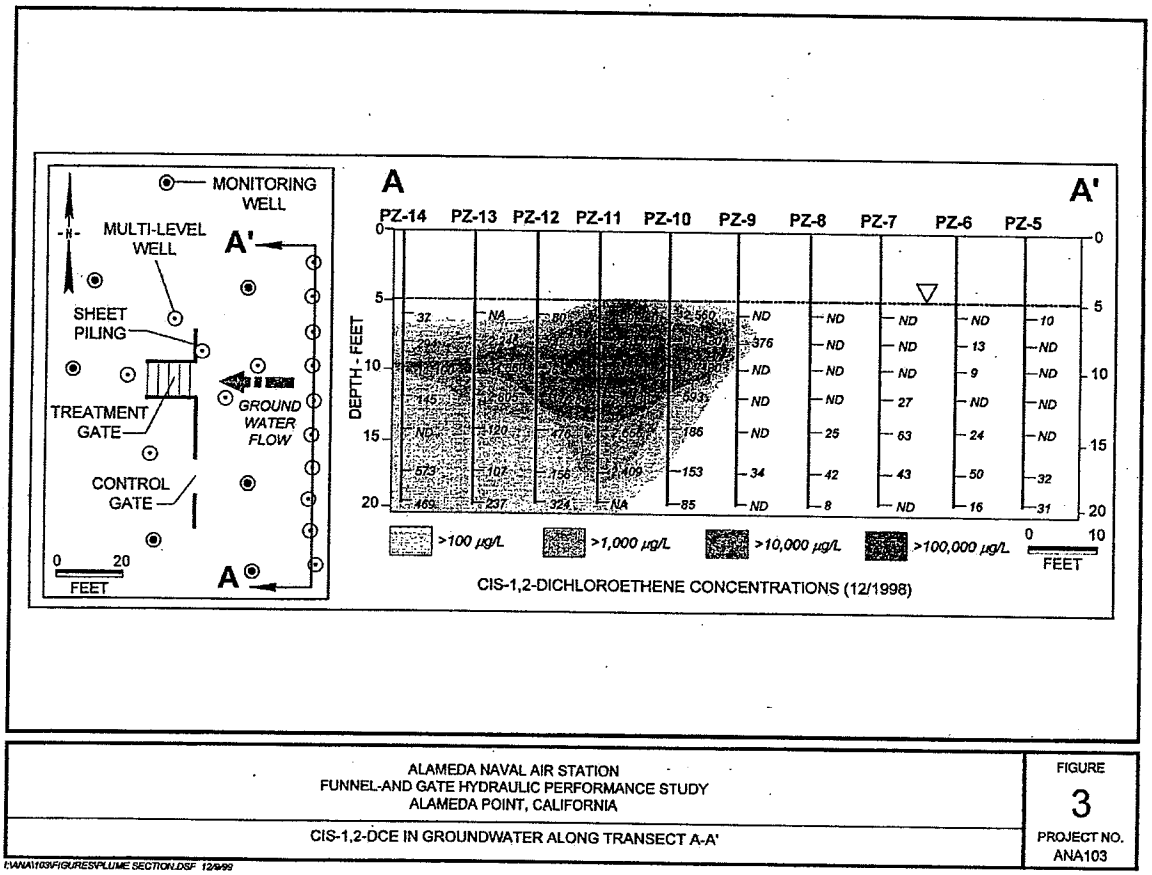

ALAMEDA NAVAL AIR STATION
FUNNEL-AND GATE HYDRAULIC PERFORMANCE STUDY
ALAMEDA POINT, CALIFORNIA

CIS-1,2-DCE IN GROUNDWATER ALONG TRANSECT A-A'

FIGURE 3

PROJECT NO. ANA103

I:\ANA\103\FIGURES\PLUME SECTION.DSF 12/9/99

Figure 3-5. Schematic View of PRB and Upgradient Contamination Profile at Former NAS Alameda Site (Einarson et al., 2000)

4.0 Performance Assessment Approach

4.1 Performance Assessment Objectives

The two primary objectives of the current project are:

- Assessing the longevity of PRBs made from iron, the most common reactive medium used so far. Longevity refers to the ability of a PRB to maintain its reactivity and hydraulic performance (residence time and capture zone) in the years following its field installation.

- Assessing the hydraulic performance of various PRBs in terms of their ability to provide the influent groundwater with the desired residence time in the reactive medium and to capture the desired portion of the upgradient plume.

The longevity evaluation focused primarily on two sites:

- Former NAS Moffett Field
- Former Lowry AFB.

The hydraulic performance evaluation focused primarily on four sites:

- Former NAS Moffett Field (funnel-and-gate)
- Former Lowry AFB (funnel-and-gate)
- Seneca Army Depot (continuous reactive barrier)
- Dover AFB (funnel with two gates).

These sites provided a range of PRB designs and hydrogeologic characteristics (see Section 3.2) that could be studied so that appropriate guidance could be provided for future applications.

4.2 Performance Assessment Strategy

The performance assessment objectives were achieved by using a select variety of tools that allowed the project to fill in the data gaps identified in the existing information from the PRB sites. Both performance objectives, longevity and hydraulic performance, presented significant challenges for the project. The strategy that evolved used a combination of tools to address each objective and overcome the limitations of each individual tool.

4.2.1 Longevity Evaluation Strategy. From the beginning of the project, it was clear that developing predictions about the life of a granular iron barrier would be difficult, given the short history of the technology in the field, the lack of information on kinetic rates of precipitation and reactivity loss that could be used in predictive models, and the difficulty of conducting any kind of laboratory simulations that would mimic the exposure of the iron to many pore volumes (i.e.,

long periods) of groundwater. Tools that were used in the current project to evaluate longevity include the following:

- Analysis of inorganic constituents in groundwater influent and effluent to the PRB
- Analysis of iron cores collected from field PRBs that have been operating for at least two years
- Geochemical modeling
- Accelerated column tests.

Tools that have become fairly conventional for evaluating precipitation in field PRBs include groundwater monitoring (influent and effluent) and iron core collection and analysis. By analyzing the groundwater influent and effluent (or upgradient and downgradient) to the PRB, the loss of inorganic constituents (e.g., calcium, magnesium, alkalinity, sulfate, silicate, etc.) sustained by the groundwater can be measured as it moves through the reactive cell of the PRB. The differences in or loss of groundwater constituents represents the potential precipitation that has occurred in the PRB. However, there are two challenges to using these tools:

- First, the losses in inorganic constituents measured in the groundwater often do not match the amount of precipitate observed on core samples of iron collected from the PRB. This mismatch can partly be explained by the fact that there is considerable uncertainty in the spatial extrapolation of the amount of precipitate observed on small core samples of iron to the rest of the reactive cell, as precipitates may be unevenly deposited in different parts of the iron.
- Second, even if the amount of precipitate formed could be accurately determined, it is unclear how these precipitates distribute on the iron surfaces (whether in mono-layers that use up maximum surface area or in multiple layers that conserve the available reactive sites). Also, because the mechanism through which the precipitates may be bound to the iron and the process by which electrons are transferred between the iron and the contaminants is unclear, it is difficult to correlate loss of surface area with loss of reactivity. In other words, could iron continue to react with the contaminants through a layer of precipitates on its surface?

Geochemical modeling previously has been used to elucidate the precipitation process (Battelle, 1998; Gavaskar et al., 2000; Sass et al., 2001). Two types of models are available – equilibrium models (models that assume an infinitely long contact time between the iron and the groundwater constituents) and kinetic models (models that can be can be calibrated to contact time, if the various reaction kinetics or rate constants involved are known). Because the kinetics of iron-

groundwater reactions have not yet been documented, although attempts have been made by some researchers (Yabusaki et al., 2001) to do that, kinetic models have limited applicability. However, equilibrium models are useful for identifying the *types*, if not the quantity, of precipitates; these models were used in the current project to understand the kinds of precipitation reactions occurring in the iron and provide some indication of what to look for when analyzing the iron cores.

Given the limitations of the indicative tools described above, there was a need for *direct* empirical evidence of any decline in reactivity of the iron due to exposure to groundwater. Therefore, in the current project, accelerated column tests were conducted to simulate the field performance of PRBs at former NAS Moffett Field and former Lowry AFB. The objective of the accelerated column tests was to examine if and to what extent the reaction rates (or half lives) of the contaminants would deteriorate when the iron was exposed to many pore volumes (i.e., long periods) of contaminated groundwater flow. Unlike tests conducted by John Hopkins University (Arnold and Roberts, 2000; Totten et al., 2001), which currently is studying the effect of individual inorganic and organic constituents in groundwater on the iron, the accelerated column tests in the current project were conducted with actual groundwater from the two sites (former NAS Moffett Field and former NAS Lowry AFB) simulated. The same iron that is in these PRBs (Peerless Metal Products, Inc., iron at for NAS Moffett Field, and Master Builder, Inc., iron at former Lowry AFB) was used to pack the two columns. A small amount of oxygen scavenger was added to the groundwater influent to the columns to restore the low dissolved oxygen (DO) levels of the native groundwater, because the groundwater is relatively anaerobic at both sites. Therefore, the interplay of factors occurring in the two field PRBs were simulated as closely as possible.

Higher groundwater flowrates were maintained in the columns than were present in the field PRBs, in order to accelerate the exposure of the iron to the groundwater. Previous studies (O'Hannesin, 1993) have shown that contaminant half-lives are independent of the flowrate; this was confirmed through half-life measurements conducted at different flowrates during the current project (see Appendix C). Accelerating the flow through the column permits an examination of the changes in reactivity of the iron when exposed to many pore volumes (or several years) of groundwater flow. Given the short history of field PRBs (6 years maximum), this simulation provides valuable insights into the future behavior of the iron-groundwater systems at these sites.

The accelerated column simulations do differ in some respects from the flow system in the field PRBs, and some of these differences may be advantageous or disadvantageous for the longevity prediction. For example, when a flow of 0.5 ft/day is accelerated in the column to 12 ft/day (24 times faster), it results in 24 years of simulation in 1 year of operation of the column. However, the precipitation that would normally occur in 1 inch of iron in the field may spread over 24 inches of iron in the accelerated column. Therefore, the column simulations may not lead to a conservative prediction of longevity; any losses in reactivity may be slower to develop in the column than in the field PRB. On the other hand, the eventual flowrate (12 ft/day) that the columns were stabilized at was determined by initial Eh and pH measurements and inorganic

analysis of the influent and effluent. These initial measurements were conducted at different flowrates (25 ft/day, 12 ft/day, and 6 ft/day) to ensure that the flowrate was not so fast that precipitation was mostly incomplete or so fast that colloidal precipitate particles were washed away with the flow. This initial analysis showed that 12 ft/day was an optimum flowrate where Eh and pH stabilized (at approximately –600 mV and 10.0 standard units, respectively) and most of the precipitates formed stayed in the column – this was determined by analyzing unfiltered and filtered samples of the effluent groundwater. When the flowrate was increased beyond 12 ft/day, there were more inorganic constituents in the unfiltered groundwater than in the filtered groundwater effluent, indicating that finer precipitate particles were being flushed out of the column.

Perhaps the main benefit of the accelerated column tests is that precipitation is spread over a long enough flow path through the iron, which enables the determination of a contaminant (trichloroethene [TCE]) half-life for the affected section of the iron. When the flow is slow and precipitation or other passivating reactions occur over a small portion (e.g., an inch or two) of the iron, measuring the loss of reactivity due to the precipitation becomes difficult. Despite such limitations in translating the rate of passivation in the columns to the rate of passivation in the field PRB, accelerated column tests were considered to be the only way of obtaining a direct determination of any future decline in reactivity of the PRB iron, something that the continued use of more conventional tools, such as groundwater monitoring, iron core analysis, and geochemical modeling, were unlikely to provide.

4.3 Sampling and Analysis Procedures

The sampling and analysis procedures used to fulfill the strategy for longevity and hydraulic performance evaluation are described in this section.

4.3.1 Longevity Evaluation. The longevity evaluation included the following elements:

- Groundwater sampling
- Iron coring
- Silt sampling from monitoring wells
- Accelerated column tests.

4.3.1.1 Groundwater Sampling. Groundwater samples were collected from selected monitoring wells at each of the PRB sites using classic sampling techniques. Teflon™ tubing (¼-inch diameter) was used to collect the groundwater samples by inserting the tubing into the monitoring well to the center of the designated screen interval. The Teflon™ tubing was then connected to a 12-inch piece of ¼-inch Viton tubing which was fed through a MasterFlex L/S peristaltic pump. Three well volumes then were purged and discharged to a waste container and the well was then sampled for volatile organic compounds (VOCs) by collecting the extracted groundwater into 40 mL volatile organic analysis (VOA) vials.

For the accelerated column tests site, groundwater from former Lowry AFB and former NAS Moffett Field was collected from two upgradient monitoring wells. The water was collected

using a peristaltic pump and contained in 2.5-gallon carboy containers. Water was collected every other month and sent to Battelle laboratories for storage. After receiving the carboy containers from the field, they were stored in a walk-in refrigerator at 4°C until they were used to fill the collapsible Teflon™ bags for use in the accelerated column tests.

4.3.1.2 Iron Core Collection at Former NAS Moffett Field. Core samples in the iron cell at former NAS Moffett Field were collected in December 1997, about 20 months after installation of the cell in April 1996. The first coring results provided an important benchmark, because chemical changes in the iron were relatively minor at that time. Core samples were taken for a second time in May 2001, five years after the pilot PRB was installed. Both vertical and angled cores were collected using a truck-mounted coring rig. A vibratory hammer was used to drive a 3-inch casing through the pavement and down to depths of up to 23 ft. Depth-discrete samples were collected at several locations within the PRB and adjacent aquifer, as show in Figures 4-1 (plan view) and 4-2 (vertical profile). Figures 4-3 and 4-4 shown photographs of the parking lot above the PRB and coring rig during the field activity. All three vertical borings samples were collected near the upgradient interface within the pea gravel section. Approximately 50 samples of iron, pea gravel, and soil were collected in six-inch stainless steel sleeves. Figure 4-5 shows pea gravel being removed from the drive casing after attempting to locate the interface between the upgradient pea gravel section and the iron. Subsequent attempts were made after repositioning the rig a few inches north (downgradient side). Figure 4-6 shows a finished core sleeve with some excess iron remaining on the core table. A field log of the core samples is contained in Appendix C.

The sample sleeves were placed in Tedlar™ bags and filled with nitrogen gas before shipping to Battelle in coolers packed with ice. After the coolers were received, the Tedlar™ bags were removed from the ice bath and were stored in a room at 4°C. Samples were prioritized and dried in batches by placing approximately twelve core sleeves in a vacuum oven. A low temperature (< 30°C) was maintained to compensate for the cooling effect of evaporation. The core sleeves were weighed periodically to determine whether the samples were dry. When drying was complete the sleeves were placed in a glove box with an inert atmosphere, where they were split and placed into glass vials for analytical procedures, which included elemental analysis by x-ray fluorescence (XRF) spectroscopy (five samples) and x-ray diffraction (XRD) (ten samples). Laboratory processing included grinding the samples to No. 325 mesh-size or smaller to improve homogeneity.

4.3.1.3 Iron Core Sampling at Former Lowry AFB. Cores were collected from the reactive cell for examination of signs of corrosion and precipitation, which were predicted by the groundwater analysis and geochemical modeling. Core samples were collected at Lowry September 16-17, 1999.

Cores were taken from a total of five locations inside the PRB with the help of a push-type rig (see Figures 4-7 and 4-8). A plan view of the coring locations in relation to the groundwater monitoring wells is shown in Figure 4-9. On this figure, the symbol ⊗ represents vertical

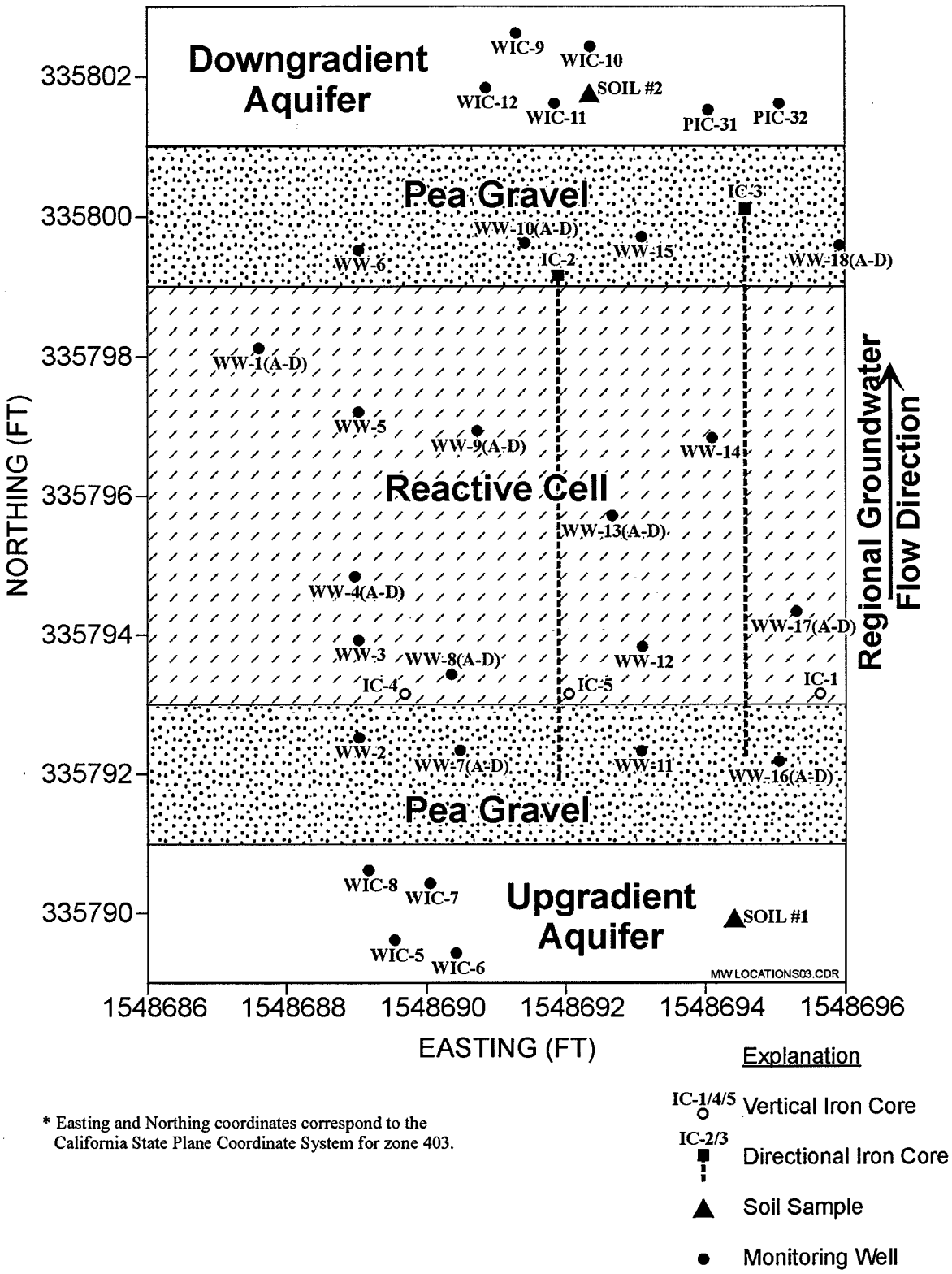

* Easting and Northing coordinates correspond to the California State Plane Coordinate System for zone 403.

Figure 4-1. Coring Locations in Moffett Field Permeable Reactive Barrier (Plan View)

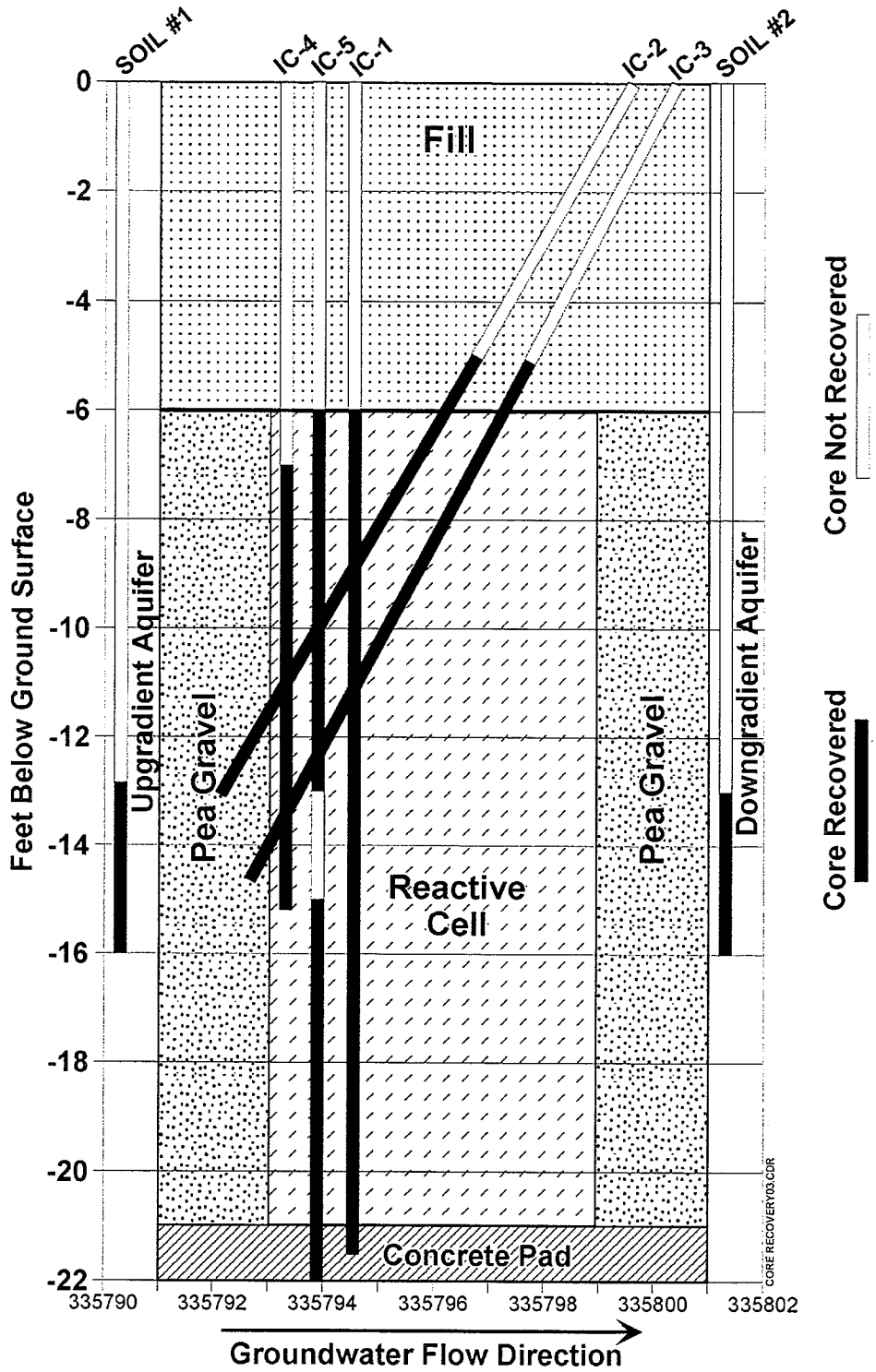

Figure 4-2. Coring Locations in Moffett Field Permeable Reactive Barrier (Vertical Profile). Note that IC-1, -4, and –5 were all cored at approximately 335793.2 ft.; the offset is not to scale.

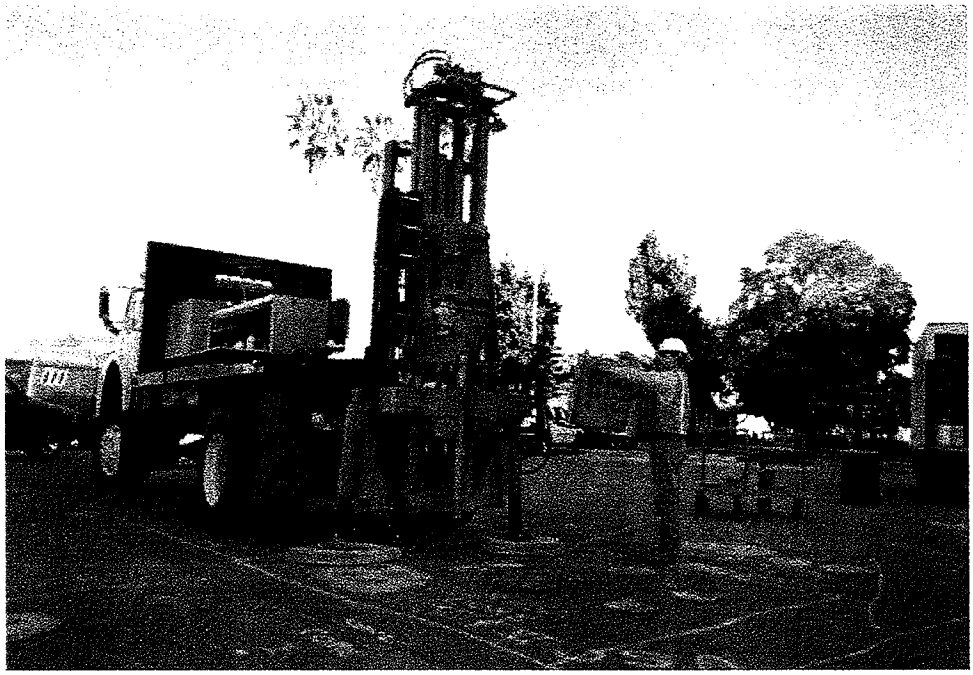

Figure 4-3. Rig Used to Collect Iron Core Samples from the Moffett Field PRB

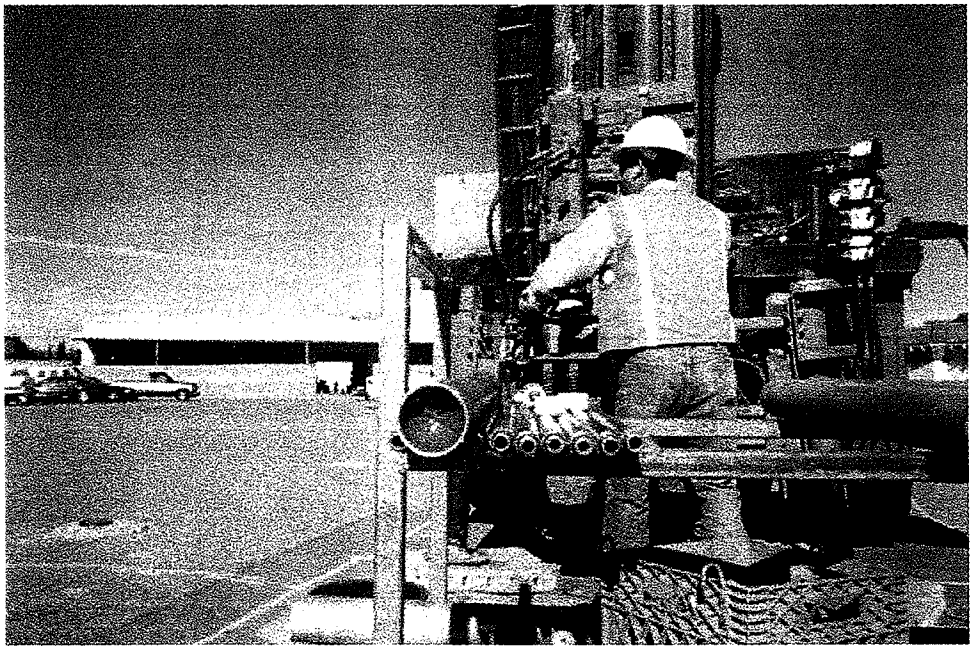

Figure 4-4. Rig Showing Sand Catcher Inside Core Barrel

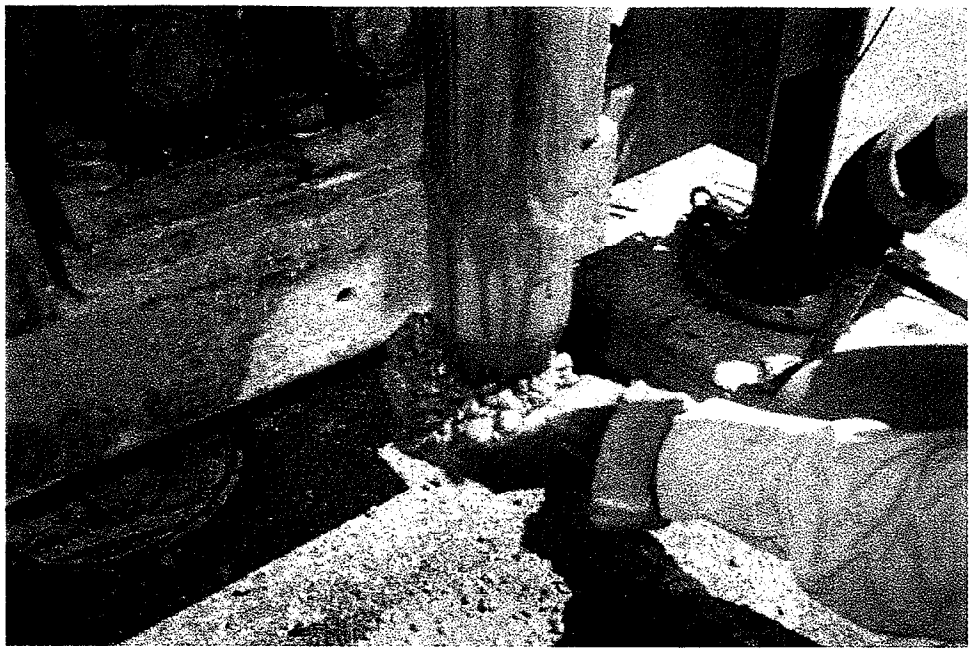

Figure 4-5. Pea Gravel Being Removed from Drive Casing

Figure 4-6. Closed Stainless Steel Sample Sleeve and Excess Iron on Core Table

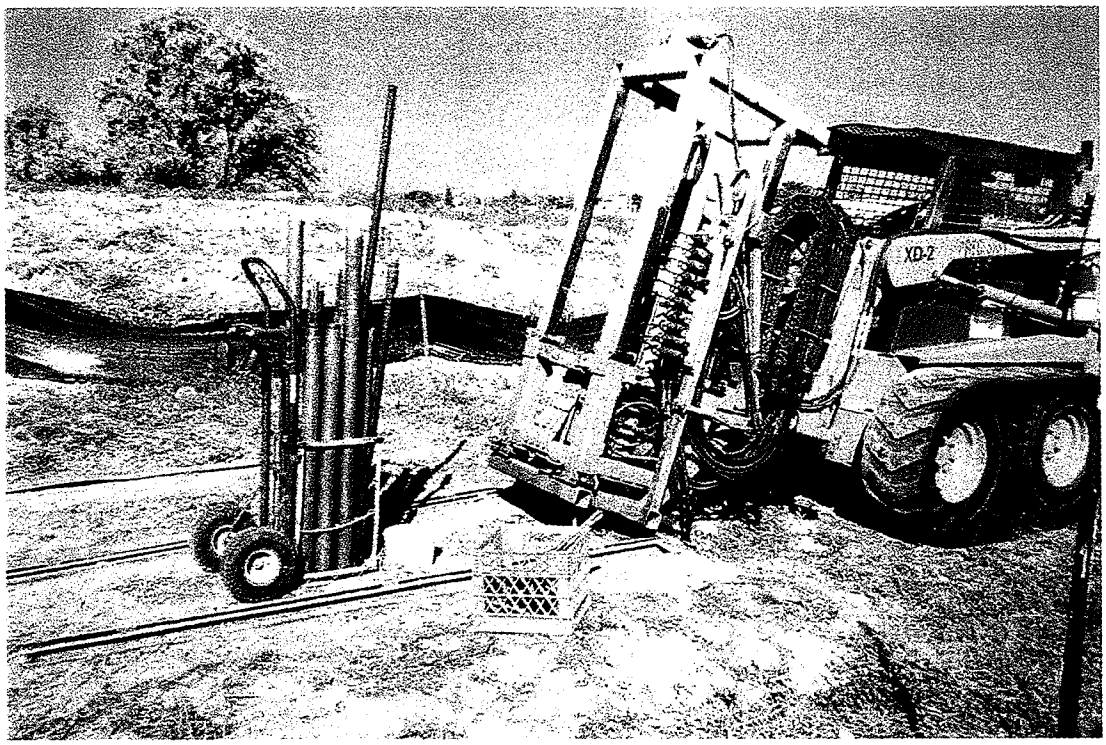

Figure 4-7. Coring Rig

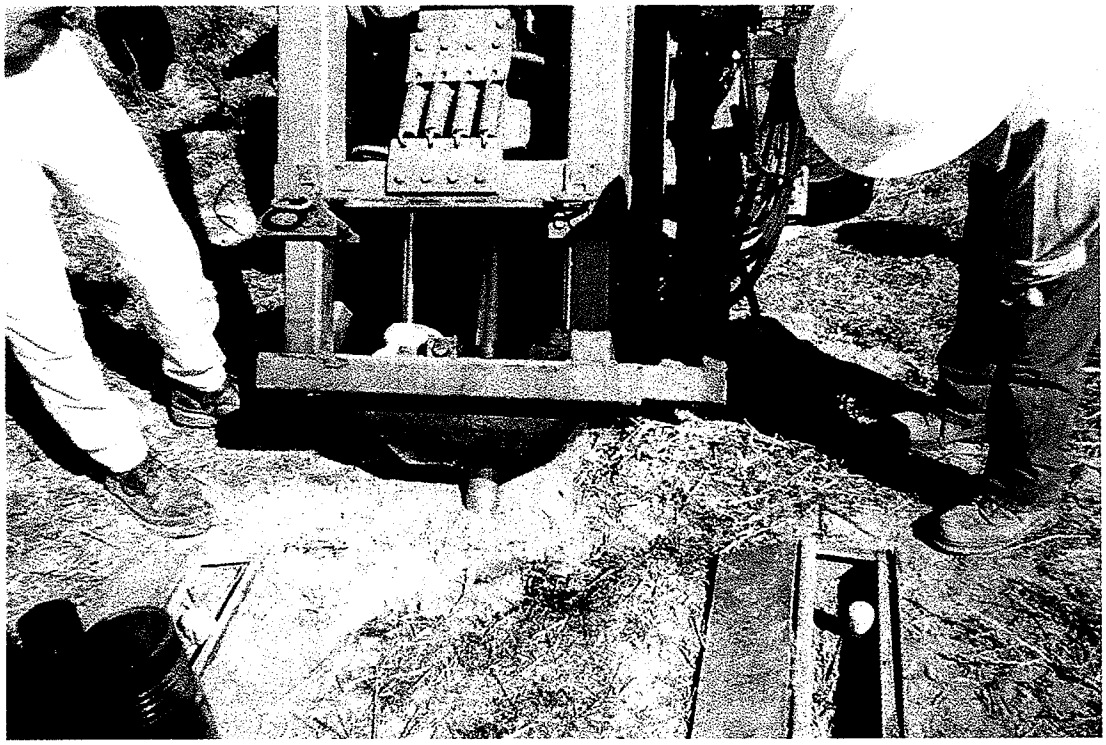

Figure 4-8. Close-Up View of Coring Rig

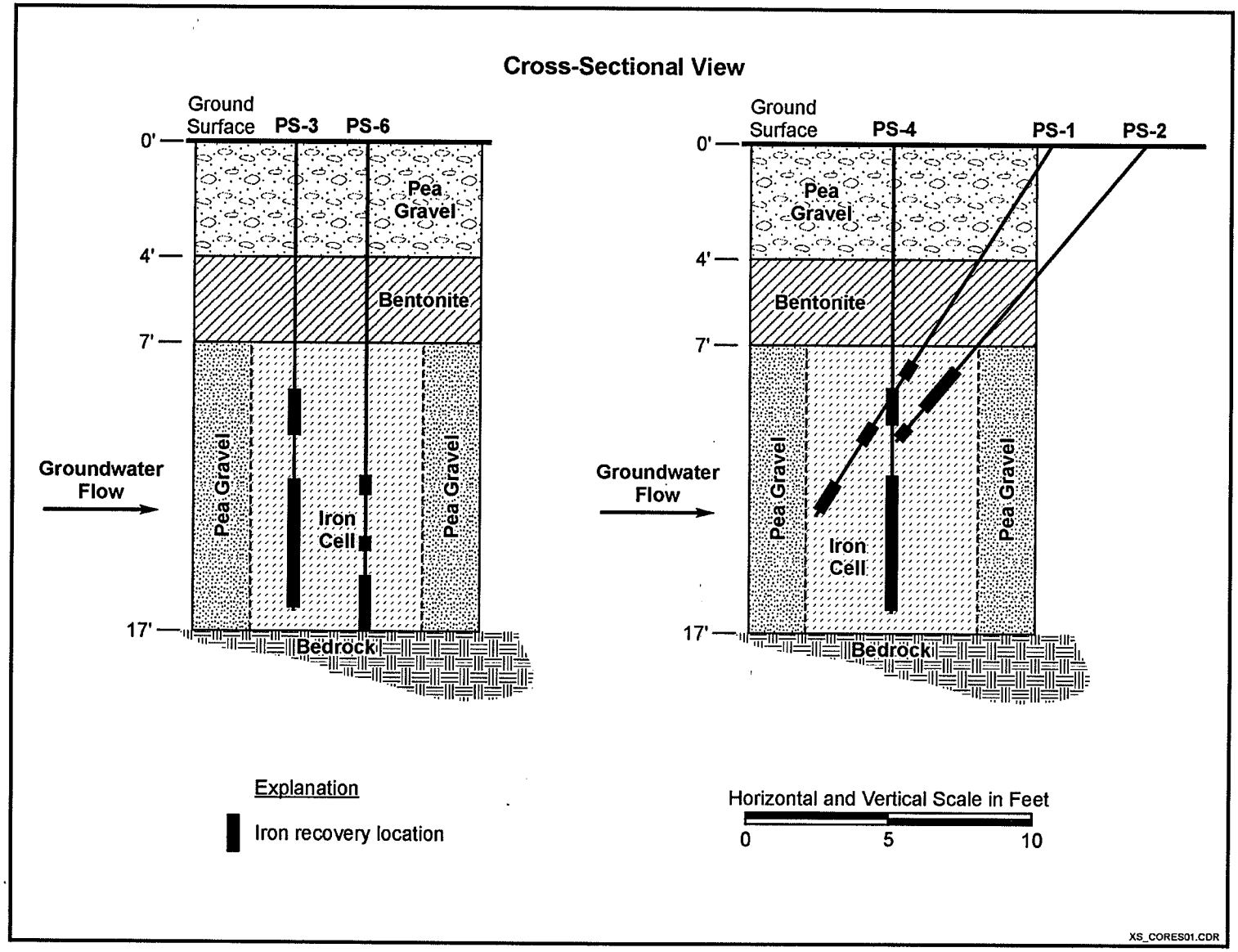

Figure 4-9. Location of Cores Collected in the PRB at Former Lowry AFB

corings and × represents angled corings. Altogether, samples were obtained from more than 40 discrete locations and depths. All of the samples that were collected and the approximate amount of recovery for each sample have been compiled into a table in Appendix C. Three of the corings were vertical and two were angled at approximately 25° off normal (see Figure 4-9, on which the thicker lines indicate depth intervals where samples were recovered). Figure 4-9 also shows vertical profiles of the PRB along the northing coordinate, which coincides approximately with the regional groundwater flow direction.

Typically, less than a full 18-inch-long section of core was recovered during each advancement of the sampler. In some cases, no sample could be recovered either because the coarseness of the medium (especially pea gravel) obstructed the opening of the core barrel or because the sample could not be retained in the sleeve by the sand catcher. The particle-size distribution of the iron is quite broad and this may have contributed to the difficulty in recovering a sample. The minimum depth that samples were collected was approximately 9 ft bgs, which corresponds with the upper level of the iron. Directly above the iron zone is a pea gravel zone; above this zone lies native soil. At the base of the PRB (approximately 17 ft bgs) is bedrock.

Coring locations were chosen to provide specimens over nearly the full extent of the PRB. Two vertical cores were taken on the western side of the reactive cell, because this side was not sampled during the previous coring event. Angled corings were taken to expose greater surface area and to cut across the interface of the iron and pea gravel. This sampling strategy was expected to yield representative cores within the treatment zone.

Precision Sampling uses the Enviro-Core® dual-tube sampling system to collect continuous and discrete-depth soil cores. The coring system consists of a small-diameter drive casing and an inner sample barrel that are simultaneously vibrated into the ground. Soil cores were collected in stainless steel liners inside the sample barrel. After being advanced 1½ ft, the full sample barrel was retrieved, and the drive casing was left in place to prevent the probe hole from collapsing. The drive casing ensures that subsequent samples are collected from the targeted interval, rather than from potentially contaminated slough located higher up in the probe hole. The sampling system was mounted on an XD series all-terrain rig with a skid loader. After the sleeves were removed from the sample barrel, the ends were covered with polyethylene caps. Plastic tape was wrapped around the ends of the sleeves to prevent the caps from leaking or becoming loose. The core sleeves then were placed into Tedlar™ bags that contained packets of oxygen scavenging material, as shown in Figure 4-10. The bags were purged with nitrogen gas and refrigerated until they were shipped to the analytical laboratories.

4.3.1.4 Iron Core Processing. Core samples were refrigerated immediately after they were collected in the field, and shipped on blue ice to a Battelle laboratory. Samples for microbiological analysis were later shipped in an airtight container to the designated laboratory. Samples for inorganic analysis were transferred to a vacuum desiccator. Vacuum drying was performed at near-room temperature. The core samples were then placed in a glove box, where they were subdivided for chemical and spectroscopic analysis.

Figure 4-10. Preservation of Core Samples in the Field

4.3.1.5 ***Iron Core Analysis Methods.*** Selected samples (Table 4-1) were analyzed by Battelle and its subcontracted laboratories using the methods shown in Table 4-2.

Samples for Raman spectroscopy were sent to Miami University (Oxford, Ohio), Molecular Microspectroscopy Laboratory for analysis. Confocal Raman spectra were collected with a Renishaw System 2000 Raman Imaging Microscope. This system employs a 25 milliwatt HeNe laser and Peltier cooled charge coupled device (CCD) detector for excitation and detection of Raman scattered light, respectively. The system features fast full range scanning (100 to 4,000 wavenumbers) and direct two-dimensional (2-D) Raman imaging. Spatial resolutions of 1 micrometer and axial resolution of 2 micrometers can be achieved with the use of the confocal feature.

Samples for scanning electron microscopy (SEM) were sent to the Battelle Microscopy Center. A JEOL 840 SEM was used to collect images. The SEM has resolutions of approximately 6 nm and magnifications ranging from 10 to 300,000X. A variety of imaging modes are possible for examination of metallic and nonmetallic samples, including secondary electron- and back-scattered electron imaging. An x-ray energy dispersive spectrometer (EDS) permits qualitative analysis of chosen areas for elements with atomic weight equal to or greater than that of sodium. The SEM 840 is interfaced with a Tracor Northern computer for automatic stage movements and data collection.

Table 4-1. Selected Core Samples for Solid Phase Characterization

Sample ID	Depth (ft bgs)	Sample ID	Depth (ft bgs)
PS-1	15.0-16.0	PS-5	10.5-13.0
PS-1	9.0-10.0	PS-5	14.5-15.0
PS-1	12.0-12.5	PS-6	11.0-12.0
PS-2	12.0-13.0	PS-6	13.5-14.0
PS-2	13.0-13.5	PS-6	15.0-17.0
PS-3	8.5-10.0	USO-1	11.5-13.0
PS-3	11.5-12.0	USO-1	13.0-16.0
PS-3	13.0-14.0	DSO-1	11.5-13.0
PS-3	14.0-16.0	DSO-1	13.5-16.0
PS-4	12.0-15.0		

Notes: PS samples were collected within the iron cell; USO samples were collected in soil zone upgradient of the barrier; and DSO samples were collected in soil zone downgradient of the barrier.

Table 4-2. Characterization Techniques for Core Samples

Analysis Method	Description
Carbon Analysis	Inorganic (carbonate) and organic carbon are converted to CO_2 following combustion of solid sample in furnace above 900°C. Evolved CO_2 is measured in a coulometric cell.
Raman Spectroscopy	Semiquantitative characterization of amorphous and crystalline phases. Suitable for identifying iron oxides and hydroxides.
Fourier Transform Infrared (FTIR) Spectroscopy	Attenuated total reflectance (ATR) cell is used to qualitatively measure absorbed silica, iron oxides, and carbonates.
Scanning Electron Microscopy (SEM)	High-resolution visual and elemental characterization of amorphous and crystalline phases. Useful for identifying morphology and composition of precipitates and corrosion materials. The SEM is also equipped for energy dispersive x-ray spectroscopy (EDS)
X-Ray Diffraction (XRD)	Qualitative determination of crystalline phases. Suitable for identifying carbonates, magnetite, goethite, etc.
Microbiological Analysis	Identification of microbial population within the cored material. Relates to presence or absence of iron oxidizing or sulfate reducing bacteria. Isolation streak and PLFA tests are performed.

Samples for x-ray diffraction (XRD) were sent to the Battelle Microscopy Center. The center's XRD capabilities include preparation of samples, automatic, unattended acquisition of data, and computer-aided interpretation of results. A pretreatment step was performed to concentrate the corrosion compounds so that that they would not be masked by the metallic iron peaks. To separate corrosion coatings from the bulk material, the iron filings were placed in a fine sieve and vibrated until a sufficient quantity of corrosion coatings were collected. A fully automated Rigaku diffractometer was used to analyze the samples.

Some iron and soil samples were sent to Microbial Insights, Inc., for microbiological analysis. These samples were removed from the core sections before vacuum drying, as required by the procedure. The samples were analyzed for heterotrophic plate counts and phospholipid fatty acid (PLFA) of microbial strains.

4.3.1.6 Silt Sampling from Monitoring Wells. Fine-grained material that collected in the silt traps at the base of the monitoring wells was sampled to determine if it was enriched in precipitates that settled out of the water column. Information about these solids may help explain the apparent discrepancy between the predicted amount of precipitates, based on groundwater analysis, and the relatively lesser amount observed by analysis of the previous core samples. The silt traps were routinely cleaned after the barrier was installed while quarterly sampling was taking place. Therefore, it was expected that silt present in the traps would have accumulated over at least two years.

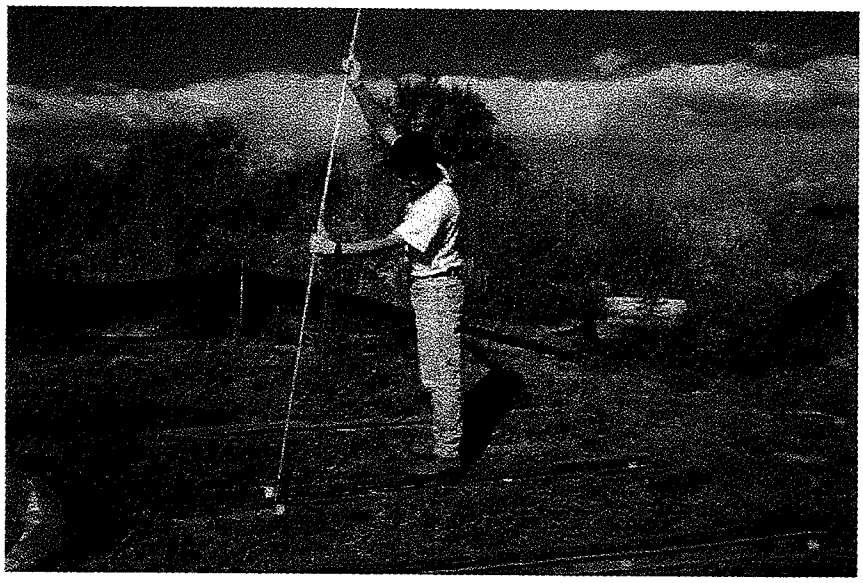

Figure 4-11. Collecting Deposits from Silt Traps in Monitoring Wells

The sediment was collected using a wireline piston core barrel (Figures 4-11 and 4-12). The device was constructed similar to a sampler described by Zapico et al. (1987). It was evident from inserting the corer that the silt traps did not contain a large amount of sediment, and some traps contained none at all. A portion of the silt was digested in concentrated nitric acid, then the solution was analyzed by inductively-coupled plasma/mass spectroscopy (ICP/MS). Some silt was reserved for other types of analyses such as XRD and SEM, to determine mineral and elemental make-up, and total carbonate analysis. Carbonate content was determined by decomposing the sample in a furnace at 950°C and analyzing evolved CO_2 in a coulometric cell.

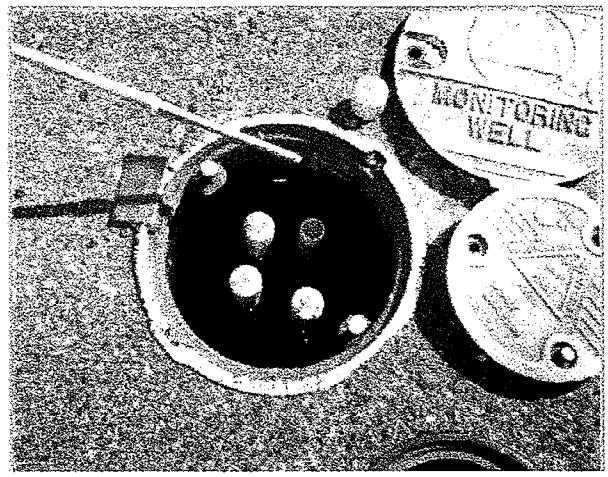

Figure 4-12. Photograph of Silt Sampler Ready to be Lowered Into a Monitoring Well

4.3.1.7 Accelerated Column Test

Setup and Sampling. The accelerated column test setup and sampling was performed to determine long-term effects on the permeable reactive media contained in the former Lowry AFB and former NAS Moffett Field PRBs. Each column was constructed of glass 36 inches in length and 1½-inches in diameter. The columns were constructed with four sampling ports located at 6 inches, 12 inches, 18 inches, and 24 inches from the bottom to top of the column. The sampling ports were fitted with ¼-inch stainless steel fittings. Inlet and effluent sampling ports were also placed on the inlet and outlet tubing to collect samples before and after the PRB material. The columns were sampled using a 22 gauge, 6-inch-long stainless steel needle inserted into each sampling port. The samples were drawn using a 40 mL glass syringe. The sample then was ejected into the appropriate container and subsequently sent to the off-site analytical laboratory. Samples were collected for VOC and inorganics analyses. Pressure gauges also were used to measure changes in inlet head pressure to the columns. A 3½-inch, 0-30 psi stainless steel gauge was used to record the inlet pressure to each of the accelerated column test setups.

Battelle began running additional long-term column tests in March 2000. These tests were configured in a way to simulate two sites under accelerated flow conditions. A diagram of the column test configuration is shown in Figure 4-13. Two identical multiple port glass columns (3 ft long, 1½ inches in diameter) were packed with iron. Sampling ports were located along the length of the columns at six-inch intervals. The effluent was equivalent to the final sampling port. Water samples were collected from the column locations shown in Table 4-3.

One column was filled with iron produced by Peerless Metal Powders and Abrasives (Detroit, MI) to simulate the former NAS Moffett Field barrier, and the other was filled with Master Builder iron to simulate the former Lowry AFB barrier. Iron filings were placed in the column

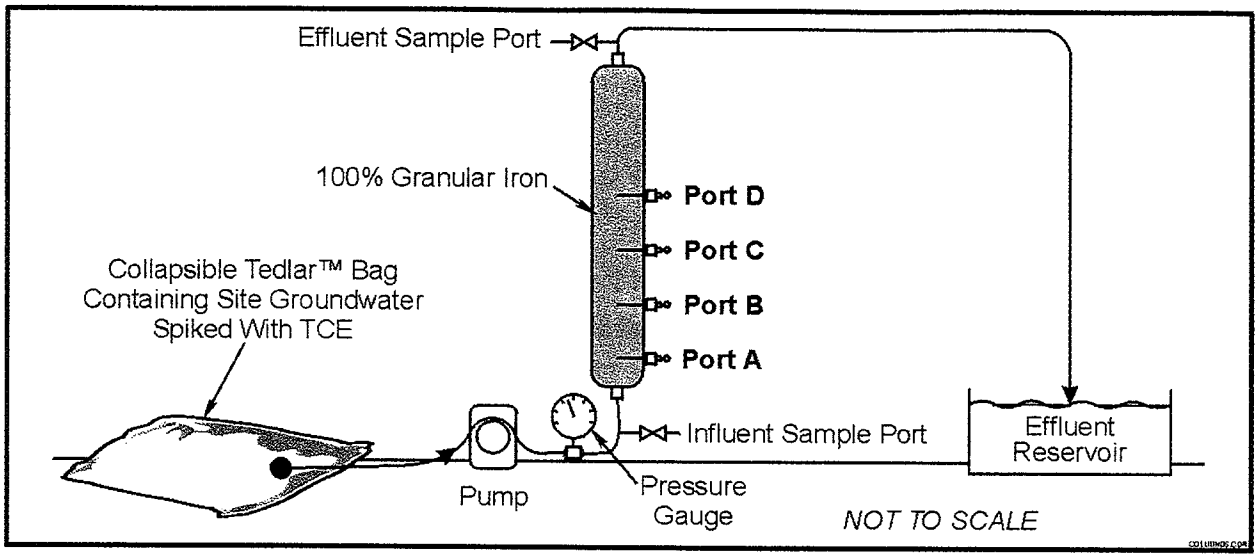

Figure 4-13. Schematic of Accelerated Column Test Setup

Table 4-3. Locations of Sampling Points in the Column Tests

Sampling Point	Distance from Inlet (inches)	Distance from Inlet (centimeters)
Influent	0	0
Port A	6	15.2
Port B	12	30.5
Port C	18	45.7
Port D	24	61.0
Effluent	36	91.4

in several lifts. After each lift, water was carefully added to fill the pore space with minimal entrainment of air bubbles. This process was repeated until the columns were filled. Average porosities were calculated based on the mass and volume of iron added to each column and the density of the iron. These data were used to calculate desired flowrates and pore volume exchanges.

Groundwater from the former NAS Moffett Field and former Lowry AFB sites were collected monthly to operate the columns. The groundwater was collected in carboys from wells in the vicinity of each of the PRBs and then shipped by overnight carrier to Battelle. The water was pumped into Tedlar™ bags to maintain the compositions as close as possible to their natural states. However, some air exchange did occur, either during shipment or in transferring to the Tedlar™ bags, causing a slight increase in DO. The aquifers at former NAS Moffett Field and

former Lowry AFB are normally anoxic (DO <0.5 mg/L), but values as high as 2 mg/L were measured after the water had been transferred to the Tedlar™ bags. To reduce the DO levels, a small amount of sodium sulfite was added to the water to react with the amount of DO measured in each bag. Sulfite reacts rapidly with molecular oxygen and is converted to sulfate. This resulted in restoring DO levels close to the native conditions before the water was pumped through the columns. The resulting minor increase in sulfate was minimal compared to the high native sulfate levels in the groundwater from both sites.

Batches of groundwater were spiked with TCE to achieve a relatively consistent concentration of contaminant throughout the study. Approximately 40 pore volumes of TCE-spiked groundwater were flowed through each of the columns before samples were taken. This approach afforded a conditioning period when sorptive sites on the iron could become saturated and flow patterns would become stabilized.

A peristaltic pump (Masterflex L/S) was used to transfer water through 0.125-inch Viton® tubing from the Tedlar bags to the base of the columns. The columns were oriented vertically so that water entered at the bottom and exited through the top. Tubing carried the effluent water to a drum for treatment and disposal. Figure 4-14 is a photograph of the laboratory setup. Periodically, the flowrate was recalibrated by measuring the volumetric flow of the effluent. Pressure gauges (WIKA, stainless steel, 0-30 psi range) were positioned at the water inlets to record water pressure throughout the duration of the study. An increase in pressure (at constant flowrate) would indicate decreased permeability caused by possible accumulation of inorganic precipitates in the iron porespace.

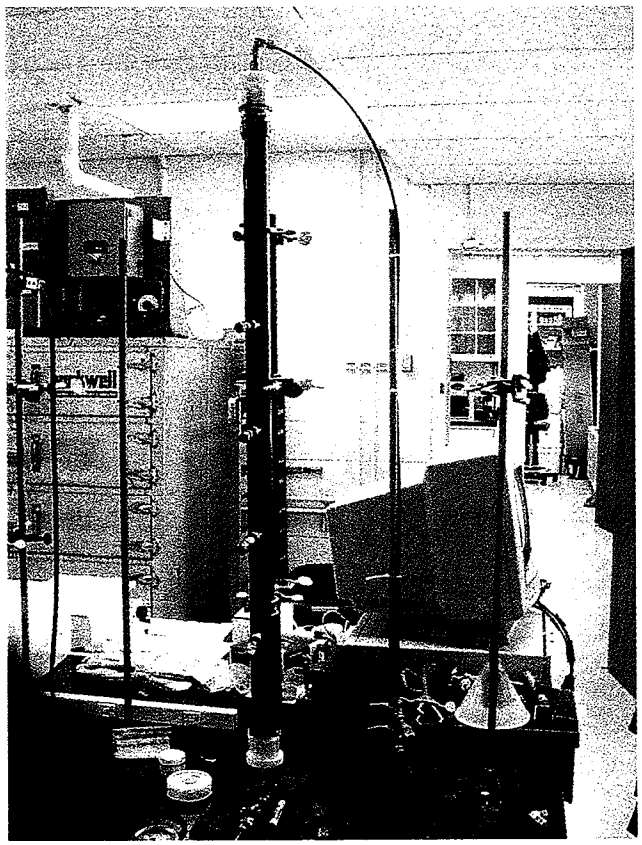

Figure 4-14. Picture of Accelerated Column Tests

Water in the columns was sampled monthly and analyzed for pH, oxidation-reduction potential (ORP), and TCE. Inorganic parameters were analyzed less frequently and typically at inlet and outlet points only. Samples for pH, ORP, and TCE were taken by withdrawing small volumes of water using a glass syringe fitted with a stainless steel needle. A 22 gauge, 6-inch-long stainless steel needle was attached to the syringe so that water could be removed from the center of the column which would be representative of the bulk flow. This technique helped avoid water from along the column wall which might be flowing at a lower rate than average.

Initially, the water flowrate in the "Moffett Field" column was adjusted so that pH would plateau by the last sampling port (Port D) in the column. Flowrates up to 30 ft/day were initially tested, but at such high flows, the pH was found to change between the final sampling port and the effluent from the column. A flowrate of 25 ft/day initially was found to be satisfactory for the Moffett Field simulation, which represents an increase of approximately 50 times the natural flowrate. After about 50 pore volumes at 25 ft/day, the pH and ORP measurements appeared to plateau at the effluent end of the column. However, subsequent pH and ORP measurements showed that, at 283 pore volumes, pH continued to rise between the last port (Port D) and the effluent (E). At that point, the capability of the column to generate and retain most of the precipitates that could be formed was studied by reducing the flowrate to 12.5 ft/day and 6 ft/day (see Section 5.3.1)

A flowrate of 12.5 ft/day was found to provide a more stable pH (compared to 25 ft/day). Also, at 12.5 ft/day analysis of filtered and unfiltered groundwater samples from the column effluent showed that much of the precipitate formed was being retained in the column, whereas at 25 ft/day, noticeable amounts of precipitate was being washed out of the column with the flow. The main difference between 12.5 ft/day and 6 ft/day was that, at the slower flowrate, magnesium also was precipitating in the column. In the interests of project time, the 12.5 ft/day flowrate was deemed as optimum and the rest of the test was run at 12.5 ft/day. A summary of column settings used in the accelerated test is given in Table 4-4.

Table 4-4. Summary of Groundwater Flowrates used in Moffett Field Column Test

Date of Adjustment	Linear Flowrate (ft/day)	Volumetric Flowrate (mL/min)	Cumulative Pore Volumes
06/14/2000	25	3.8	15
06/20/2000	25	3.8	58
06/23/2000	25	3.8	84
06/30/2000	25	3.8	134
07/06/2000	25	3.8	153
07/13/2000	25	3.8	203
07/20/2000	25	3.8	249
07/28/2000	25	3.8	283
08/072000	12.5	1.9	317
08/12/2000	6	0.92	327
09/07/2000	12.5	1.9	408
10/10/2000	12.5	1.9	499
11/16/2000	12.5	1.9	592
12/19/2000	12.5	1.9	739
01/24/2001	12.5	1.9	816
02/12/2001	12.5	1.9	923
04/12/2001	12.5	1.9	1,047
05/07/2001	12.5	1.9	1,103
06/27/2001	12.5	1.9	1,310

As with the Moffett Field column, the water flowrate in the "Lowry" column was adjusted so that pH would become stabilized by the final sampling port. Flowrates up to 30 ft/day were tested, but at such high flows, the pH was found to change between Port D and the outlet. A flowrate of 25 ft/day initially was found to be satisfactory for the Lowry simulation. Flowrates of 12.5 and 6 ft/day also were used to determine if flowrate had a bearing on the column test measurements (see Section 5.3.2). A summary of settings for the Lowry column test is given in Table 4-5.

Table 4-5. Summary of Groundwater Flow Rates used in Lowry Column Test

Date of Adjustment	Linear Flowrate (ft/day)	Volumetric Flowrate (mL/min)	Cumulative Pore Volumes
06/12/2000	25	3.95	15
06/15/2000	25	3.95	35
06/20/2000	25	3.95	55
06/23/2000	25	3.95	84
06/30/2000	25	3.95	137
07/06/2000	25	3.95	155
07/13/2000	25	3.95	196
07/20/2000	25	3.95	252
07/28/2000	25	3.95	292
08/07/2000	12.5	1.97	324
08/12/2000	6	0.95	334
09/07/2000	12.5	1.97	412
10/10/2000	12.5	1.97	505
11/16/2000	12.5	1.97	612
12/19/2000	12.5	1.97	744
01/24/2001	12.5	1.97	844
02/12/2001	12.5	1.97	937
04/12/2001	12.5	1.97	1,057
05/07/2001	12.5	1.97	1,113
06/27/2001	12.5	1.97	1,316

4.3.2 Hydraulic Performance Evaluation. The hydraulic performance evaluation included the following elements:

- Water-level measurements
- Slug tests
- In-situ flow sensors
- Colloidal borescope.

4.3.2.1 ***Water-Level Measurements.*** Groundwater flow directions were determined by measuring water levels in the individual monitoring wells at each site. Numerous water-level surveys were conducted in the field. The water-level surveys were done utilizing a water-level indicator probe. The probe was washed and decontaminated prior to each measurement in each individual well, and then was inserted into the monitoring well and field staff waited for the alarm signal to sound when the groundwater was encountered. The depth to water measurement was recorded from reading the markings on the probe cable. Each of the monitoring wells was surveyed to obtain the relative elevation of the location of each monitoring well. The data then were entered into a computer program to generate groundwater flow gradients.

4.3.2.2 ***Slug Tests.*** The slug test sampling procedure consisted of placing a pressure transducer to a depth of more than 5 ft below the measured water level within the test well. After the transducer was in position and its depth was recorded, a 1.5-inch-diameter by 5-ft-long solid polyvinyl chloride (PVC) slug was inserted into the monitoring well. After the water level reached an equilibrium, the slug was rapidly removed from the well and slug test was started using software manufactured by WinSitu, Inc. The removal of the slug created approximately 1.6 ft of change in water level within each test well. Water-level recovery then was monitored for approximately 10 minutes using the TROLL pressure transducer/data logger. The data were downloaded to a notebook computer using the WinSitu software. Replicate tests were performed for each well.

The recovery rates of the water levels were analyzed with the Bouwer (1989) and Bouwer and Rice (1976) methods for slug tests in unconfined aquifers. Graphs were made showing the changes in water level versus time and curve fitted on a semi-logarithmic graph. The slope of the fitted line then was used in conjunction with the well parameters to provide a value of the permeability of the materials surrounding the test well.

4.3.2.3 ***In-Situ Flow Sensors.*** The in situ groundwater velocity sensor from HydroTechnics™ (see Figure 4-15) uses a thermal perturbation technique to directly measure the three-dimensional (3-D) groundwater flow velocity vector in unconsolidated, saturated, porous media. The technology allows for long-term, continuous monitoring of the groundwater flow in the immediate vicinity of the down-hole probe. The probes and associated data acquisition system were obtained from Hydrotechnics, Inc.

The instrument consists of a cylindrical heater that is 30 inches long by 2.37 inches in diameter. The instrument has an array of 30 calibrated temperature sensors on its surface. The probe was installed directly in contact with the aquifer media at each site at the depth of interest. A data transmission lead wire connected the probe to the ground surface. The heater was activated by supplying 70 watts of power that heated the sediment and groundwater surrounding the probe to approximately 20 to 30°C above background temperatures. The temperature distribution from the ground surface to the probe was affected by the groundwater movement resulting from the advective flow of the heated groundwater. The measured temperature distribution was then converted into flow velocity (3-D in magnitude and direction) by a computer program. The

Figure 4-15. HydroTechnics™ Flow Sensor

technology specifications of the down-hole probe indicate that the Darcy velocity range of 0.01 to 1.0 ft/day could be measured to a resolution of 0.001 ft/day and an accuracy of 0.01 ft/day. The life span of the down-hole probes is typically 1 to 2 years.

4.3.2.4 ***Colloidal Borescope.*** The colloidal borescope (see Figure 4-16) was used during the field activities to provide direct visual means for observing colloids in the monitoring wells. Colloidal size, density, and flow patterns were assessed, and an evaluation of the sampling effects on the natural groundwater flow system were made. The colloidal borescope also was used to determine flow velocity and direction in monitoring wells by the direct observation of colloidal particle movement.

The colloidal borescope consists of a CCD camera, optical magnification lens, an illumination source, and stainless steel housing. The device is approximately 60 cm long and has a diameter of less than 5 cm. These dimensions allowed the borescope to be utilized in 2-inch-diameter monitoring wells, which are prevalent at the test sites investigated. The electronic image from the borescope could be seen at the surface on a monitor and was recorded on a VHS tape. The magnified image corresponds to a field view of approximately 1.0 mm by 1.4 mm by 0.1 mm. The colloidal borescope was inserted into each test well by a set of rigid quick-connect tubes. These tubes maintained the alignment of the borescope in the well so that the flow directions could be determined. The flow velocity and direction then were measured after a waiting period (usually 10 minutes) during which the flow changes from the turbulent (due to the probe insertion) to laminar (due to the natural groundwater flow) flow.

4.4 Characterization Tools Considered but Not Used

Some characterization tools were seriously considered for this project but not used. However, these tools could be useful for future investigations, so a brief summary of these tools is presented here.

Figure 4-16. Colloidal Borescope Used at Former Lowry AFB

4.4.1 Down-Hole Velocity Probes (Heat Sensors). The flowmeter used in this investigation was the Model 40L Geoflo Groundwater Flowmeter System manufactured by KVA Analytical Systems (Falmouth, MA). The system is a portable self-contained instrument consisting of: a 2-inch-diameter flowmeter probe and associated packer assembly attached to 80 feet of electronic cable, aluminum suspension rods, and a control unit with battery packs. The submersible probe consists of a central heating element surrounded by four pairs of opposed thermistors. The heating element and thermistors are contained within a packer assembly that is filled with 2-mm-diameter glass beads. The measurement of groundwater velocity and direction by the flowmeter is based on initiating a short-term heat pulse at the center of the probe. The distribution of the resulting heat in the glass beads is measured by the thermistors and the relative difference between opposed thermistors is displayed. The values read from the display are resolved into the rate and direction of flow in the well through a process of vector resolution and then computation with a flow velocity calibration equation. The quality of the tests can be evaluated by use of cosine test as described in the user's manual. Hand calculations and graphical methods for vector resolution provided by the manufacturer are cumbersome. Therefore, a customized spreadsheet program using Microsoft® Excel was setup to perform vector resolution, velocity calculation, and cosine test for the permeable barrier site.

Calibration of the flowmeter instrument is required to ensure accurate results. Factors potentially affecting the instrument response include aquifer matrix type, well screen type and orientation, type and amount of the fill in the annular space of the well, adherence of uniform and horizontal groundwater flow through the well screen, and operator techniques. The flowmeter used during a previous study at former NAS Moffett Field was rented from the manufacturer (Battelle, 1998). It was calibrated by the manufacturer based on the information on site-specific conditions prior to shipping. The calibration is based on measuring the instrument response in a laboratory tank with flow velocity, probe screen, and glass beads similar to that expected at the site. The flow velocity calculated for several flowrates in the tank is plotted against the instrument reading and the slope of the resulting calibration curve is used to calculate field velocity in the wells. Thus, a site-specific calibration equation is obtained for each site.

4.4.2 Diffusion Samplers. Although diffusion samplers (see Figure 4-17) were not used in conjunction with this project, they can be used at PRB sites for gathering VOC samples from monitoring wells, in the long term. The diffusion sampling technique relies on natural molecular diffusion to cause the molecules from volatile organic compounds to pass from the groundwater through a semi-permeable 42-mm-diameter sampler that is prefilled with deionized water. After sufficient time has elapsed the concentrations in the sampler approximate those in the well. The field technician then simply removes one sampler and replaces it with another for the next quarter or round of sampling. No bailing or purging is required when using diffusion samplers, minimizing on site time.

The diffusion sampling method produces significant cost savings over traditional sampling methods by eliminating field time for well purging, equipment decontamination/ maintenance, and purge water disposal.

Diffusion samplers typically are placed within the screened interval of a well where groundwater flow is known to occur. Wells with long screened intervals or bedrock wells that intersect known fractures can utilize samplers connected in series to monitor more than one interval or fracture set. Stainless steel weights are used to position the samplers at the required depths. Locking caps with a bottom fastener are used to secure the suspension cord at the wellhead.

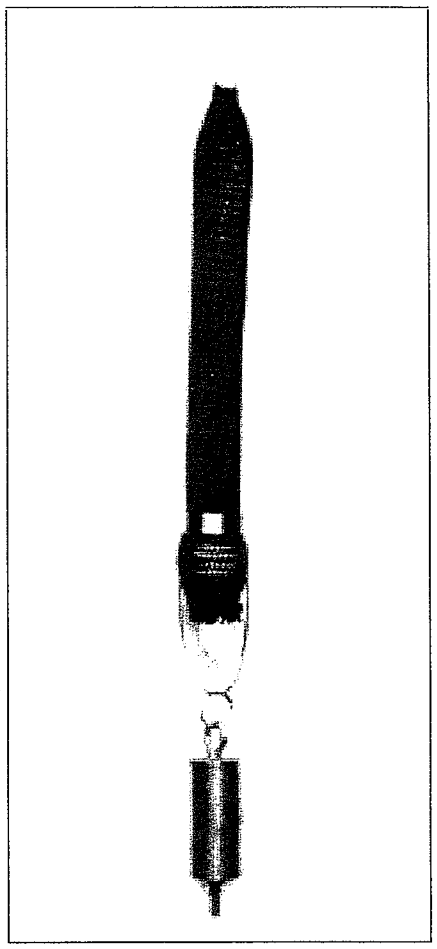

Figure 4-17. Diffusion Sampler

5.0 Performance Assessment for Longevity of PRBs

The longevity evaluation in this project focused on three lines of investigation:

- Field investigations of geochemical changes occurring in PRBs installed at least a year or more ago at DoD sites. The tools used for the field investigation included collection and analysis of:

  - Groundwater from monitoring wells in the PRB and surrounding aquifer.
  - Cores of the PRB medium (iron)
  - Silt from the silt traps at the bottom of monitoring wells in PRBs

- Long-term accelerated column tests that simulated approximately 30 years of groundwater flow through PRBs at former NAS Moffett Field and former Lowry AFB. The same iron and groundwater involved in the field PRBs were used in these tests to obtain some indication of how much groundwater flow would have to occur before the reactivity of the iron is significantly affected.

- Geochemical modeling with computerized codes to evaluate the types of precipitates expected and compare them to the field results.

5.1 Field Evaluation of Longevity at Former NAS Moffett Field

The longevity evaluation at former NAS Moffett Field included:

- Groundwater sampling and analysis for organics and inorganics
- Iron coring and analysis
- Silt sampling and analysis
- Microbiological analysis of iron cores and aquifer samples.

5.1.1 Groundwater Sampling at Moffett Field. Following installation of the Moffett Field barrier in April 1996, groundwater inside the barrier and vicinity was monitored for six consecutive quarters. Results of each quarterly monitoring event were reported at the conclusion of the previous performance evaluation (Battelle, 1998). In the current project, a selected number of groundwater samples were collected in May 2001 (five years after installation), to determine whether any changes in performance had occurred. In each event, samples were collected from the following PRB locations:

- Upgradient A1 and A2 aquifer zone wells
- Upgradient pea gravel wells
- Reactive cell wells
- Downgradient pea gravel wells
- Downgradient A1 and A2 aquifer zone wells.

The locations of the monitoring wells in and near the PRB at former NAS Moffett Field are shown in Figure 4-1 (in Section 4.3.1).

Historically, TCE, *cis*-DCE, and PCE are the predominant contaminants in the groundwater at the permeable barrier location. However, several other CVOCs are detectable in the A1 aquifer zone groundwater upgradient from the permeable barrier. Table 5-1 shows the average and range in concentrations of CVOCs in the groundwater entering the barrier over multiple sampling events (Battelle, 1998). These values are based on results of analyses from wells WIC-1, WIC-6, and WIC-7, which are located immediately upgradient of the barrier.

Table 5-1. Concentrations of CVOCs in the Upgradient A1 Aquifer Zone Groundwater for the Five Monitoring Events

Analyte[a]	n[b]	Average (µg/L)	Minimum (µg/L)	Maximum (µg/L)
PCE	11	16	5.9	32
TCE	16	1,360	920	2,900
cis-DCE	17	230	170	310
VC	2	<0.5	< 0.5	0.4 J
1,1-DCA	12	22	18	26
1,2-DCA	0	<0.5	<0.5	<0.5
1,1-DCE	12	31	18	58
trans-DCE	3	2	<0.5	3
Carbon Tetrachloride	0	<0.5	<0.5	<0.5
Chloroform	5	<1	<0.8	0.9
CFC-113	10	27	13	56
Methylene Chloride	0	<0.5	<0.5	<0.5
1,1,1-TCA	1	<3	<0.5	2.9

(a) Combined results for upgradient wells WIC-1, WIC-6, WIC-7, and WIC-8.
(b) Number of analyses above detection limit.
J Indicates that the value is qualitatively identified but is reported at an estimated quantity.
DCA = dichloroethane. TCA = trichloroethane.
CFC = chlorofluorocarbon. DCE = dichloroethene.

As shown in Table 5-1, TCE is the dominant contaminant entering the upgradient aquifer. The average concentration of TCE is 1,360 µg/L. The next most abundant analyte is *cis*-DCE, which has an average concentration of 230 µg/L. *cis*-DCE is a degradation product of TCE by the hydrogenolysis pathway and is indicative of possible natural attenuation of TCE and PCE in the plume. Similarly, vinyl chloride is also a degradation product of TCE by hydrogenolysis, but is mostly absent from the influent groundwater. Other CVOCs were detected, but at much lower concentrations; these include 1,1-DCA; 1,1-DCE; PCE; CFC-113; and 1,1,1-TCA.

5.1.1.1 ***TCE Degradation.*** In October 1997, when the quarterly sampling program ended, the concentration of TCE in the upgradient aquifer well WIC-1 was 2,800 µg/L, and between 1,000 and 1,600 µg/L in the upgradient pea gravel, where intense horizontal and vertical mixing occurs (Battelle, 1998). However, less than 1 ft into the reactive cell, TCE was reduced to the maximum contaminant level (MCL) value of 5 µg/L. Approximately 4 ft into the zero-valent iron zone, TCE was below detection (<0.5 µg/L). In fact, the majority of water samples collected elsewhere in the reactive cell are below the detection limit of 0.5 µg/L for TCE. In general, TCE concentrations in the downgradient pea gravel tended to fall between 1 and 10 µg/L. This result was explained by mixing of contaminated groundwater from the downgradient aquifer with treated water emerging from the reactive cell (Battelle, 1998).

Table 5-2 show the concentrations of key contaminants for selected wells at the October 1997 sampling event. These wells were sampled in May 2001 as well. These early results demonstrated that the permeable barrier is capable of reducing influent TCE concentrations to well below MCLs.

Table 5-2. Target CVOC Concentrations During Quarterly Monitoring (October, 1997)

Well ID	PCE (µg/L)	TCE (µg/L)	*cis*-DCE (µg/L)	Vinyl Chloride (µg/L)
Upgradient A1 Aquifer Well				
WIC-1	32	2,800	310	<0.5
Upgradient Pea Gravel Well				
WW-11	9	1,200	220	<0.5
Reactive Cell Wells				
WW-12	<0.5	5	110	<0.5
WW-14	<0.5	<0.5	0.6	<0.5
Downgradient Pea Gravel Well				
WW-15	<0.5	6	1	<0.5
Downgradient A1 Aquifer Wells				
WIC-3	28	2,500	290	0.9
WIC-9	13	830	82	<0.5
WIC-12	71	3,400	360	<25

Contrary to the declining trend in the downgradient pea gravel and in the immediately downgradient aquifer well cluster (WIC-9 to WIC-11), the concentration of TCE in WIC-12 (the deepest well in the cluster) was consistently higher than in the other wells (3,400 µg/L in October 1997). High concentrations of contaminants in the deepest well in the A1 aquifer may be caused either by migration of TCE in the gap underneath the PRB (the PRB was not keyed into the thin aquitard below the A1 aquifer zone for fear of breaching it) or by upward migration

of groundwater from the more contaminated A2 aquifer zone below. This is borne out by the water-level measurements, which show an upward hydraulic gradient present on the downgradient side of the barrier (Battelle, 1998). TCE concentrations were also somewhat higher in relatively more distant downgradient A1 aquifer zone wells WIC-3 and W9-35 (2,500 and 6,000 μg/L, respectively). In the A2 aquifer zone, TCE concentrations ranged from 7,100 μg/L in WIC-4 to 9,700 μg/L in W9-20, which are greater than those detected in any of the A1 aquifer zone wells.

Table 5-3 shows the concentrations of key contaminants in select wells sampled during the current project in May 2001, five years after installation. The TCE concentration in the upgradient A1 aquifer well, WIC-1, is 1,700 μg/L, which is not as high as in October 1998, but may be within the range of natural variability. Similarly, TCE concentrations decrease slightly in the upgradient pea gravel (due to mixing) and quite substantially in the reactive cell (due to contact with the iron). Also, a water sample from PIC-31, located a few feet east of WIC-11 (Figure 4-1), has very low concentration of TCE (160 μg/L). Elevated levels of TCE in the downgradient pea gravel wells in May 2001 were unexpected, as these wells remained relatively clean during the quarterly sampling program and as the wells within the reactive cell continued to show TCE levels below MCL. It is possible that contaminated water from the downgradient side has entered the pea gravel, although levels of TCE in both the downgradient *and* upgradient aquifer may have dropped slightly since the October 1997 event.

Table 5-3. Target CVOC Concentrations After Five Years of Operation (May 2001)

Well ID	PCE (μg/L)	TCE (μg/L)	*cis*-DCE (μg/L)	Vinyl Chloride (μg/L)
Upgradient A1 Aquifer Well				
WIC-1	21 J	1,700	270	<10
Upgradient Pea Gravel Well				
WW-11	13 J	960	230	<5
Reactive Cell Wells				
WW-12	<3	2.4 J	100	1.3
WW-14	<3	0.70 J	0.65 J	<1
Downgradient Pea Gravel Well				
WW-15	<3	21	3.9 J	<1
WW-15-Dup	<3	22	4.3 J	<1
Downgradient A1 Aquifer Wells				
WIC-3	<30	1,400	240	<10
WIC-9	<15	480	60	<5
WIC-12	24 J	1,500	260	<10
PIC-31	<6	160	17	<2.0

Because the reactive cell is incorporated in a sand channel with the funnel walls embedded in silty clay layers on the sides, advective flow of TCE around the PRB is expected to be minimal. Yet a clean front of treated groundwater emerging from the PRB (or at least a substantial improvement in groundwater quality) on the downgradient side is still not clearly visible. Possible reasons for the persistence in elevated levels of TCE on the downgradient side of the PRB are:

- Migration of TCE through the gap under the PRB and aquitard
- Migration of TCE from the more contaminated lower aquifer zone (A2)
- Diffusion of TCE from the surrounding clay.

A closer examination of historical trends of CVOCs and inorganic constituents in groundwater influent and effluent from the PRB shows that some dilution of these components in select wells in the aquifer is visible (see Section 5.1.1.6). These trends indicate that treated water is emerging from the PRBs, but may be mixing with the surrounding contaminated water.

5.1.1.2 cis-DCE Degradation. Based on results from the October 1997 sampling event, concentrations of *cis*-DCE were approximately 170 to 340 μg/L in the upgradient A1 aquifer zone and upgradient pea gravel wells (Battelle, 1998). The *cis*-DCE concentration was 310 in WIC-1 (see Table 5-2). In the reactive cell, *cis*-DCE concentrations declined along the flow direction. The decline was slower than the declines for TCE and PCE, as evidenced by the persistence of elevated *cis*-DCE concentrations in the reactive cell, because *cis*-DCE has a longer half-life. Also, some *cis*-DCE probably is being produced as a byproduct concurrent with TCE and PCE degradation. Therefore, *cis*-DCE persists over a longer distance in the reactive cell. The *cis*-DCE concentration declined to less than 0.5 μg/L, four feet into the reactive cell. Results were similar for the May 2001 sampling event in the current project, but there appears to be a slight reduction in *cis*-DCE overall. Results throughout the five-year history show that *cis*-DCE has been reduced to well below its MCL of 70 μg/L inside the reactive cell.

5.1.1.3 PCE Degradation. In October 1997, PCE concentrations were relatively low (between 16 and 32 μg/L) in the upgradient A1 aquifer zone (32 μg/L in WIC-1; see Table 5-2). PCE concentrations in the upgradient pea gravel wells were generally very similar to those in the aquifer. In the upgradient pea gravel zone, PCE concentrations ranged between 12 to 16 μg/L. In all the reactive cell wells, PCE concentrations were uniformly below the detection limit of 0.5 μg/L, indicating that degradation took place rapidly and completely. PCE remained below detection in the downgradient pea gravel (<0.5 μg/L), but rebounded somewhat in the downgradient aquifer cluster. This pattern parallels the degradation patterns for TCE and *cis*-1,2-DCE, and was consistent over the five quarters studied previously (Battelle, 1998). This trend continued into the May 2001 sampling event, indicating that there were no significant changes in the PCE degradation pattern over five years of operation.

5.1.1.4 Vinyl Chloride. During the quarterly sampling program, vinyl chloride was below detection (0.5 μg/L) in nearly all of the reactive cell wells and did not exceed 1.0

μg/L in any well. Results were similar for the May 2001 sampling event. Some vinyl chloride was detected near the upgradient interface; this vinyl chloride is probably a byproduct of TCE degradation. All vinyl chloride detected was below its MCL of 2 μg/L. In some wells, vinyl chloride may have been masked during analysis because of the higher levels of TCE and *cis*-1,2 DCE.

5.1.1.5 ***Results of Field Parameter Measurements.*** Field parameter measurements collected during the quarterly sampling program included pH, ORP, temperature, and DO. Table 5-4 lists selected results of field parameter measurements taken during the April 1997 monitoring event, which was the most recent event in the previous study (Battelle, 1998) from which a complete set of groundwater samples was analyzed. These results are representative of other sampling results during the quarterly sampling program. Table 5-5 lists results of field parameter measurements taken during May 2001 activities.

Table 5-4. Selected Results of Field Parameter Measurements for April 1997

Well ID	Temperature (°C)	pH	ORP (mV)	DO (mg/L)
		Upgradient A1 Aquifer Well		
WIC-1	19.9	6.8	177.2	0.0
		Upgradient Pea Gravel Well		
WW-11	20.3	7.1	358.8	0.1
		Reactive Cell Wells		
WW-12	20.4	10.1	-291.4	0.0
WW-14	20.3	10.5	-674.3	0.1
		Downgradient Pea Gravel Well		
WW-15	20.5	9.3	-382.4	0.1
		Downgradient A1 Aquifer Wells		
WIC-3	20.1	6.9	62.1	0.1
WIC-9	20.4	7.1	-16.4	0.2
WIC-12	20.2	7.0	9.6	0.0

Results of ORP measurements indicate that values are generally positive in the aquifer wells and generally negative within the reactive cell, indicating strongly reducing conditions created by the iron. Similarly, pH is close to neutral in the aquifer zone wells and become alkaline (pH ~ 9 to 11) within the reactive cell. A decrease in ORP and an increase in pH are expected trends in the reactive cell, due to chemical reactions involving the strongly reducing zero-valent iron. In the downgradient pea gravel and aquifer, ORP values increase somewhat and pH values decrease. As with the measured VOCs, this behavior seems to signify some mixing of treated effluent from the reactive cell with untreated groundwater flowing around or under the barrier.

Table 5-5. Selected Results of Field Parameter Measurements for May 2001

Well ID	Temperature (°C)	pH	ORP (mV)	DO (mg/L)
		Upgradient A1 Aquifer Well		
WIC-1	19.8	7.0	133.9	0.6
		Upgradient Pea Gravel Well		
WW-11	20.6	7.0	229	0.7
		Reactive Cell Wells		
WW-12	20.4	10.0	-40.2	1.0
WW-14	20.5	10.9	-820.8	0.4
		Downgradient Pea Gravel Well		
WW-15	20.6	9.7	-8	0.4
		Downgradient A1 Aquifer Wells		
WIC-3	20.7	7.0	121.9	0.6
WIC-9	21.0	7.3	141.1	3.2 [(a)]
WIC-12	20.6	7.0	-13.2	0.7
PIC-31	20.2	9.3	-137.3	0.4

(a) The DO value of 3.2 mg/L from WIC-9 is unusually high and is inconsistent with the ORP reading from the same well and other aquifer wells. This value is considered to be an outlier.

Comparing the data in Tables A-5 and A-6, one can see that the field parameters have remained very consistent during the five years that the PRB has been operating. This is an encouraging finding, because pH and ORP are indicators of iron corrosion and iron reactivity.

5.1.1.6 Results of Inorganic Chemical Measurements. The predominant ions in the A1 aquifer zone groundwater are sodium, potassium, magnesium, calcium, sulfate, bicarbonate, and chloride. On a molar basis, calcium is the dominant cation, followed by Mg ~ Na >K. Sulfate and bicarbonate are the dominant anions, followed by chloride. Nitrate is a minor constituent in the A1 aquifer zone (~1 to 3 mg/L). Other minor ionic constituents include bromide, which is close to 0.5 mg/L in all groundwater samples, and fluoride and phosphate, at average concentrations of 0.15 and 0.1 mg/L, respectively (Battelle, 1998). Table 5-6 lists selected results of inorganic chemical measurements for wells from the April 1997 sampling event. These results are representative of results obtained during all quarterly sampling events in the previous study. Table 5-7 lists selected results for May 2001.

Table 5-6 and 5-7 show similar distributions of ions for both the quarterly sampling program and May 2001 event. The trend is that concentrations of alkalinity, calcium, magnesium, nitrate, silica, and sulfate are significantly lower in the reactive cell than either the upgradient aquifer or pea gravel. Tables 5-6 and 5-7 show alkalinity values are greater than 300 mg/L upgradient of the reactive cell and fall below 100 mg/L in the reactive cell. Calcium concentrations are approximately 160 to 180 mg/L in the aquifer and typically less than 20 mg/L in the reactive cell. The magnesium concentration in the aquifer is about 60 to 70 mg/L and decreases below

Table 5-6. Selected Results of Inorganic Chemical Measurements for April 1997 Sampling Event

Well ID	Ca (mg/L)	Fe (mg/L)	Mg (mg/L)	Na (mg/L)	K (mg/L)	Alk[a] (mg/L)	Cl (mg/L)	SO_4 (mg/L)	NO_3 (mg/L)
Upgradient A1 Aquifer Zone Wells									
WIC-1	158	< 0.02	58.3	30.3	1.42	314	45.1	349	3.2
Upgradient Pea Gravel Wells									
WW-11	164	< 0.02	68.2	36.5	1.75	314	39.5	404	1.8
Reactive Cell Wells									
WW-12	1.77	< 0.02	17.9	36.4	1.95	78.5	38.3	22.4	< 0.05
WW-14	0.62	< 0.02	0.44	30.4	1.64	10.7	35.9	10.1	< 0.05
Downgradient Pea Gravel Wells									
WW-15	6.87	0.0456	1	26.4	0.967	287	40.4	8	< 0.5
Downgradient A1 Aquifer Zone Wells									
WIC-3	162	< 0.02	57.9	29.2	1.12	209	45	347	3
WIC-9	58	< 0.02	20.9	29.3	2.11	< 1,000 [b]	42.2	121	< 0.5
WIC-12	132	< 0.02	44.1	40.5	1.46	270	40.7	308	1.8

(a) Alkalinity as $CaCO_3$
(b) High dilution

Table 5-7. Selected Results of Inorganic Chemical Measurements for May 2001

Well ID	Ca (mg/L)	Fe (mg/L)	Mg (mg/L)	Na (mg/L)	K (mg/L)	Alk[a] (mg/L)	Cl (mg/L)	SO_4 (mg/L)	NO_3[b] (mg/L)	Silica[c] (mg/L)	TDS (mg/L)
Upgradient A1 Aquifer Well											
WIC-1	180	0.12	65	38	1.5	390	45	360	3.1	24	820
Upgradient Pea Gravel Well											
WW-11	170	0.11	66	41	1.6	370	43	410	1.1	20	810
Reactive Cell Wells											
WW-12	1.3	0.037	14	43	1.5	94	34	20	1.9	1	130
WW-14	1.0	<0.05	<0.5	52	3.2	66	39	3.2	<0.05	1	110
Downgradient Pea Gravel Well											
WW-15	6.2	<0.05	0.18	41	0.99	44	45	5	<0.05	9	92
WW-15-Unfiltered	5.9	0.058	<0.5	41	<1	NA	NA	NA	NA	NA	NA
Downgradient A1 Aquifer Wells											
WIC-9	26	<0.05	8.3	33	1.1	140	32	81	0.024	12	270
WIC-12	180	0.097	65	38	2.1	360	43	350	<0.05	25	830
PIC-31	14	0.022	2.5	44	0.86	62	39	37	<0.05	18	150
WIC-3	190	0.1	65	37	1.4	380	45	390	2.9	25	820

(a) Alkalinity as $CaCO_3$
(b) Analysis includes NO_2, if present
(c) Silica as SiO_2
NA = not analyzed.

detection in the reactive cell. Nitrate levels are about 1 to 3 mg/L in the aquifer and below detection (0.05 mg/L) in the reactive cell. Sulfate typically ranges from 350 to 400 mg/L in the aquifer and pea gravel and decreases to less than 20 mg/L in most reactive cell wells.

Table 5-7 also shows that dissolved silica decreased from 24 mg/L in the aquifer to 1 mg/L in the reactive cell. Losses in silica from groundwater were first observed from a partial sampling event by Tetra Tech in October 1998 (Tim Mower, personal communication). The results of this event, which are illustrated in Table 5-8, confirms that dissolved silica levels decrease to approximately 1 mg/L or below in the reactive cell, and rebound in the downgradient aquifer. These results are shown in Figure 5-1, where silica concentrations (circles) are plotted against distance from the upgradient aquifer-pea gravel interface. The line is not a regression curve, but simply helps illustrate the concentration trend.

Table 5-8. Silica Concentrations in Groundwater from October 1998

Well ID	Silica Result (mg/L)
Upgradient A1 Aquifer Zone Wells	
WIC-1	20.8
WIC-6	13.5
WIC-7	21.4
Upgradient A2 Aquifer Zone Wells	
WIC-2	20.5
Upgradient Pea Gravel Wells	
WW-7A	18.6
Reactive Cell Wells	
WW-8C	0.4
WW-8D	1.2
WW-13D	0.9
WW-17C	0.3
WW-17D	0.4
Downgradient A1 Aquifer Zone Wells	
WIC-3	23.7
WIC-10	9.4
WIC-11	16.8
Downgradient A2 Aquifer Zone Wells	
WIC-4	23.1
Downgradient Pea Gravel Zone Wells	
WW-18A	7.0

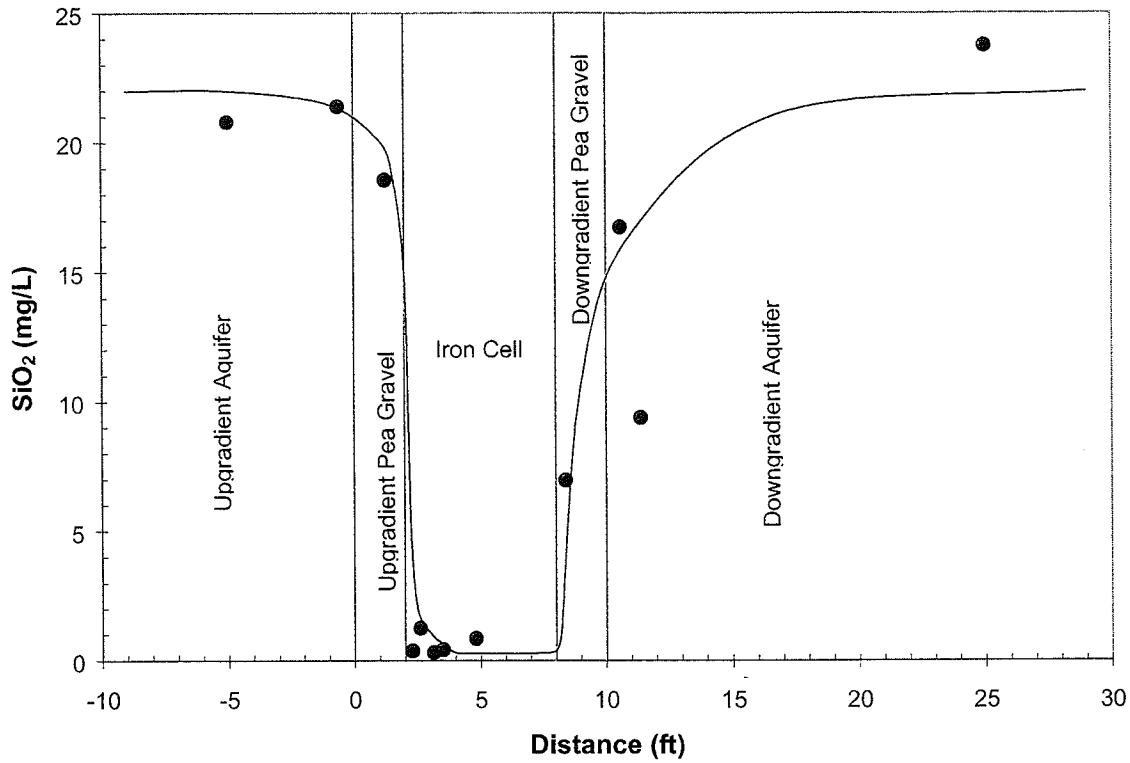

Figure 5-1. Plot Showing the Distribution of Dissolved Silica in the Moffett Field PRB in October 1998

The decrease in calcium, nitrate, sulfate and silica concentrations appears to take place quickly in the iron. Concentrations of these species decrease sharply (relative to the aquifer) as the water enters the reactive cell. However, following this initial decline, the concentrations of these species remain stable as the water moves through the rest of the reactive cell. This suggests that the kinetics of the controlling reactions for these ions are fast, relative to the residence time within the reactive cell.

The converse seems to be true for alkalinity and magnesium, which appear to decrease more gradually in the downgradient direction in the reactive cell. It is presumed at this point that species concentrations are controlled by an equilibrium chemical mechanism, such as precipitation-dissolution or sorption-desorption. For example, reductions in the concentrations of alkalinity, and calcium are believed to be caused by precipitation of calcite or aragonite ($CaCO_3$), based on geochemical modeling predictions and analysis of iron cores from the barrier by core sampling. Sorption as a controlling mechanism was not investigated in detail because sorption densities needed to explain the observed changes in groundwater concentration would

have to be unrealistically high. The implication of precipitation inside PRBs on performance is further discussed in Sections 5.3 and 5.4.

Table 5-9 shows the historical trend of several groundwater parameters in select monitoring wells in the upgradient and downgradient aquifer. The concentrations of several parameters show a noticeable declining trend over time in wells WIC-9 and PIC-31, which are located within 2 ft of the downgradient edge of the PRB. WIC-3 is further downgradient in the aquifer and WIC-12 is at the same depth as the gap between the base of the PRB and the clay aquitard. These trends indicate that, except for wells that are affected by groundwater flowing around (WIC-3) or below (WIC-12) the PRB, the immediately downgradient wells are experiencing some sustained decline in groundwater constituents that are either treated (TCE) or precipitated (calcium, alkalinity) by the PCB. This observation supplements some hydraulic data which indicate that groundwater is flowing through the PRB.

5.1.2 Iron Coring at Former NAS Moffett Field. The first iron coring event at former NAS Moffett Field was done as part of a separate project (Battelle, 1998) in December 1997, approximately two years after installation of the PRB (in April 1996). In the current project, a second iron coring event was conducted in May 2001, approximately 5 years after installation. Both vertical and angled cores were collected as described in Section 4.3.1 (Figures 4-1 and 4-2).

5.1.2.1 XRF Analysis of Cores. Results of XRF analysis of the cores is shown in Table 5-10. It should be noted that this analysis does not include light elements such as sodium, oxygen, and carbon. Since oxygen is not reported it cannot be determined whether other metals are present as oxides or are in elemental form. The results presented in Table 5-10 are summed to 100% of the *analyzable* elements and not the full composition. Therefore, concentrations determined by XRF are qualitative and should be used only for comparison between samples in the same table.

Some core samples collected in the reactive cell contained admixtures of pea gravel with the iron. This occurred as a result of coring as close as possible to the pea gravel-iron interface. Cores containing mixtures of media were noted on the field log and were also evident from the analyses. Two of the five samples analyzed by XRF, IC-1 and IC-4, contained high concentrations of silicon and trace potassium, indicating the presence of pea gravel. The remaining three samples that did not contain pea gravel had no measurable silicon. Samples IC-1 and IC-4 were recalculated without Si and K to eliminate the contribution from pea gravel (see footnote to Table 1). After this was done, the Ca content in the vertical borings ranged from 10 to 32%. The Ca is presumed to be due to mineral precipitation, which will be discussed with the XRD results, below. However, it should be mentioned again that these values do not include light elements such as oxygen and carbon, which are very likely to be present as carbonate. Actual concentrations of Ca would be lower if the "missing" elements were included.

Despite these qualifications, Ca concentrations in the angled cores appear to be significantly lower than in the vertical cores: 1% Ca in IC-2 and 6 % Ca in IC-3. The reason for this is that the angled cores were not as successful in reaching the upgradient interface with the pea gravel

Table 5-9. Time Series Measurements in Upgradient and Downgradient Aquifer Wells at Former NAS Moffett Field

Parameter	Upgradient Aquifer Well WIC-1 19-24 ft bgs	Downgradient Aquifer Wells			
		WIC-9 11-12 ft bgs	WIC-12 25-26 ft bgs	PIC-31 10-20 ft bgs	WIC-3 19-24 ft bgs
TCE (µg/L)					
Jun-96	1,180	NA	NA	NA	1,680
Sep-96	1,400	NA	NA	NA	1,600
Jan-97	ND	800	3,200	NA	1,900
Apr-97	NA	550	3,400	NA	2,900
Oct-97	2,800	830	3,400	NA	2,500
01-May	1,700	480	1,500	160	1,400
Calcium (mg/L)					
Jun-96	154	NA	NA	NA	164
Sep-96	162	NA	NA	NA	177
Jan-97	165	73	125	NA	159
Apr-97	158	58	132	NA	NA
Oct-97		42	131	NA	179
May-01	180	26	180	14	190
Alkalinity (mg/L)					
Jun-96	266	NA	NA	NA	299
Sep-96	ND	NA	NA	NA	371
Jan-97	377	172	243	NA	362
Apr-97	314	ND	270	NA	NA
Oct-97	NA	117	308	NA	345
May-01	390	140	360	62	380
pH					
Jun-96	7.0	NA	NA	NA	7.2
Sep-96	7.1	NA	NA	NA	NA
Jan-97	6.1	7.0	7.1	NA	7.0
Apr-97	6.8	7.1	7.0	NA	6.9
Oct-97	7.1	7.3	7.4	NA	7.1
May-01	7.o	7.3	7.0	NA	7.0
ORP (mV)					
Jun-96	100	NA	NA	NA	148
Sep-96	NA	NA	NA	NA	NA
Jan-97	10	10	-3	NA	34
Apr-97	177	-16	10	NA	62
Oct-97	109	49	43.5	NA	84
01-May	134	141	-13	-137	122

NA = not analyzed.
ND = not detected.

Table 5-10. Results of XRF Analysis of Five Iron Core Samples from the Moffett Field PRB

Boring Direction	Vertical					Angled	
Boring Location	IC-1	IC-1 [(a)]	IC-4	IC-4 [(a)]	IC-5	IC-2	IC-3
Depth (ft)	12.0	12.0	12.5	12.5	12.5	12.0	15.0
Ca	7	10	8	32	15	1	6
Cr	ND	ND	ND	ND	ND	1	1
Cu	ND	ND	ND	ND	ND	ND	ND
Fe	65	90	17	68	70	92	85
K	1	--	1	--	ND	ND	ND
Mn	ND	ND	ND	ND	ND	ND	ND
S	ND	ND	ND	ND	13	5	7
Si	26	--	73	--	ND	ND	ND

Note: units are weight percent and total 100% for each sample; analytes do not include Na and lighter elements.
ND = Not detected (< 1 %)
(a) Recalculated without Si and K to eliminate the contribution from pea gravel

as were the vertical cores. Calculations based on a 25° penetration angle indicate that iron retrieved in both angled cores shown in Table 2-1 were about one foot downgradient of the pea gravel section. In contrast, iron retrieved in the vertical cores was in some cases intermixed with the pea gravel (IC-1 and IC-4). Also, the sample from IC-5 may have been only a few centimeters away from the interface. These results indicate that more Ca precipitation occurs close to the upgradient interface than occurs further downgradient.

Sulfur was detected in only one vertical core, IC-5, where the analysis value was 13%. It is possible that sulfur was not detected in IC-1 and IC-4 due to dilution below the detection limit by the pea gravel. Compared to IC-5, less S was detected in the two angled cores, IC-2 and IC-3 (5 and 7%). As with Ca, this trend may indicate that there was more precipitation of sulfur compounds at the upgradient interface than in the downgradient direction.

5.1.2.2 XRD Analysis. Results of the XRD analysis for ten core samples are shown in Table 5-11. Abundances of mineral phases were reported based on peak intensity as major, minor, or ND (not detected). Cores from IC-1 and IC-4 contained large amounts of quartz and a magnesium-iron silicate (magnesian ferrosilite, a peroxene mineral), confirming the presence of pea gravel in the samples, but also potentially obscuring diffraction lines for iron compounds. Samples without pea gravel (IC-2, IC-3, and IC-5) contain major or minor amounts of graphitic carbon, which is normally present on the surfaces of granular iron due the manufacturing process. Minor amounts of magnetite were observed where iron was a major phase. Magnetite is also present as an oxide coating on the initial iron.

Table 5-11. Results of XRD Analysis Iron Core Samples from the Moffett Field PRB

Boring Direction	Vertical							Angled		
Boring Location	IC-1	IC-1	IC-1	IC-4	IC-5	IC-5	IC-5	IC-2	IC-3	IC-3
Depth (ft)	12.0	15.5	16.0	12.5	7.0	12.5	19.0	12.0	14.5	15.0
Iron	Minor	Minor	ND	ND	Major	Major	Major	Major	Major	Major
Carbon	ND	ND	ND	ND	Major	Major	Minor	Minor	Minor	Minor
Aragonite	ND	ND	ND	ND	Minor	Minor	ND	ND	ND	ND
Calcite	ND	Minor	ND	ND	ND	ND	ND	ND	ND	ND
Magnetite	ND	ND	ND	ND	Minor	Minor	Minor	Minor	Minor	Minor
Iron Carbonate Hydroxide	ND	ND	ND	ND	Minor	Minor	ND	ND	ND	ND
Quartz	Major	Major	Major	Major	ND	ND	ND	ND	ND	ND
Magnesian Ferrosilite	Minor	Minor	Minor	Minor	ND	ND	ND	ND	ND	ND

ND = Not detected.

Two samples from IC-5 (7.0 and 12.5 ft) contained a calcium carbonate mineral, aragonite, and one sample from IC-1 (15.5 ft) contained calcite. The two samples that contained aragonite also contained iron carbonate hydroxide. This compound is related to siderite, although true siderite was not detected in any of the samples by XRD analysis. These results are in apparent agreement with the XRF analysis, in that precipitation of carbonate minerals occurs close to the upgradient interface with the pea gravel.

No sulfur-bearing phases were observed by XRD, so it is not possible to corroborate the presence of sulfur that was detected by XRF. Iron sulfide minerals had been identified in the previous iron-core sampling event at former NAS Moffett Field in December 1997 (Battelle, 1998).

5.1.3 Silt Collection from Monitoring Wells at Moffett Field. Fine-grain material that collected in the silt traps at the base of the monitoring wells was sampled in August 2000, to determine if the materials is enriched in precipitates that settled out of the water column (see Section 4.3.1.6). Information about these solids may help understand whether colloidal transport of precipitates is taking place. The silt traps were routinely cleaned after the barrier was installed and for the first two years while quarterly sampling was taking place; subsequently the silt traps were not maintained for the next two or three years. Therefore, it was expected that silt present in the traps is colloidal material that has accumulated for at least two years.

The masses of silt recovered from the wells at former NAS Moffett Field are shown in Table 5-12. It was not possible to determine how much silt was present in the traps. However, when using the coring tool, one could sense that more silt was present in the two-inch long-screen wells than in the one-inch short-screen wells. Therefore, the amount of silt in the traps was no doubt related to the well screen area. In addition to the wells shown in Table 5-12, other wells were sampled, but no silt was collected, either because there was none present, or because the material did not remain intact inside the sampler and was not recovered.

Table 5-12. Recoverable Material from Silt Traps at Moffett Field Monitoring Wells

Sample ID	Location	Sample Weight (g)[a]
WW-3	Upgradient iron (west side)	1.0429
WW-3DUP[b]	Upgradient iron (west side)	0.2003
WW-12	Upgradient iron (east side)	2.5511
WW-14	Downgradient iron (east side)	3.6448
WW-15	Downgradient pea gravel (east side)	7.2070
WW-16A	Upgradient pea gravel (east side)	4.8068
WW-17B	Upgradient iron (east side)	4.6776
WW-17C	Upgradient iron (east side)	3.6890
WW-17D	Upgradient iron (east side)	0.1808

(a) Weight determined after drying.
(b) Duplicate sample recovered from WW-3 by inserting the silt corer a second time.

Results of the bulk chemical analysis are shown in Table 5-13. In most samples the analytes do no sum to 100%. This is due to the presence of insoluble compounds, principally quartz, and because oxygen was not determined. The carbon data in Table 5-13 are expressed as carbonate (CO_3), which is believed to be the dominant form of carbon in these samples. It can be seen that the carbonate content ranges from 1.9 to 26.5%. Carbonate varies in proportion to the abundance of calcium, but there is always less carbonate present than would be required to form calcium carbonate. (Calcium carbonate is approximately 40% Ca and 60% CO_3 by weight).

XRD analysis (Table 5-14) confirms that calcite is present in these samples; in a few cases calcite is the predominant mineral. The iron content of the silt samples ranges from 5.6 to 82.5%. XRD shows that elemental iron is present in only one sample (WW-14), which also has the highest total iron content. The sample from WW-14 also contained magnetite and iron oxy-hydroxide (FeOOH). Neither iron carbonates nor iron sulfides were not detected in the silt samples by XRD. Also, amorphous iron hydroxide, if it were present in the samples, is not detectable by XRD. The Mg content ranges from 1.1 to 9.3%; the lowest value was for WW-14 (downgradient iron) and the highest value was for WW-3 (upgradient iron). However, no discrete Mg-bearing minerals were detected by XRD. Mn is a minor element in these samples which does not seem to scale with any other elements in the samples.

Ettringite was detected by XRD in four samples (Table 5-14). Ettringite, given by the formula $Ca_6Al_2(SO_4)_3(OH)_{12} \cdot 26H_2O$, is best know for its importance in controlling setting times in hydraulic cements. Figure 5-2 is an SEM photograph of silt from WW-12 showing needle-shaped ettringite; the platy crystals are calcite. The occurrence of ettringite in the silt traps was unexpected because it has not been observed in the iron cores. It is not know whether ettringite

Table 5-13. Results of Chemical Analysis from Moffett Field Silt Traps

Sample ID	n	Mg	Ca	Fe	Mn	CO_3	Sum
WW-3	2	9.3	33.3	13.5	0.2	26.5	82.8
WW-12	2	2.4	12.5	50.0	0.3	8.2	73.4
WW-14	1	1.1	11.1	82.5	0.5	11.1	106.3
WW-15	1	3.1	4.5	6.0	0.2	2.7	16.5
WW-16a	1	2.9	2.1	5.6	0.1	1.9	12.8
WW-17b	1	3.3	5.2	11.1	0.2	3.3	23.1
WW-17c	1	2.6	8.9	24.6	0.2	6.2	42.6
WW-17d	1	6.4	32.1	18.3	0.2	14.2	71.2

Note: results are in weight percent
n = Number of samples analyzed; if n>1 the results were averaged.

Table 5-14. Results of XRD Analysis from Moffett Field Silt Traps

Sample ID	Quartz	Calcite	Ettringite	Iron	Magnetite	FeOOH	Albite	Muscovite-1M	Other
PDF #	33-1161	05-0586	41-1451	06-0696	19-629	13-0087	09-0466	07-0025	see footnotes
WW-3	ND	Major	ND	ND	ND	ND	ND	Minor	ND
WW-3DUP	Minor	Major	ND	ND	ND	ND	Minor	Minor	ND
WW-12	Major	Major	Minor	ND	ND	ND	ND	ND	Trace[a]
WW-14	Major	Major	Minor	Minor	Minor	Trace	Minor	ND	Trace[b]
WW-15	Major	Minor	Trace	ND	ND	ND	Minor	ND	ND
WW-17B	Major	Minor	ND	ND	ND	ND	ND	ND	Trace[b]
WW-17C	Major	Major	ND	ND	ND	ND	ND	ND	Trace[c]
WW-17D	Major	Major	Trace	ND	ND	ND	Minor	Trace	Trace[d, e]

Note: Sample WW-16A was not analyzed by XRD.
ND = not detected.
(a) Katoite (PDF# 38-0368)
(b) Illite-$2M_1$ (PDF# 26-0911)
(c) Chlorite (PDF# 21-1227)
(d) Ca-montmorillonite (PDF# 13-0135)
(e) Lazurite, pyroxene (PDF# 44-1458)

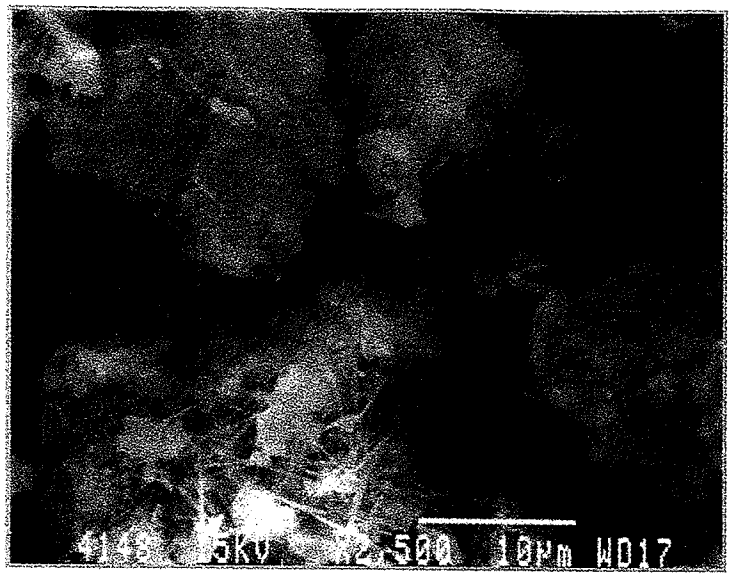

Figure 5-2. SEM Micrograph of Silt from Well WW-12 Showing Ettringite (Needles) Adjacent to Calcite (Plates)

forms elsewhere in the barrier, or if its formation is simply an artifact of conditions inside the silt traps. It is possible that some of the calcium and sulfate losses from the groundwater as it travels through the PRB (see groundwater analysis in Tables 5-7 and 5-8) can be accounted to the formation of ettringite.

The XRD results show that one of the samples that contained ettringite, also contained a trace amount of katoite. This sample was WW-12, located in the upgradient portion of the iron cell. Katoite, given by the endmember formula, $Ca_3Al_2(SiO_4)_{1.5}(OH)_6$, is a type of hydrogarnet (sometimes called hydrogrossular), with a partial replacement of silica for hydroxyl in the mineral structure. Because only one sample had evidence of katoite, and the amount indicated by the diffraction intensity was very low, the significance of this phase is questionable. Nevertheless, the XRD data presented here serves to note that katoite may be a possible precipitate in the Moffett Field PRB.

Several types of aluminosilicate minerals were detected by XRD (Table 5-14). These include fine grain sizes of plagioclase feldspar (albite), muscovite mica, and clay minerals (illite, Ca-montmorillonite, and chlorite). This suite of minerals, along with quartz, is indicative of granitic rock, from which the pea gravel is made. Also, the clays are typical products of granite weathering. The presence of these minerals in the silt traps is evidence that the pea gravel is being eroded and weathered by the movement of groundwater into the reactive barrier. This indicates that transport of fine particulate is taking place throughout the reactive barrier and that the minerals being transported include not only components of the pea gravel, but also precipitates produced inside the barrier. These precipitates are mainly calcium carbonate (calcite), but they also include the calcium-aluminum-sulfate compound, ettringite, and the

calcium-aluminum compound, katoite. In contrast, the analysis of the iron cores shows they contain small amounts of calcium carbonate (in two forms), calcite and aragonite, and iron hydroxide carbonate. The differences between the minerals found in the silt traps versus those found in the iron, itself, may be related to mobility. It is possible that calcite is more easily transported by groundwater movement than either aragonite or iron hydroxide carbonate. In any case, colloidal transport seems to be prevalent, as is evident by the presence of quartz in both the iron cores and the silt traps and the numerous types of aluminosilicates in the silt traps.

In addition to XRD and XRF analysis of the silt cores, chemical analysis was performed by EDS while the samples were being examined by SEM. EDS results, presented in Table 5-15, are considered semiquantitative and do not include light elements such as carbon, oxygen, and sodium. Comparing these results to the wet chemical analysis (Table 5-13), it can be seen that the two types of analyses are in close *relative* agreement. They differ quantitatively because the sums include different sets of elements. Using the EDS analysis set, concentrations of various elements were compared to determined if other meaningful trends could be observed.

Table 5-15. Results of EDS Analysis from Moffett Field Silt Traps

Element	WW-3	WW-3 (dup)	WW-12	WW-14	WW-15	WW-16A	WW-17B	WW-17C	WW-17D
Al	1.7%	3.5%	1.9%	1.5%	8.7%	10.1%	7.9%	6.1%	2.9%
Ca	41.8%	45.1%	33.9%	24.7%	16.2%	5.6%	12.0%	15.4%	51.7%
Cl	0.6%	0.5%	0.6%	0.0%	0.0%	0.0%	0.0%	0.0%	0.6%
Fe	11.1%	13.4%	37.9%	61.4%	23.6%	23.9%	32.7%	44.1%	14.6%
K	0.8%	0.6%	0.3%	0.3%	3.9%	5.5%	4.5%	2.3%	0.9%
Mg	14.4%	7.1%	3.1%	0.5%	1.8%	1.7%	2.0%	2.1%	3.6%
Mn	1.6%	1.0%	3.3%	1.8%	1.1%	0.0%	0.0%	0.7%	0.0%
S	0.6%	1.8%	2.5%	1.4%	0.6%	0.2%	0.6%	0.3%	3.0%
Si	26.7%	25.5%	15.6%	7.7%	43.4%	50.9%	39.2%	28.2%	21.2%
Ti	0.6%	1.6%	0.9%	0.6%	0.7%	2.1%	1.1%	0.9%	1.5%
Total[(a)]	100.0%	100.0%	100.0%	100.0%	100.0%	100.0%	100.0%	100.0%	100.0%

Note: results are in weight percent.
(a) Total includes only the elements listed; this excludes sodium and lighter elements.

Figure 5-3 is a plot of the aluminum and silicon concentrations in the silt samples (data are in Table 5-15). The plot shows an approximately linear correlation where silicon increases approximately 5 percentage points for each percentage point of aluminum. Based on the XRD analysis, it is known that quartz is present in all samples except WW-3, and quartz is probably the main contributor to the Si content. The correlation between Al and Si may be due to the transport of fine-grain aluminosilicate minerals along with quartz though the PRB, some of which becomes deposited in the silt traps. The nearly constant ratio of Si/Al (~5) suggests that the availability of quartz and certain aluminosilicate minerals is relatively everywhere within the permeable barrier. Interestingly, the source of these minerals may be the pea gravel, itself, since

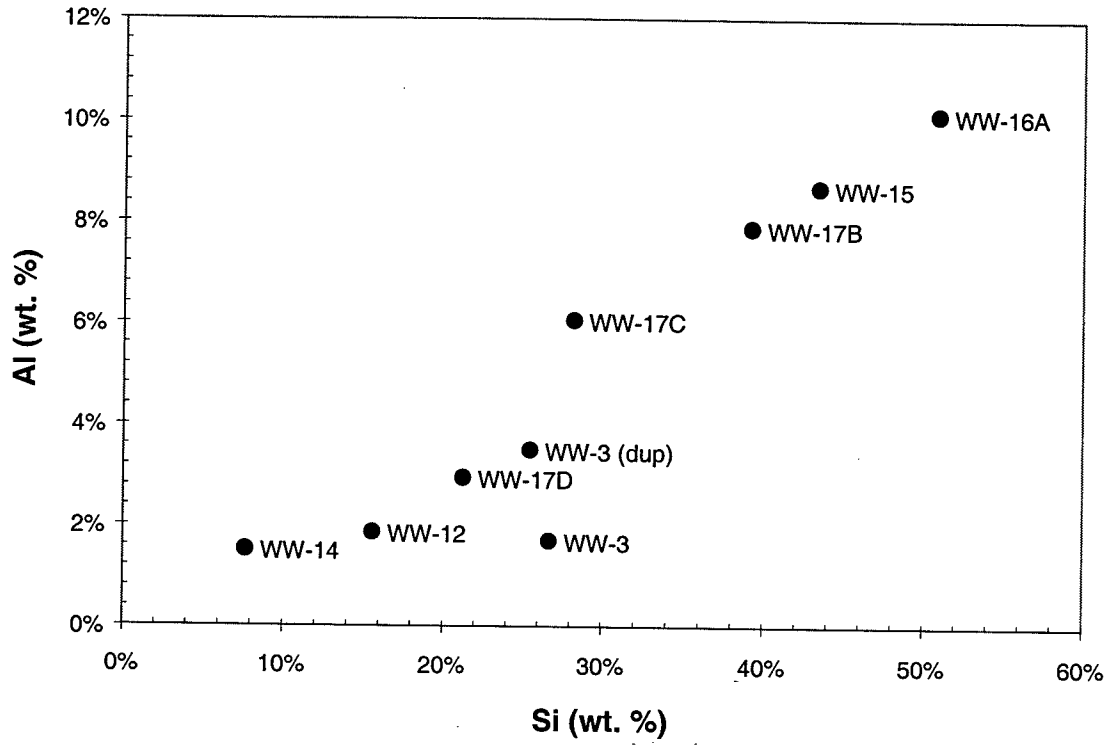

Figure 5-3. Plot of Aluminum and Silicon in Moffett Field Silt

the sample containing the highest fractions of Al and Si (WW-16A) is from the upgradient pea gravel and the sample containing the second-highest fractions of Al and Si (WW-15) is in the downgradient pea gravel. Conversely, the sample from the downgradient iron (WW-14) has the least amount of Al and Si.

To better understand the nature of the aluminous phases, plots were made of the ratios K/Al (Figure 5-4) and S/Al (Figure 5-5). Included with these plots is the ratio of K/Al for muscovite and S/Al for ettringite. It can be seen in Figure 5-4 that the data plot close to the muscovite line, indicating that muscovite (or perhaps the compositionally similar clay mineral illite) is a dominant potassium- and aluminum-bearing phase in the silt samples. Muscovite and illite were identified by XRD as a minor aluminosilicate mineral in several silt samples (see Table 5-14). In Figure 5-5 the line showing the S/Al ratio for ettringite is arbitrarily offset by 1% Al. This figure show that five silt samples roughly obey the compositional trend for ettringite, whereas four samples clearly do not. Based on XRD evidence, ettringite was identified in three of the five samples falling near the ettringite line (WW-3 and its duplicate did not contain ettringite). However, these five samples contained the highest amount of sulfur of the entire set (see Table 5-15). In the group that does not plot near the ettringite line, three samples did not contain ettringite according to XRD, and one contained a trace level. All four samples in this group contained the least amount of sulfur.

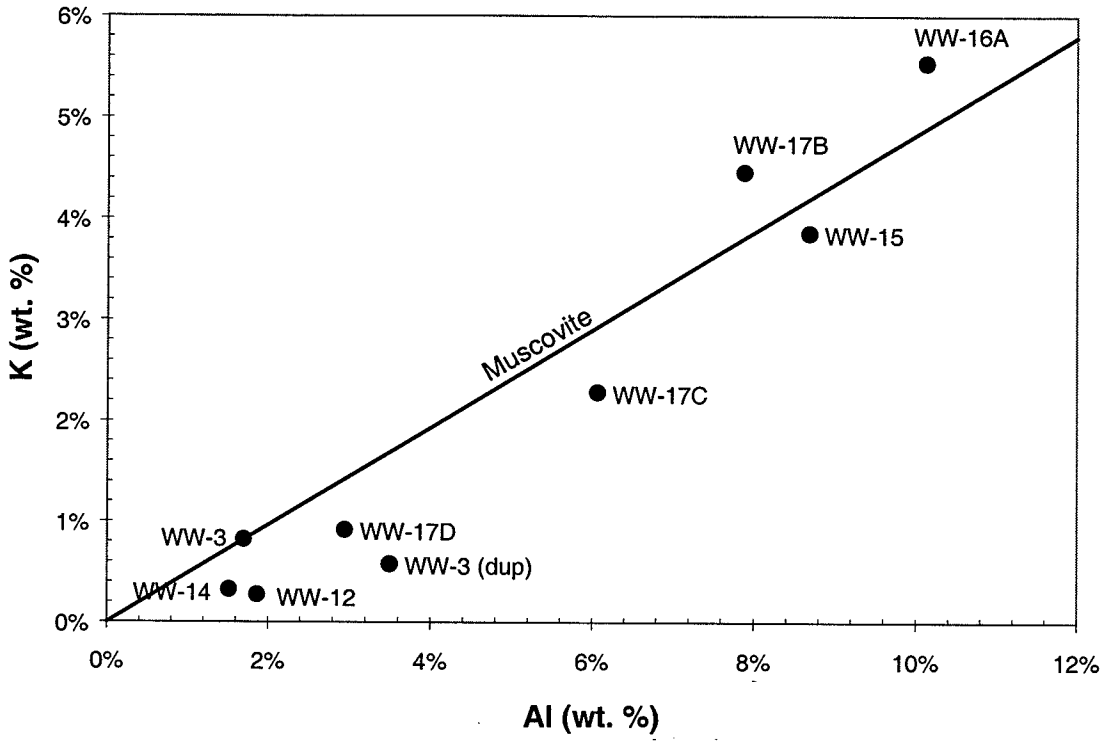

Figure 5-4. Plot of Potassium and Aluminum in Moffett Field Silt

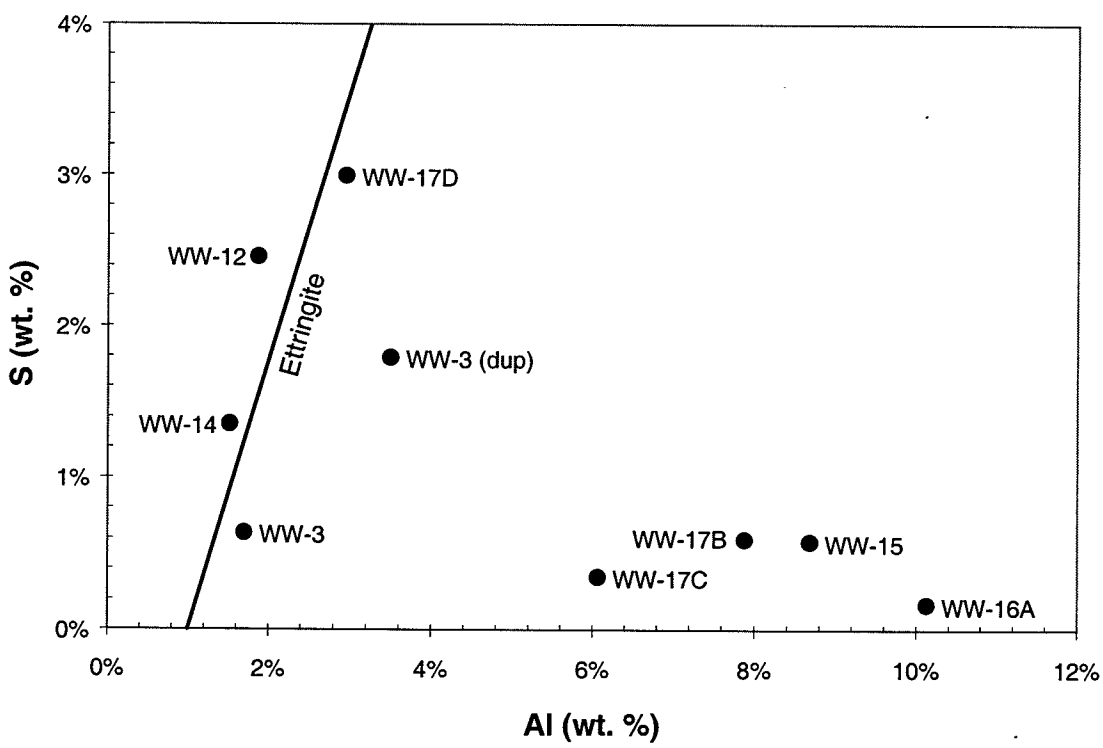

Figure 5-5. Plot of Sulfur and Aluminum in Moffett Field Silt

Figure 5-6 is a plot showing the relative concentrations of Mg and Ca in the Moffett Field silt samples. It appears that there is not a good correlation between these two elements, even though small amounts of Mg can substitute for Ca in some solid phases, such as calcite. While Ca has so far been attributed to calcite, ettringite and possibly katoite, no discrete phase containing Mg has been identified. It can be seen in Table 5-15, or Figure 5-6, that Mg ranges from 0.5 to 4% (not including oxygen, carbon, etc.) for all silt samples except for WW-3 and WW-3DUP. This range is approximately 1 to 6% according to the absolute measurements in Table 5-13. WW-3 contains nearly 15% Mg according to the EDS measurement (Table 5-15) or about 9% absolute (Table 5-13). There may be two possible explanations why a Mg-rich phase was not detected by XRD. One is that Mg is present in the mineral brucite [$Mg(OH)_2$], but it was not detected due to poor crystallinity. The other explanation is that Mg is contained in an amorphous silicate matrix that cannot be detected by diffraction methods. Whatever reason an Mg-rich phase has not been found, it is clear that some phase is precipitating inside the reactive barrier, both from the decline of Mg in the water analyses and from elemental analysis of the silt.

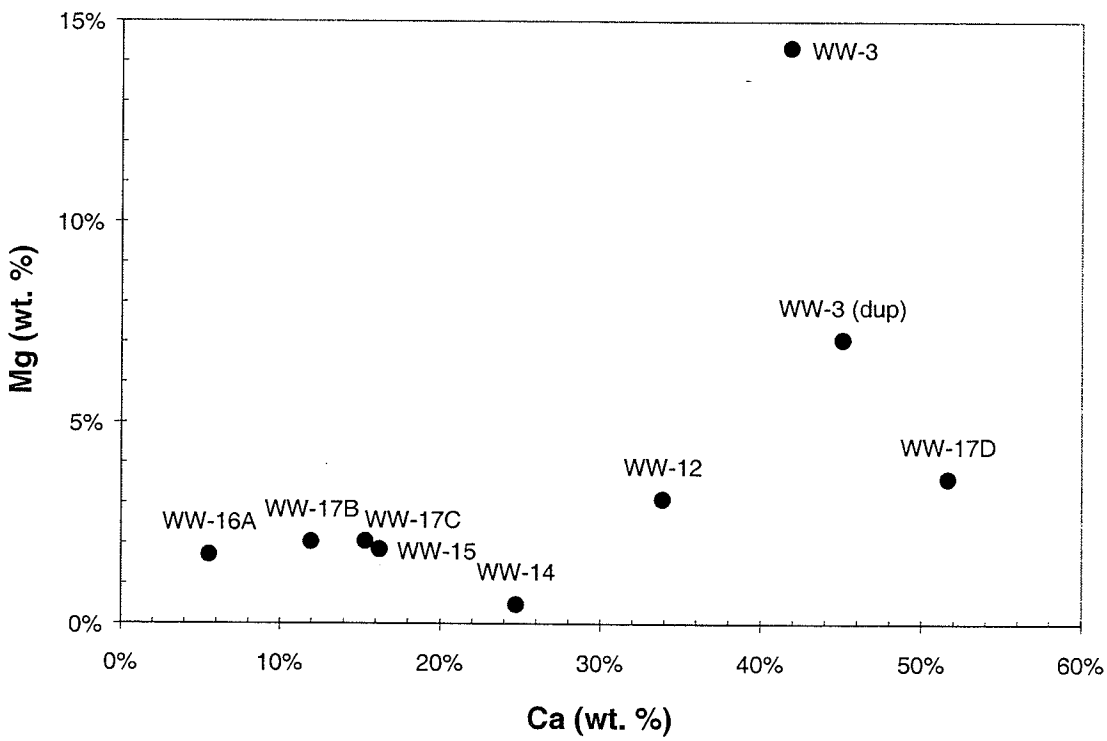

Figure 5-6. Plot of Aluminum and Silicon in Moffett Field Silt

Polished thin sections were prepared for elemental mapping of mineral grains using SEM with an EDS analyzer. Results for silt from WW-12 are shown in Figure 5-7, which includes a backscatter electron image (BEI) and EDS maps for Ca, Mg, and Si. In backscatter mode the

lighter shades indicate elements with higher atomic weight. For example, a fragment of iron is clearly visible in the upper left corner of the backscatter image in Figure 5-7. The remainder of the BEI micrograph consists of irregularly shaped, medium-gray grains on dark background. EDS maps show that the irregular grains are composed principally of Ca, which indicates they are calcite grains according to the XRD results presented in Table 5-14. The other two EDS maps show that the Mg and Si make up most of the infilling material between the calcite and iron grains. The distribution of aluminum (not shown) is similar to the distribution of Mg and Si. These elements may be present in very fine grain clays and other aluminosilicate minerals.

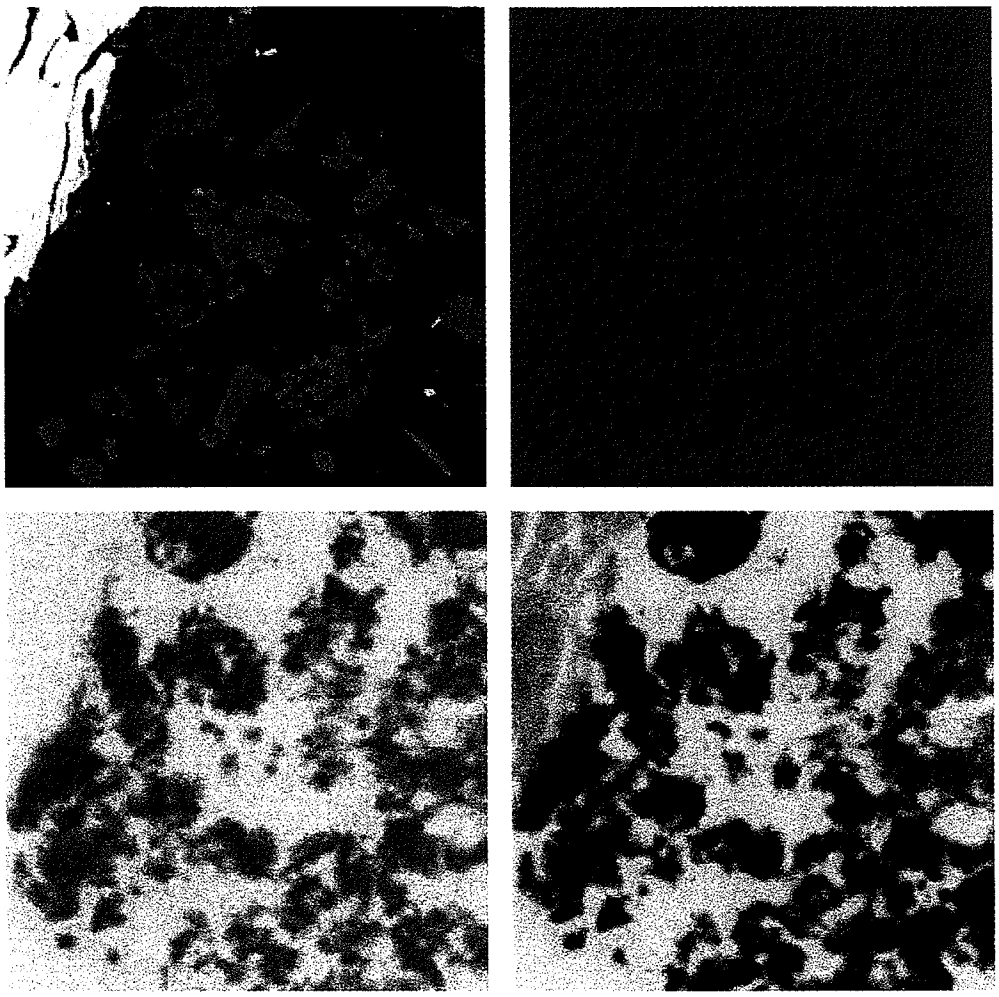

Figure 5-7. Silt Sample From WW-12. Clockwise from top left are BEI showing iron and calcium; and EDS maps showing calcium (red), magnesium (green), silicon (violet).

5.1.4 Microbiological Evaluation of the PRB at Former NAS Moffett Field. Samples were collected in the iron cell and adjacent aquifer regions. Samples from the iron cell were taken from vertical cores IC-1 and IC-5 (see plan view figure of PRB). Aquifer material designated Soil #1 was collected upgradient of the PRB and Soil #2 was collected downgradient. Sample information and results of the phosphlipid fatty acid (PLFA) analysis are shown in Table 5-16.

Table 5-16. Samples for Microbiological Evaluation in May 2001

Sample Name	Soil #1	Soil #2	IC-1	IC-5
Sample Date	05/15/2001	05/15/2001	05/16/2001	05/15/2001
Weight of wet sample (g)	51.36	50.45	50.94	50.55
Moisture content (% water)	22%	10%	10%	10%
Weight of dry sample (g)	40.15	45.18	46.03	45.74

For these samples, biomass content was similar between Soil #1 and IC-1 (~10^6 cells/g) all of which was essentially bacterial. Sample IC-5 had approximately 1/3 the amount of biomass detected in Soil #1 and IC-1. Biomass content in Soil #2 was very low, differing by more than an order of magnitude from Soil #1 (see Table 5-17). A full report of the microbiological investigation, conducted by Microbial Insights (Rockford, Tennessee), is included in a Microbial Analysis Report (Appendix C).

PLFA profiles showed a predominance of Gram-negative bacteria in all four samples (indicated by percentage of monoenoic PLFA). Comparison of the two soil samples showed a noticeable difference between their community structures with soil #1 having a more diverse community composition (as define by the variety of PLFA detected). The most notable difference between the soil samples was high proportions of biomarkers indicative of metal-reducing bacteria (see Table 5-17 and Figure 5-8) in Soil #1 (no such markers were detected in Soil #2).

Specifically, high proportions of the mid-chain branched biomarker 10me16:0, which is prominent in sulfate reducing bacteria *Desulfobacter*, was detected in Soil #1. Compared to the iron samples (IC-1 and IC-5), Soil #1 had proportionally about five times the amount of 10me16:0.

Although, both soil samples were primarily composed of Gram-negative bacteria (monoenoic PLFA), the proportions of fatty acids contributing to this structural group differed greatly. Effectively all of the fatty acids for this group in Soil #2 were derived from 18-carbon fatty acids whereas the biomarkers for Gram-negative bacteria were more evenly distributed within Soil #1.

The most notable difference between the iron samples comes from the amount of i17:1w7c, which was very prominent in the IC-1 sample. IC-1 also had the highest proportion of i15:0, whereas IC-2 had the highest proportion of a17:0. Again, these differences indicate different bacteria contributed to the anaerobic Gram-negative populations in these samples.

Table 5-17. Summary of Microbiological Results

Property	Measurement	Sample Name			
		Soil #1	Soil #2	IC-1	IC-5
Total Biomass	pmols PLFA/g dry wt.	245	6	238	71
Cell Equivalent Value	Cells/g dry wt.	4.80E+06	1.19E+05	4.75E+06	1.41E+06
Bacterial Biomass	picomoles prokaryote PLFA	240	6	238	70
Eukaryotic Biomass	picomoles eukaryote PLFA	5	ND	ND	1
Ratio bacteria/eukarya	ratio prokaryote/eukaryote	48	NC	NC	69
Gram+/anaerobic Gram	TerBrSats	5.7	0.0	17.0	16.2
Gram	Monos	44.7	57.6	46.0	55.7
Anaerobic metal reducers	BrMonos	0.5	0.0	18.3	5.3
SRB/Actinomycetes	MidBrStats	17.7	0.0	6.9	2.4
Genera	Nsats	29.3	42.4	11.7	18.9
Eukaryotes	polyenoics	2.1	0.0	0.0	1.4

ND = not detected.
NC = not calculated.

Finally, biomarker ratios indicative of growth rates and environmental stress showed that the Gram-negative bacterial populations in the soil samples and iron core samples differed in their responses to their environmental conditions. Some Gram-negative bacteria preferentially synthesize 16-carbon fatty acids, whereas others preferentially synthesize 18-carbon acids. Organisms with 16-carbon fatty acids had much faster growth rates than bacteria with 18-carbon fatty acid in Soil #1, in large part because of the very slow growth rates of the latter organisms. Within Soil #2, the 18-carbon fatty acid bacteria also showed slow growth, but still had faster rates than the same group in Soil #1. Biomarkers for 16-carbon fatty acid were not even detected in Soil #2. The opposite trend was present in the iron samples, where bacteria with 18-carbon fatty acid had much faster growth rates than the 16-carbon bacteria.

5.2 Field Evaluation of Longevity at Former Lowry AFB

5.2.1 Groundwater Sampling at Lowry. Groundwater samples were collected from the PRB at former Lowry AFB in the current project in September 1999, approximately four years after installation of the PRB. Locations of the existing monitoring wells in the vicinity of the PRB are shown in Figure 5-9. Groundwater samples were collected in all three rows of wells inside the reactive cell and in the upgradient and downgradient pea gravel zones that are adjacent to the reactive cell. In addition, aquifer wells were sampled immediately upgradient and downgradient of the reactive cell.

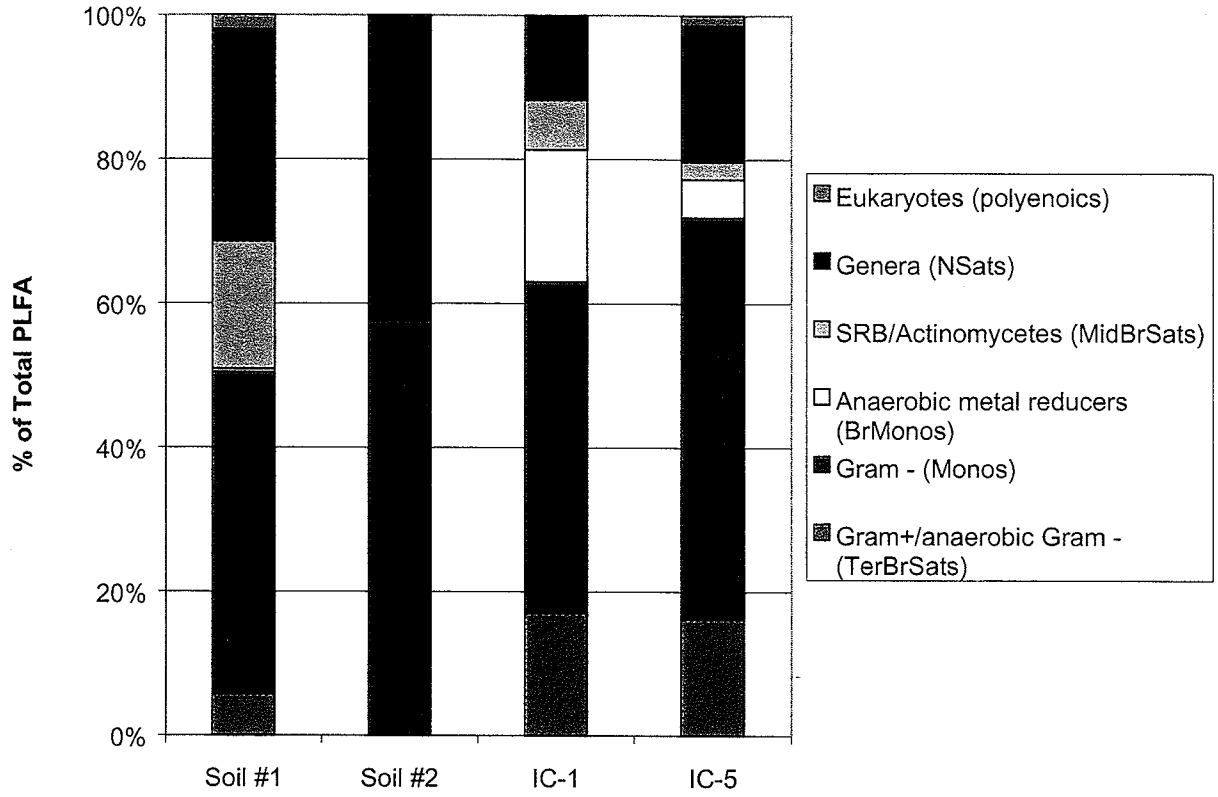

Figure 5-8. Comparison of the Relative Percentages of Total PLFA Structural Groups

Results of groundwater sampling are shown in Tables 5-18 (CVOCs), Tables 5-19 (inorganic analysis), and Table 5-20 (field parameters). Table 5-20 shows that TCE is the major contaminant in the groundwater; smaller concentrations of *cis*-DCE and *trans*-1,2-DCE also were observed in the aquifer. CVOC concentrations declined slightly in the upgradient pea gravel due to quick horizontal and vertical mixing in the porous zone. PCE tentatively was observed at levels below the method detection limit (3 µg/L). The contaminants were undetectable in most of the reactive cell wells and are entirely below detection in the downgradient portion of the cell. These results demonstrate that the reactive cell is degrading the contaminants to below their respective MCLs (<5 µg/L for PCE and TCE; <70 µg/L for DCE). TCE, *cis*-DCE, and *trans*-1,2-DCE are present in the downgradient aquifer as a result of mixing with contaminated groundwater flowing around the pilot-scale PRB.

Results of field parameter measurements are given in Table 5-19. Trends such as rising pH, declining ORP, and declining DO as water moves into the reactive cell indicate that the barrier was functioning normally, after four years of operation. Lower conductivity values in the reactive cell wells compared to aquifer wells suggests some precipitation of solids inside the reactive cell.

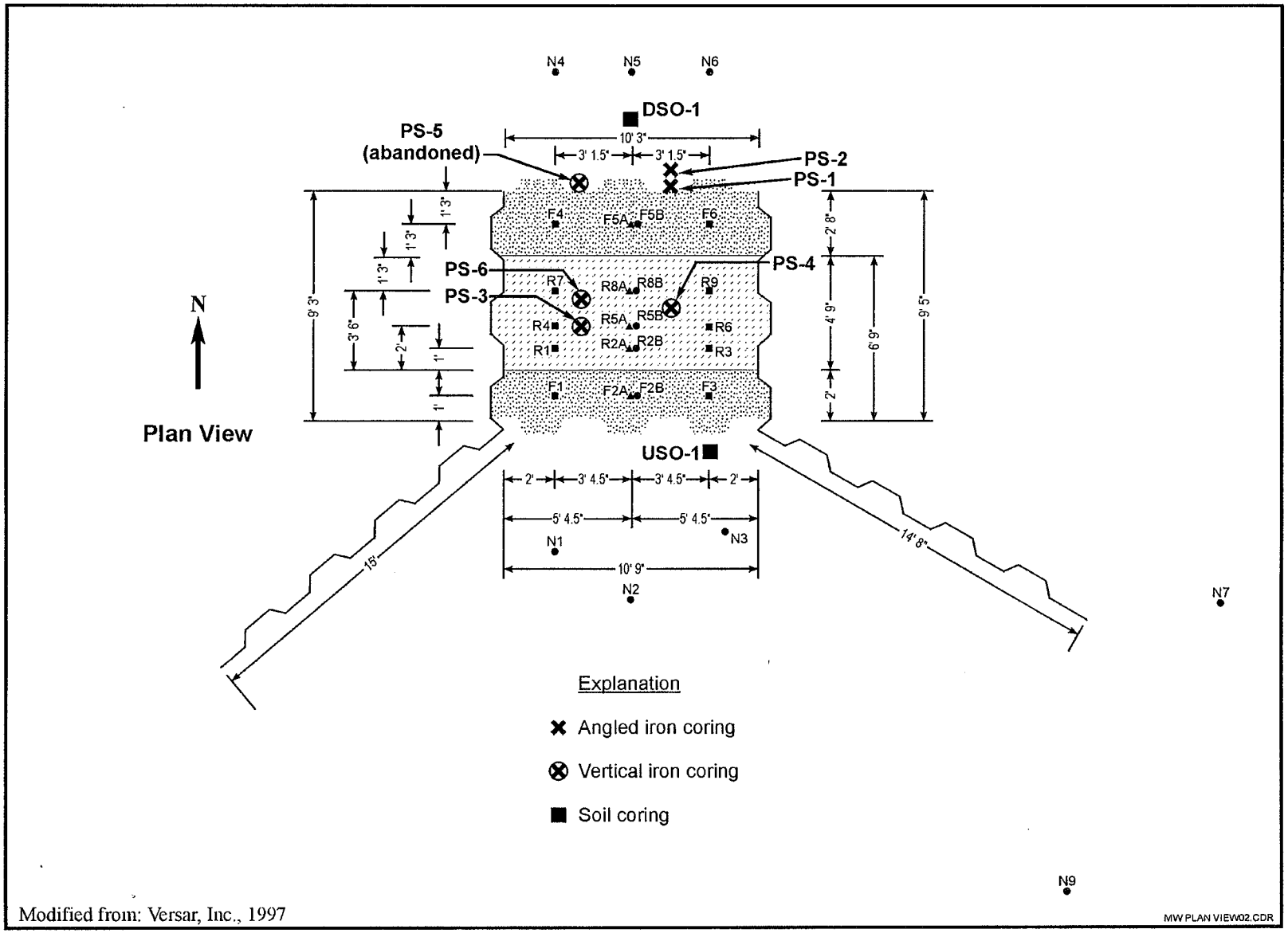

Modified from: Versar, Inc., 1997

Figure 5-9. Sampling Well Locations in the PRB and Vicinity at Former Lowry AFB

Table 5-18. CVOC Distribution in the Groundwater in the PRB and Vicinity at Former Lowry AFB (September 1999)

Well ID[(a)]	PCE (μg/L)	TCE (μg/L)	*cis*-DCE (μg/L)	*trans*-1,2-DCE (μg/L)	Vinyl Chloride (μg/L)
Upgradient Aquifer Well					
N2	1.8 J	71	30	11	<1
Upgradient Pea Gravel Wells					
F1	<3	11	9.5	3.7 J	<1
F2-A	<3	<3	1.2J	<5	<1
F2-B	<3	9	13	4.3 J	<1
Reactive Cell Wells					
R2-A	<3	<3	<5	<5	<1
R2-B	<3	<3	20	5.7	<1
R5-A	<3	<3	<5	<5	<1
R5-A-DUP	<3	<3	<5	<5	<1
R5-B	<3	<3	3.8J	<5	<1
R8-A	<3	<3	<5	<5	<1
R8-B	<3	<3	<5	<5	<1
R9	<3	<3	<5	<5	<1
Downgradient Pea Gravel Wells					
F5-A	<3	<3	<5	<5	<1
F5-B	<3	<3	<5	<5	<1
Downgradient Aquifer Well					
N5	1.7J	59	18	6.9	<1
Quality Assurance (QA) Samples					
Rinsate[(a)]	<3	0.54J	<5	<5	<1
Trip Blank	<3	<3	<5	<5	<1

Units are in μg/L.
J: The result was estimated below the detection limit.
(a) A refers to shallow wells and B refers to deep wells.
(b) Rinsate sample was collected after R2-B sampling.

Results of inorganic analysis are shown in Table 5-20. These data show a considerable decline in alkalinity, calcium, magnesium, silica, and sulfate as the groundwater flows through the reactive cell, which suggests mineral precipitation inside the barrier. Further discussion on mineral precipitation is included in Section 5.3 and 5.4.

5.2.2 Iron Coring at Lowry. Iron cores were collected at Lowry AFB in September 1999, approximately four years after PRB installation. Results of solid phase analysis are presented in this section.

5.2.2.1 Carbon Analysis. Iron samples were analyzed for total carbon using a UIC Model 5120 Total Carbon Analyzer. The combustion temperature was set to 950°C, so that both organic and carbonate carbon could be detected. Results indicate that the average carbon content of the unused iron was 2.2 ±0.1% by weight (Table 5-21). The carbon

Table 5-19. Field Parameter Measurements in Groundwater in the PRB and Vicinity at Former Lowry AFB (September 1999)

Well ID[a]	pH	ORP (mV)	DO (mg/L)	Temp (°C)	Conductivity (mS/cm)
Upgradient Aquifer Well					
N2	6.87	-13.2	0.66	16.94	6.921
Upgradient Pretreatment Zone Wells					
F1	8.68	-168.2	0.77	15.92	4.067
F2-A	10.06	-267.7	0.83	18.11	2.887
F2-B	7.72	-73.5	0.71	16.59	4.296
Reactive Cell Wells					
R2-A	10.98	-664.3	0.69	18.15	2.870
R2-B	10.14	-376.8	0.73	16.76	3.500
R5-A	11.39	-714.0	0.83	18.00	3.281
R5-B	11.15	-443.8	0.78	16.65	3.709
R8-A	11.52	-724.9	0.86	17.03	3.306
R8-B	11.37	-648.6	0.69	16.22	3.776
R9	11.42	-460.4	0.81	16.27	3.834
Downgradient Exit Zone Wells					
F5-A	10.38	-300.1	0.88	18.24	2.968
F5-B	10.34	-278.4	0.87	16.25	3.156
Downgradient Aquifer Well					
N5	6.84	-46.9	0.59	16.01	7.884

(a) A refers to shallow wells and B refers to deep wells.

detected in the unused iron samples may be the graphite-like carbon detected by Raman spectroscopy. Results of carbon analysis of the core samples were approximately the same as the unused material, indicating that measurable amounts of carbonate precipitates were not detected in the core samples.

5.2.2.2 ***XRD.*** XRD spectra yield peaks for metallic iron and magnetite, as well as a minor amount of wustite (FeO) (Table 5-22). These results were typical of both unused iron and material sampled from the former Lowry barrier. The iron oxide composition is characteristic of the Master Builders iron. In the past, wustite was not observed in iron from either Peerless Metal Products, Inc., (former NAS Moffett Field; Battelle, 1998) or Connelly, Inc., (Dover AFB; Battelle, 2000a). In addition, the former Lowry AFB samples contained a variable amount of quartz, which could be explained by an accumulation of silt onto iron grains.

Table 5-20. Inorganic Analysis of Groundwater in the PRB and Vicinity at Former Lowry AFB (September 1999)

Well ID[a]	Alkalinity as $CaCO_3$ (mg/L)	Calcium (mg/L)	Chloride (mg/L)	Iron (mg/L)	Magnesium (mg/L)	Manganese (mg/L)	Nitrate + Nitrite-N (mg/L)	Potassium (mg/L)	Dissolved Silica (mg/L)	Sodium (mg/L)	Sulfate as SO_4 (mg/L)	TDS (mg/L)
Upgradient Aquifer Well												
N2	530	290	100	0.25	86	2.7	4	6	24	480	1,000	2,900
Upgradient Pretreatment Zone Wells												
F1	400	82	24	0.27	26	0.72	0.51	10	10	380	310	1,400
F2-A	410	4.2	60	<0.05	0.53	<0.01	<0.05	7.4	8.3	340	120	960
F2-B	420	93	18	1.9	29	1.2	<0.05	10	11	370	1,400	1,500
Reactive Cell Wells												
R2-A	270	0.77	64	<0.05	<0.5	<0.01	<0.05	8.9	1	290	150	780
R2-B	370	2.1	85	0.05	10	0.012	<0.05	9.7	0.87	380	240	4,000
R5-A	280	1.1	57	<0.05	<0.5	<0.01	<0.05	9.6	2.3	310	150	840
R5-B	400	1	76	<0.05	<0.5	<0.01	<0.05	11	1.2	390	180	1,100
R8-A	340	1.4	64	<0.05	<0.5	<0.01	<0.05	8.8	2.9	320	120	790
R8-B	350	0.92	73	<0.05	<0.5	<0.01	<0.05	9.5	1.6	390	180	940
R9	280	0.68	82	<0.05	<0.5	<0.01	<0.05	10	0.91	370	250	1,000
Downgradient Exit Zone Wells												
F5-A	370	4	74	<0.05	<0.5	<0.01	<0.05	5.4	9.9	340	140	910
F5-B	350	3.8	75	<0.05	<0.5	<0.01	<0.05	5.9	8.1	350	170	980
Downgradient Aquifer Well												
N5	510	380	160	0.29	100	2.2	9.1	9.8	20	490	1,100	3,300

Units are in mg/L.

(a) A refers to shallow wells and B refers to deep wells.

Table 5-21. Carbon Composition (Weight Percent) of Iron from Lowry PRB

Sample ID	Average [(a)]	Standard Deviation[(a)]
PS-4 14.0 -15.0	2.01	0.091
PS-5 10.5 -11.0	2.11	0.291
PS-5 12.5 - 13.0	2.05	0.085
PS-6 11.0 - 11.5	2.15	0.202
PS-6 13.5 - 14.0	2.04	0.139
PS-6 16.5 - 17.0	2.14	0.036

(a) Statistics based on analysis of three independent samples

5.2.2.3 ***Raman Spectroscopy.*** Raman spectra were recorded at three different grain locations for each sample. Multiple locations were chosen because the material was found to be heterogeneous in appearance.

In general, most samples yielded Raman spectra characteristic of magnetite (Fe_3O_4) and reduced carbon (Table 5-22). An exception was sample PS-3 (9.0-9.5 ft bgs) which also contained iron oxyhydroxide, which could be similar to goethite (FeOOH).

Table 5-22. Results of Core Sample Analysis of the PRB at Former Lowry AFB

Core ID	Depth (ft bgs)	Sample Composition According to Each Analysis		
		XRD	Raman Analysis	FTIR
Unused Iron	N/A	Magnetite, iron, quartz, wustite	Magnetite, carbon	Iron oxide (hydrous)
PS-1	9.0 - 9.5	Magnetite, iron, goethite, quartz, wustite	Magnetite, carbon	Iron oxide (hydrous)
PS-1	12.0 - 12.5	Magnetite, iron, quartz, wustite	Magnetite, carbon	Iron oxide (hydrous)
PS-1	15.5 - 16.0	Magnetite, iron, quartz, wustite	Magnetite, carbon	Iron oxide (hydrous)
PS-2	12.0 - 12.5	Magnetite, iron, quartz, wustite, illite	Magnetite, carbon	Iron oxide (hydrous), organic salt
PS-2	13.0 - 13.5	Magnetite, iron, quartz, wustite	Magnetite, carbon	Iron oxide (hydrous)
PS-3	9.0 - 9.5	Magnetite, iron, quartz, wustite	Magnetite, iron oxyhydroxide, carbon	Iron oxide (hydrous)
PS-3	11.5 - 12.0	Magnetite, iron, quartz, wustite, hematite	Magnetite, carbon	Iron oxide (hydrous), silicate
PS-3	15.0 - 16.0	Magnetite, iron, quartz, wustite	Magnetite, carbon	Iron oxide (hydrous)
PS-4	12.0 - 12.5	Magnetite, iron, quartz, wustite, microcline	Magnetite, carbon	Iron oxide (hydrous)
PS-4	14.0 - 15.0	Magnetite, iron, quartz, wustite, hematite	Magnetite, carbon	Iron oxide (hydrous)
PS-6	11.0 - 11.5	Magnetite, iron, quartz, wustite, hematite	Magnetite, carbon	Iron oxide (hydrous), silica
PS-6	13.5 - 14.0	Magnetite, iron, quartz, wustite	Magnetite, carbon	Iron oxide (hydrous), silica
PS-6	16.5 - 17.0	Magnetite, iron, quartz, wustite	Magnetite, carbon	Iron oxide (hydrous)

N/A: not applicable.

5.2.2.4 ***FTIR.*** Infrared analysis yielded spectra characteristic of a hydrated iron oxide, but in some instances absorption for silica were also observed (Table 5-22). Silica is believed to absorb onto iron surfaces from the groundwater.

5.2.3 Silt Coring at Lowry. Fine-grain material that collected in the silt traps at the bases of the monitoring wells was sampled on 21 September 2000, to determine if the materials is enriched in precipitates that settled out of the water column (see Section 4.3.1.6). Information about these solids was sought to help in understanding whether colloidal transport of precipitates is taking place within the PRB. Information was not available on whether or how often the silt traps were cleaned in the past. Therefore, it is uncertain whether the silt present in the traps had accumulated for a few years or up to the age of the barrier at that time, which was approximately five years.

Compared to the Moffett Field PRB, it appeared that there was less silt present in the silt traps at Lowry. There could be a number or reasons for this difference, including well construction, screen size and length, geochemistry, and water flow patterns. Silt was recovered from only four wells, as shown by the recovered mass in Table 5-23. In addition to these, other wells were sampled, but no silt was collected, either because there was none present, or because the material did not remain intact inside the sampler and was not recovered.

Table 5-23. Material Sampled from Silt Traps at Lowry Monitoring Wells

Well ID	Location	Sample Weight (g)[a]
R6	Middle of Iron (East)	3.4988
R8A	Downgradient Iron (Center)	0.0024
R9	Downgradient Iron (East)	2.2225
F4	Downgradient Pea Gravel (West)	0.1118

(a) Weight determined after drying.

XRD analysis of the silt from wells R6 and R9 is shown in Table 5-24. Due to the small amount of material recovered from R8A and F4, these samples were not analyzed. Both samples, which are from inside the iron cell, contain iron, magnesium, and wustite, which are indicative of the Master Builder iron. In addition both samples contain a small amount of quartz which could have originated from the pea gravel or aquifer. In addition, the sample from well R6 contains a small amount of rankinite, a calcium silicate with formula $Ca_3Si_2O_7$. Rankinite belongs to the melilite mineral group, which is uncommon in sediments. Although it is possible this mineral could have precipitated in the reactive cell, no other analysis were performed to corroborate its existence in the silt sample. Therefore, rankinite is considered a possible, rather than likely mineral phase. Due to the small sample recoveries and absence of carbonates in the XRD evaluation, no chemical tests were performed on these samples.

Table 5-24. Results of XRD Analysis of Silt from Lowry AFB Monitoring Wells

Sample ID	Quartz	Iron	Magnetite	Wustite	Rankinite
PDF #	33-1161	06-0696	19-629	06-0615	22-0539
R6	Minor	Major	Major	Minor	Minor
R9	Minor	Major	Major	Minor	ND

5.2.4 Microbiological Evaluation of the PRB at Former Lowry AFB. Seven samples of iron were analyzed for PLFA content. Sample PS-5 14.5-15.0 was lost during PLFA Analysis. Of the remaining samples, biomass content was lowest in sample PS-6 15.0-15.5 and highest in upgradient aquifer sample USO-1 11.5-12.0. A comparison of the PLFA profiles showed that all but samples PS-3 14.0-15.0 and PS-6 15.0-15.5 contained relatively diverse microbial communities primarily composed of Gram negative bacteria. Sample PS-3 14.0-15.0 was primarily composed of eukaryote PLFA and sample PS-6 15.0-15.5 was equally distributed between both eukaryote PLFA and normal saturated PLFA. The Gram negative communities with detectable biomarkers were in a stationary phase of growth and were not showing any signs of decreased membrane permeability, a bacterial response to environmental stress.

5.3 Accelerated Column Tests

Iron reactivity has not been studied in the field for sufficiently long times to define the performance lifetime of a reactive barrier. Longevity issues were partly addressed in a preliminary column test experiment under accelerated flow conditions by Gavaskar et al. (1998), in which 1,200 pore volumes of groundwater (from a site in Ohio) were passed through granular iron. In this test, an accelerated flowrate of 12 ft/day was used to investigate whether changes in performance could be detected between start-up and end of the experiment. After an equilibration period of about 40 pore volumes, the half-life for TCE degradation was approximately 30 minutes. Toward the end of the experiment, when approximately 1,200 pore volumes had passed through, the half-life had increased by 33%. Analysis of the iron grains by SEM and XRD indicated the presence of iron oxyhydroxide and iron carbonate nearest the influent end. Other carbonate precipitates (calcite and aragonite) were found on the iron throughout the column.

More focused accelerated long-term column tests were run during the current project to simulate several years of operation of the PRBs at former NAS Moffett Field and Lowry AFB. The columns were filled with the same iron used in the field PRBs and groundwater was obtained on a monthly basis from local site representatives. The objective was to observe the kind of aging of the iron that would not be visible in the field PRBs for many years in the future and get some idea about the change in performance of the iron over time (represented by pore volumes of flow).

5.3.1 Former NAS Moffett Field Column Simulation. The column setup for the former NAS Moffett Field simulation is described in Section 4.3.1.7. About 1,300 pore volumes of

groundwater obtained from the site was run through the column that was packed with iron from Peerless Metal Products, Inc., (the same iron as was used in the field PRB). As described in Section 4.3.1.7, the flowrate was initially set to 30 ft/day, but shortly thereafter was reduced to 25 ft/day to ensure that the pH and ORP would reach a plateau between the final port within the column, Port D, and the effluent (E). Figure 5-10 shows the pH and ORP profile after 15 pore volumes of water had passed through the column and at a flowrate of 25 ft/day. However, subsequent measurements showed that the pH was continuing to climb, indicating that some precipitates may not be getting enough time to form in the column. Also, analysis of filtered and unfiltered samples showed that more of the precipitates were being retained in the column at 12.5 ft/day; at 25 ft/day, colloidal precipitate particles were being washed out of the column. Therefore, the flowrate was reduced to 12.5 ft/day at 317 pore volumes and was maintained at that level until the end of the test. It is possible that in the first part of the test (until 317 pore volumes), precipitate formation and retention had not reached their maximum in the column.

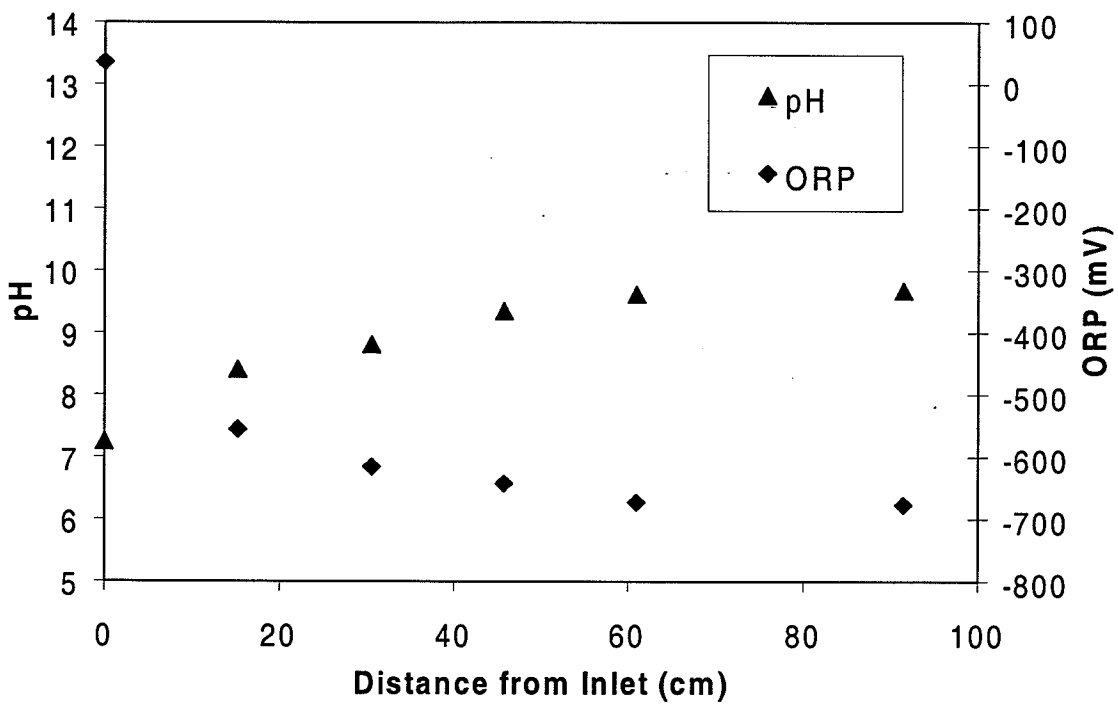

Figure 5-10. Plot Showing Stability of pH and ORP After 15 Pore Volumes of Groundwater

A 6 ft/day-flowrate was tested briefly, but did not appear to provide any significant advantage in terms of pH increase or precipitate retention. At the end of the test, the effect of flow velocity on the half-life measurements in the column was checked; the results are provided in Appendix C.

The TCE half-life remained relatively constant at all three flowrates tested (25 ft/day, 12.5 ft/day, and 6 ft/day), indicating that the flowrate did not affect the half-life determination. However, the half-life increased slowly and monotonically over the duration of the column test, which is believed to be an effect of iron aging.

5.3.1.1 ORP and pH in the Moffett Field Column. Trends in pH and ORP measurements were monitored from the initial setup to the end of the test, which represents approximately 1,300 pore volumes. (See Appendix C for a compilation of column test measurements). Figure 5-11 shows these results graphically at individual sampling ports and combined into a single plot. At each of the sampling ports the data show a trend of increasing pH values and decreasing ORP values as the number of pore volumes increase. This behavior can be explained by the fact that faster flowrates were used at the beginning of the tests and slower flowrates were used later. This would have had the effect of shifting the point of equilibrium (or steady state condition) toward the inlet end of the column. However, once the flowrate had been changed (at 317 pore volumes), the pH and ORP values returned to an equilibrium (or steady state) condition and fluctuated in a relatively narrow band.

The pH stability during the test may preclude the use of pH and ORP as inexpensive field indicators of the long-term reactivity changes in the iron. As seen in Section 5.3.1.2, the TCE half-life continued to progressively increase over the duration of the test, whereas pH and ORP remained relatively constant. This indicates that the reactivity of the iron may have continued to decline, even as the pH and ORP conditions in the iron remained relatively current.

5.3.1.2 TCE Degradation. Water samples were collected periodically for analysis from the inlet and outlet points, and from the four sampling ports in the column. Results of water sample analysis for TCE are show in Table 5-25. Relative concentrations (c_{rel}) were calculated by dividing concentration values (c) at every sampling point i by the concentration in the effluent (c_0); i.e. $c_{i,rel} = c_i/c_0$ (see Table 5-26). Relative concentrations were used instead of actual concentrations to evaluate reaction rates, because TCE levels varied continuously over the course of the study due to differences in the batch of groundwater and in spike levels.

Rate constants for TCE degradation were calculated from relative concentration data. It was assumed that rate reactions were first order, and thus would obey Eq. (1)

$$c_{rel}(\tau) = e^{-k\tau} \tag{1}$$

where τ is residence time and k is a first-order rate constant. Residence time was calculated by Eq. (2)

$$\tau = xnA/u \tag{2}$$

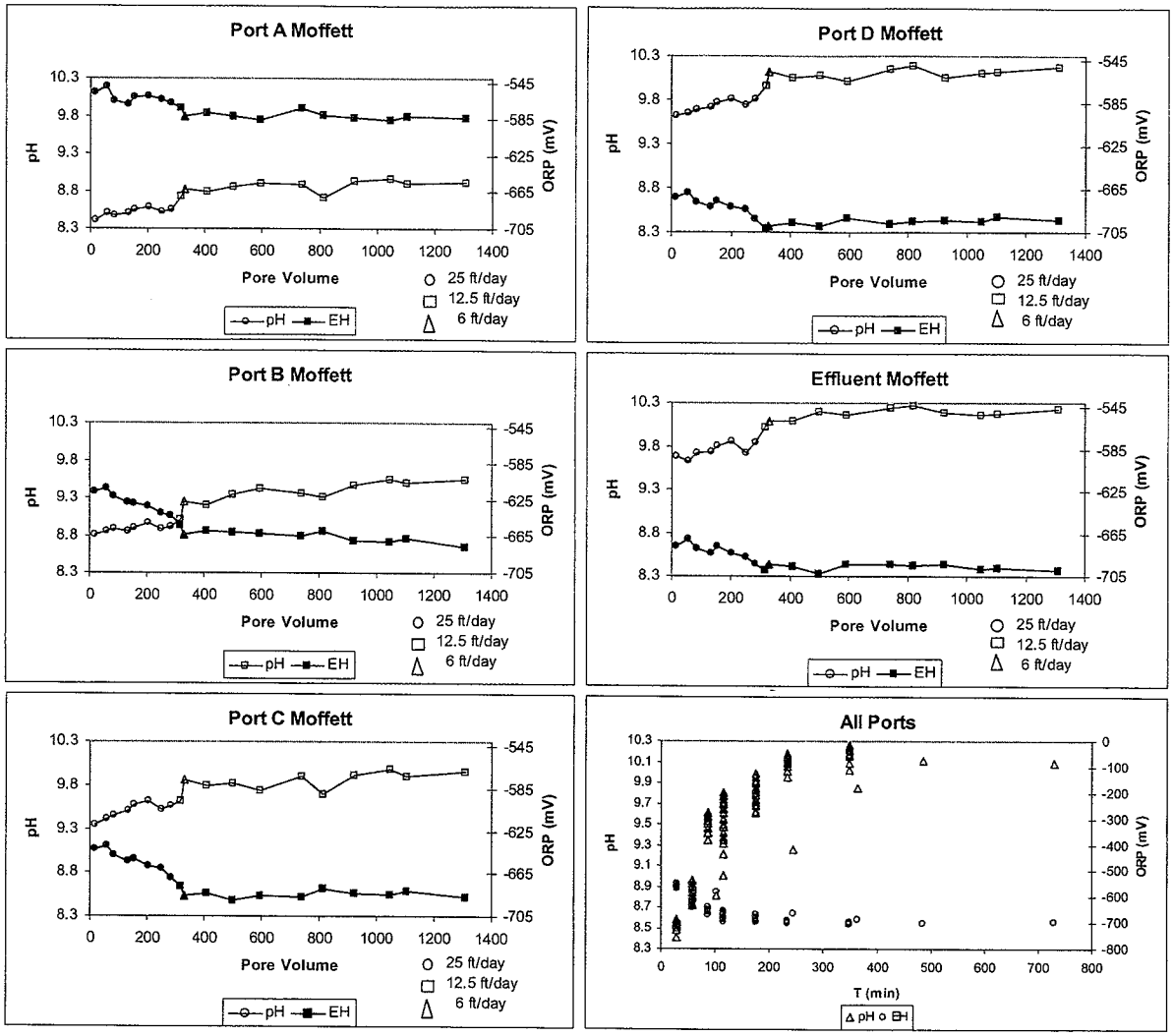

Figure 5-11. pH and ORP Values in the Moffett Field Column at Different Pore Volumes (Ages of Iron)

where x is the flow distance (i.e., the distance from the inlet port to the sampling port), n is the porosity (0.637 for Peerless iron), A is the cross-sectional area of the column (11.5 cm^2) and u is the volumetric flowrate (see Table 4-3).

After plotting the data using a logarithmic concentration scale it was apparent that Eq. (1) did not fit the data equally well throughout the entire range. Regression results based on Eq. (1) deviated most strongly from the data at the shortest residence times and at the longest residence times. The shortest times correspond to fluid flow between the inlet to the column and the first sampling port (Port A). The longest times were those between Port D and the outlet. In general, log-linear regressions of the data produced "good" fits after restricting the data points to ports A, B, C, and D (4 points).

Table 5-25. Results of TCE Measurements (mg/L) in Moffett Field Column Test

PVs	Influent	Port A	Port B	Port C	Port D	Effluent
42	69.4	37.5	34.1	31.4	31.9	30.5
84	759	304	152	88.6	53.1	47.5
140	1260	524	224	131	95.3	79.6
187	477	205	112	79.8	45.7	20.9
223	523	230	120	92.4	52.3	56.4
257	460	200	127	86.0	43.1	32.4
317	484	210	124	76.7	33.8	19.7
475	797	299	171	91.2	61.0	42.1
1,012	643	301	185	113	85.6	72.5
1,047	523	248	156	97.2	76.9	61.8
1,295	575	251	161	107	79.2	66.4

Table 5-26. Relative TCE Concentrations (C/C_0) in Moffett Field Column Test[(a)]

PVs	Influent	Port A	Port B	Port C	Port D	Effluent
42	1.00	0.540	0.491	0.452	0.460	0.439
84	1.00	0.400	0.201	0.117	0.070	0.063
140	1.00	0.415	0.177	0.104	0.075	0.063
187	1.00	0.430	0.236	0.167	0.096	0.044
223	1.00	0.439	0.229	0.177	0.100	0.108
257	1.00	0.435	0.276	0.187	0.094	0.070
317	1.00	0.435	0.256	0.159	0.070	0.041
475	1.00	0.375	0.215	0.114	0.077	0.053
1,012	1.00	0.469	0.288	0.176	0.133	0.113
1,047	1.00	0.474	0.299	0.186	0.147	0.118
1,295	1.00	0.437	0.281	0.186	0.138	0.115

(a) Concentration at a sampling location divided by the influent concentration.

Graphs showing the experimental data from Table 5-26 and the regression curves are given in Appendix C. In these figures closed symbols represent points that were used in the regression analysis and open symbols represent points that were not used. Note that the fitted lines do not intercept the concentration axis at $c/c_0 = 1$ at $\tau = 0$, but instead intercepts at a value between 0.27 and 0. 47. This is probably because of the end effect of the column; water entering the column from a small-diameter tube mixes with water in the column as it travels to the first port, before plug flow is established. Table 5-27 lists the results of the regression analysis. The rate constant, k, was calculated by fitting a linear function to the logarithmic value of TCE concentration to residence time. A least-squares regression fit provided the slope of the line,

from which k was derived and also gave the standard error. The 'intercept' is the calculated value of the fitting function at $\tau = 0$.

The half life for the reaction was determined by the relation $t_{½} = ln\ (2)/k$. It should be noted that results of water analyses collected at 42 and 317 pore volumes are not represented in Table 5-27. In case of the 42 pore volume data, the profile is more like that of absorption, rather than first-order decay. Apparently, sorption sites were not sufficiently saturated after 42 pore volumes. In the case of the 317 pore volume data, the flowrate had been adjusted from 25 ft/day to 12.5 ft/day a relatively short time before the samples were collected. It is possible that the column had not re-equilibrated by that time.

Table 5-27. Results of Regression Calculation on Moffett Field Column Test

Cumulative Pore Volumes	Linear Flowrate (ft/day)	Number of Fitted Points	k (min^{-1})	Standard Error (min^{-1})	$t_{½}$ (min) Average (range)		Intercept
84	25	4	0.0201	0.0010	34.5	(32.9 - 36.4)	0.389
140	25	4	0.0196	0.0029	35.4	(30.7 - 41.5)	0.452
187	25	4	0.0168	0.0012	41.3	(38.5 - 44.3)	0.395
223	25	4	0.0163	0.0018	42.5	(38.3 - 47.7)	0.408
257	25	4	0.0174	0.0016	39.8	(36.6 - 44.0)	0.293
317	12.5	4	0.0103	0.0009	67.3	(61.5 - 73.7)	0.185
475	12.5	4	0.0094	0.00056	73.7	(69.8 - 78.8)	0.465
1,012	12.5	4	0.0085	0.00004	81.5	(81.2 - 82.0)	0.267
1,047	12.5	4	0.0081	0.00007	85.6	(84.5 - 86.0)	0.275
1,295	12.5	4	0.0074	0.00017	93.7	(91.7 - 96.0)	0.408

The half-life of TCE increased by a factor of approximately 2 over the exposure to 1,300 pore volumes of groundwater from NAS Moffett Field. Therefore, the long-term exposure to groundwater flowing through the PRB is likely to reduce the reactivity of the iron.

A plot of rate constants at different pore volume ages (Figure 5-12) shows that the degradation rate of TCE in the Moffett Field column decreases exponentially during the course of the experiment. Least-squares regression of the data gives the following expression for k

$$k\ (\text{min}^{-1}) = 0.024\exp\ (-0.0016\ \text{PV}) \qquad (3)$$

The coefficient of determination (R^2) for the fit is = 0.8643. Using this function for k, the half-life at different pore volume ages was calculated and is shown in Figure 5-13. The intercept at zero pore volumes is approximately 36 minutes, which is the extrapolated half-life of TCE before any aging of the iron has occurred. This calculation omits the effect of absorption, which normally obscures the measurement of half-life in laboratory experiments without proper conditioning.

Table 5-28. Inorganic Analysis of Filtered Water Samples From Moffett Field Column

Pore Volumes	Flowrate	pH inlet	pH outlet	pH % change	ORP (mV) inlet	ORP (mV) outlet	ORP (mV) % change
249	25	7.38	9.73	32	31.5	-686.9	-2281
317	12.5	7.36	10.03	36	10.5	-699.5	-6762
327	6	7.36	10.09	37	3.9	-693.4	-17879
1,310	12.5	7.35	10.23	39	22.3	-699.1	-3235
Pore Volumes	**Flowrate**	**Calcium (mg/L) inlet**	**Calcium (mg/L) outlet**	**Calcium (mg/L) % change**	**Magnesium (mg/L) inlet**	**Magnesium (mg/L) outlet**	**Magnesium (mg/L) % change**
249	25	90	69	-23	64	65	2
317	12.5	200	85	-58	59	59	0
327	6	200	65	-68	60	49	-18
1,310	12.5	250	139	-44	63	75	19
Pore Volumes	**Flowrate**	**Alkalinity (mg/L) inlet**	**Alkalinity (mg/L) outlet**	**Alkalinity (mg/L) % change**	**Sulfate (mg/L) inlet**	**Sulfate (mg/L) outlet**	**Sulfate (mg/L) % change**
249	25	395	375	-5	675	575	-15
317	12.5	400	160	-60	550	550	0
327	6	390	32	-92	575	725	26
1,310	12.5	330	258	-22	650	550	-15
Pore Volumes	**Flowrate**	**Dissolved silica (mg/L) inlet**	**Dissolved silica (mg/L) outlet**	**Dissolved silica (mg/L) % change**	**Iron (µg/L) inlet**	**Iron (µg/L) outlet**	**Iron (µg/L) % change**
249	25	N/A	N/A	N/A	<30	<30	NA
317	12.5	17.0	8.4	-51	<30	240	>700
327	6	16.45	3.25	-80	<30	<30	NA
1,310	12.5	18.00	15.5	-14	160	13,300	8,213

readily achieving steady state conditions as residence times increase. It is known from core sample analysis and geochemical modeling that precipitation of calcium carbonate can accompany a pH rise if the groundwater is close to saturation before encountering the iron.

The possibility of calcium carbonate precipitation can be observed by the changes in concentrations of calcium and alkalinity (see Table 5-28 or Figure 5-14). The changes in calcium concentration are -23, -58, and -68% as the flowrates decrease from 25, 12.5, and 6 ft/day, respectively. These values correspond to 249, 317, and 327 pore volumes, respectively, so the age of the iron is an unlikely factor. Also, when the flowrate is increased from 6 to 12.5 ft/day after 1,310 PVs, the calcium concentration increases once again, which suggests that the precipitation rate slows down accordingly. Similarly, alkalinity concentrations follow a similar pattern, which would be required if calcium carbonate were precipitating (e.g., calcite or aragonite). The 'rebound' in alkalinity after the flowrate is increased from 6 to 12.5 ft/day (corresponding to 327 and 1,310 PVs) parallels the calcium rebound. However, the decline in

Table 5-29. Inorganic Analysis of Unfiltered Water Samples From Moffett Field Column

Pore Volumes	Flowrate	Calcium (mg/L) inlet	Calcium (mg/L) outlet	Calcium (mg/L) % change	Magnesium (mg/L) inlet	Magnesium (mg/L) outlet	Magnesium (mg/L) % change
148		305	325	7	90	80	-11
249	25	89	52	-42	63	53	-16
317	12.5	195	82	-58	59	57	-3
327	6	195	58	-70	59	68	15
1,310	12.5	165	212	28	61	63	3

Pore Volumes	Flowrate	Alkalinity (mg/L) inlet	Alkalinity (mg/L) outlet	Alkalinity (mg/L) % change	Sulfate (mg/L) inlet	Sulfate (mg/L) outlet	Sulfate (mg/L) % change
148		423	562	33	1,870	1,920	3
249	25	400	395	-1	625	600	-4
317	12.5	410	215	-48	575	550	-4
327	6	450	45	-90	575	850	48
1,310	12.5	330	298	-10	425	575	35

Pore Volumes	Flowrate	Dissolved silica (mg/L) inlet	Dissolved silica (mg/L) outlet	Dissolved silica (mg/L) % change	Iron (μg/L) inlet	Iron (μg/L) outlet	Iron (μg/L) % change
148		21.3	16.5	-23	290	32,300	11038
249	25	NA	NA	NA	50	2,180	4260
317	12.5	18.25	10.25	-44	<30	9,100	>30233
327	6	16.25	4.44	-73	<30	970	>3133
1,310	12.5	18	15.5	-14	280	15,700	5507

Pore Volumes	Flowrate	Sodium (mg/L) inlet	Sodium (mg/L) outlet	Sodium (mg/L) % change	Potassium (mg/L) inlet	Potassium (mg/L) outlet	Potassium (mg/L) % change
148		845	882	4	3.08	2.97	-4

Pore Volumes	Chloride (mg/L) inlet	Chloride (mg/L) outlet	Chloride (mg/L) % change	Nitrate (mg/L) inlet	Nitrate (mg/L) outlet	Nitrate (mg/L) % change
148	152	184	21	1.86	1.92	3

Pore Volumes	Flowrate	TOC (mg/L) inlet	TOC (mg/L) outlet	TOC (mg/L) % change	Dissolved Residue (mg/L) inlet	Dissolved Residue (mg/L) outlet	Dissolved Residue (mg/L) % change
148		7.2	9.8	36	2,600	2,710	4

Pore Volumes	Flowrate	Manganese (μg/L) inlet	Manganese (μg/L) outlet	Manganese (μg/L) % change
148		1,530	1,360	-11

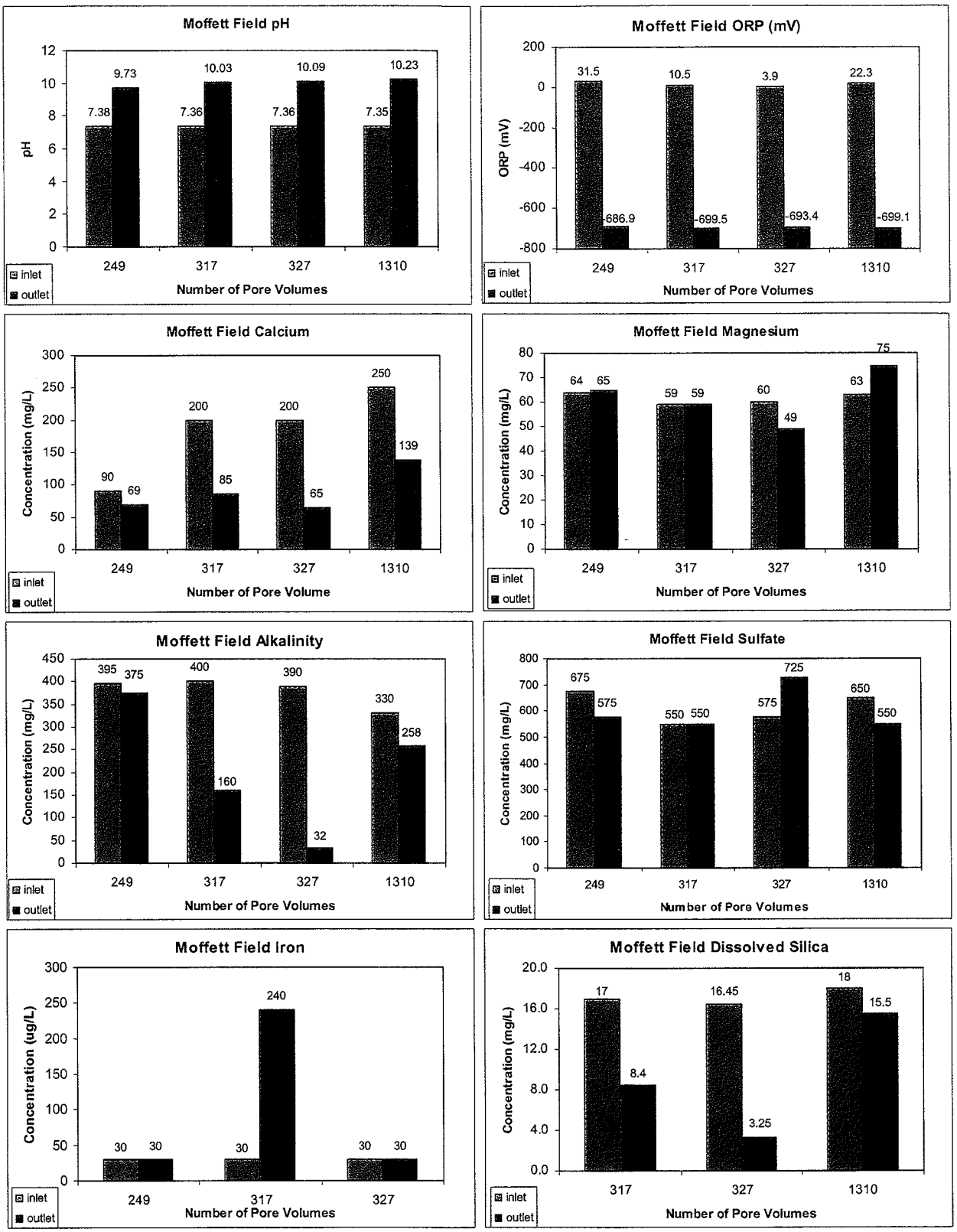

Figure 5-14. Bar Graphs for Moffett Field Column Showing Input and Output Concentrations of Inorganic Analytes (Filtered)

alkalinity is greater than that of calcium. This is true even when calculated on a molar basis. The proportionally higher loss of alkalinity could be precipitation of another carbonate compound, in addition to calcite or aragonite, such as iron carbonate (siderite, $FeCO_3$) or iron carbonate hydroxide ($Fe_2CO_3(OH)_2$).

Magnesium in the effluent is approximately the same as in the influent at the two faster flowrates (25 and 12.5 ft/day), but decreases measurably (-18%) at 6 ft/day. Possible Mg-bearing phases likely to form are magnesium hydroxide (brucite, $Mg(OH)_2$) and magnesium silicate.

Silica concentrations change by -51 and -80 %, corresponding to 12.5 and 6 ft/day. A rebound is also observed when the flowrate is increased (-14 % at 1310 PV).

Changes in the iron and sulfate concentrations do not show particularly consistent patterns. Sulfate concentrations in the effluent decrease at 25 ft/day, remain steady at 12.5 ft/day and increase at 6 ft/day. These results do not indicate that sulfate is converting to sulfide, although a small amount may do so without noticeably affecting the sulfate concentration. In field barriers it is believed that iron concentrations are controlled at very low levels by the solubility of iron sulfides or carbonates. This could certainly explain the behavior of iron in the column test. With the exception of very high iron concentrations in the effluent at 1310 PVs, typical iron concentrations are below detection (30 μg/L).

Inorganic species that were expected to behave conservatively (e.g., sodium, potassium, and chloride) behaved as such. For example, changes in effluent concentrations in unfiltered samples (Table 5-29) were as follows: Na, 4%; K, -4%; Cl, 21%. These results indicate that the iron had no affinities for these species. Interestingly, nitrate was not degraded in the column test, whereas nitrate is typically immeasurable in the Moffett Field reactive cell. This could indicate the residence time in the column was too short for reduction by microbes to occur. Manganese concentration did not change appreciable in the effluent, suggesting that manganese carbonate (rhodochrosite, $MnCO_3$) did not precipitate in the column.

After approximately 1300 pore volumes of water had passed through the Moffett Field column, a bromide tracer test was conducted to determine if the porosity had changed over the course of the evaluation. After momentarily stopping the water flow, 30 mL of 100 mg/L KBr solution was injected into the influent port. The water flow was restarted and maintained at an average rate of 1.89 mL/min, and the bromide concentration in the effluent was monitored continuously with a selective ion probe. The mid-point of the tracer peak emerged approximately 285 minutes after the pump was restarted (see figure in Appendix C). The porosity of the iron was calculated to be 0.518, which was determined by dividing the pore volume determined from the tracer peak (540 mL) by the volume of the column (1042.5 mL). This porosity value is smaller than the value of 0.637 determined by bulk density at the beginning of the column test. Because the methods used to determine porosity in the two situations were different, these values are not directly comparable. However, the difference between them is only about 19%, which suggests that the porosity change over 1300 pore volumes is not very great. Therefore, it appears that any precipitation that occurred in the Moffett Field simulation over the course of the column test

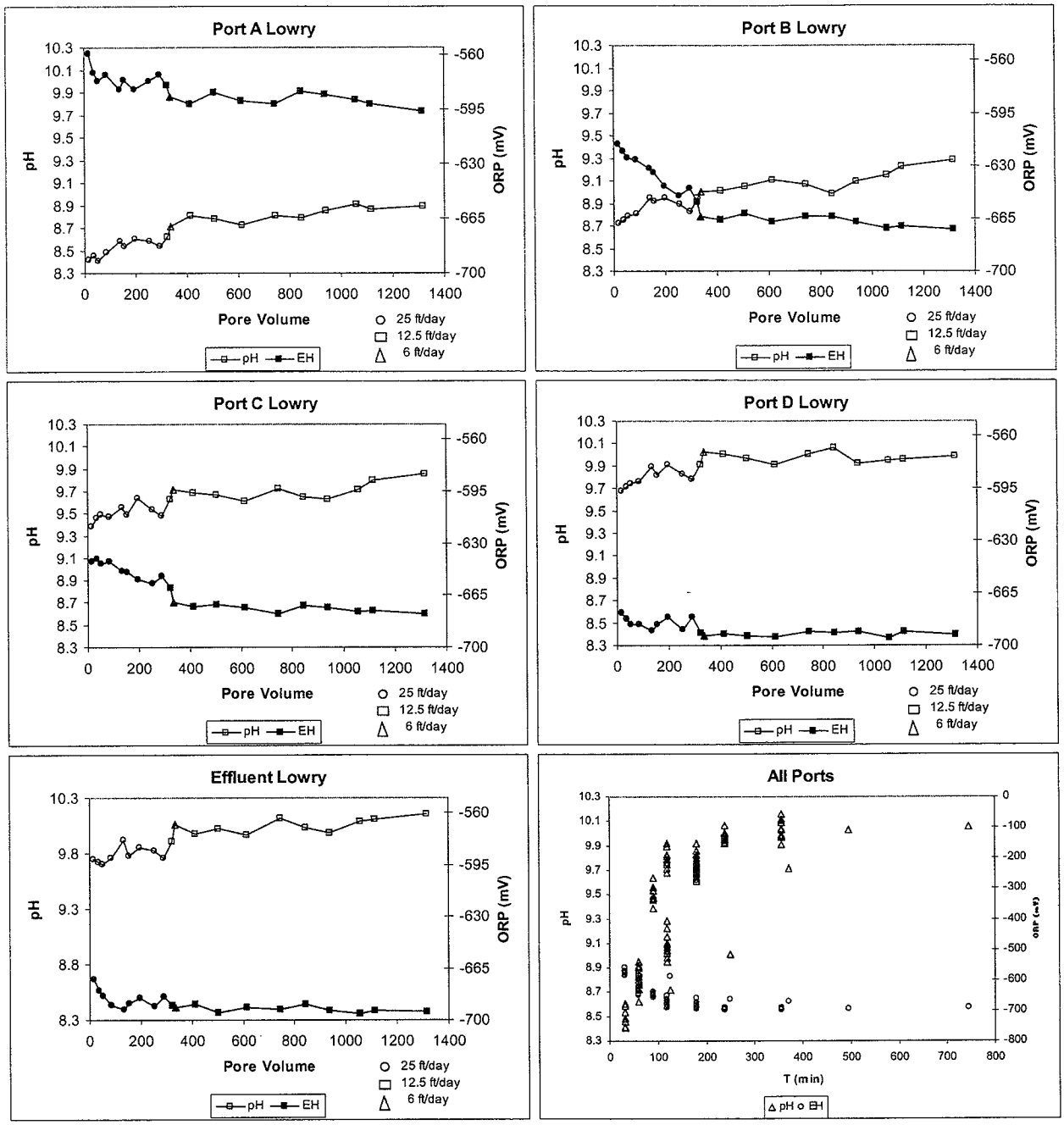

Figure 5-15. pH and ORP Values in the Lowry Column at Different Pore Volumes Ages

evaluation was not appreciable. This result confirms speculation that degradation of performance over time is due to passivation by iron corrosion coatings distributed over all of the iron grains, rather than by infilling of pore space, particularly at the influent end of the column.

5.3.2 Former Lowry AFB Column Simulation. The column set up for the Lowry AFB PRB simulation was conducted in exactly the same manner as the Moffett Field column simulation. The setup and methods are described in Section 4.3.1.7.

5.3.2.1 ORP and pH in the Lowry Column. Trends in pH and ORP measurements were monitored after the initial setup to the completion of the test, which was over 1,300 pore volumes. (See Appendix C) for a compilation of column test measurements). Figure 5-15 shows these results graphically at individual sampling ports and combined into a single plot. At each of the sampling ports the data show a trend of increasing pH values and decreasing ORP values as the number of pore volumes increases. This behavior can be explained by the faster flowrates used at the beginning of the tests and slower flowrates used later. This would have had the effect of shifting the point of equilibrium (or steady state condition) toward the inlet end of the column. However, once the flowrate had been changed, the pH and ORP values returned to an equilibrium (or steady state) condition.

5.3.2.2 TCE Degradation. Water samples were collected periodically for analysis from the inlet and outlet points, and from the four sampling ports. Results of water sample analysis for TCE are shown in Table 5-30. Relative concentrations (c_{rel}) were calculated by dividing concentrations (c) at every sampling point i by the concentration in the effluent (c_0); i.e. $c_{i,rel} = c_i/c_0$. Relative concentrations (presented in Table 5-31) were used instead of actual concentrations to evaluate reaction rates, because the TCE concentration in the feed was not perfectly constant over the course of the test, due to differences in the batch of groundwater and variations in spike levels.

Table 5-30. Results of TCE Measurements (mg/L) in Lowry Column Test

Pore Volumes	Influent	Port A	Port B	Port C	Port D	Effluent
46	77.8	47.6	41.3	38.5	34.2	35.1
84	569	235	107	75.6	55.2	43.6
148	4455	2055	1096	565	294	232
196	445	201	142	129	118	105
229	577	224	172	151	113	101
265	652	279	173	146	103	92.3
324	529	258	176	141	93.1	79.6
482	896	444	261	185	115	86.4
1,023	646	288	222	192	153	134
1,057	583	302	216	188	159	145
1,298	591	305	229	196	161	149

(a) Concentration values are in mg/L.

Table 5-31. Relative TCE Concentrations (C/C_0) in Lowry Column Test[a]

PV	Influent	Port A	Port B	Port C	Port D	Effluent
46	1.00	0.612	0.531	0.495	0.440	0.451
84	1.00	0.412	0.188	0.133	0.097	0.077
148	1.00	0.461	0.246	0.127	0.066	0.052
196	1.00	0.453	0.320	0.291	0.265	0.236
229	1.00	0.388	0.297	0.262	0.196	0.175
265	1.00	0.427	0.266	0.223	0.159	0.141
324	1.00	0.487	0.333	0.267	0.176	0.150
482	1.00	0.495	0.292	0.206	0.128	0.096
1,023	1.00	0.445	0.344	0.297	0.238	0.208
1,057	1.00	0.519	0.370	0.323	0.273	0.250
1,298	1.00	0.516	0.387	0.332	0.273	0.251

(a) Concentration at a sampling location divided by the influent concentration.

Rate constants for TCE degradation were calculated from relative concentration data. As with the Moffett Field column test, it was assumed that reaction rates were first order, and would obey Eq. (1). Residence time was calculated by Eq. (2) ($\tau = xnA/u$), where the porosity for Master Builder iron was 0.652.

As with the Moffett Field column test, the Lowry column test data did not fit a first-order decay curve equally well throughout the entire range. In general, log-linear regressions of the data produced "good" fits after restricting the data points to ports A, B, C, and D (4 points).

Plots of the relative concentration data (Table 5-31) and the regression curves are contained in Appendix C. In these plots closed symbols represent points that were used in the regression analysis and open symbols represent points that were not used. Selection of data points for regression analysis was based on appearance of first-order decay behavior, as described in Section 5.3.1.2. Note that the fitted lines do not intercept the concentration axis at $c/c_0 = 1$ at $\tau = 0$, but instead intercept between 0.12 and 0.74. Table 5-32 lists the results of the regression analysis, which includes the rate constant, k, the standard error, half- life, $t_{½}$ and half-life range, and intercept.

The rate constant and half-life for TCE degradation changed exponentially (see Figures 5-16 and 5-17) as the number of pore volumes increases. Least-squares regression of the rate data gives the following expression for k

$$k\ (\text{min}^{-1})\ 0.013 \exp(-0.0012\ \text{PV}) \qquad (4)$$

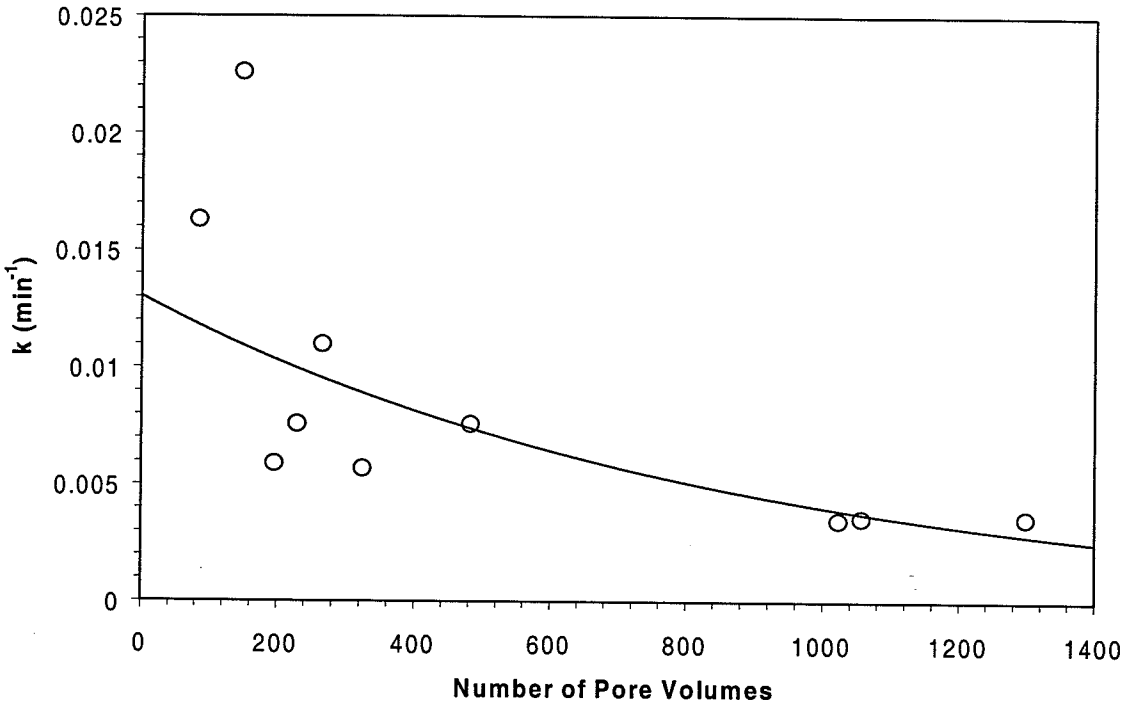

Figure 5-16. Plot of TCE Degradation Rates for Lowry Column at Different Cumulative Pore Volumes

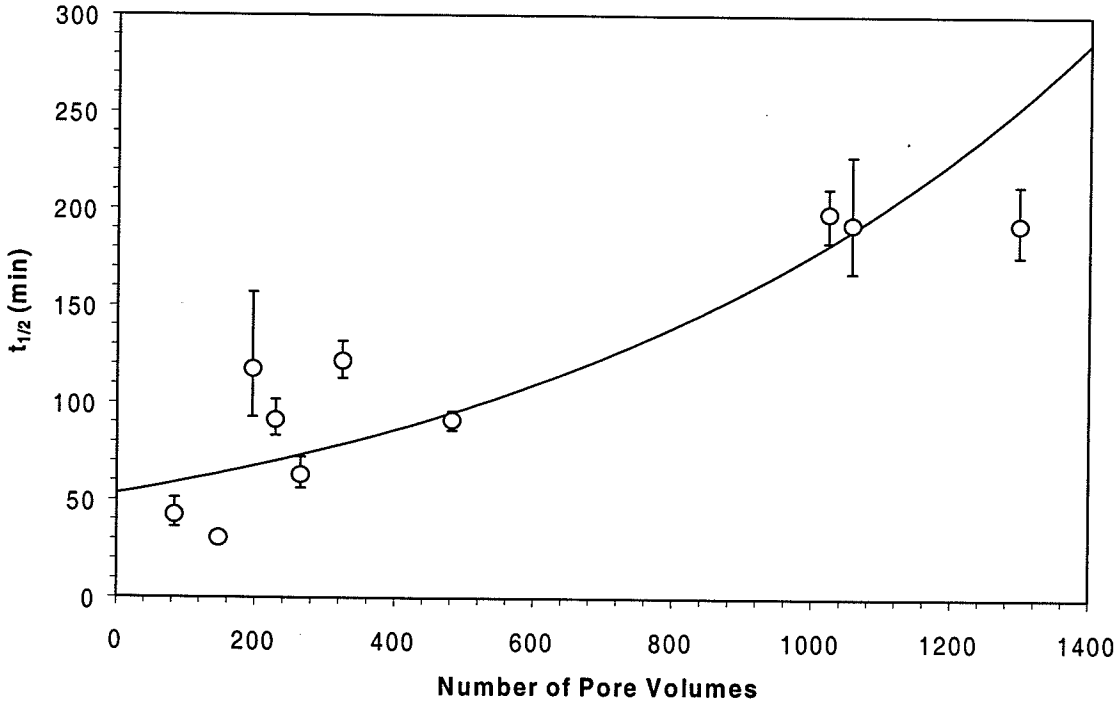

Figure 5-17. Plot of TCE Half-Lives for Lowry Column at Different Cumulative Pore Volumes

Table 5-32. Results of Regression Calculation for Lowry Column Test

Cumulative PVs	Linear Flowrate (ft/day)	Number of Fitted Points	k (min^{-1})	Standard Error	$t_{½}$ (min) Average	(range)	Intercept
84	25	4	0.0163	0.00279	42.5	(36.2 - 51.2)	0.5568
148	25	4	0.0226	0.00017	30.7	(30.4 - 30.8)	0.1162
196	25	4	0.0059	0.00153	117.5	(92.8 - 157)	0.6977
229	25	4	0.0076	0.00076	91.2	(83.2 - 102)	0.7389
265	25	4	0.0110	0.00136	63.0	(56.2 - 72.1)	0.5922
324	12.5	4	0.0057	0.00044	122	(113 - 132)	0.3998
482	12.5	4	0.0076	0.00041	91.2	(86.0 - 95.8)	0.2921
1,023	12.5	4	0.0035	0.00025	198	(183 - 211)	0.6241
1,057	12.5	4	0.0027	0.00017	257	(245 - 279)	0.5032
1,298	12.5	4	0.0030	0.00023	231	(212 - 246)	0.5926

The coefficient of determination (R^2) for the fit is = 0. 6496. This rate of increase for the Lowry simulation is more than three times greater than the rate observed in the Moffett Field column test. The intercept at zero pore volumes is 53 minutes, which is somewhat longer than the 36-minute half-life calculated for the Moffett Field column. As noted in the description of the Moffett Field column, this calculation omits the effect of absorption and gives a number for the half-life of TCE before the iron is conditioned.

The half-life of TCE increased by a factor of approximately 5 times over 1,300 pore volumes of exposure to groundwater from Lowry AFB. Therefore, long-term exposure to groundwater flow is likely to reduce the reactivity of the PRB at Lowry AFB. This increase in half-life is considerably higher for the Lowry AFB column than for the NAS Moffett Field column because of the higher TDS content of the Lowry AFB groundwater.

5.3.2.3 ***Inorganic Measurements.*** Water samples from the inlet and outlet ports were collected at five different pore volume intervals and analyzed for inorganic species. Filtered samples were collected at four such intervals (Table 5-33) and unfiltered samples were collected at all five intervals (Table 5-34).

Comparing changes in concentrations between the inlet and outlet ports reveals the effect of precipitate formation, similar to what is found or believed to occur in field barriers. For convenience, bar graphs showing concentrations of filtered solutions at the two end points are presented in Figure 5-18. For example, pH increased from approximately 7.4 to greater than 10, while ORP decreased from positive numbers to nearly –700 mV. The change in pH and ORP become greater as the flowrate was decreased, as can also be seen in the full record of pH and ORP measurements presented in Figure 5-15. This effect is due to the system achieving steady state conditions as residence times increase. It is known from core sample analysis and geochemical modeling that precipitation of calcium carbonate can accompany a pH rise if the groundwater is close to saturation before encountering the iron.

Table 5-33. Inorganic Analysis of Filtered Water Samples from Lowry Column

PVs	Flowrate (ft/day)	pH Inlet	pH Outlet	pH % change	ORP (mV) Inlet	ORP (mV) Outlet	ORP (mV) % change
252	25	7.41	9.83	33	43.9	-691.0	-1,674
324	12.5	7.45	9.91	33	21.4	-690.4	-3,326
334	6	7.39	10.06	36	28.3	-691.4	-2,543
1,316	12.5	7.45	10.16	36	20.7	-694.5	-3,455
Pore Volumes		**Calcium (mg/L) Inlet**	**Calcium (mg/L) Outlet**	**Calcium (mg/L) % change**	**Magnesium (mg/L) Inlet**	**Magnesium (mg/L) Outlet**	**Magnesium (mg/L) % change**
252	25	146	41.8	-71	75	33.1	-56
324	12.5	279	177	-37	70	73	4
334	6	276	69	-75	70	44.9	-36
1,316	12.5	277	210	-24	72	69	-4
Pore Volumes		**Alkalinity (mg/L) Inlet**	**Alkalinity (mg/L) Outlet**	**Alkalinity (mg/L) % change**	**Sulfate (mg/L) Inlet**	**Sulfate (mg/L) Outlet**	**Sulfate (mg/L) % change**
252	25	510	150	-71	1,400	1,425	2
324	12.5	610	315	-48	1,375	1,350	-2
334	6	610	65	-89	1,250	1,100	-12
1,316	12.5	525	420	-20	1,175	1,300	11
Pore Volumes		**Dissolved Silica (mg/L) Inlet**	**Dissolved Silica (mg/L) Outlet**	**Dissolved Silica (mg/L) % change**	**Iron (μg/L) Inlet**	**Iron (μg/L) Outlet**	**Iron (μg/L) % change**
252	25	NA	NA	NA	40	< 30	> -25
324	12.5	19.4	8.8	-55	< 30	< 30	N/A
334	6	17.6	2	-89	< 30	< 30	N/A
1,316	12.5	18.3	10.4	-43	180	1,760	878

The possibility of calcium carbonate precipitation can be observed by the changes in concentrations of calcium and alkalinity (see Table 5-33 and Figure 5-18). In the Lowry simulation, changes in calcium concentration and alkalinity are concomitant to one another. Also, the percentage changes are greatest at the slowest flowrate (6 ft/day), which corresponds to the highest residence time inside the column. However, as in the Moffett Field simulation, the decline in calcium on a molar basis is lower than that of alkalinity species, bicarbonate and carbonate. Therefore, these data suggest that not only is calcium carbonate precipitating within the iron, but some other carbonate phases must be precipitating as well. In terms of mass, the magnesium concentrations do not change very much. The most likely carbonate precipitate to occur is an iron carbonate.

Table 5-34. Inorganic Analysis of Unfiltered Water Samples from Lowry Column

PVs	Flowrate (ft/day)	Calcium (mg/L)			Magnesium (mg/L)		
		Inlet	Outlet	% change	Inlet	Outlet	% change
148	25	268	298	11	65	72	11
252	25	143	95	-34	75	66	-12
324	12.5	276	136	-51	69	64	-7
334	6	270	89	-67	69	79	14
1,316	12.5	263	224	-15	71	72	1
Pore Volumes	**Flowrate (ft/day)**	**Alkalinity (mg/L)**			**Sulfate (mg/L)**		
		Inlet	Outlet	% change	Inlet	Outlet	% change
148	25	329	453	38	1880	2,020	7
252	25	575	415	-28	1350	1,175	-13
324	12.5	590	278	-53	1225	1,375	12
334	6	580	95	-84	1300	1,275	-2
1,316	12.5	453	443	-2	1250	1,275	2
Pore Volumes	**Flowrate (ft/day)**	**Dissolved Silica (mg/L)**			**Iron (μg/L)**		
		Inlet	Outlet	% change	Inlet	Outlet	% change
148	25	21.3	14.9	-30	300	40,100	13,267
252	25				50	2,820	5,540
324	12.5	18.75	7.75	-59	30	2,730	9,000
334	6	17.9	2.37	-87	30	610	1,933
1,316	12.5	18.3	10.4	-43	190	21,100	11,005
Pore Volumes	**Flowrate (ft/day)**	**Sodium (mg/L)**			**Potassium (mg/L)**		
		Inlet	Outlet	% change	Inlet	Outlet	% change
148	25	440	530	20	2.13	2.04	-4
Pore Volumes	**Flowrate (ft/day)**	**Chloride (mg/L)**			**Nitrate (mg/L)**		
		Inlet	Outlet	% change	Inlet	Outlet	% change
148	25	119	174	46	1.65	1.73	5
Pore Volumes	**Flowrate (ft/day)**	**TOC (mg/L)**			**Residue, Dissolved (mg/L)**		
		Inlet	Outlet	% change	Inlet	Outlet	% change
148	25	7.3	10.2	40	2,940	3,320	13
Pore Volumes	**Flowrate (ft/day)**	**Manganese (mg/L)**					
		Inlet	Outlet	% change			
148	25	1,360	1,170	-14			

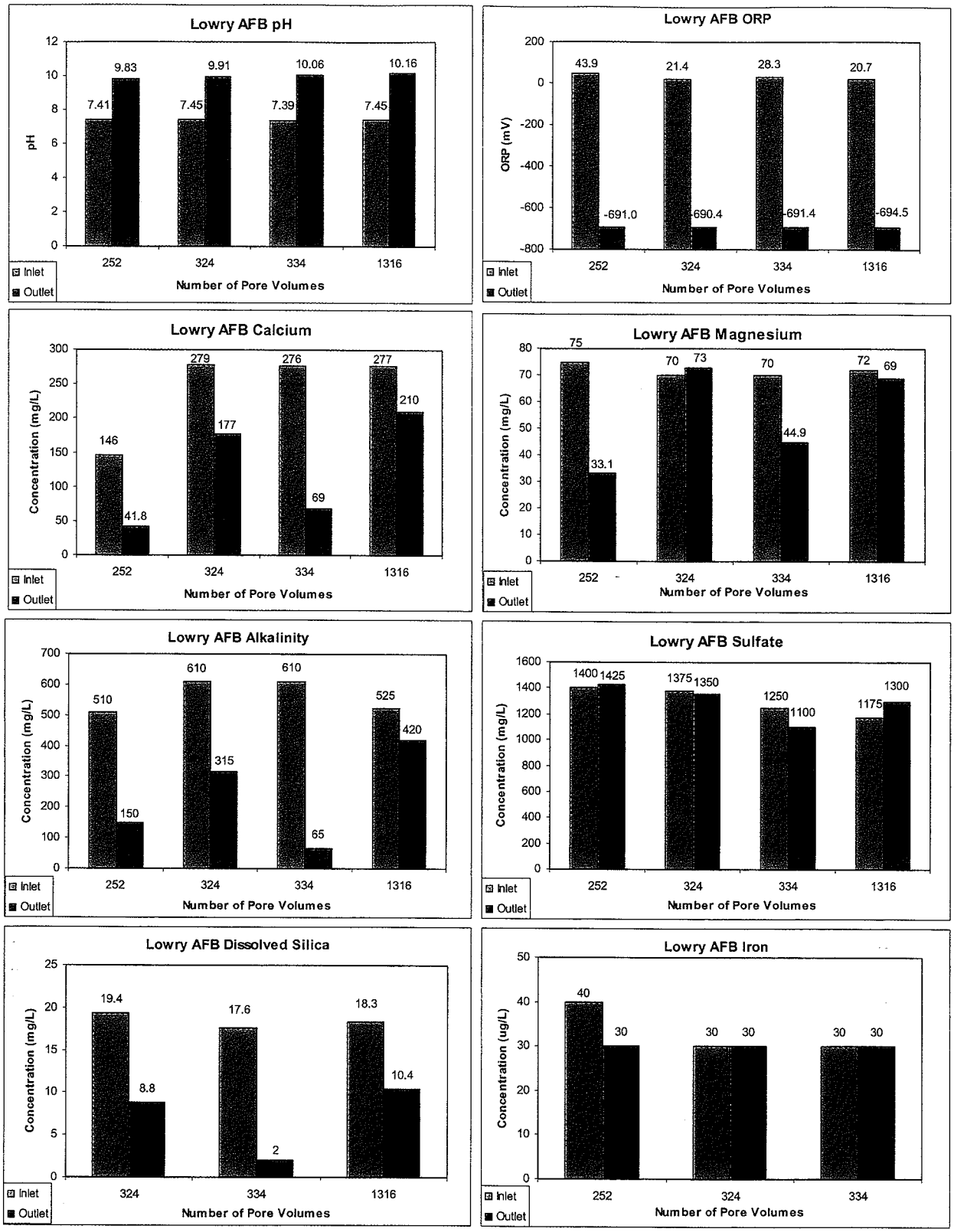

Figure 5-18. Bar Graphs Showing Input and Output Concentrations of Inorganic Analytes (Filtered)

Iron and sulfate concentrations do not change significantly throughout the testing. The sulfate data do not indicate a conversion to sulfide, although a small amount may do so without noticeably affecting the sulfate concentration. However, the measured iron concentrations do not rule out the presence of iron sulfides or carbonates, which may be controlling the iron at very low levels. With the exception of very high iron concentrations in the effluent at 1,316 PVs, typical iron concentrations are below detection (30 mg/L).

Sodium and chloride concentration are higher in the unfiltered effluent than in the influent (Table 5-34). The relative change is 20% (Na) and 46% (Cl). Because both Na and Cl are expected to behave conservatively in an iron system, these results are unexpected. These number could indicate that Na and Cl are desorbing from the iron or from colloidal material, possibly as a result of pH or other changes in the water. Potassium and nitrate concentrations, on the other hand, do not change significantly between the influent and effluent.

5.3.2.4 Analysis of Iron Cores from the Lowry AFB Column Test. At the conclusion of the Lowry simulation, the iron inside the column was dried by alternately flowing acetone and dry nitrogen gas through one end of the column. After drying, the glass was scored and taken inside a nitrogen-filled glove box, where the column was broken open along the score marks and the iron was removed in eight sections (Table 5-35). A portion of each section of iron was crushed and transferred to small vials for analysis by XRF and XRD. Results are shown in Tables 5-36 and 5-37.

Table 5-35. Dimensions of Iron Sections from Lowry AFB Column Test

Sample ID	Section (Distance from inlet in inches)
LOW 1	0 – 2
LOW 2	2 – 5
LOW 3	5 – 10
LOW 4	10 – 15
LOW 5	15 – 20
LOW 6	20 – 25
LOW 7	25 – 36

Elemental analysis of the granular iron reveals that, in addition to iron, Ca and S are also present. It can be seen in Table 5-36 that Ca ranges from 10 to 15% and S ranges from 6 to 12%, according to XRF. Other elements such as Cr, Cu, and Mn were analyzed but not detected. It should be noted that the XRF analysis includes only elements with atomic weight greater than that of Al. Therefore, the weight percentages listed in Table 5-36 are relative, rather than absolute values. Important missing elements include C, O, Mg, and Al. Also, Si was not reported because none was detected in the samples.

Table 5-36. Results of XRF Analysis of Five Iron Samples from the Lowry Column Test

Sample ID	LOW 1	LOW 2	LOW 3	LOW 4	LOW 7
Ca	14	21	13	15	10
Cr	ND	ND	ND	ND	ND
Cu	ND	ND	ND	ND	ND
Fe	72	66	79	75	82
Mn	ND	ND	ND	ND	ND
S	12	12	6	9	6

Values are in weight percent
ND = not detected; approximately < 1%
Light elements with atomic numbers less than Al were not detected.

Table 5-37. Results of XRD Analysis from Lowry Column Simulation

Sample ID	Calcite	Aragonite	Iron	Magnetite	Carbon	Iron Carbonate Hydroxide
Formula	$CaCO_3$	$CaCO_3$	Fe	Fe_3O_4	C	$Fe_2(OH)_2CO_3$
PDF #	05-0586	41-1475	06-0696	19-629	26-1080	33-650
LOW-1	Minor	ND	Major	Minor	Minor	ND
LOW-2	Minor	ND	Major	Minor	Minor	Trace
LOW-3	ND	Minor	Major	Minor	Minor	ND
LOW-4	ND	Minor	Minor	Minor	Minor	Minor
LOW-5	ND	Minor	Major	Minor	Minor	ND
LOW-6	Minor	ND	Major	Minor	Minor	ND
LOW-7	ND	ND	Major	Minor	Minor	Trace

ND = not detected.

5.4 Geochemical Modeling

XRD analysis indicates that the granular iron contains calcium carbonate compounds in the first through sixth sections (0 – 25 inches), but none were detected in the final section (25 – 36 inches). Interestingly, the form of the calcium carbonate was calcite (hexagonal) in the initial two sections of iron (0 – 5 inches) and in the sixth section; then aragonite (orthorhombic) was found in the third through fifth sections (5 – 20 inches). No $CaCO_3$ was reported in the final section, possibly because of the instrument detection limit. Disregarding surface effects, calcite is the more stable phase under these experimental conditions. However, aragonite is known to precipitate in lieu of calcite certain environments, including when favored to do so by surface effects. Both calcite and aragonite are minor phases in the column test samples; iron is the predominant crystalline phase. Assuming that all of the Ca is present as $CaCO_3$, the average

amount of $CaCO_3$ in the samples is 30%; the following amounts were calculated to be present in individual sections:

- LOW 1 – 29% $CaCO_3$
- LOW 2 – 40% $CaCO_3$
- LOW 3 – 28% $CaCO_3$
- LOW 4 – 31% $CaCO_3$
- LOW 7 – 22% $CaCO_3$

These are approximate values, which are likely overestimates, because of the aforementioned missing elements that are likely to be present, but were not detectable by XRF.

According to Table 5-36, the S content of the iron ranges from 6 to 12%, with the high concentrations near the water influent end of the column. Because no sulfur-bearing phases were detected by XRD, the form of the S phases is not known. Predictions based on geochemical modeling indicate that iron sulfide phases might form. Also, silt from inside the Moffett Field barrier contained the calcium-aluminum-sulfate mineral, ettringite; however, ettringite was not detected in the silt from the Lowry barrier.

Other mineral phases detected by XRD were magnetite, graphitic carbon, and iron carbonate hydroxide (Table 5-37). Magnetite and graphitic carbon are present in the granular iron received from the manufacturer. Because the analysis was qualitative, it is not known whether any additional magnetite was produced during the column test.

Analysis of core samples from the field barrier at Lowry revealed the following minerals: iron, magnetite, wustite, quartz, graphitic carbon, hematite, hydrous iron oxides, and silicates (see Table 5-20). Interestingly, no form of calcium carbonate was detected in the field barrier. One explanation for the disparity in calcium carbonate is that groundwater flow through the barrier could be slow. If that is the case, then most of the calcium carbonate would have precipitated in the upgradient end of the iron cell, where it is possible that none of the core samples were taken.

Geochemical modeling was used to evaluate the types of precipitates that are likely in the iron and to understand the precipitation processes seen in the field evaluation and column tests.

5.4.1 Geochemical Modeling Approach. Reductive dechlorination of TCE and other chlorinated VOCs in PRBs is driven by corrosion of zero-valent iron. In general, corrosion processes are affected by groundwater composition, temperature, and properties of the metal such as purity, heat treatment, and the presence of surface coatings. It is well know that corrosion is affected by pH, salinity, alkalinity, and hardness of the water that comes into contact with the metal. Typically, granular iron that is used in permeable reactive barriers is a cast material with purity of approximately 92-95% iron. For example, Peerless Metal Powders and Abrasives reports the composition of its product to be 92% Fe, 3.5% C, 2.5% Si, 1.0% Mn and 1.0% Cu. Granular iron commonly has coatings of magnetite, hematite, wustite, and reduced (graphitic) carbon.

Corrosion of iron is an oxidation process that releases ferrous ions and electrons, as show by the half-cell reaction

$$Fe^0 \rightarrow Fe^{2+} + 2e^- \tag{5}$$

When oxygen is present in aqueous solution, it can undergo reduction according to

$$\frac{1}{2}O_2 + H_2O + 2e^- \rightarrow 2OH^- \tag{6}$$

Combining Eqs. (1) and (2), results in an oxidation-reduction (redox) reaction that describes oxygen "scrubbing" by iron

$$Fe^0 + \frac{1}{2}O_2 + H_2O \rightarrow Fe^{2+} + 2OH^- \tag{7}$$

This reaction is relatively fast, with a first-order rate constant of 4×10^{-7} mol m^{-2} s^{-1}, which is multiplied by the activity of dissolved oxygen, $[O_{2(aq)}]$ (Yabusaki et al., 2001). At relatively slow advective groundwater movement, typical of flow in permeable barriers, dissolved oxygen would become depleted very quickly inside the iron zone. This was found to be the case in column tests conducted by General Electric, in which dissolved oxygen was found to be consumed at the entrance and did not affect the bulk of the iron (Mackenzie et al., 1999). Furthermore, many contaminated aquifers are anoxic, so the amount of oxygen available for reaction is small. For these reasons, neither the pH of the water nor the amount of ferrous ion released inside a reactive barrier are significantly affected by the reaction describe by Eq. (3).

After oxygen has been scrubbed from the groundwater, anoxic corrosion of the iron can then take place. In this regime, oxidation of the iron can still occur, but it is coupled to the reduction of water (hydrolysis) according the following reaction step

$$2H_2O + 2e^- \rightarrow 2OH^- + H_2 \tag{8}$$

Combining Eqs. (1) and (4), results in a reaction describing the hydrolysis of water by iron

$$Fe^0 + 2H_2O \rightarrow Fe^{2+} + 2OH^- + H_2 \tag{9}$$

The reaction rate for Eq. (5) has been reported to be 0.7 ± 0.05 mmol/kg-Fe/day (Reardon, 1995) and 0.06 ± 0.003 mmol/kg-Fe/day (Fort, 2000), where both values predict slower corrosion rates than would normally occur under toxic conditions, i.e., Eq. (3). In both studies, corrosion rates were determined by evolution of hydrogen gas, which is expected to be constant, according to Eq. (5). The roughly factor of ten difference between Reardon's and Fort's rate constants may have to do with differences in salinity, alkalinity, and pH, of the water used in their experiments, as well as grain size and its effect on surface area (as well as surface porosity) and product manufacturer. Reardon's study was based on Master Builder iron, while Fort used Peerless iron. These materials may have undergone different treatments prior to being sold and therefore could have had different corrosion coatings that may have affected passivation of the iron at the beginning of the experiments (Fort, 2000).

More recently, Yabusaki et al. (2001) derived the rate constant for Eq. (5) from a column study (PRC, 1996) that used Peerless iron and Moffett Field groundwater. In this study, a 4 ft long, 4 in diameter column was packed with an equivalent mass mixture of iron and sand. The estimated rate constants for hydrolysis ranged from 3×10^{-12} to 5×10^{-12} mol m^{-2} s^{-1}. Using a specific surface area of 1.5 m^2/g (Johnson et al., 1996), the hydrolysis rates are 0.39 to 0.65 mmol/kg-Fe/day, which are very close to Reardon's (1995) results. While these rate constants are much larger than the value obtained by Fort (2000) for the same manufacturer of iron, the disparity could be due to changes in manufacturing process during the 5-year time span, and differences in reactivity caused by dissolved components in water. For example, Fort (2000) used Madison, Wisconsin tap water, which is pumped for a deep, dolomitic aquifer. The groundwater makeup for these two studies is compared in Table 5-38. Both waters have similar alkalinity, but Moffett Field groundwater has much higher levels of all major ions. Higher chloride and sulfate concentrations, in particular, could be responsible for the faster corrosion of Peerless iron in Moffett Field groundwater. Scherer et al. (1998) point out that sustained reduction reactions require the existence of localized defects in the passive oxide films (by corrosion pitting, for example) in order for electrons to be transferred to the surface.

Table 5-38. Comparison of Typical Analytes for Moffett Field Groundwater and Madison Tap Water

Parameter	Moffett Field Groundwater [(a)]	Madison Tap Water [(b)]
pH	7.1	7.1
Total Alkalinity (as $CaCO_3$)	300	290
Sodium	32	2
Magnesium	60	34
Calcium	155	71
Iron	< 0.02	0.24
Chloride	42	0.6
Sulfate	350	7
Nitrate	3.2	0.5
Fluoride	0.15	0.1

(a) Typical values during a two year long monitoring study (Battelle, 1998).
(b) Fort (2000).

Evidence from field evaluations (Battelle, 2000) and laboratory experiments (Sivavec, 2000) shows that pH values tend to become uniform in the anoxic regime after moderate residence times, which can be explained by steady state oxidation of iron. The existence of steady state behavior makes it possible to simulate conditions inside the barrier with a modeling code and predict the effects of corrosion on secondary mineral precipitation and changes in pore water chemistry.

To correctly model the interaction between iron and solution requires rate information for mineral precipitation reactions that are *known* to occur inside the barrier. This approach was used successfully by Yabusaki et al. (2001). However, precipitate formation inside iron barriers

is not always well known. Moreover, mineral phases determined by optical techniques or x-ray diffraction may not be well characterized. This is particularly true when materials are amorphous or poorly crystalline, and if their compositions vary greatly due to solid solution behavior (e.g., "green rusts"). Therefore, some assumptions are normally made about the phases involved. By modeling different sets of potential precipitates, it is generally possible to deduce the most likely controlling reactions based on a comparison of predicted parameters (e.g., pH, Eh, dissolved species) with measured values. Unfortunately, precipitation rates are not all known with great accuracy, and reaction kinetics are complicated by environmental factors such as surface energy effects, solid solution behavior, temperature, salinity, and particle size.

In this study, a geochemical modeling code was used to simulate the *reaction path* as iron interacts with the solution to simulate steady state corrosion of iron and to understand geochemical conditions inside a barrier. This approach was used to explore additional factors that may affect barrier performance. In contrast to the kinetic modeling study conducted by Yabusaki et al. (2001), the objective of reaction path modeling is to develop a better understanding of the overall process of precipitate formation, rather than predicting precipitation dynamics inside a column or barrier. In reaction path modeling, a small amount of iron is allowed to dissolve, then equilibrium is calculated using thermodynamic constraints. The size of the increments can be made arbitrarily small, so the evolution of the system can be observed in small steps. For the reaction path approach to be valid, the aqueous species and solid phases (other than iron) must equilibrate quickly, relative to the time-scale of process. In a real system, the appropriate time-scale is the residence time of the water inside the reactive medium, which is typically several hours or days, depending on thickness and flowrate. In the column tests conducted for this study, as well as in the field PRBs, steady state conditions are believed to prevail, based on pH, Eh, and ion concentration profiles. Therefore, the modeling approach is assumed to be valid.

The geochemical modeling code PHREEQC (Parkhurst and Appelo, 1999) was used to perform the simulations. The thermodynamic database was adapted from *thermo.com.V8.R6.230*, which was prepared by Jim Johnson at Lawrence Livermore National Laboratory (LLNL), in Geochemist's Workbench format, and converted to PHREEQC format by Greg Anderson and David Parkhurst.

The modeling runs were intended to simulate stepwise equilibration of Moffett Field groundwater with zero-valent iron. Results of a typical water analysis was used for the input parameters. Initially, the model was run to determine if the water was oversaturated with respect to any mineral phases. Because the water was found to be slightly oversaturated with respect to calcite, the input data were modified by allowing the code to simulate calcite saturation. In addition, because iron levels were typically below the detection limit of 0.02 mg/L, the program was allowed to simulate saturation with respect to goethite (FeOOH), a common soil mineral with very low solubility. These preconditions requiring calcite and goethite saturation ensured that no the water was not oversaturated with respect to any mineral phase prior to dissolving zero-valent iron. Finally, charge balance was imposed by addition of sodium. Results of the pre-equilibration step are shown in Table 5-39.

Table 5-39. Input Parameters for Moffett Field Groundwater after Pre-equilibration

Elements	Concentration	
	Molality	mg/L
Alkalinity (as $CaCO_3$)	7.85E-03	393
Ca	4.11E-03	165
Cl	1.13E-03	40.1
Fe	1.79E-08	0.0010
K	5.12E-05	2.00
Mg	2.47E-03	60.1
Na	4.57E-03	105
SO_4^{-2}	5.21E-03	501
SiO_2	1.88E-04	18.0
pH	6.88	SU
Eh	91.5	mV

Zero-valent iron was allowed to dissolve in increments of 1 mmole. After each increment, the model calculates whether the solution is oversaturated with respect to any solid phases in the thermodynamic database. If any of these compounds could reasonably be expected to precipitate on the time-scale of the column tests, they were allowed to do so and the equilibrium solution was calculated accordingly. Examples of compounds likely to precipitate from solution include carbonates and hydroxides such as calcite, brucite, $Fe(OH)_2$ and green rusts. Names and formulas of potential phases are listed in Table 5-40.

If the oversaturated compounds were not expected to precipitate, either because they are know to form only at high temperatures or pressures, or if precipitation kinetics are very long, they were not allowed to precipitate and the solution remained oversaturated with respect to these phases. Examples of compounds in this group include most silicates and oxides. Note, that one silicate compound, tobermorite-14Å, is allowed to precipitate if required to maintain equilibrium. Tobermorite is an amorphous calcium silicate hydrate that is an important phase in hydration of hydraulic cement. Tobermorite was included in the database as a potential sink for dissolved silica, which was found to decline significantly inside the columns and field barriers. No other

siliceous minerals were identified in the LLNL database which we thought to be likely possibilities for precipitation under conditions inside the columns or field barriers.

Iron-bearing mineral phases are very important to the modeling exercise, because they are potential sinks for the dissolving zero-valent iron. Without them, aqueous iron concentrations would become unrealistically high. In addition, their presence or absence can affect pH, alkalinity, sulfate, and sulfide, depending on whether they contain hydroxide, carbonate, sulfate, or sulfide groups. To examine the implications of precipitating iron-bearing compounds, four different cases were modeled, which are summarized in Table 5-41.

Table 5-40. Formulas for Mineral Phases with Favorable Precipitation Kinetics

Mineral	Formula
Aragonite	$CaCO_3$ (*ortho*)
Brucite	$Mg(OH)_2$
Calcite	$CaCO_3$ (*rhom*)
Ferrous Hydroxide	$Fe(OH)_2$
Ferric Hydroxide	$Fe(OH)_3$
Green Rust I	$3Fe(OH)_2\ Fe(OH)_2Cl\ nH_2O$ [(a)]
Green Rust IIa	$4Fe(OH)_2\ 2Fe(OH)_3\ [SO_4\ 2H_2O]$ [(b)]
Green Rust IIb	$4Fe(OH)_2\ 2Fe(OH)_3\ [CO_3\ 2H_2O]$ [(c)]
Mackinawite	FeS
Magnesite	$MgCO_3$
Magnetite	Fe_3O_4
Marcasite	FeS_2
Siderite	$FeCO_3$
Tobermorite-14Å	$Ca_5Si_6H_{21}O_{27.5}$
Tobermorite-11Å	$Ca_5Si_6H_{11}O_{22.5}$
Tobermorite-9Å	$Ca_5Si_6H_6O_{20}$

(a) $3 \geq n \geq 2$ Refait and Génin (1994)
(b) Génin et al. (1996)
(c) Odziemkowski et al. (1998)

Table 5-41. Minerals Considered in Modeling Cases

All	Calcite, Magnesite, Brucite, $Fe(OH)_2$, Tobermorite-14Å			
Case 1	Siderite	Mackinawite	Marcasite	—
Case 2	—	Mackinawite	Marcasite	—
Case 3	Siderite	—	—	—
Case 4	Siderite	Mackinawite	Marcasite	Magnetite

Some phases were common to all runs and are listed as such in Table 5-41. Note that the minerals shown are only those that precipitated at some point in the modeling runs. Aragonite, for example, is not shown, because it was less stable than calcite in each of the runs. Similarly, tobermorite-14Å was the only such compound to have a stability region in the simulations.

Three types of iron-bearing minerals were considered in the cases listed in Table 5-41. These were, iron carbonate, iron sulfide (mackinawite and marcasite), and magnetite. Green rusts were not evaluated due to insufficient thermo-chemical data. Iron carbonate (siderite) has often been cited as a precipitate in iron barriers (Puls et al., 1995; Battelle, 1998). Also, iron sulfides are also thought to be possible, due to bacterial reduction of sulfate. Magnetite can be converted from $Fe(OH)_2$ at low temperature (> 0°C) under anoxic conditions by a disproportionation reaction (Schikorr, 1929):

$$3Fe(OH)_2 \rightarrow Fe_3O_4 + H_2 + 2H_2O \quad (10)$$

At temperatures typical of most groundwater environments, the Schikorr reaction is thought to be too slow to quantitatively convert $Fe(OH)_2$ to Fe_3O_4 (Reardon, 1995). However, magnetite has been observed to form on electrolytic iron powder after only 17 hours (Odziemkowski et al., 1998). Because magnetite is the predominant oxide coating on zero-valent iron commonly used in permeable barriers, it is difficult to determine whether additional magnetite forms inside barriers by the Schikorr reaction.

5.4.2 Geochemical Simulation Results. The purpose of these cases was to explore the effects different reaction pathways on groundwater composition. Results of these simulations are lengthy, and therefore, graphical representations will be used to illustrate the behavior of each of the four systems. Results for the first case are described below and the results for all four cases are presented in Appendix C.

Case 1. Iron carbonate and sulfide precipitation allowed. Figure 5-19 shows the pH and Eh profiles that were generated by reaction path modeling, according to the phase constraints for Case 1 (Table 5-35). It can be seen that the initial pH and Eh values are 6.88 and 91.5 mV, respectively, in accordance with the input parameters (Table 5-33). In these simulations the amount of iron reacted ranges from 1 to 50 mmoles per liter of pore water. As zero-valent iron is allowed to react with the groundwater, the pH increases and Eh decreases rapidly at first, then change more slowly. In this case there appear to be three regions where pH and Eh are somewhat stable: at approximately 6 mmol Fe/L (pH ~ 9.8; Eh ~ -350); 20 mmol Fe/L (pH ~ 10.8; Eh ~ -430); 45 mmol Fe/L (pH ~ 12; Eh ~ -560).

Figure 5-20 shows that alkalinity, total calcium, and total sulfate concentrations decrease rapidly in the first part of the simulation. These changes in dissolved species concentrations result from precipitation of solid phases, which will be discussed shortly. As more iron dissolves, the alkalinity and calcium concentrations increase. This is due to instability of phases that control the concentrations of these ions. Figure 5-21 shows the concentration profiles for dissolved silica, total ferrous iron, and total magnesium. Silica levels remain unchanged until approximately 30 mmoles Fe/L have reacted, then silica drops to low concentrations. Iron (II) concentration rise to a maximum near 4 mg/L at 1 mmol Fe/L, then decrease to low concentration (minimum values are near 0.2 mg/L). Magnesium concentrations decrease from the initial concentration of 60 mg/L to < 1 mg/L after approximately 13 mmoles Fe/L have reacted.

Figures 5-22 shows the masses of precipitates and the sum (total mass) of the individual phases. It can be seen that ferrous hydroxide is the dominant solid phase after approximately 10 mmole Fe/L have dissolved. Figure 5-23 shows the same results without ferrous hydroxide and the sum to better illustrate the behavior of the minor compounds. It can be seen that calcite, siderite, and marcasite precipitate immediately. Other minerals do not begin precipitating until add ional iron dissolves (brucite, 5 mmol Fe/L; $Fe(OH)_2$, 6 mmol Fe/L; tobermorite-14Å, 32 mmol Fe/L).

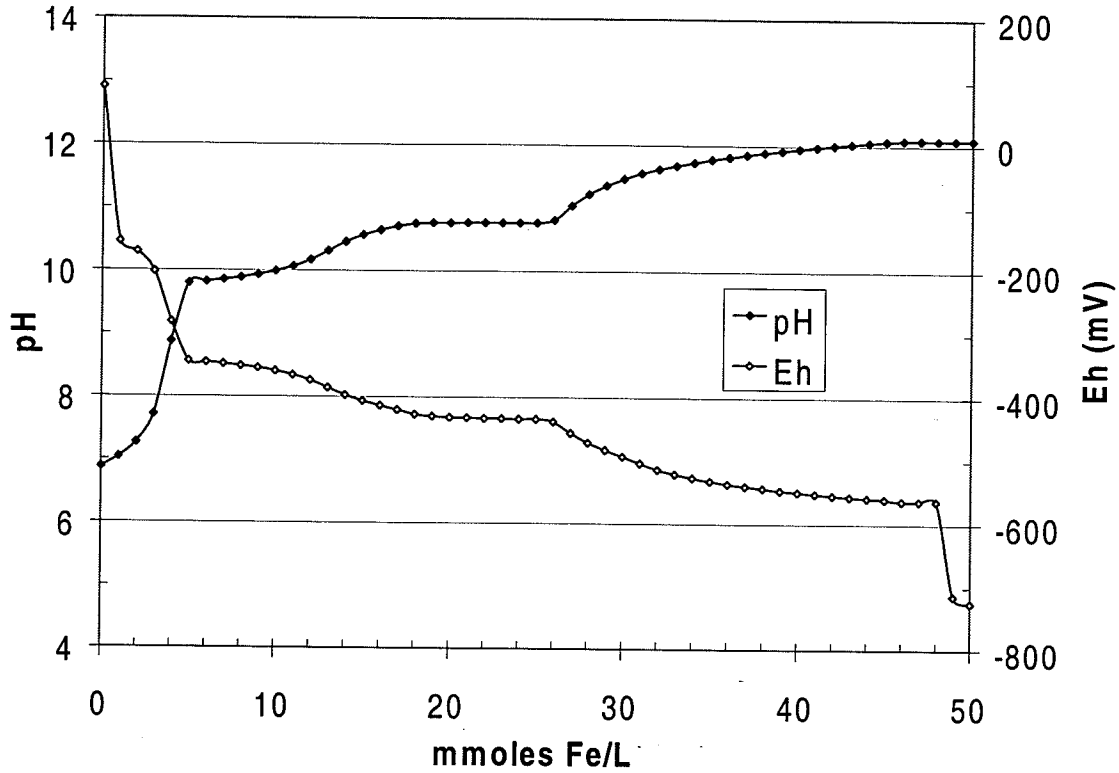

Figure 5-19. pH and Eh Profile Based on Case 1

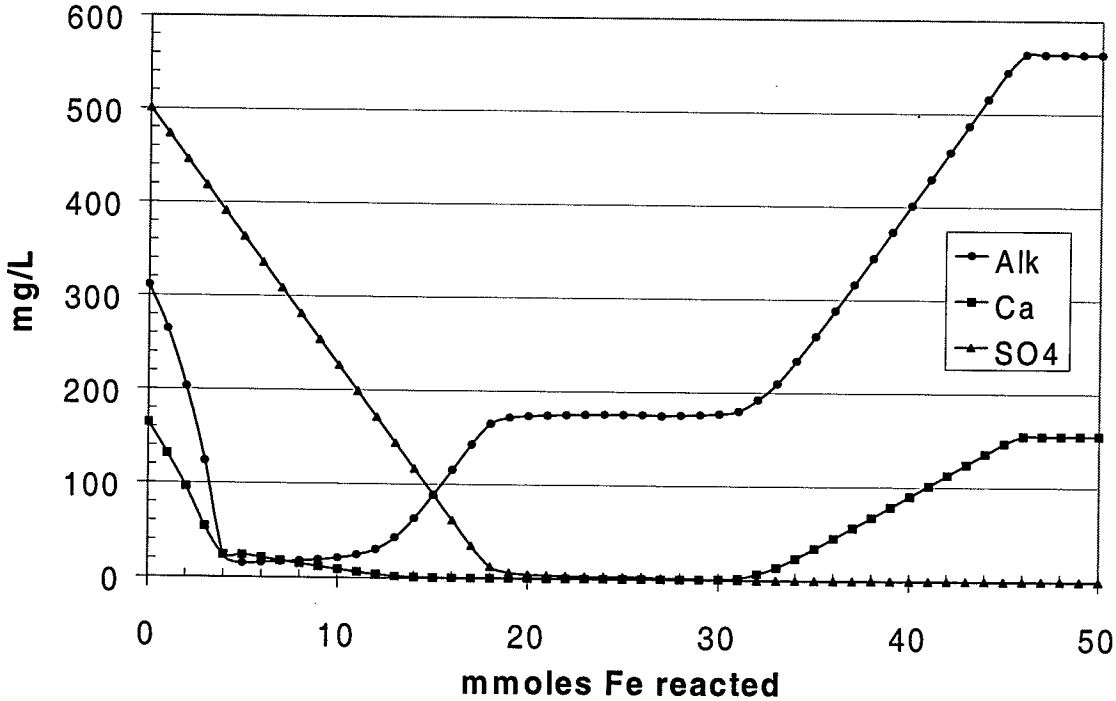

Figure 5-20. Profiles of Alkalinity, Ca, and Sulfate Based on Case 1

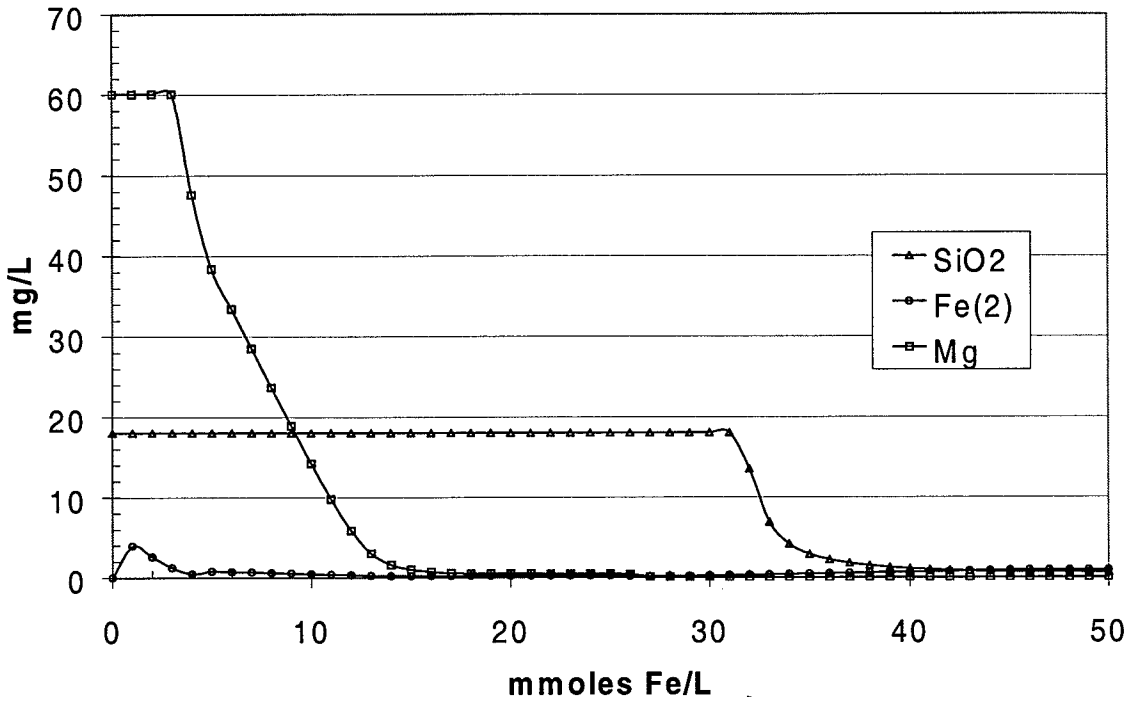

Figure 5-21. Profiles of Silica, Fe(II), and Mg Based on Case 1

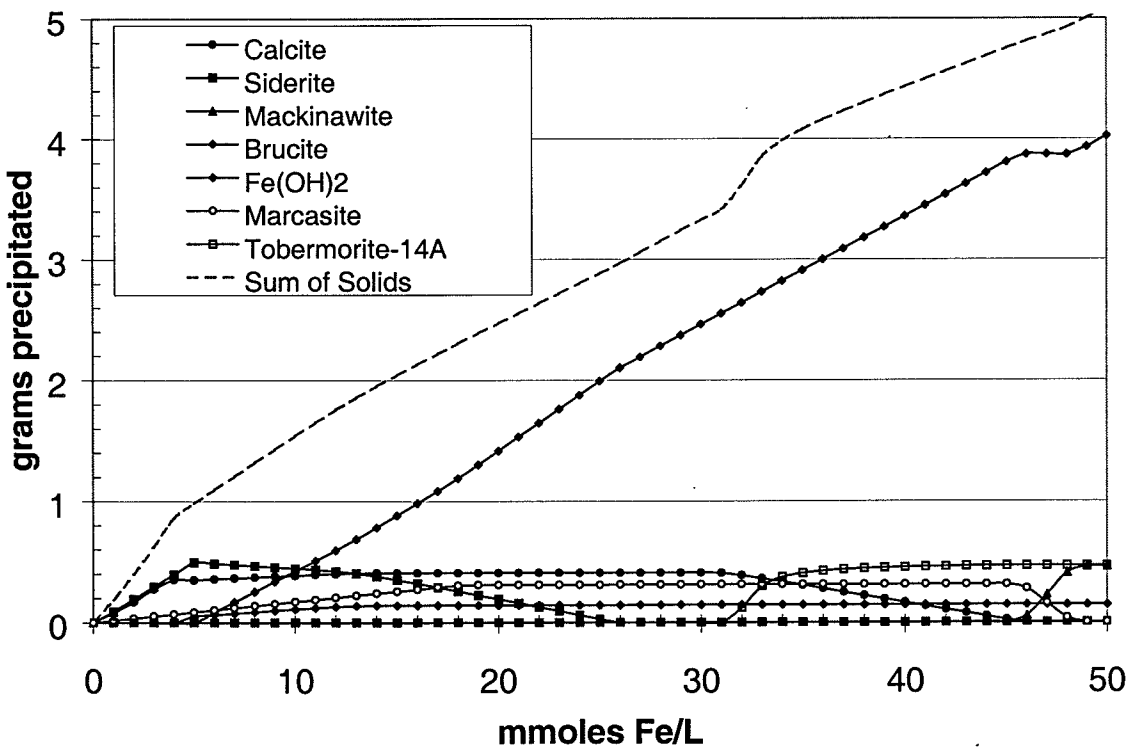

Figure 5-22. Masses of Precipitates Based on Case 1

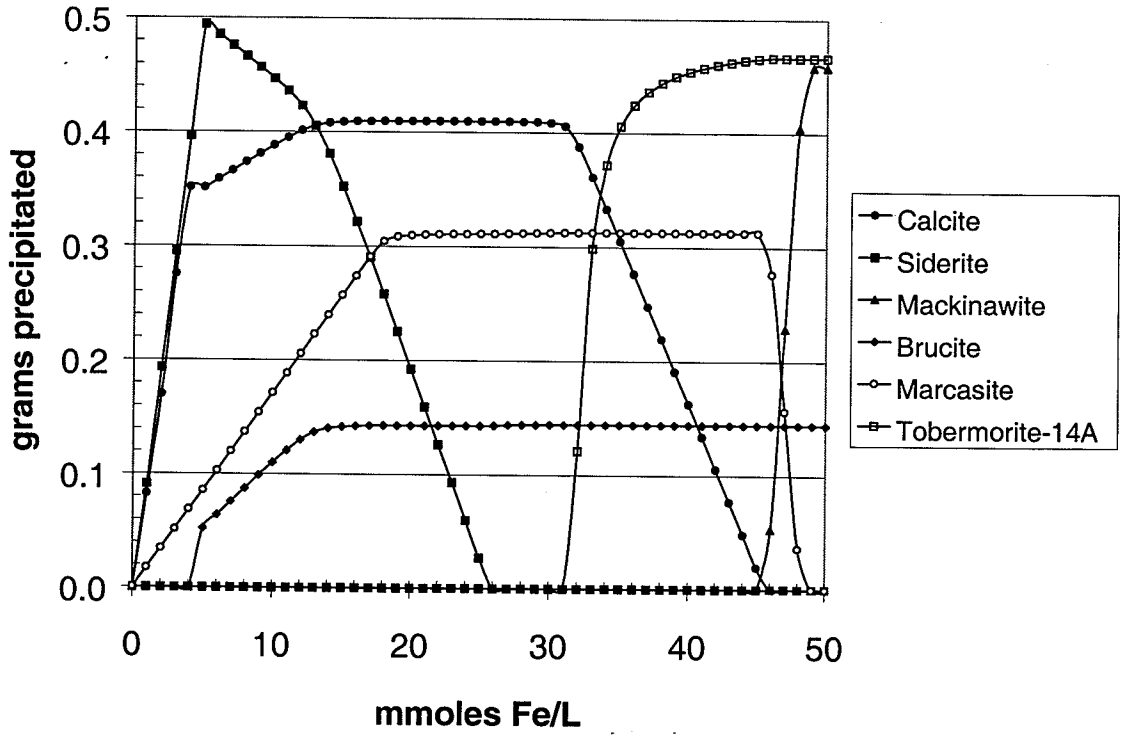

Figure 5-23. Masses of Minor Precipitates Based on Case 1

As more iron dissolves some minerals become unstable and dissolve. For example, siderite begins to dissolve above 5 mmol Fe/L (where $Fe(OH)_2$ becomes stable) and calcite begins to dissolve above 30 mmol Fe/L (where tobermorite-14Å becomes stable). Also, marcasite [S(-I)] dissolves above 45 mmol Fe/L, but is replaced by mackinawite, which contains a more reduced form of sulfur [S(-II)].

Similar results were produced by the other three cases (see Appendix C). Qualitative differences are described below:

Case 2. Siderite precipitation not permitted. This constraint appears to cause aqueous iron concentration to reach a maximum value of approximately 150 mg/L. After more iron dissolves aqueous iron is controlled by marcasite precipitation. Magnesite is stable between 2 and 26 mmol Fe/L, which delays the precipitation of brucite until 17 mmol Fe/L. pH and Eh do not change as quickly at the initial part of the reaction, but the later portion of the plots are similar. At approximately 6 mmol Fe/L, pH ~ 8.7 and Eh ~ -260 mV. Alkalinity does not decline as quickly, and never decreases below 90 mg/L.

Case 3. Iron sulfides not permitted. An important effect is that sulfate concentrations remain high, initially. After more than 20 mmol Fe/L have dissolved, sulfate is converted to sulfide, which remains in aqueous solution. Siderite and calcite precipitate immediately after iron begins to dissolve, but neither approaches the same level as in Case 1, and both dissolve more quickly.

Also, tobermorite-14Å begins precipitating earlier (at 25 mmol Fe/L), causing dissolved silica to decline sooner. Similarly, brucite does not begin precipitating before 17 mmol Fe/L have dissolved, allowing magnesium concentrations in solution to remain high until that point. The initial rate of decline in alkalinity is about the same as in Case 1. The pH and Eh profiles are similar, initially, but do not change as much as in Case 1.

Case 4. Magnetite precipitation allowed. Calcite, siderite and marcasite precipitate immediately, followed by magnetite after 2 mmol Fe/L has dissolved. Only a small amount of siderite is produced and it is very short-lived. Note that $Fe(OH)_2$ does not form at all in this case. Magnesite is stable between 7 and 20 mmol Fe/L, which delays the precipitation of brucite until 13 mmol Fe/L. The marcasite-mackinawite transition occurs at a lower amount of dissolved iron (36 mmol Fe/L), compared to Case 1. Also, alkalinity remains higher and calcium concentration in aqueous solution does not diminish as quickly. Profiles of other ions (silica, ferrous iron, magnesium) are similar to Case 1. The rise in pH and decline in Eh are much slower in this case, compared to Case 1. For example, after 10 mmol Fe/L have dissolved, the pH increases only one unit (pH~8) and Eh is approximately –300 mV.

5.4.3 Comparison of Results with Estimated Corrosion Rates. It is of interest to determine how much iron was likely to dissolve inside the columns, as well as in the field barrier, so that there is a possibility of comparing the modeling predictions with experimental data. For these calculations we assume that the iron corrosion rate is 1 mmol Fe/kg/day, based on the previous discussion about corrosion rates. Residence time at each of the sampling ports was calculated based on flowrates and porosity (assumed to remain constant throughout the tests). Iron dissolution at each port distance was calculated based on the assumed corrosion rate and mass of iron in each section of the column.

Results of residence time and iron dissolution calculations are shown in Table 5-42 for two different flowrates, 25 and 12.5 ft/day. Even at the slower flowrate the amount of iron dissolution is less than 1 mmol/L in the effluent. One can see that these values are small when viewed at the scale of the modeling calculations presented in Figures 10-14. Based on these corrosion levels the modeling runs predict there would be very little change in water composition between influent and effluent. For example, based on the results for Case 1, the pH would increase by less than one-tenth of a unit and the concentrations of aqueous species (e.g., bicarbonate, calcium, sulfate) would barely change as predicted. Perhaps only the concentration of ferrous iron would increase noticeably. In terms of precipitate formation, a small amount of calcite, siderite (~ 0.1 g/L each), and marcasite (~ 0.02 g/L) would form within the entire length of the column.

Due to longer residence times in a field barrier, iron dissolution was calculated to be much higher in the Moffett Field barrier than in the column test. Residence times and iron dissolution are shown in Table 5-43 for the two extremes in flowrates, which were determined by Battelle (1998). For example, at 1 ft inside the barrier, iron dissolution was calculated to be 7.5 mmol/L at 0.5 ft/day and 18.8 mmol/L at 0.2 ft/day. Using Case 1 as an example, and assuming a

Table 5-42. Residence Times and Iron Dissolution in Moffett Field Column Test

Port	x (cm)	Residence Time (days)		Fe Dissolution (mmol/L)	
		25 ft/day	12.5 ft/day	25 ft/day	12.5 ft/day
A	15.2	0.020	0.041	0.077	0.153
B	30.5	0.041	0.082	0.154	0.307
C	45.7	0.061	0.122	0.230	0.460
D	61.0	0.082	0.163	0.307	0.614
Outlet	91.4	0.122	0.245	0.460	0.920

flowrate of 0.5 ft/day, solution parameters were predicted by the same method as used for the column test. Results for the field barrier simulation, listed in Table 5-44, are compared with the initial values that were used for the column model (see Table 5-39). A third column contains sampling results for a well located 1 ft inside the Moffett Field barrier. While the simulation results do not necessarily match up with field measurements, the trend is similar. For example, significant declines in alkalinity, calcium, magnesium, and sulfate concentrations observed in the field measurements are predicted by the simulation. Silica, on the other hand, does not decrease in the simulation, which puts it in poor agreement with the field measurement. The reason for the disagreement is that the silica phase used by the model (tobermorite) does not begin to precipitate until 31 mmol Fe/L have dissolved. This discrepancy suggests that tobermorite precipitation is not representative of the silica-controlling mechanism in the Moffett Field barrier.

Table 5-43. Residence Times and Iron Dissolution Encountered in the PRB at Former NAS Moffett Field

x (ft)	x (cm)	Residence Time (days)		Fe Dissolution (mmol/L)	
		0.5 ft/day	0.2 ft/day	0.5 ft/day	0.2 ft/day
0.5	15.2	1.0	2.5	3.8	9.4
1.0	30.5	2.0	5.0	7.5	18.8
1.5	45.7	3.0	7.5	11.3	28.2
2.0	61.0	4.0	10.0	15.0	37.6
3.0	91.4	6.0	15.0	22.6	56.4

The corresponding masses of precipitates are shown in Table 5-45. Note that the masses were calculated in terms of grams per liter of porewater. Furthermore, these values refer to the residence time listed in Table 5-43 (2 days in this example) and therefore represent one pore volume of groundwater. As each additional pore volume of water flows through the barrier, an equivalent amount of solids would precipitate.

Table 5-44. Comparison of Simulation Results for the Moffett Field PRB with Initial Conditions and Field Measurements

Solution Parameter	Units	Initial Values Used for Simulation [a]	Results of Simulation [b]	Results of Field Measurements [c]
pH	SU	6.88	9.87	10.1
Eh	mV	91.5	-350	-469
Dissolved iron	mmoles/L	0.00	7.50	N/A
Alkalinity	mg/L	393	17.2	78.5
Ca	mg/L	165	16.4	1.77
Fe(2)	mg/L	0.001	0.64	< 0.02
Mg	mg/L	60.1	26.1	17.9
K	mg/L	2.0	2.0	1.95
S(-2)	mg/L	0.0	2.1E-06	N/A
SO_4^{-2}	mg/L	501	295	22.4
Cl	mg/L	40.1	40.1	38.4
SiO_2	mg/L	18.0	18.0	1.2 [d]

N/A = not available (not measured).

(a) Input value (see Table 5-33).

(b) Simulation results are for a residence time of 2 days, which is equivalent to a location 1 ft inside the iron barrier at a flowrate of 0.5 ft/day.

(c) April 1997 sampling results for a long-screen 2-inch ID well (WW-12) located 1 ft inside the iron zone (Battelle, 1998).

(d) Silica was not measured during the regular sampling program. This value was obtained from the October 1998 sampling event for well WW-8D, located 0.6 ft inside the iron zone (Battelle, 1999).

Table 5-45. Calculated Mass of Precipitate at 1 ft Inside Moffett Field PRB

Precipitate	Mass/Volume (g/L)[a]
Calcite	0.37
Siderite	0.47
Magnesite	0.00
Mackinawite	0.00
Brucite	0.082
$Fe(OH)_2$	0.21
Marcasite	0.13
Tobermorite-14Å	0.00
Sum of Solids	1.26

(a) Calculation of precipitate mass is based on throughput of one pore volume of Moffett Field groundwater.

5.5 Summary of Results and Conclusions from the Longevity Evaluation

Longevity refers to the period over which a PRB continues to retain an acceptable level of reactivity and hydraulic performance. In the current project, longevity was evaluated primarily at two sites – former NAS Moffett Field and former Lowry AFB, which have groundwater containing moderate and high levels of dissolved solids, respectively. Dissolved solids, especially inorganic geochemical constituents of the groundwater, such as oxygen, calcium and alkalinity, can precipitate out under the strongly reducing conditions created by the iron reactive medium. These precipitates can potentially coat the reactive surfaces of the iron and reduce its reactivity. In addition, water itself can be reduced by iron to form hydrous iron oxides, which potentially cause passivation of the iron. Both PRBs were installed five or more years ago and have been exposed to groundwater flow over this period. The following monitoring tools were used to evaluate longevity at these two sites:

- Sampling and analysis of groundwater influent to and effluent from the PRB to evaluate loss of geochemical groundwater constituents.

- Sampling and analysis of iron cores from the two PRBs. In addition, silt was collected from the silt traps in monitoring wells in the iron to analyze the deposits that were either formed in the vicinity of these wells or had been transported by advective flow from the upgradient direction.

- Accelerated long-term column tests to establish a direct link between period of exposure of the iron to groundwater and the reactivity of the iron. The same iron and groundwater used at the former NAS Moffett Field and former Lowry AFB were used in the columns.

- Geochemical modeling to evaluate possible reactions and products contributing to the loss of reactivity of the iron

The results of the longevity evaluation indicate that the reactivity of the iron deteriorates progressively over time or over exposure to groundwater. The results of the longevity evaluation can be summarized as follows:

- At former NAS Moffett Field, TCE, PCE, and cis-1,2 DCE in the effluent from the reactive cell iron continues to be below their respective MCLs and below detection. Most of the treatment occurred in the upgradient half of the iron. A noticeable clean groundwater front is not clearly identifiable in the downgradient aquifer, although there are some preliminary signs that it could occur in the future. After five years of PRB operation in the sand channel enclosed by silty clay sides, it was expected that introduction of CVOC-free groundwater effluent would lead to a noticeable improvement in downgradient groundwater quality, despite some contrary site conditions. One or more of the site conditions that could be acting to delay or prevent an improvement in downgradient groundwater quality are:

- Less groundwater flowing through the more conductive reactive cell or gate than is predicted or than is flowing around or below the PRB. In some wells screened at shallower depths, a proportionate relative decline in CVOC and inorganic constituents (e.g., calcium) is noticeable over time, which would support this scenario. CVOC levels have declined somewhat over time in the upgradient aquifer too, making the determination more difficult.

- Recontamination of cleaner groundwater effluent from the PRB with contaminated groundwater flowing under the PRB (the pilot-scale PRB intentionally was not keyed into the clay layer for fearing of breaching a thin aquitard) or from the lower aquifer zone. The downgradient monitoring wells that are screened at a depth near the base of the PRB continue to be the most contaminated, indicating that there is underflow. However, vertical gradients that were upward in the vicinity of the PRB before PRB installation have consistently turned downward after the installation; this would tend to reduce the mixing of groundwater flowing under and through the PRB.
- Contaminated groundwater flowing around the funnel walls of the pilot-scale PRB that was designed to capture only a small part of a regional plume. This is less likely because the sand channel, which probably accounts for most of the groundwater flow in the local region of the PRB, directs flow mostly through the gate. The funnel walls encounter minimal additional groundwater flowing through the silty-clay deposits around the channel.
- Diffusion of CVOCs trapped in the silty clay layers surrounding the sand channel. This type of contaminant persistence has been observed at other sites, even with pump-and-treat systems. However, diffusion is a slow process and water quality improvement immediately downgradient of the PRB would still be expected.

- At former Lowry AFB, TCE, cis-1,2 DCE, and trans-1,2 DCE were treated to below MCLs and below detection in the upgradient half of the reactive cell iron. This indicates that, given sufficient residence time, not only the primary contaminants, but also the reduction byproducts can be treated by iron to below detection. At this site too, a noticeable clean groundwater front was not visible on the downgradient side of the PRB, after four years of operation. Possible reasons include:

  - Mixing of the PRB effluent with contaminated groundwater flowing around the pilot-scale PRB installed inside the plume to capture only part of the plume.
  - Less groundwater flowing through the more conductive reactive cell or gate than predicted or than may be flowing around the PRB.

- Most of the dissolved calcium, iron, magnesium, sulfate, nitrate, and silica in the groundwater flowing through the PRB at former NAS Moffett Field were removed. Levels of alkalinity and total dissolved solids were considerable reduced. These constituents are likely to have precipitated out in the PRB. The groundwater pH rose from 7.0 to 10.9 and the ORP dropped from 134 to –821 mV in the iron. These trends are consistent with previous monitoring events conducted after the PRB was installed. There is no sign that the pH or ORP conditions in the reactive cell are being carried over into the downgradient aquifer. However, some of the shallower downgradient wells located just two feet from the downgradient edge of the PRB are showing some signs of decline in levels of inorganic constituents, such as calcium and alkalinity, indicating the effects of treated groundwater emerging from the reactive cell.

- At former Lowry AFB, most of the dissolved calcium, iron, magnesium, manganese, nitrate, and dissolved silica were removed from the groundwater flowing through the reactive cell. Levels of alkalinity, sulfate, and dissolved solids were considerably reduced. The groundwater pH rose from 6.9 to 11.5 and ORP dropped from –13 to –725 mV in the iron. These trends are consistent with trends seen in previous monitoring events. There were no signs that any of the geochemical changes in the reactive cell were being transmitted to the downgradient aquifer; a downgradient well, about 5 ft away from the PRB, had the same geochemical constitution as the upgradient groundwater, indicating that any contribution of the treated water emerging from the PRB was overwhelmed by groundwater flowing around the PRB.

- At former NAS Moffett Field, geochemical analysis of iron cores from the PRB showed the following:

  - Calcium, silicon, and small amounts of sulfur were the elements identified on the iron particles.
  - Aragonite, calcite (both forms of calcium carbonate), and iron carbonate hydroxide (similar to siderite) were the mineral species identified on the iron particles.
  - Most of these minerals were concentrated in the iron samples collected from the upgradient edge of the reactive cell, indicating that the rest of the iron had not encountered much precipitation.

- Calcite, iron oxyhydroxide (FeOOH) or goethite, ettringite (calcium-aluminum sulfate), and katoite (calcium-aluminum silicate) were the mineral species identified in the silt from the silt traps in the monitoring wells in the PRB at former NAS Moffett Field. The elements iron and magnesium were identified in the silt, but could not be associated with any particular mineral species. Some mineral species (such as feldspar, muscovite, mica and clay minerals) that

probably originated from the pea gravel (granite) were also identified. The presence of minerals in the silt traps that are traceable to the groundwater indicates that not all the precipitates formed deposit on the iron medium. Finer, colloidal particles can be transported by the flow to other locations within the PRB, some of which become trapped in the monitoring wells.

- Iron oxyhydroxide (goethite) and silica were the main minerals traceable to the groundwater that were found on the iron cores from the upgradient edge of the reactive cell at former Lowry AFB. Surprisingly, no calcium or carbonate was detected on the iron core samples analyzed. This finding is in marked contrast to the results of the column test simulation using Lowry site groundwater and Master Builder iron, where two forms of calcium carbonate were detected throughout most of the column. The disparity in these results could be due to extremely slow groundwater movement in the Lowry field barrier, which would have caused most of the precipitation to occur in the most upgradient portion of the iron that may not have been represented in any of the cores samples taken.

- In terms of mass and vertical thickness of deposits in the wells, less silt was found in the monitoring wells at former Lowry AFB than at former NAS Moffett Field, even though the silt traps at Moffett Field had been flushed periodically. A minor amount of rankinite (calcium silicate), though tentatively identified, was the only mineral traceable to a precipitation reaction within the barrier . The groundwater at Lowry AFB is particularly high in dissolved solids, especially sulfate, alkalinity, and calcium. It is surprising that no signs of precipitates associated with these constituents were found on the iron medium or in the monitoring well silt. Once again, the column test results differed from the field measurements in that sulfur was detected on the iron medium used in the column test. Similarly, one possible explanation for this is that the groundwater flow through the PRB is much less than predicted.

- Microbiology results, based on PLFA profiles, from the Moffett Field reactive cell and adjacent aquifer showed a predominance of Gram-negative bacteria, indicating that highly adaptable bacterial communities were present. These results also showed that the aquifer soil downgradient of the Moffett Field PRB had a less diverse microbiological community than the soil upgradient of the PRB. Furthermore, the upgradient soil contained a high proportion of biomarkers indicative of metal-reducing bacteria, whereas no such markers were detected in the downgradient soil. Total cell mass was highest in the upgradient soil and lowest in the downgradient soil; the cell mass in the iron cell was between these extremes. PLFA analysis of the iron samples indicates that different bacteria contributed to the anaerobic Gram-negative populations in these samples. The iron samples contained proportionally five times less the amount of a biomarker for sulfate reducing bacteria than the upgradient soil. Altogether, these results may be indicating that the microbial community is still becoming acclimated to

conditions inside the PRB. No significant buildup of microbial populations was visible on the iron itself.

- Samples of iron from the Lowry PRB too contained a highly diverse microbial communities composed primarily of Gram-negative bacteria. However, some iron samples were composed mainly of eukaryote PLFA or had equal distributions of eukaryotes and normal saturated PLFA. The Gram-negative communities were in a stationary phase of growth and did not show signs of environmental stress.

- Geochemical modeling was used to predict a likely sequence of mineral precipitation events, based on groundwater responses to changes in pH and ORP in the presence of zero-valent iron. Four separate scenarios were run with the following possible phases common to each run: calcite, magnesite, brucite, ferrous hydroxide, and tobermorite. In each of the four scenarios, one or more of the following minerals were allowed to form: siderite, mackinawite; marcasite, and magnetite. All four scenarios predicted changes in pH and ORP that were similar to those observed in the field or laboratory column tests. Also, all four scenarios predicted declines in inorganic species in the groundwater, but at somewhat different proportions. When iron corrosion rate data from available literature were used to predict precipitation rates, the model predictions matched the trends in groundwater chemistry in the Moffett Field barrier for all major species except dissolved silica. The reason for failing to predict silica loss in the barrier was that the likely silica-controlling phase is not known, although thermodynamic data for such a phase may not be available anyway. However, published iron corrosion rate data are much too slow to model the changes occurring during short residence times inside the columns. Despite providing ample indication of the types and quantities of precipitates formed in the PRB, groundwater monitoring, iron core analysis, and geochemical modeling provided no links between time and reactivity of the iron, as it was unclear how these precipitates affected the reactivity of the iron in the long-term. To establish some preliminary links between period of exposure to groundwater and potential loss of reactivity of the iron, long-term accelerated column tests were conducted with the same groundwater and iron as from the field PRBs at former NAS Moffett Field and former Lowry AFB.

- The two columns were adjusted to a flow rate whereby pH and ORP reached a plateau (indicating that majority of the reactions between the iron and groundwater had occurred in the column), but was fast enough that many pore volumes of groundwater could be passed through the column (or many years of PRB operation could be simulated). After some trial-and-error, a flow rate of 12.5 ft/day was eventually established as optimum for the column test. At this flow rate, all the precipitates generated stayed in the column (at higher flow rates, there was a tendency for finer precipitates to be transported out with the flow. If a

representative normal flow rate of 0.5 ft/day is assumed at both sites, than the flow in the columns is accelerated 25 times. The 1,300 pore volumes of groundwater passed through each column and the 1.5 years of column testing represented approximately 25 to 30 years of operation in the field PRBs. A related test conducted with the same columns showed that the TCE half-life was independent of the flow rate over a wide range of flow rates.

- The column tests show that over the 1,300 pore volumes of flow that the iron was exposed to, the half-life of TCE increased approximately by a factor of 2 in the Moffett Field column and by a factor of 4 in the Lowry AFB column. While some effects of aging may be intrinsic to the iron, itself, or to the manufacturing process, other differences may be due to the inorganic content of the water and the subsequent precipitation of dissolved solids. Former NAS Moffett Field has groundwater with a moderate level of dissolved solids and former Lowry AFB has groundwater with relatively high levels of dissolved solids; consequently, Lowry AFB showed a greater decline in reactivity over the same period of exposure to groundwater as the Moffett Field column. The mechanism for the loss of TCE reactivity is not known with certainty. However, it does appear from the column testing that iron in both column tests lost reactivity fairly uniformly, rather than developing a front of inactivated iron that progressively migrates along the length of the column. One reason for the uniform change in reactivity may be deposition of non-electrically conductive coatings on the iron grains, such as calcium carbonate, amorphous silicates, sulfide and sulfate minerals, and ferrous hydroxide. Because of the accelerated flow rate in the columns, these precipitates were distributed along a longer distance than would normally occur in a field barrier. However, it is important to note that ferrous hydroxide can form by reaction of water with iron, even if the water has no ionic content. So, for example, if a barrier is very thick or if water moves through very slowly, most of the ionic content of the water will be scrubbed out near the influent end, leaving water with low ionic content in a downgradient portion of the barrier. In this downgradient portion of the barrier, corrosion by hydrogenolysis may still occur at a fixed rate and the iron may become coated by ferrous hydroxide. An explanation for the decrease in reaction rate of iron is that non-conductive coatings inhibit the beta-elimination pathway, where TCE is converted to ethene and ethane following a transition state that involves creation of an acetylene-based molecule. Due to the complexity of the process and number of electrons that must be involved, the probability of forming the acetylene transition state may decline as the coating thickness increases. However, since the pH and ORP do not seem to be much affected by aging of the iron, it seems that reduction of water continues as it did prior to aging. This could indicate that TCE and other chlorinated ethenes could continue to be reduced by a simpler mechanism, such as the hydrogenolysis pathway, which is known to occur, but which is also a slower and less efficient reaction than beta-elimination. In addition to a reduced rate of TCE degradation, one consequence of the hydrogenolysis pathway replacing beta-

elimination as the dominant degradation mechanism is that byproducts such as DCE and VC would be produced in greater quantity. If this supposition is correct, then TCE half-lives would not become infinitely long as predicted by the exponential decline in reaction rate described in the column test results. Rather, TCE half-lives would migrate from a predominantly beta-elimination process to one that is predominantly driven by hydrogenolysis.

- One practical consequence of declining degradation rate while hydrogenolysis is still occurring is that measurement of pH and ORP may not be indicative of declining performance. Thus, these simple measurements may not be useful tools for predicting the long-term decline of a barrier.

- The pH and ORP distribution in the two columns remained relatively constant once the test flow rate of 12.5 ft/day was established in the columns, even though the reactivity of the iron declined. This indicates the following:

  - The geochemical constituents of the groundwater *do* affect the reactivity of the iron upon long-term exposure to groundwater.
  - The rate of decline in iron reactivity over time is dependent on the native level of dissolved solids in the groundwater.
  - The PRB is likely to be passivated before the entire mass of zero-valent iron is used up, unless some way of regenerating or replacing the reactive medium is developed and implemented.

- The porosity and permeability of the iron (and hence the residence time) was not considerably affected over the duration of the test, as indicated by a tracer test conducted in the column after 1,300 pore volumes of flow. Therefore, the reactive performance of the iron is likely to decline much faster than any potential decline in long-term hydraulic performance.

- The progressive decline in iron reactivity over time indicates that the residence time required to meet groundwater cleanup targets also will be progressively higher in the long term. One way of ensuring that sufficient residence time is available in the future is to incorporate a higher safety factor in the currently designed flow-through thickness of the reactive medium in the PRB. Therefore, there is a tradeoff between current cost and future PRB performance.

6.0 Hydraulic Evaluation of PRBs at DoD Sites

The permeable reactive barriers technology relies upon the use of hydraulic characteristics of the site for successful performance over the short- and long-term. Therefore, a careful consideration of the hydrogeologic issues must be incorporated at all stages of the project: site screening, characterization, design, construction, and performance assessment. Most of the reports about sub-optimum performance at some PRB sites may be attributed to hydraulic factors. The issues of concern include insufficient residence time resulting in contaminant breakthrough, inability to verify flow through the reactive cell, plume bypass around, under, or over the barrier, seasonal fluctuations in groundwater flow that result in variation in performance, and effect of nearby site features such as drains, surface water, operating pump-and-treat systems, etc. Almost all of these issues can be related to the two primary objectives involved in designing a PRB and monitoring its hydraulic performance:

- Ensuring that the PRB will capture the desired portion of the plume, and
- Ensuring that the desired residence time in the reactive cell will be met.

Thus the two primary interdependent parameters of concern when designing a PRB are *hydraulic capture zone width* and *residence time*. Capture zone width refers to the width of the zone of groundwater that will pass through the reactive cell or gate (in the case of funnel-and-gate configurations) rather than pass around the ends of the barrier or beneath it. Capture zone width can be maximized by maximizing the discharge (groundwater flow volume) through the reactive cell or gate. Residence time refers to the amount of time contaminated groundwater is in contact with the reactive medium within the gate. Residence times can be maximized either by minimizing the discharge through the reactive cell or by increasing the flowthrough thickness of the reactive cell. Thus, the design of PRBs must often balance the need to maximize capture zone width (and discharge) against the desire to increase the residence time. Contamination occurring outside the capture zone will not pass through the reactive cell. Similarly, if the residence time in the reactive cell is too short, contaminant levels may not be reduced sufficiently to meet regulatory requirements.

The basic tools and methods that can be used at various stages of a PRB project for improving the probability of successful implementation have been discussed in details in the design guidance (Gavaskar et al., 2000). The two classes of design tools mentioned in the design guidance document for improving the probability of hydraulic success are:

- Site Characterization – this includes developing a detailed understanding of the site geology, hydrogeology, contaminant distribution, and seasonal fluctuations and incorporating the ranges in these aspects into the PRB design to maximize successful implementation.

- Groundwater Flow Modeling – this includes incorporating the site parameters into the computer simulation tools so that the spatial and temporal variations in these

parameters can be evaluated and the appropriate safety factors can be determined for PRB design and monitoring system configuration.

The purpose of hydrogeologic investigations conducted under the current project was to evaluate the major issues related to *capture zone* and *residence time* based on these existing two classes of tools. These two hydraulic issues were investigated by:

- Conducting a field evaluation of PRBs at various DoD sites, and
- Conducting computer simulations to evaluate the effects of hydraulic variations and characterization uncertainties.

The following sections provide a brief discussion of the monitoring and modeling efforts, followed by a discussion of key findings and their implications for design and performance assessment at future PRB sites.

6.1 Field Evaluations of Hydraulic Performance at DoD Sites

A thorough characterization of site geology and hydrology is required to understand flow conditions and how they will be impacted by installation of a PRB. Site characterization usually involves an initial regional or property-wide investigation (e.g., Remedial Investigation/ Feasibility Study or RCRA Facility Investigation) followed by additional localized characterization to assess the hydrogeology, contaminant distribution, and geochemistry at the prospective PRB location(s). The property-wide site characterization usually offers the first indication of the presence of a contaminant plume and is used to conduct a feasibility study of potential remediation methods. The Design Guidance document (Gavaskar et al., 2000) provides various site and contaminant characteristics that can be used to screen a site for potential PRB application. If a PRB is determined as feasible at a site, additional localized characterization is generally necessary at the prospective PRB location (s) to further delineate the subsurface and collect information required for a good PRB design. It is this localized characterization and the subsequent (post-construction) monitoring of the PRB that were the focus of the current project.

Key site characterization tasks may include soil sampling or cone penetrometer testing (CPT) logging to delineate hydrostratigraphic units, water level surveys to determine gradient, geotechnical tests to assess hydrologic parameters, and groundwater sampling for plume delineation. Geologic cross sections then can be prepared and are useful for determining how aquifer heterogeneity may influence results. For example, lenses of low permeability clay near the water table at the Dover site had higher contamination levels, which caused plume concentrations to vary with water table fluctuations.

PRBs have been installed at DoD sites with a variety of site characteristics. Table 6-1 summarizes the hydraulic parameters encountered during the field evaluation at five different DoD sites that were the particular focus of this project. Some of the supporting data for this table are presented in Appendix E. Overall, PRBs have been fairly effective over a wide range of site conditions. Many PRBs have been installed in unconfined aquifers. Key issues for

Table 6-1. Representative Hydraulic Parameters Measured for Aquifers at the DoD PRB Sites Evaluated

Site	Former NAS Moffett Field	Former Lowry AFB	Seneca Army Depot	Dover AFB	Former NAS Alameda
Aquifer Type	Semi-confined	Unconfined	Unconfined	Unconfined	Unconfined
Aquifer Material	Sand Channel	Silty Sand to Sand and Gravel	Glacial Till	Silty Sand	Artificial Fill
Depth of Aquitard (ft)	25	17	8-10	35-40	20
Aquifer Vertical Thickness (ft)	20	11	8	15-25	14
Aquifer Porosity	0.30	0.30	0.18	0.31	0.35
Aquifer Hydraulic Conductivity (ft/d)	0.1-633	1.1-3.1	0.4-126	1.8-101	0.001-33.4
Typical Hydraulic Conductivity (ft/d)[a]	30	1.7	25	7.4	18.4[b]
Hydraulic Gradient (ft/ft)	0.005-0.009	0.035	0.005-0.01	0.0015-0.002	0.007
Typical Hydraulic Gradient	0.007	0.035	0.006	0.0018	0.007
Range of Groundwater Velocity (ft/day)	0.0017-19.0	0.013-0.36	0.011-7.0	0.0087-0.65	<0.001-0.67
Approximate Groundwater Velocity (ft/day)	0.7	0.2	0.83	0.04	0.37
Reactive Cell Thickness (ft)	6	5	1	4	7
Range of Residence Times (days)	0.3-3,529	14-385	0.1-91	6-456	10-7,000
Typical Residence Time (days)	9	25	1	100	19

(a) The typical hydraulic conductivity is the most prevalent value from the range of values measured.
(b) Hydraulic conductivity used in modeling (Einarson et al., 2000).

unconfined aquifers include ensuring that the PRB is keyed into an underlying confining layer and ensuring that the wall is thick enough to accommodate fluctuations in water levels. Whereas none of the DoD PRBs were installed in a confined aquifer, the Moffett field PRB was installed in a semi-confined setting. In confined or semi-confined aquifers settings, the potential for affecting vertical gradients may affect the PRB performance. PRBs have been installed mainly in unconsolidated aquifers, where groundwater flow is likely to be more predictable than in fractured and/or consolidated media. However, emerging construction techniques, such as high pressure jetting, are making the installations in consolidated rocks more feasible.

Several different types of aquifer materials were encountered at DoD's PRB sites, with soil ranging from alluvial silty sands to artificial fill to glacial till. Aquifer thickness ranged from 8 to 20 ft. The deepest DoD site where a PRB was installed was Dover AFB, where the aquifer

was 35 ft below ground surface. Aquifer porosity was generally around 0.30, except at Seneca Army Depot, where it was more variable due to aquifer heterogeneity. Representative aquifer permeability varied from 6 to 221 ft/day. However, when all of the slug and pump test data from various sites were examined, permeability of the aquifer materials showed a much greater range, spanning several orders of magnitude from less than 0.001 ft/day to more than 633 ft/day. This exemplifies the wide variability in aquifer characteristics at sites, and the importance of capturing it in designing and monitoring PRBs. Aquifer gradients ranged from 0.001 to 0.01 ft/ft. This parameter may have a considerable effect on PRB performance, since it affects residence times in the reactive cell. Several sites exhibited seasonal variations in gradient due to seasonal trends and/or precipitation events. Based on reported hydraulic parameters, linear groundwater flow velocities at the investigated PRB sites ranged from 0.04 to 0.83 ft/day.

The hydraulic aspects of PRB performance were evaluated with data obtained from the above-mentioned sites. Characterization and monitoring efforts for the current project included water level surveys, hydraulic conductivity measurements using slug tests, and velocity measurements using HydroTechnics™ sensors and colloidal borescope measurements. These tools were used to estimate groundwater gradients, directions, residence times, and capture zones. In addition, the measured parameters were utilized in computer modeling scenarios of the hydraulic regime in and around the PRB.

6.1.1 Water Level Surveys. Water level surveys provide information on groundwater gradients and capture zones for PRBs to demonstrate that groundwater is flowing through the barrier at a rate, which will ensure adequate destruction of the contamination. Several rounds of water level surveys were performed at the selected DoD PRB sites during the current project. In general, the groundwater surveys demonstrated a positive gradient in the expected flow direction through the PRBs, that is, when gradients were measured from upgradient to downgradient aquifer. For example, positive gradients were observed in periodic monitoring of PRBs at Dover AFB, former NAS Moffett Field, Seneca Army Depot, and former Lowry AFB, as shown in Table 6-2.

Table 6-2. Summary of Hydraulic Gradients Through PRBs*

Site	Gradient Through PRB	Basis
Dover AFB	0.005	Periodic Water Level Surveys (Battelle, 2000a)
Former Lowry AFB	0.02 to 0.03	Periodic Water Level Surveys (Battelle, 2000b)
Former NAS Moffett Field	0.026	Periodic Water Level Surveys (Battelle, 1998)
Seneca Army Depot	0.01 to 0.02 ft/day	Quarterly Water Level Surveys (Parsons Engineering Service, Inc., 2000)

*Gradients were based on measured water levels from wells upgradient of the PRB to wells downgradient of the PRB.

Within the PRBs themselves, hydraulic gradients were extremely flat, which is expected of highly permeable and porous media. A few transient flow reversals were reported, for example, at the Moffett Field site, but these occurrences appear to have been temporary and generally within the measurement error (Battelle, 1998). At former NAS Moffett Field, monitoring conducted during a previous project showed that some mounding appeared to be occurring at the downgradient end of the PRB, which may indicate that groundwater discharge from the highly permeable PRB media to the generally less permeable aquifer meets with some resistance. The results of water levels measured in May 2001 as part of the current project are shown in Figure 6-1. Among all the PRB sites evaluated under the current project, the PRB at former NAS Moffett Field provided the most certainty in terms of verifying a groundwater capture zone and occurrence of flow through the PRB, probably because the sand channel surrounded by silty-clay deposits constrained flow from diverging to the sides. Close examination of the water level map in Figure 6-1 shows flow divides occurring about half way across the length of each funnel wall. Based on these water levels an approximate estimate of capture zone is 30 ft. The capture zone includes the flow directly upgradient of the 10-ft-wide gate and halfway across 20-ft-wide funnel wall. Water-level surveys are a key monitoring activity for confirming gradients at PRB sites.

Based on a typical hydraulic gradient of 0.007, observed during water level mapping events, and a typical hydraulic conductivity of 30 ft/day, representative of slug test results in the sand channel, a typical groundwater velocity of 0.7 ft/day and a residence time of 9 days are estimated as shown in Table 6-1. This residence time estimate matches the results of a tracer test (Battelle, 1998) conducted during a previous project. The wide variability in the hydraulic conductivities measured at different locations in the aquifer and the likelihood of preferential pathways in the iron medium itself, as seen in the tracer test, create substantial uncertainty in the groundwater velocity and residence time estimates.

Although the water level information at the DoD sites usually showed capture by the PRBs, at some sites the groundwater gradient was often so low that water level surveys were less conclusive than expected. Because there is a limit to the accuracy of a groundwater survey (usually 0.01 ft or 1/10 inch), careful design of a monitoring well network is required to obtain useful water level information. A general rule for water levels is to space the monitoring wells at distances equivalent to at least the measurement accuracy divided by the gradient. For example, wells in an aquifer with a gradient of 0.001 would require spacing of at least ten feet to acquire a measurable 0.01 ft or higher difference in water levels. In practice, PRB dimensions along the groundwater flow directions are often smaller (generally less than 10 ft) than the monitoring well spacing required for sufficient resolution in water level measurements. Therefore, at most sites, water level surveys are likely to be challenging.

One way of improving the accuracy of water level measurements for evaluating horizontal gradients is to ensure that the screened intervals of all the wells in the monitoring network are at uniform depth throughout the network. This approach has improved the feasibility of water level surveys at sites, such as Dover AFB, with very low hydraulic gradients. Figure 6-2 shows a water level map for shallow wells in February 1998 that indicates that gradients in the upgradient aquifer are in the expected direction toward the gates (Battelle, 2000a). Not all monitoring

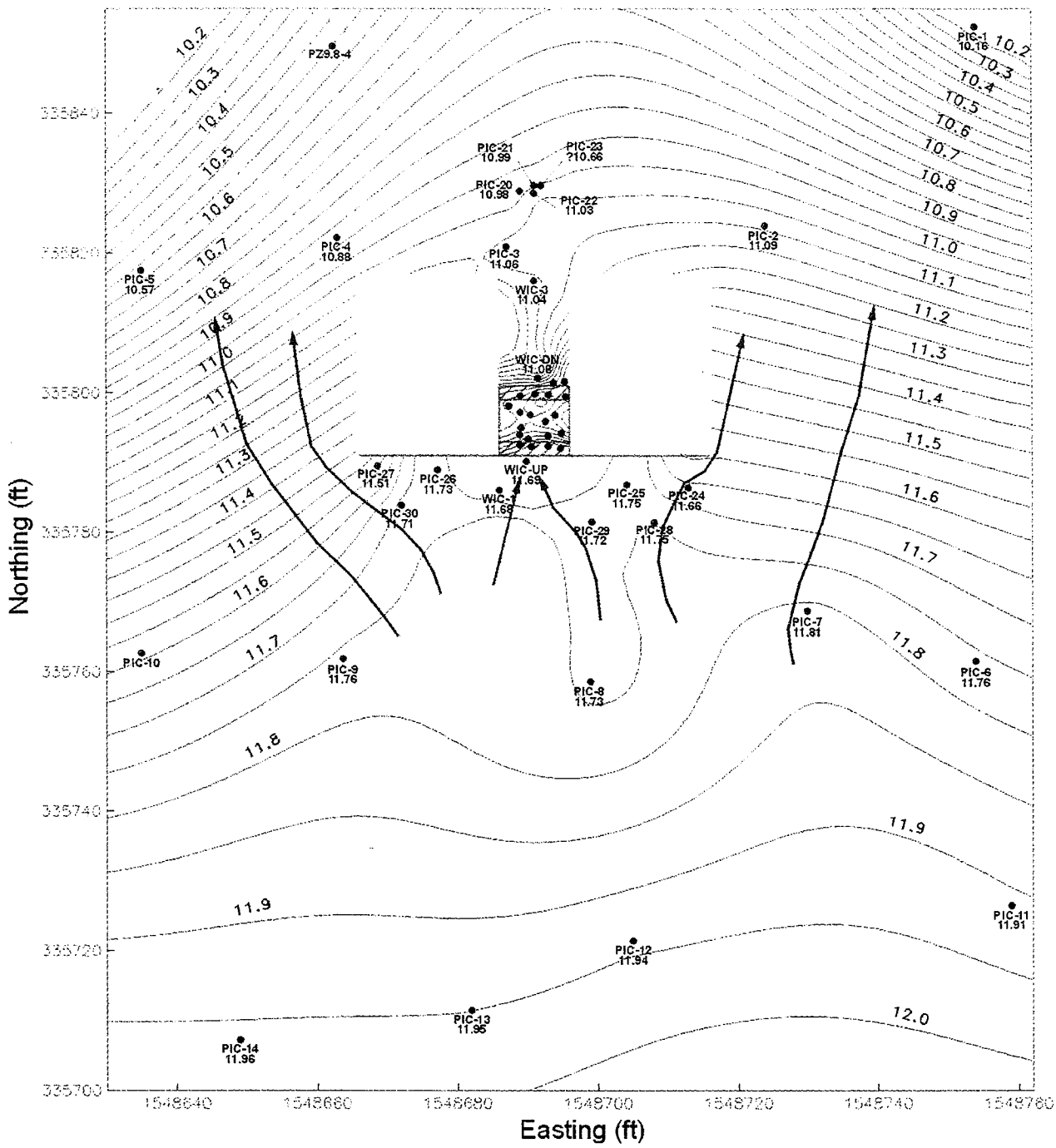

Figure 6-1. May 2001 Water Levels and Flow Patterns in the Vicinity of Former NAS Moffett Field PRB

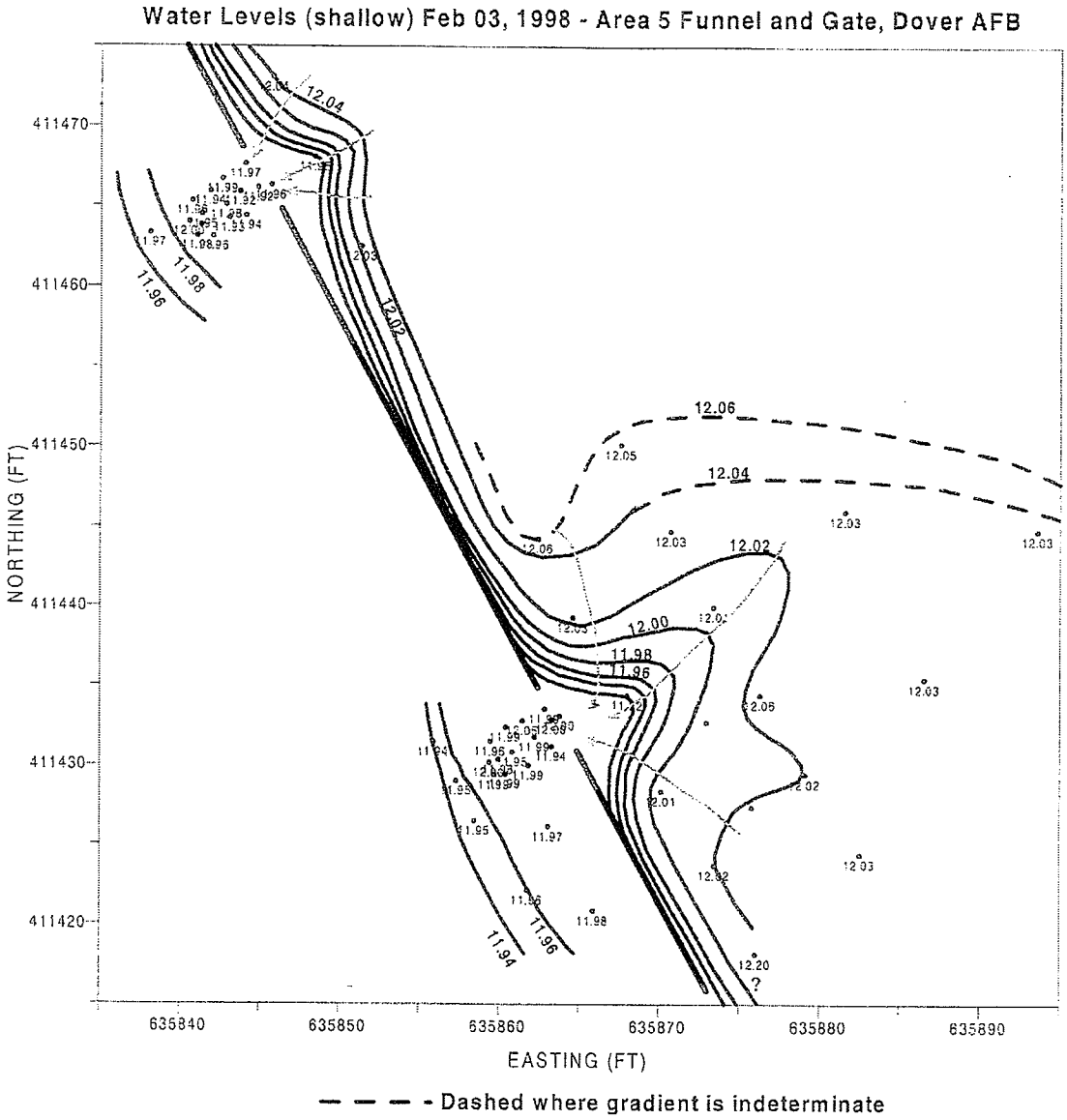

Figure 6-2. Water Levels and Flow Patterns at Dover AFB PRB Site for February 1998 (Battelle, 2000a)

events at this site provided water-level maps that were as amenable to interpretation as the map in Figure 6-2. For example, the water-levels obtained during December 1999 at this site were essentially flat (Figure 6-3) and did not show any discernible flow patterns. However, during certain seasons, it was possible to obtain measurable gradients in the aquifer upgradient of the PRB at this low-flow site. Within the reactive cells however, the gradient was too low to obtain meaningful measurements.

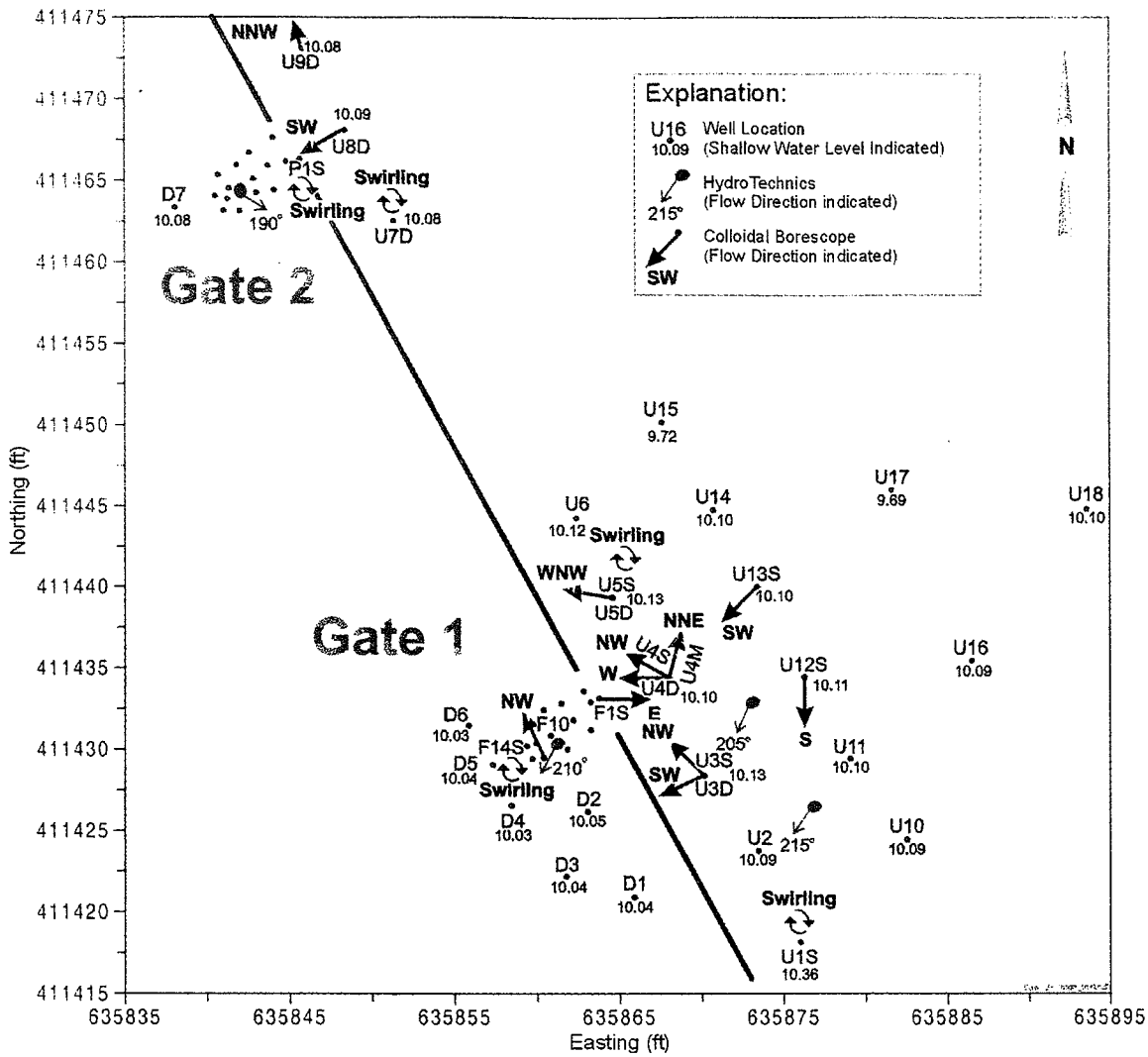

Figure 6-3. December 1999 Water Levels and other Hydraulic Measurements for Dover AFB PRB

Seasonal fluctuations in the gradient must be accounted for in the analysis of water level data. For example, at Dover AFB, historical measurements indicated that groundwater flow direction changed by about 30° on a seasonal basis (Battelle, 2000a). This had a considerable effect in determining an optimum design and orientation of the PRB so that the PRB was perpendicular to the flow during most times of the year. At least four quarters of water level data should be obtained to account for seasonal fluctuations in groundwater velocity and direction, before designing a PRB. In addition, information on long-term extremes in water levels and flow directions obtained from historical records, where available, should be considered in the designing PRBs.

The capture zone produced by a PRB in the upgradient aquifer may be determined by contouring the water levels for wells in and around the PRB. However, these maps are not always conclusive, due to a limited number of data points, limitations in obtaining accurate water level differences over short distances, and low magnitude of the gradient itself. While most maps of observed water levels demonstrate flow through the PRB, a well-defined capture zone was rarely apparent from the field data.

For example, at Lowry AFB (see Figure 6-4), gradients were relatively strong in the upgradient aquifer and indicated not only flow progressing in the expected direction toward the reactive cell, but also the asymmetric nature of the capture zone due to the effect of an adjacent stream on the east side. The capture zone at Lowry AFB appears to be approximately 20 ft wide, with 10 ft of capture directly upgradient of the gate and 10 ft along the western funnel wall. Most of the flow upgradient of the eastern funnel wall appears to be directed towards the flowing stream on the east. Based on the hydraulic conductivities measured during slug tests and the hydraulic gradient obtained from water level measurements, a typical groundwater velocity of 0.2 ft/day and a typical residence time of 25 days are estimated, as shown in Table 6-1. A moderate variability in the hydraulic conductivity estimates in the sandy aquifer creates some uncertainty in these estimates.

On the other hand, at Seneca Army Depot and Dover AFB, the flow divide and therefore the capture zone were difficult to determine. At Dover AFB, the native gradient itself is low. At Seneca Army Depot (Figures 6-5 and 6-6), the difficulty was that the PRB was relatively thin (1 ft flowthrough thickness) and generated a very minor disturbance in the natural flow patterns.

At both these sites, uniformly screened monitoring wells and multiple monitoring events led to at least some events that afforded discernible groundwater flow trends. To conserve limited resources, the monitoring well network at Seneca Army Depot was limited to one end of the relatively long PRB. The water level map for this site for April 2001 (Figure 6-5) shows a steep gradient immediately upgradient of the PRB and flat water levels farther away. It also shows that the flow lines are pointing towards the PRB at the northern end of the site indicating capture of the plume from that area. However, during July 2001 (Figure 6-6) the water levels are flat upgradient of the PRB showing the seasonal effects on the flow patterns and residence times. In both cases there is a downward gradient from upgradient to downgradient wells indicating the flow is occurring through the PRB.

At the Former NAS Moffett Field where a large number of monitoring wells installed at similar depth are available and the flow is constrained through a sand channel, it was possible to draw a capture zone upgradient of the funnel-and-gate PRB (Figure 6-1). In this case, the capture zone appears to be the soft-wide zone directly upgradient of the reactive cell and extending to about half the width of the funnel wall on each side.

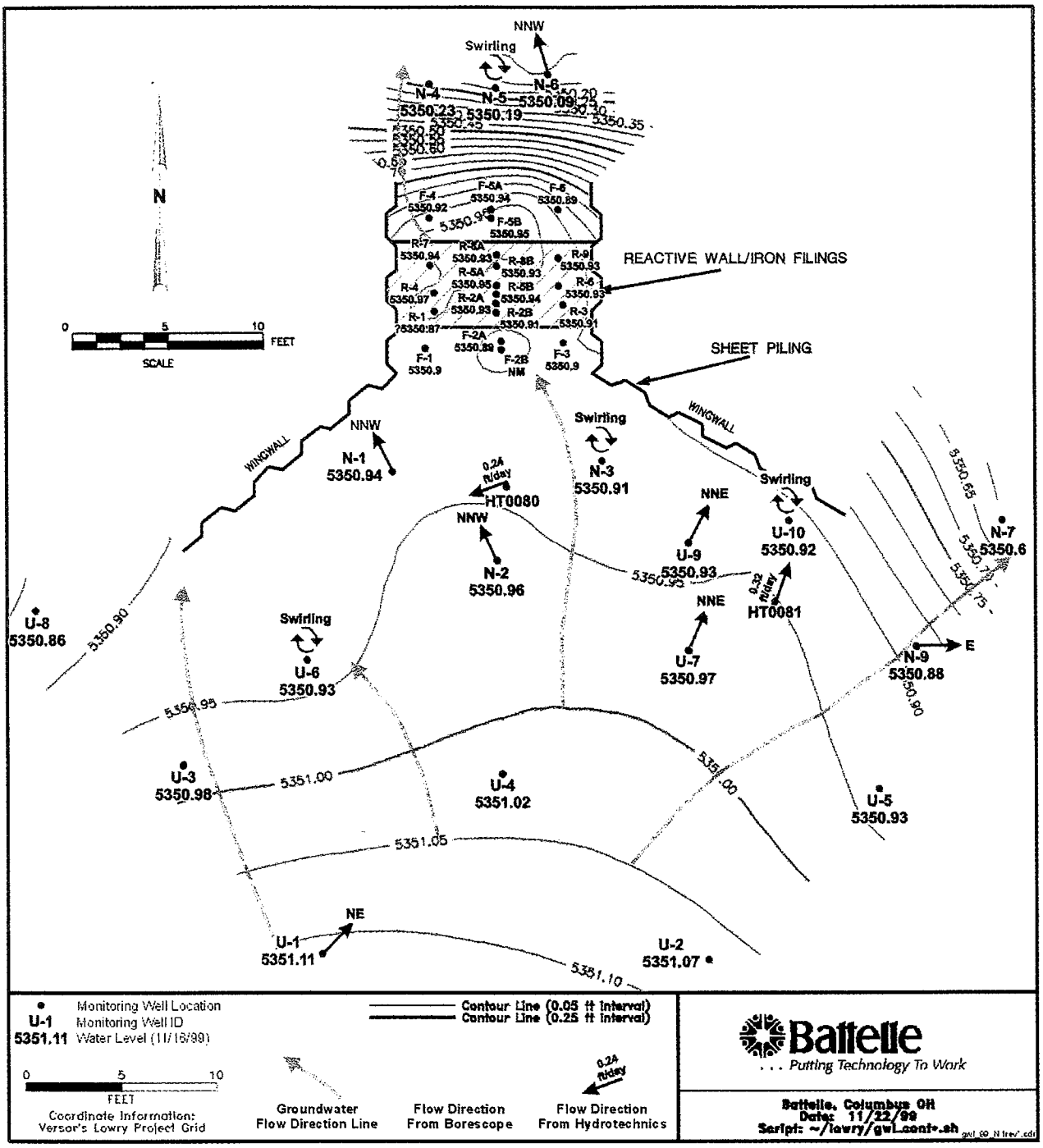

Figure 6-4. November 1999 Water Levels and Other Hydraulic Measurements at Lowry AFB PRB

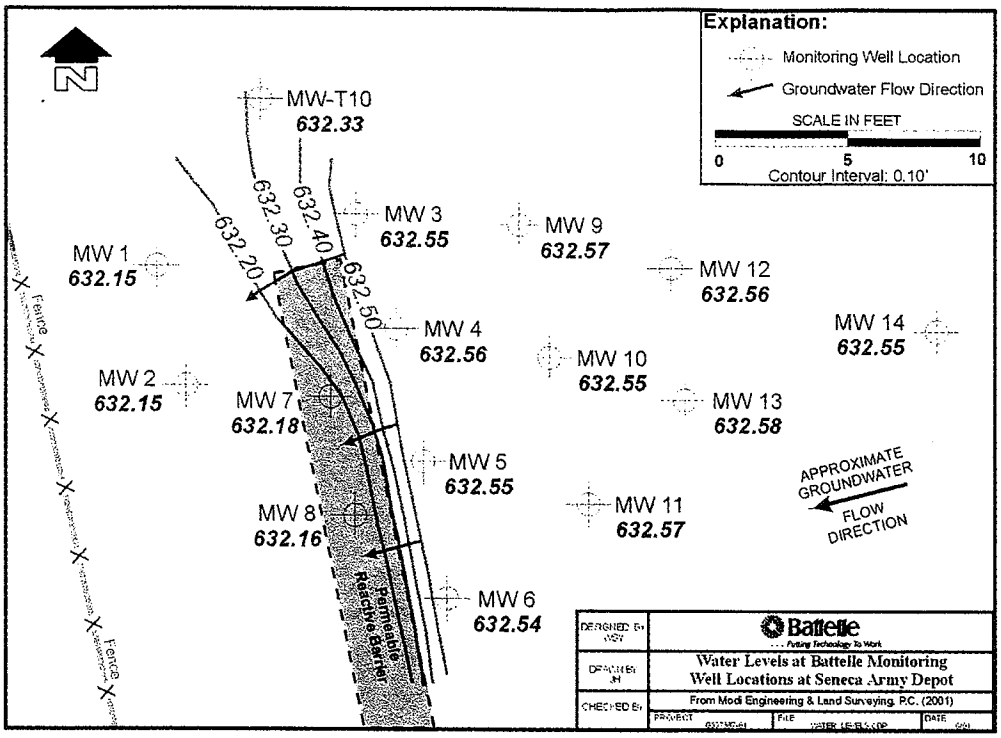

Figure 6-5. April 2001 Water Levels at Seneca Army Depot PRB

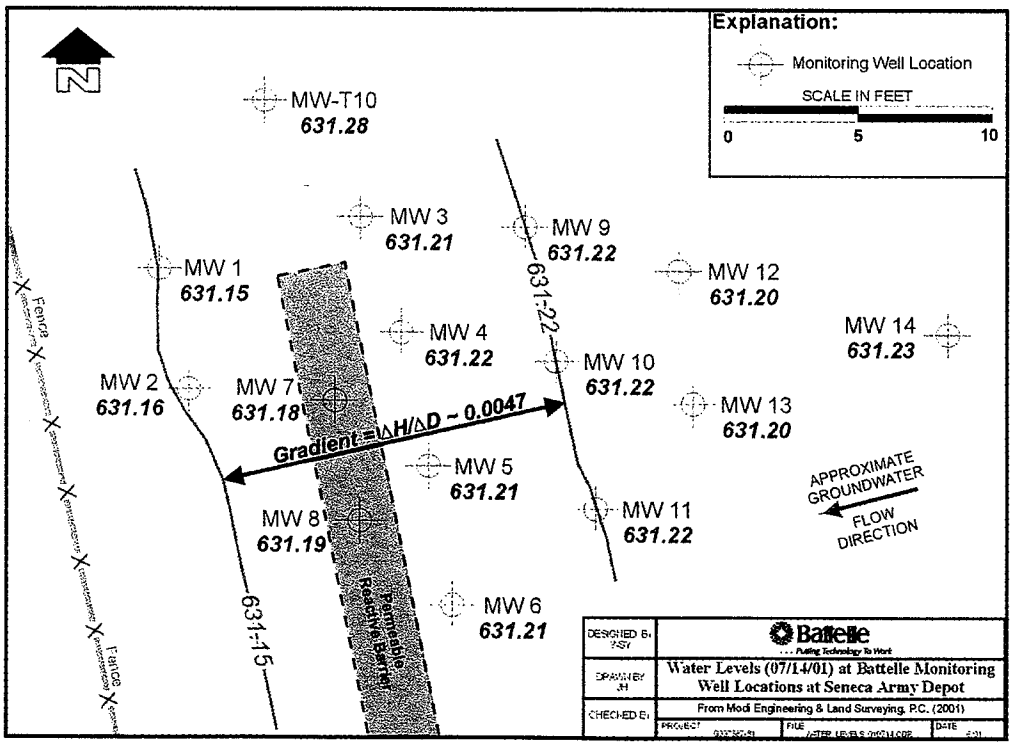

Figure 6-6. July 2001 Water Levels at Seneca Army Depot PRB

Vertical gradients were analyzed previously at the Moffett Field site, where upgradient wells were installed at four different depth intervals. Analysis of these water levels (Battelle, 1998) suggests that a slight downward gradient was induced by the installation of the PRB. A moderate, but progressively downward, gradient was observed from the shallower wells to the deeper wells. In addition, the previously upward (pre-construction) gradient between the lower aquifer to the upper aquifer in which the PRB was placed was reversed to a downward gradient after installation. The effect of such changes in flow patterns on plume capture should be considered in designing and monitoring PRBs at sites with layered aquifers or PRBs that are not keyed into the underlying confining layers.

In addition to periodic water level measurements, continuous water level monitoring in selected wells can provide important information on fluctuations in water levels at the site. No continuous water level monitoring was performed as part of the current project. However, previous data were available from the Former NAS Moffett Field and Dover AFB (Figure 6-7) PRB sites. In general, these data showed seasonal trends that correlate with low and high water levels and precipitation trends. In the example shown in Figure 6-7, the water levels in the downgradient sand (Well P14S) appear to be about 0.25 ft higher than those in the iron cell (Well P7S), indicating stagnation or some backflow in the iron cell during June/July 1998. Other sites may have different trends depending on the local climate and geologic conditions. At NAS Moffett Field PRB, water level response was similar in wells both inside and outside the PRB, suggesting that flow conditions were affected the same in the PRB media as in the undisturbed aquifer. Water levels also remain the same in relation to each other, which suggests that the overall flow patterns are not altered with seasonal water level fluctuations. Continuous water level monitoring is most useful at sites where seasonal fluctuations may be large or where precipitation events cause rapid changes in water levels. In addition, it can be used to evaluate relative water levels over a period of time in groups of wells in a consistent manner.

6.1.2 Hydraulic Conductivity Measurements. Hydraulic conductivity is generally determined in the field using slug tests or pumping tests. The methods and their relative merits are described in the design guidance (Gavaskar et al., 2000). Although pumping tests are considered more accurate, slug tests have been employed for field measurement of aquifer or reactive media K measurements in most PRB studies. Some limitations of pump tests include:

- A proper network of monitoring wells is required for a pump test. An array of multiple wells surrounding the pumping well and screened at similar depths in the same aquifer is the best setup. If wells are too far from the pumping well, they may not be influenced during the test.

- Pumping requirements for a test may be large and long in duration for highly transmissive aquifers. Sometimes, this presents a challenge in disposing of contaminated water. The test may also influence hydrologic conditions.

- Aquifer heterogeneity may interfere with pumping test results, as the test requires a homogeneous, isotropic aquifer for best results.

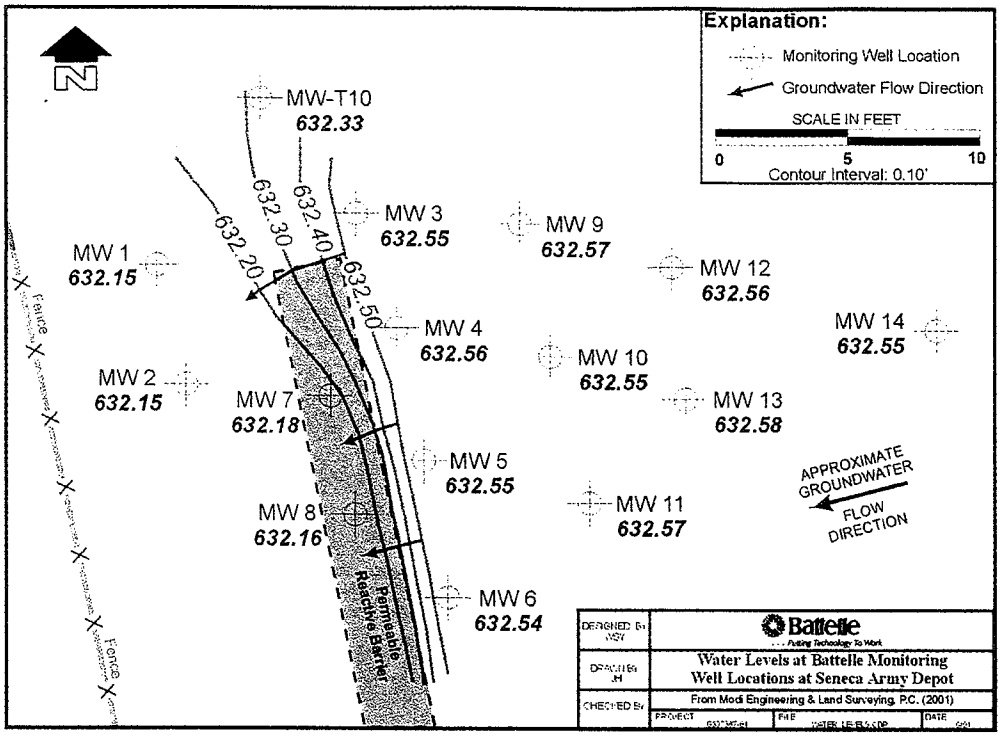

Figure 6-5. April 2001 Water Levels at Seneca Army Depot PRB

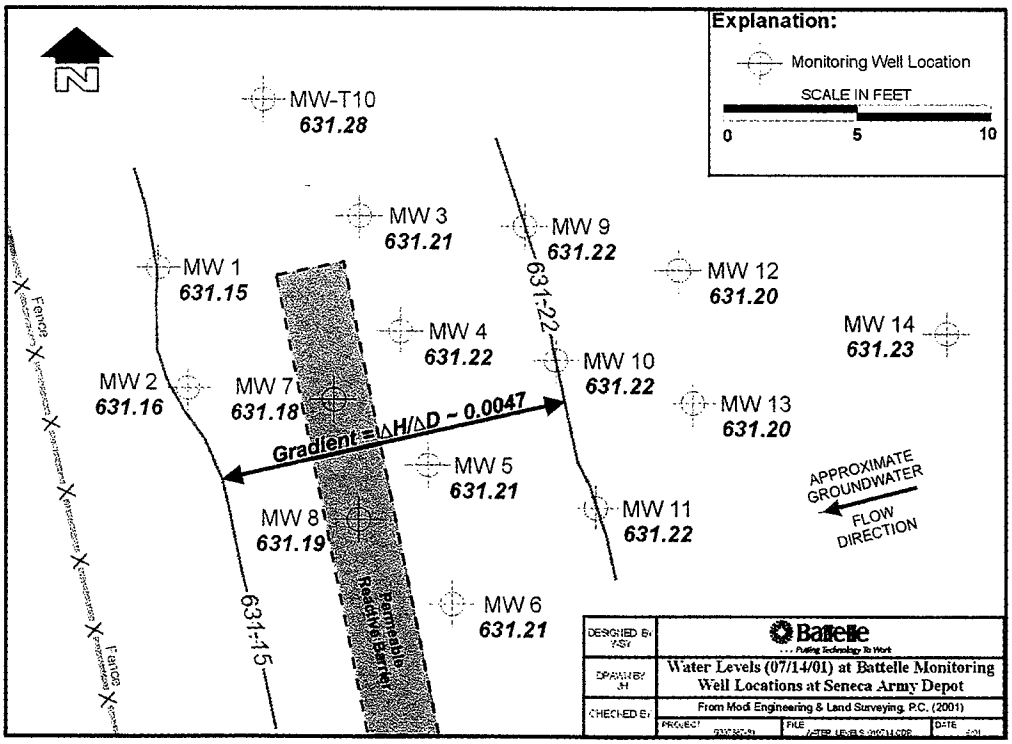

Figure 6-6. July 2001 Water Levels at Seneca Army Depot PRB

Vertical gradients were analyzed previously at the Moffett Field site, where upgradient wells were installed at four different depth intervals. Analysis of these water levels (Battelle, 1998) suggests that a slight downward gradient was induced by the installation of the PRB. A moderate, but progressively downward, gradient was observed from the shallower wells to the deeper wells. In addition, the previously upward (pre-construction) gradient between the lower aquifer to the upper aquifer in which the PRB was placed was reversed to a downward gradient after installation. The effect of such changes in flow patterns on plume capture should be considered in designing and monitoring PRBs at sites with layered aquifers or PRBs that are not keyed into the underlying confining layers.

In addition to periodic water level measurements, continuous water level monitoring in selected wells can provide important information on fluctuations in water levels at the site. No continuous water level monitoring was performed as part of the current project. However, previous data were available from the Former NAS Moffett Field and Dover AFB (Figure 6-7) PRB sites. In general, these data showed seasonal trends that correlate with low and high water levels and precipitation trends. In the example shown in Figure 6-7, the water levels in the downgradient sand (Well P14S) appear to be about 0.25 ft higher than those in the iron cell (Well P7S), indicating stagnation or some backflow in the iron cell during June/July 1998. Other sites may have different trends depending on the local climate and geologic conditions. At NAS Moffett Field PRB, water level response was similar in wells both inside and outside the PRB, suggesting that flow conditions were affected the same in the PRB media as in the undisturbed aquifer. Water levels also remain the same in relation to each other, which suggests that the overall flow patterns are not altered with seasonal water level fluctuations. Continuous water level monitoring is most useful at sites where seasonal fluctuations may be large or where precipitation events cause rapid changes in water levels. In addition, it can be used to evaluate relative water levels over a period of time in groups of wells in a consistent manner.

6.1.2 Hydraulic Conductivity Measurements. Hydraulic conductivity is generally determined in the field using slug tests or pumping tests. The methods and their relative merits are described in the design guidance (Gavaskar et al., 2000). Although pumping tests are considered more accurate, slug tests have been employed for field measurement of aquifer or reactive media K measurements in most PRB studies. Some limitations of pump tests include:

- A proper network of monitoring wells is required for a pump test. An array of multiple wells surrounding the pumping well and screened at similar depths in the same aquifer is the best setup. If wells are too far from the pumping well, they may not be influenced during the test.

- Pumping requirements for a test may be large and long in duration for highly transmissive aquifers. Sometimes, this presents a challenge in disposing of contaminated water. The test may also influence hydrologic conditions.

- Aquifer heterogeneity may interfere with pumping test results, as the test requires a homogeneous, isotropic aquifer for best results.

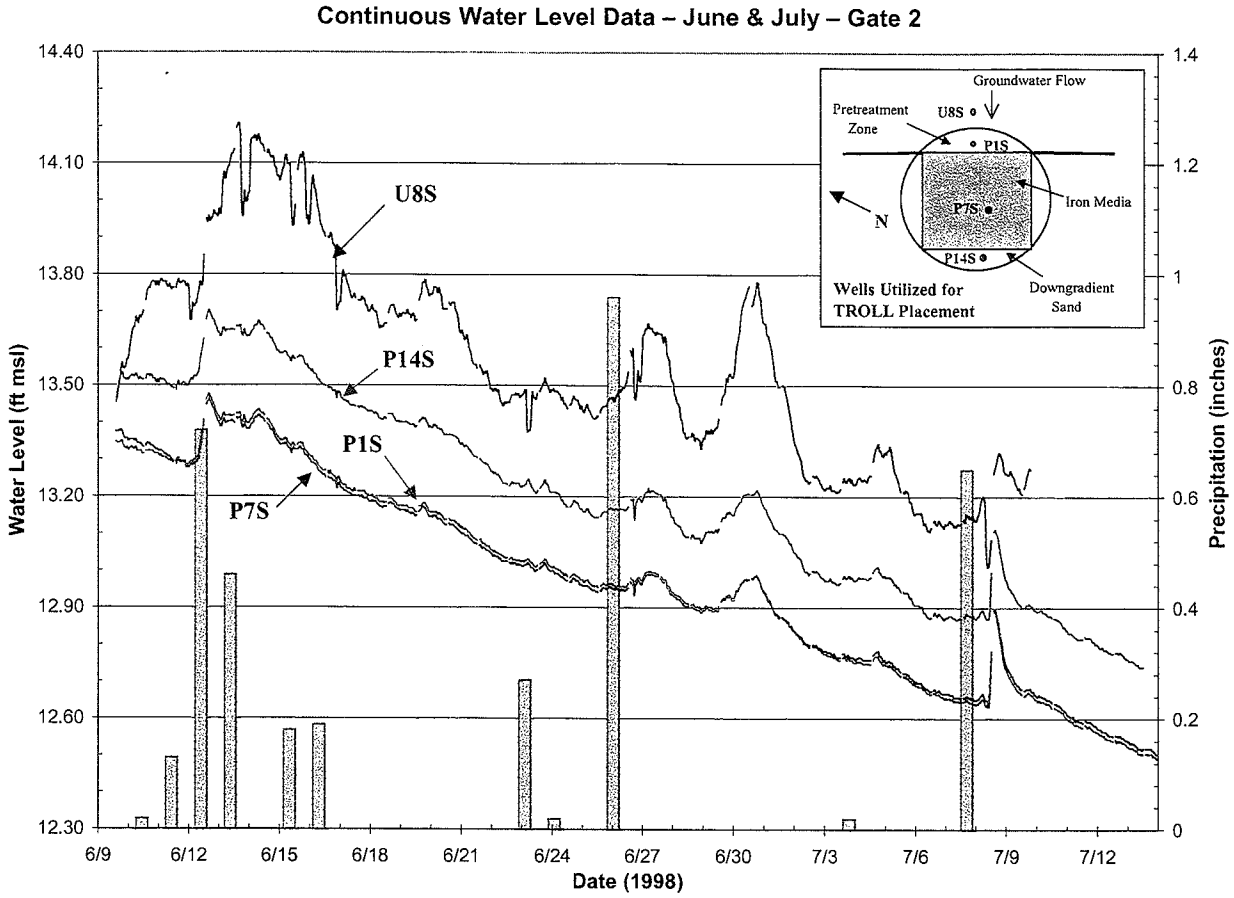

Figure 6-7. Example of Continuous Water Level Monitoring Data from Dover AFB PRB (Battelle 2000a)

- Hydrologic influences such as tides, lakes, streams, and ditches have a substantial effect on well tests. Consequently, these factors must be accounted for by removing long-term trends in water levels from observed results.

- Analysis of pumping test response curves may be challenging. There are many analytical methods for pump tests based on the aquifer properties and well specifications. Some of the methods require estimates of such factors as aquifer thickness and storativity, which may not be readily available.

Slug tests are hydrologic tests designed to determine the hydraulic conductivity of sediments immediately surrounding a well screen. The major limitation of slug tests is that they only provide a hydraulic conductivity estimate for the material immediately surrounding a well screen. In the case of PRBs, this local estimate may actually be advantageous for evaluating

small-scale heterogeneities. However, for sites with large-scale heterogeneities, such as sand channels, slug tests may provide misleading information on sediments in one particular location. Some other limitations of slug tests involve:

- Shallow wells (with less than approximately 10 ft of standing water) may not be large enough to permit a substantial slug to be inserted into the well. Consequently, water level recovery may not be adequate for analysis. This may be problematic for slug tests in wells within PRBs, which are commonly shallow.

- Materials with very high or low conductivity may not provide a good response curve for calculation of hydraulic conductivity. High K material will have a very rapid recovery (less than 10 seconds) and there may not be enough data to fit a line. Conversely, low K material may have a prolonged recovery curve, which is not practical to monitor.

- Slug tests in wells that have a sand pack around the screen may reflect the K of the sand pack rather than the aquifer materials. In general, it is possible to detect a break in the response curves when the recovery starts to reflect the aquifer rather than the sand pack, but smaller wells and slugs may not induce enough stress to impact the aquifer.

Eventually, pumping tests and slug tests, as well as, the laboratory column tests provide a relatively wide range of K values applicable to the site. This range represents both the aquifer variability and the method limitations. Generally it is difficult to determine the K value with a confidence better than half an order of magnitude. This range also results in an uncertainty in the groundwater velocity calculations using modeling or Darcy's law.

No pumping tests or laboratory cores analysis were performed as part of the current project. Slug tests were conducted at former Lowry AFB (Figure 3-2) and Seneca Army Depot (Figure 3-3) PRB sites. In addition, data are also available from previous testing at Moffett and Dover sites. These data are summarized in Table 6-3. In general, the slug tests showed a contrast of several orders of magnitude between the aquifer sediments and the barrier material. In fact, at most sites it has been difficult to obtain reliable slug test data because the extremely high conductivity of iron particles. It is reasonable to assume that conductivity of reactive barrier is typically several orders of magnitude higher that the aquifer media. This is noteworthy from a hydraulic standpoint in that extreme contrasts in permeability may cause variations in flow conditions such as refraction of flow lines and gradient deviations. Another potential difficulty is that on the downgradient side, some flow backup may occur when the water is exiting the high conductivity barrier into the lower conductivity aquifer media.

Within the aquifer media, the tests at Moffett field (Figure 3-2) and Seneca (Figure 3-3) revealed aquifer heterogeneity. The Moffett site contains a relatively specific sand channel within silty sand, while the Seneca site suggested more widespread variations in permeability associated with the glacial till aquifer and presence of anthropogenic preferential pathways. These differences

Table 6-3. Comparison of Slug Test Data in Aquifer Sediments and PRB Material

Site	Hydraulic Conductivity (ft/day)	
	Aquifer	PRB
Dover	1.8 to 101	234 to 812
Lowry	1.1-3.1	NA
Moffett	0.1 to 633	NA
Seneca	0.4 to 126	NA

were reflected in the barrier designs: the Moffett PRB was a 30 ft wide funnel which intercepted the sand channel, while the Seneca design was a 600 ft long trench. At Lowry AFB, all the slug tests showed an exceptionally narrow conductivity range indicating a relatively homogeneous aquifer.

6.1.3 Measurement of Velocity with HydroTechnics™ Sensors and Colloidal Borescope. The velocity of the groundwater in the aquifers and PRBs can also be measured directly using in-situ sensors such as the HydroTechnics™ sensor or borehole probes such as the colloidal borescope. During the current project the HydroTechnics™ sensors were deployed at the Former Lowry AFB and the colloidal borescope was used at the Dover AFB and Former Lowry AFB sites. In addition the KV-meter downhole velocity probe has previously been used at the Former NAS Moffett Field PRB (Battelle, 1998). As shown below, all of these probes have encountered mixed success.

HydroTechnics™ sensors provide information on groundwater flow velocity and direction based on propagation of induced thermal gradients. The sensors were developed at Sandia National Laboratory (Ballard, 1996) and use a thermal perturbation technique to directly measure the three-dimensional groundwater flow velocity vector in unconsolidated, saturated, porous media. The sensors are installed directly in a boring. A heating element within the probe heats the surrounding aquifer materials and groundwater to a temperature of about 20 to 30°C above background. The temperature distribution at the surface of the probe is affected by the groundwater movement resulting from advective flow of the heated groundwater. The technology allows for long-term, remote, continuous monitoring of the groundwater flow regime in the immediate vicinity of the probe.

Four HydroTechnics™ sensors were installed at Dover PRB site (Battelle, 2000a). Two sensors were installed upgradient of the PRB and the other two sensors were installed within the PRB (Figure 6-3). The sensors were monitored for six months. Results from the sensors at the Dover site showed periods of substantial groundwater velocity fluctuations after the initial installation. Each sensor appeared to stabilize, but flow velocities appeared to be less than velocity determined by groundwater simulations. It was also difficult to determine whether the observed flow directions from the probes inside the reactive cells are the true representation of groundwater flow or if they have been affected by the iron media.

Two HydroTechnics™ sensors were installed at the Lowry PRB site in October 1999. One sensor was installed about 5 ft directly upgradient of the PRB and the other was installed towards the end of the eastern funnel wall to assess the flow divide (Figure 6-4). Table 6-4 summarizes the power supply specifications for the sensors. The sensors were monitored for 18 months from October 1999 to April 2001. However, data recorder malfunction resulted in the loss of data from March 2000 to early April 2001. Figure 6-8 summarizes the results of the monitoring at Lowry based on available data. Contrary to expectation, groundwater velocities do not appear to respond to precipitation as strongly as at Dover AFB PRB. Velocities upgradient of the reactive cell (probe HT0080) appear to increase slightly, while velocities upgradient of the funnel wall appeared to decrease over the monitoring period. Both sensors are within a reasonable range of the water levels based velocities of 0.2 ft/day at the site.

Table 6-4. Power Supply for HydroTechnics™ Sensors.

Probe ID	Medium	R (ohms)	V (volts)	I (amps)	P (watts)
A (HT0080)	Aquifer	43	50.0	1.16	58.1
B (HT0081)	Aquifer	44	50.0	1.14	56.8

In the sensor upgradient of the Lowry barrier (HT0080) flow direction drifts from about 160 to 220° indicating flow to south and southwest, away from the reactive gate. This is contrary to the expectation that the flow just upgradient of the reactive gate should be directed towards the reactive gate. It is impossible to determine if the water at this location is actually flowing away from the barrier, stagnating, or indicative of sensor anomalies. It is also possible that the anomalous flow direction at this location is due to a localized flow cell or slight mounding within the PRB. The other sensor near the end of the east funnel wall (HT0081) indicates that groundwater is being flowing towards north (0°) as expected.

Overall, the flow sensors at both Lowry and Dover sites performed reasonably well. The major limitation is due to the requirement that flow patterns need to be determined over very short distances, especially within the reactive cells. This is the same problem encountered with the water level measurements because the short distances of interest in both cases make it difficult to interpret the results with certainty. Major limitation is that it is difficult to distinguish between bulk flow in the aquifer and local-scale preferential flow. The objectives of the PRB monitoring, determining capture zone and residence times, require and understanding of both the local flow patterns and bulk flow patterns in the aquifers. The HydroTechnics™ sensors probably provide information on the local patterns. However, it is difficult to determine how the local flow lines sampled by the probes fit with the overall flow patterns at the site. It has also been difficult to match the sensor based data with the water levels based flow patterns.

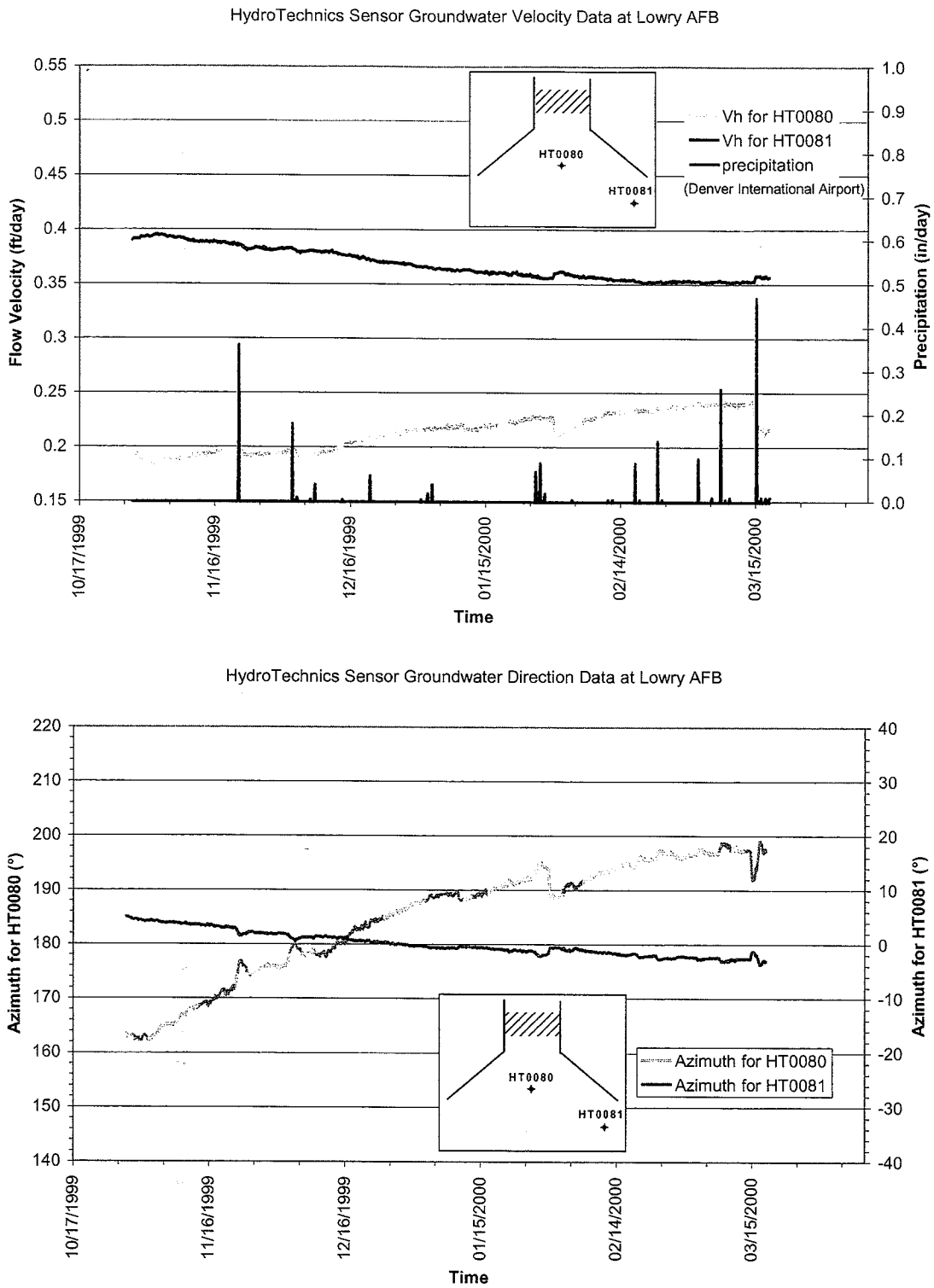

Figure 6-8. HydroTechnics™ Results for Lowry PRB Site Showing Groundwater Flow Velocity, Groundwater Flow Direction (Azimuth), and Precipitation Over Time at the Site

The second velocity sensor used in the current project, the colloidal borescope, was developed at Oak Ridge National Laboratory (ORNL) for the measurement of flow conditions in monitoring wells (Kearl et al., 1992). The instrument relies on the use of a specialized downhole camera for observation of colloidal particle movement across the well screen. The moving particles are recorded on a computer screen for calculation of flow direction and velocity. The borescope is limited to observations in the preferential flow zones within the well and therefore the results may be biased towards the faster flow zones in the aquifer (Kearl, 1997).

The borescope was used at the Dover PRB site in fourteen wells at the site (Table 6-5). The results at Dover were generally mixed, with many of the wells showing a swirling pattern or flow directions not matching the conceptual model of flow through the barrier (Figure 6-2). The mixed flow direction results using the borescope appear to match the extremely flat water levels at the site. Therefore, based on the December 1999 monitoring with borescope and water level measurements the flow directions at the Dover PRB are inconclusive.

Table 6-5. Colloidal Borescope Measurement Results in the Dover PRB (December 1999)

Well ID	Depth of Flow Zone(s) (ft)	Predominant Flow Direction	Preferential Flow Zone Velocity (ft/d)
U1-S	18.5	SW	4.8-9.6
U3-S	18	NW	6-12
U4-S	35.5	WSW	7.7-15
U4-M	19	NW	6.5-13
U4-D	26	NNE	1.8-3.6
U5-S	32	SW	1-2.1
U5-D	None	None	None
U-12-S	34	WNW	7.8-15.7
U-12-D	18	S	5.9-11.9
U-13-S	None	None	None
F1-S	None	SW	None
F10	None	W	None
F14-S	None	None	None
P1-S	None	None	None
U7-D	34	ENE	7.7-15.5
U8-M	None	None	None
U8-D	33	WSW	3.6-7.1
U9-D	34	N	5.9-11.7

The borescope was also employed at the Lowry site in a total of eleven wells both upgradient and downgradient of the barrier (Figure 6-4). No measurements could be made inside the reactive cell the diameter of the monitoring wells in the cell was too small. Table 6-6 summarizes the results of the colloidal borescope testing at the Lowry barrier and an example output plot is shown in Figure 6-9. Although three of the wells showed swirling flow directions,

Table 6-6. Colloidal Borescope Measurement Results in the Vicinity of Former Lowry AFB PRB (October 1999)

Well ID	Depth of Flow Zone(s) (ft)	Flow Direction	Preferential Flow Zone Velocity (ft/d)
Upgradient Aquifer Wells			
U-1	11	NE	4.54
U-6	Non located	Swirling Flow	NA
U-7	10, 12.5	N, N	3.76, 2.24
N-9	13	ESE	11.29
N-2	10	NNW	4.38
U-9	12.5	E	2.16
U-10	None located	Swirling Flow	NA
N-1	11	NNW	6.15
N-3	None located	Swirling Flow	NA
Downgradient Aquifer Wells			
N-5	None located	Swirling Flow	NA
N-6	10.5	NW	6.01

the other wells generally indicated flow to the north into the PRB (Figure 6-4). Groundwater flow velocities in preferential flow zones were much higher (2.2 to 11.3 ft/day) than the 0.2 ft/day flow velocity other observations suggest for the site. This reveals that the borescope may be limited to measure velocities in high flow zones rather than flow throughout the aquifer thickness (bulk flow). The flow directions in most wells show a reasonable match with the flow vectors determined from water-level vectors. However, there is not a good match between flow vectors from the HydroTechnics™ probe upgradient of the reactive cells.

Overall, it appears that the borescope has limited applicability in the low flow settings such as Dover AFB, where few preferential pathways exist. At sites with a reasonably high flow velocity or presence of preferential pathways, the borescope appears to be more useful. If the objective of monitoring is to find preferential flow zones at a site, then this instrument can be used at a reasonable cost.

6.2 Groundwater Modeling for Performance Assessment

Groundwater modeling has been performed at most PRB sites (see Table 6-7), although to varying degrees of detail, to evaluate capture of the contaminant plumes. The major advantage of constructing a detailed groundwater flow model is that several design configurations, site parameters, and performance and longevity scenarios can be readily evaluated once the initial model has been set up. Thus, the combined effect of several critical parameters can be incorporated simultaneously into one model. The hydraulic performance of PRBs is affected by many variables including: barrier dimensions, hydraulic properties of the reactive media, and variations in aquifer conditions. To assess the impact of these parameters, groundwater flow modeling was performed to illustrate various scenarios. Such factors as groundwater flow velocity, residence times within the PRB, capture zones, and gradients were evaluated as

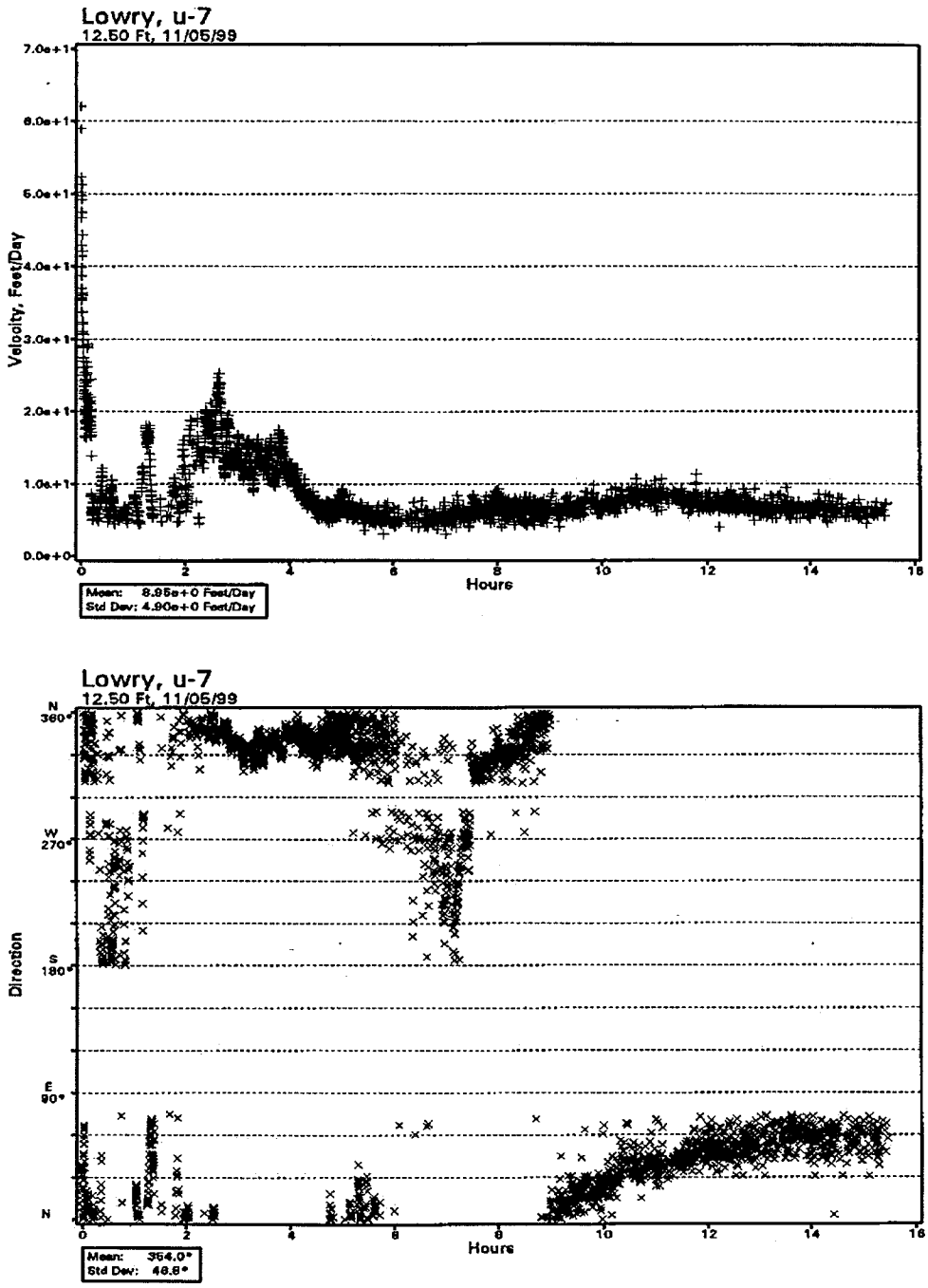

Figure 6-9. Example of Colloidal Borescope Results for Well U-7 at Former Lowry AFB PRB

Table 6-7. Summary of Groundwater Modeling at DoD PRB Sites

Site	Former NAS Alameda PRB	Dover AFB PRB	Former NAS Moffett PRB	Seneca Army Depot PRB
Flow Model	MODFLOW	MODFLOW	MODFLOW	MODFLOW
Transport Model	MODPATH	RWALK3D	RWALK3D	MODPATH
Model Dimensions (ft)	600 by 600	1,600 by 1,800	700 by 1,000	1,600 by 2,100
# Layers	6	1	7	3
Minimum grid block size (ft)	1 by 1	0.25 by 0.25	0.5 by 0.5	5 by 5
Calibration	Calibrated to Steady State and Transient Water Levels	Calibrated to Pre-installation Water Levels	Calibrated to Pre-installation Water Levels	Calibrated to Average Water Levels
PRB Setup	Horizontal Flow Barrier[(a)]	Horizontal Flow Barrier[(a)]	Horizontal Flow Barrier[(a)]	Horizontal Flow Barrier[(a)]
Summary	Modeling indicated general plume capture with or without extraction wells.	Modeling demonstrated that the PRB capture zone would be adequate, to accommodate seasonal fluctuations in flow directions.	Modeling showed capture by the wall with an asymmetric capture zone due to aquifer heterogeneity.	Modeling demonstrated effective capture of the plume and suggested that no mounding would occur upgradient of the PRB

(a): Hsieh and Freckelton, 1993.

indicators of PRB effectiveness. Issues related to field observations in operational PRBs were addressed with respect to how hydraulic conditions affect PRB performance. More detailed discussion of the modeled scenarios is presented in Battelle (2000c) modeling report. A general discussion on the use of computer simulations to design and evaluate PRBs is presented in Gupta and Fox (1999). The rest of this section provides general examples of modeling capture zones and residence times in PRBs, a example of a CRB modeling for Seneca Army Depot PRB, and illustrations of some unique hydrogeologic scenarios related to PRBs. The modeling of other DoD sites, especially Former NAS Moffett Field and the Dover AFB PRBs, has been presented in previous Battelle reports and will not be repeated here.

In general, modeling involves two parts: groundwater-flow modeling and transport modeling. Groundwater flow modeling involves simulating the flow volumes and velocities in and around the PRB. The finite difference computer program MODFLOW (McDonald and Harbaugh, 1988) is the accepted industry standard for groundwater flow modeling and capable of simulating PRB scenarios. Depending on the site, modeling of the flow conditions before and after the installation of the PRB may be performed to assess the overall impact of the PRB on the flow system. Flow output may be coupled with a groundwater transport model, which simulates the movements of particles or plumes in the flow field. Typical transport models include MODPATH (Pollack, 1989), MT3D (Zheng, 1990), and RWALK3D (Battelle, 1995).

6.2.1 Capture Zones and Residence Times. The two primary parameters involved in performance assessment of PRBs are the capture zones and residence times. In addition, modeling may also be used to evaluate hydraulic gradients, zone of influence of PRBs, different design scenarios, and effect of surface features such as ponds, streams etc., on the PRB design. Figure 6-10 shows examples of modeling output that may be used to assess PRB performance.

6.2.1.1 Capture Zone. Groundwater flow and transport models can aid in determining the capture zone of PRBs. Modeling is especially valuable at sites where there is a low hydraulic gradient or it is not possible to install many monitoring wells. Several different methods may be used to assess PRB capture zones:

- Simulated heads from groundwater flow models indicate the direction and rate of groundwater flow.
- Flow vectors from groundwater flow models illustrate both the magnitude and direction of groundwater flow in relation to the PRB.
- Particle tracking with transport modeling can delineate capture zones.
- Simulation of a slug source with transport models shows the actual plume capture.

Measured concentrations may be used as inputs into a transient model to simulate the movement of a contaminant plume into the PRB. Other transport model configurations such as continuous sources may also be used to determine capture zone of the PRB. Figure 6-10 illustrates the various methods available to model PRB capture zones. Of the methods, particle tracking provides the most definite representation of the capture zone and can reveal stagnation zones.

Simulation of a tracer or plume source adds value in that it reveals chemical concentration gradients in and around the PRB.

6.2.1.2 Residence Time. Modeling may be used to estimate the residence time in a PRB. In general, transport modeling is the best computer simulation option for determining residence times within the PRB media (Figure 6-11), although, plume simulation methods may also be used to assess the residence time in the PRB. These methods provide a more detailed view of the migration of groundwater through the PRB than traditional velocity equations based on monitoring data. Particle tracking predicts the path and rate that a particle travels in a flow field. Transport codes may integrate several different processes such as dispersion, sorption, and chemical reaction to predict the contaminant concentration over time within and around the PRBs. Darcy's Law groundwater velocity equations are based on gradients in the PRB:

$$V_x = \frac{K(dh/dl)}{n_e} \qquad (6\text{-}1)$$

where V_x = the average linear groundwater flow velocity
K = the hydraulic conductivity of the aquifer material (L/t)
dh/dl = the hydraulic gradient
n_e = the effective porosity.

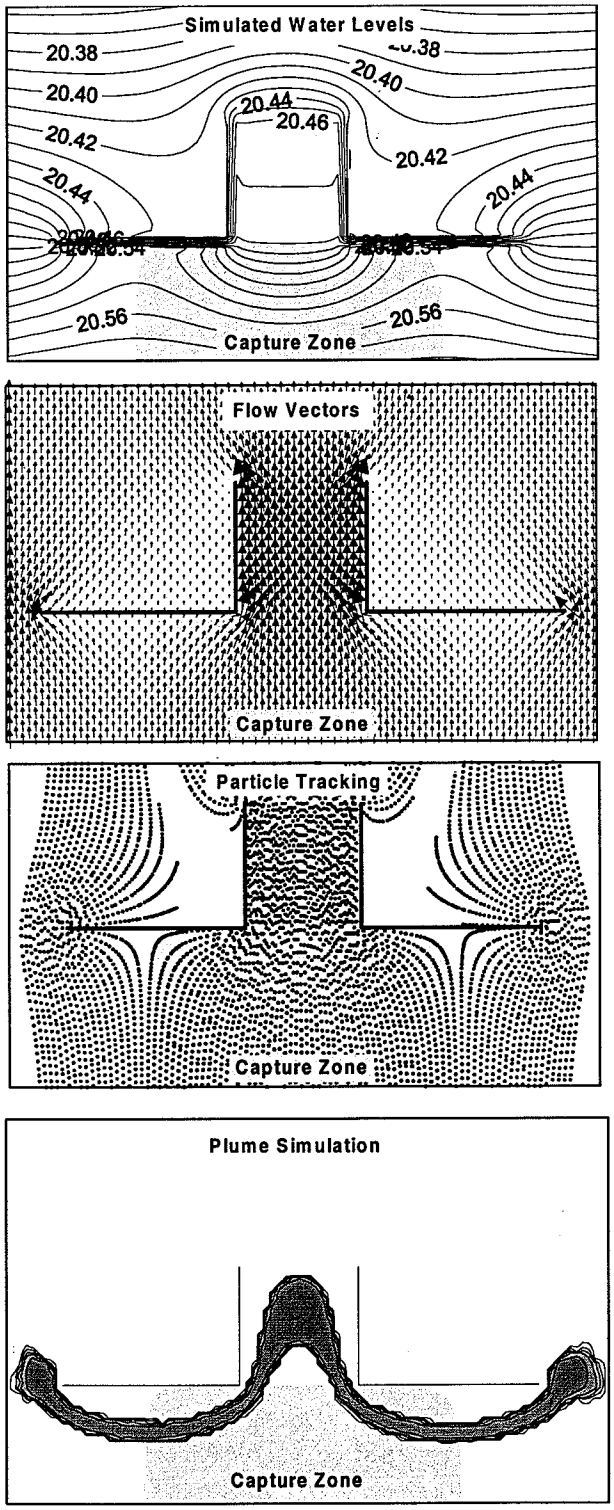

Figure 6-10. Modeling Methods Used to Illustrate Capture Zone of PRBs (Battelle, 2000c)

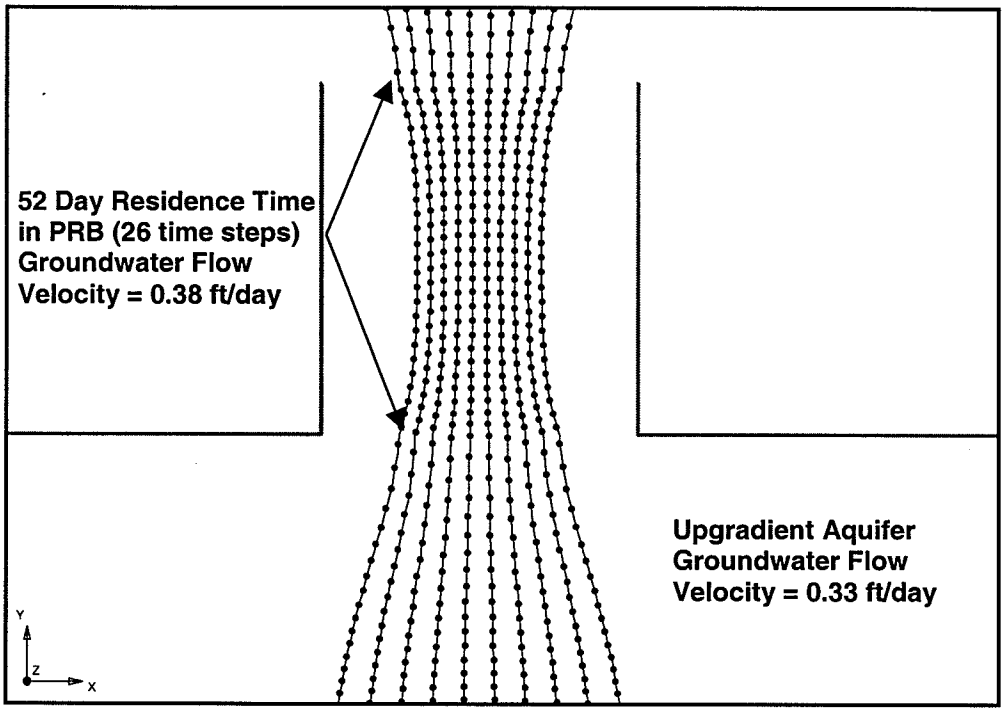

Figure 6-11. Example of Particle Tracking Used to Determine Residence Time Within a PRB. In the example, groundwater takes 52 days to travel through the PRB. There is only a small increase in groundwater flow velocity through the PRB (0.38 ft/day) compared to the upgradient aquifer groundwater flow velocity (0.33 ft/day).

In the field, it is difficult to measure water level differences within the small area of the PRB. This is further complicated by the fact that gradients in highly permeable PRB media are low. For instance, if modeling indicates a gradient of 0.001 ft/ft in a PRB 20 ft long, then water levels would vary by only 0.02 ft from the entrance of the PRB to the exit of the PRB. These differences in water levels approach the limits of the accepted accuracy of water level measurements (0.01 ft). Consequently, transport modeling is valuable to simulate groundwater movement to determine potential range of residence times where traditional monitoring methods are limited.

6.2.2 Seneca Army Depot CRB Modeling. To illustrate the effects of hydraulic conductivity affecting flow around the PRB at Seneca Army Depot, a basic groundwater flow model with heterogeneous hydraulic conductivity was created. The objective of the modeling was to demonstrate the effects of heterogeneity around the north end of the PRB on the flow system rather than to accurately match the observed water levels through calibration. Fourteen new wells were installed at the northern end of the barrier (Figure 6-5 [MW1-MW14]) to assess groundwater flow conditions through and around the wall. Water-level surveys performed in April 2001 showed groundwater flow through the PRB with some deflection around the end of the barrier (Figure 6-5). More recent survey performed in July 2001 showed a much flatter water

table with a low hydraulic gradient of 0.005 (Figure 6-6). This indicates that the system is subject to seasonal fluctuations in groundwater flow. The model was approximately calibrated to the higher flow velocity observed in April 2001, an event which provided more discernible hydraulic gradients.

The model was set up in MODFLOW (McDonald and Harbaugh, 1988) as a 1-layer, unconfined aquifer. Model domain was 40 ft by 30 ft and includes the northern 15 ft of the PRB. Constant head nodes were specified at the east and west ends of the model domain to simulate a gradient of 0.01 ft/ft, which has been the average gradient observed at the site. Several zones of hydraulic conductivity were specified based on the slug test results (Figure 6-12). The permeability zones range from 1.5 ft/day to 75 ft/day in the aquifer. The reactive media hydraulic conductivity was specified as a zone of 300 ft/day.

The model was run to a steady-state solution. Figure 6-13 shows the simulated heads. As shown, the simulation does not predict the steep head increase directly upgradient of the PRB. However, the model does show contours bending around the northern end of the PRB similar to those in the observed water level map (Figure 6-5). Flow vectors (Figure 6-14) suggest that much of the groundwater flow occurs in high permeability zones. The vectors also indicate some lateral movement within the PRB, a process that is not usually considered in the design and monitoring of reactive barriers. This lateral flow appears to be caused by the conductivity zones in the upgradient aquifer.

The observed high gradient along part of the PRB (Figure 6-5) may have been caused by smearing effect at the boundary between the PRB and the aquifer media. To evaluate this hypothesis, the model was modified to include a low permeability region in front of the PRB. Results of this model are shown in Figure 6-15. This simulation shows more closely matches the observed water level map immediately upgradient of the PRB. No attempt was made to match the water levels near to northern edge of the PRB in this scenario. While this is far from a conclusive indication of smearing along the PRB wall, it does lend support to concern that a low permeability smear zone upgradient of the PRBs at some sites may be affecting flow through the PRB. On the hand, it is also possible that the natural conductivity variations or season water level fluctuations in the aquifer are causing the observed high gradients seen in the April 2001 maps.

6.2.3 Modeling the Hydraulic Aspects of PRBs. Models are especially useful in the design of barriers and selection of barrier materials because the models may be used to optimize the design and evaluate effects of future changes in site conditions before investing in the PRB installation. This section summarizes some of the modeling scenarios simulated as part of the current project. These modeling scenarios provide useful guidance for design and monitoring of PRBs.

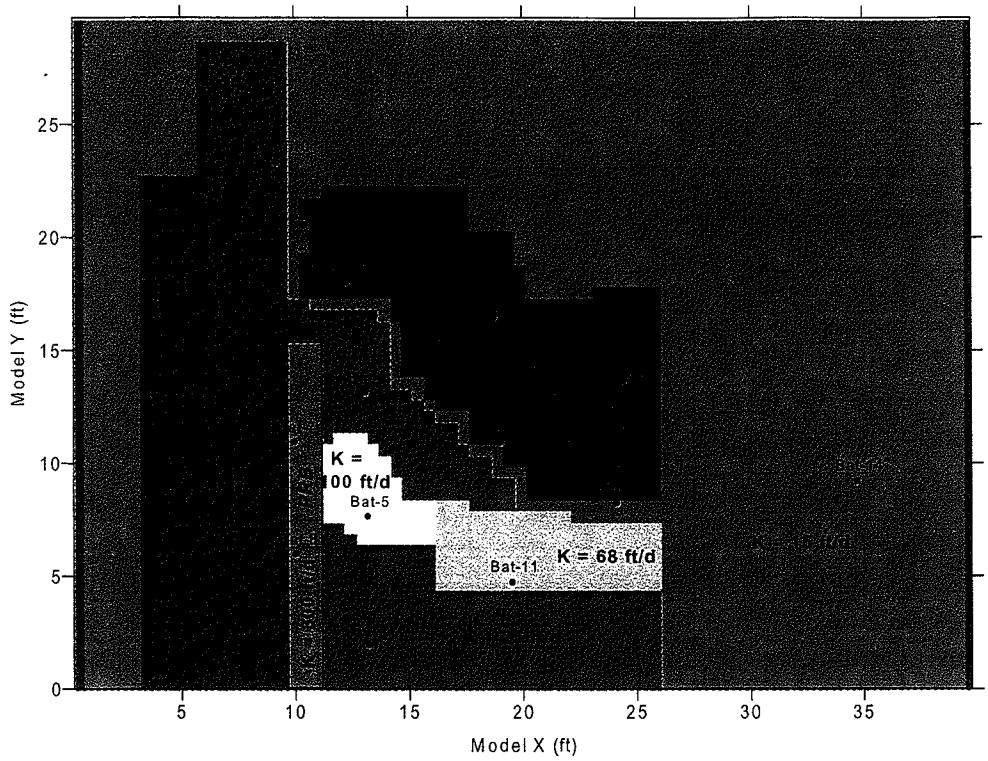

Figure 6-12. Model Setup and Permeability Zones at Seneca Army Depot PRB

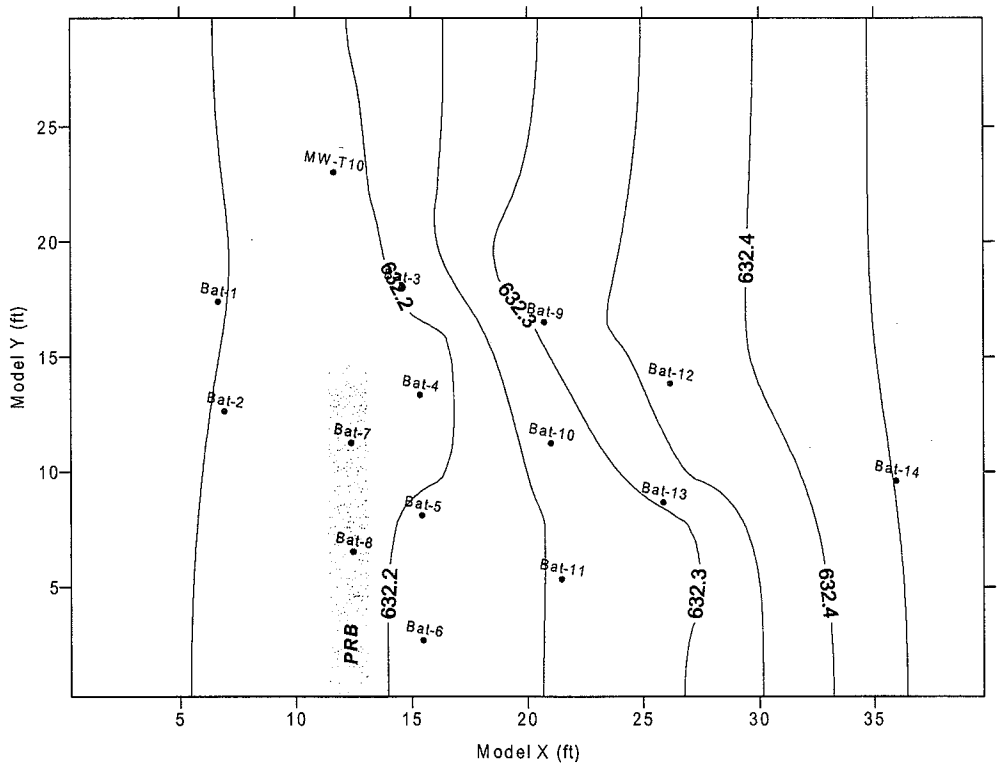

Figure 6-13. Simulated Water Levels at Seneca Army Depot PRB

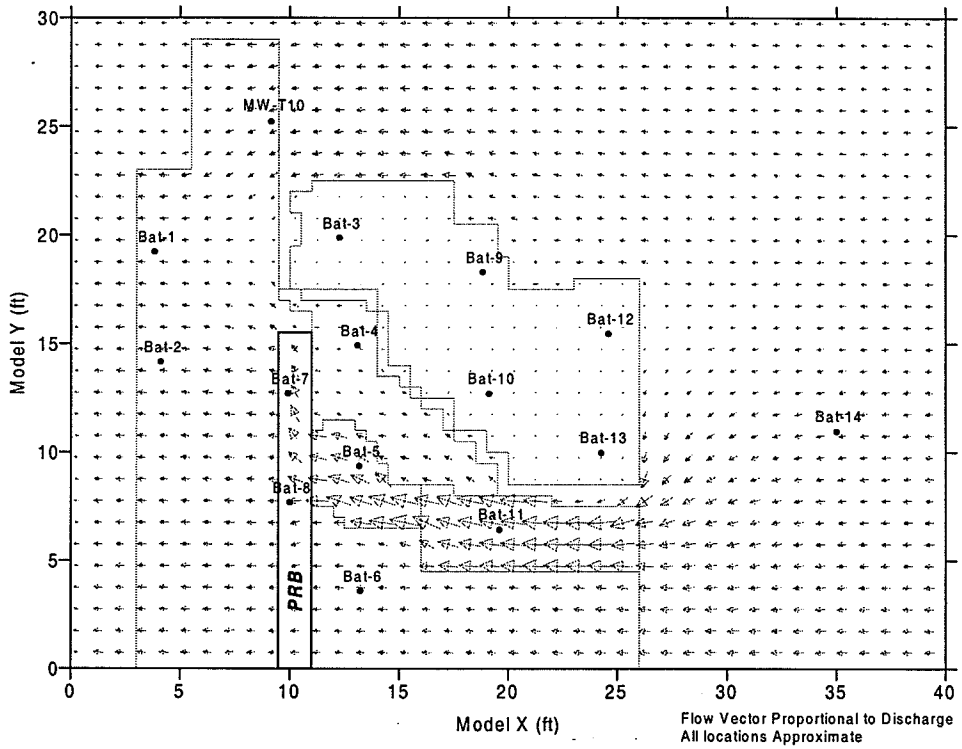

Figure 6-14. Simulated Flow Vectors at Seneca Army Depot PRB

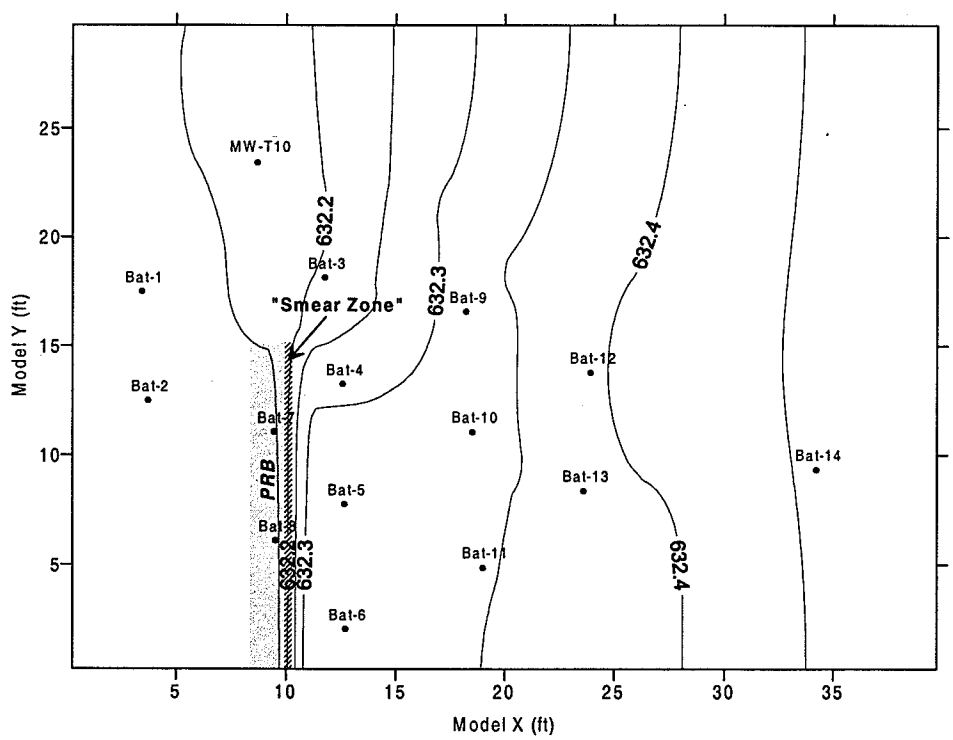

Figure 6-15. Simulated Water Levels at Seneca Army Depot CRB with a Low Permeability Zone Upgradient of the PRB

6.2.3.1 Effect of Hydraulic Parameters. The key hydraulic parameters controlling PRB performance are derived from the Darcy's Law. These include hydraulic gradient, hydraulic conductivities of aquifer and reactive media, porosity, and the PRB dimensions. The hydraulic conductivity of PRBs is typically much greater than the aquifer. Modeling shows that this increases the flow of groundwater into the barrier as long as PRB conductivity is slightly higher than the aquifer conductivity (Gupta and Fox, 1999). Figure 6-16 shows the effect of PRB conductivity on capture of a plume. When the conductivity of the PRB is less than that of the aquifer, the entire plume bypasses the PRB. The plume capture progressively improves as the PRB conductivity increases relative to the aquifer. However, as the PRB conductivity increase, the gradient within the PRB becomes essentially flat (Figure 6-17). This condition is common in most PRBs because the reactive media conductivity is several orders of magnitude higher than the aquifer conductivity in an effort to increase plume capture. The monitoring of the PRB for residence times and flow velocities at such low gradients is extremely difficult.

The porosity of the PRB media will affect the rate of groundwater flow through the PRB. In general, material with high porosity will have a lower groundwater velocity through the PRB gate. PRB media often have high porosity (up to 0.70). Consequently, residence time in the PRB will increase for highly porous reactive media. In addition, groundwater flow velocity measurements based on sensors or measured gradient will be more uncertain. The actual discharge through the PRB may remain acceptable because groundwater is discharging through a larger cross sectional area for media with higher porosity.

Variations in the hydraulic gradient and flow direction in the aquifer also affect the capture zone and residence times in PRBs. Changes in flow direction may be accounted for with a correction factor. Variations in gradient may also be accounted for by increasing the width of the barrier to ensure that groundwater will remain in the barrier long enough for complete treatment.

6.2.3.2 Hanging Wall Configurations. A hanging wall configuration may be appropriate at sites where the aquifer is deep and/or the contamination plume is limited to a defined depth interval. In the setup, the barrier wall only partially penetrates the aquifer rather than fully penetrating the affected aquifer. To evaluate groundwater flow for a hanging wall configuration, a three-layer model was developed with a funnel-and-gate PRB in the middle layer. Thus, the model can predict if groundwater will be captured by the gate or if groundwater will flow under or over the PRB. Figure 6-18 shows the results of particle tracking through a hanging wall PRB with hydraulic conductivity of 30 ft/day and 300 ft/day (aquifer hydraulic conductivity of 30 ft/d). As shown, particles move under the barrier walls even if the PRB has a K greater than the surrounding aquifer. Cross-section views of particle tracking illustrate how groundwater moves under and over portions of the barrier walls that would normally capture groundwater for a fully penetrating configuration. The PRB section of the funnel-and-gate continues to capture groundwater from areas immediately upgradient. Thus, a PRB without barrier walls is a more suitable configuration for a site where a hanging wall configuration is necessary. Other conditions that may encourage flow under or over a PRB include high downward vertical gradients, vertical anisotropy, and aquifer heterogeneity. A continuous

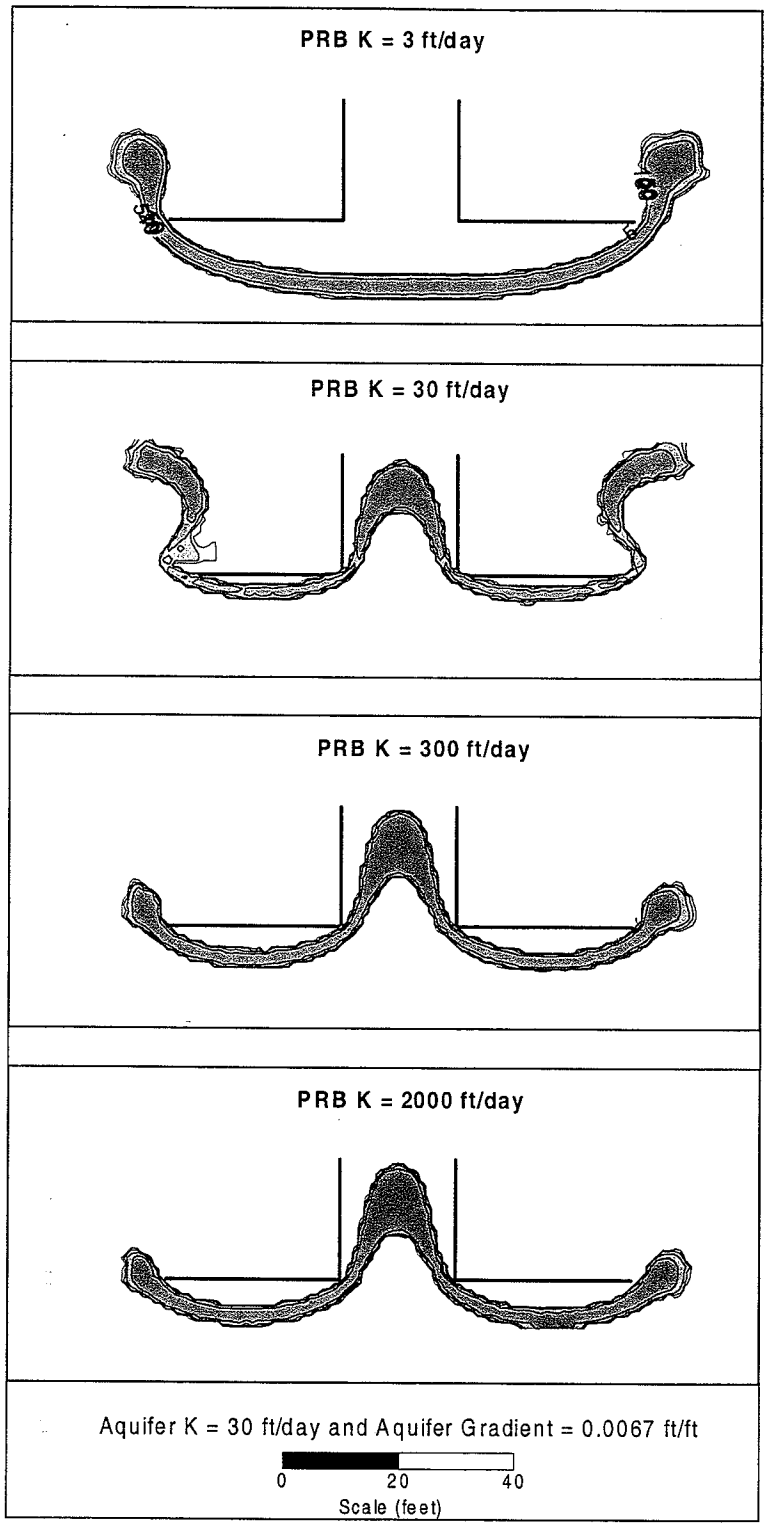

Figure 6-16. Transport Modeling of a Slug of Contamination Through a Funnel-and-Gate PRB for a Range Hydraulic Conductivity in the PRB. Flow is diverted around the PRB at lower hydraulic conductivity. At higher hydraulic conductivity, the capture zone does not substantially increase in size.

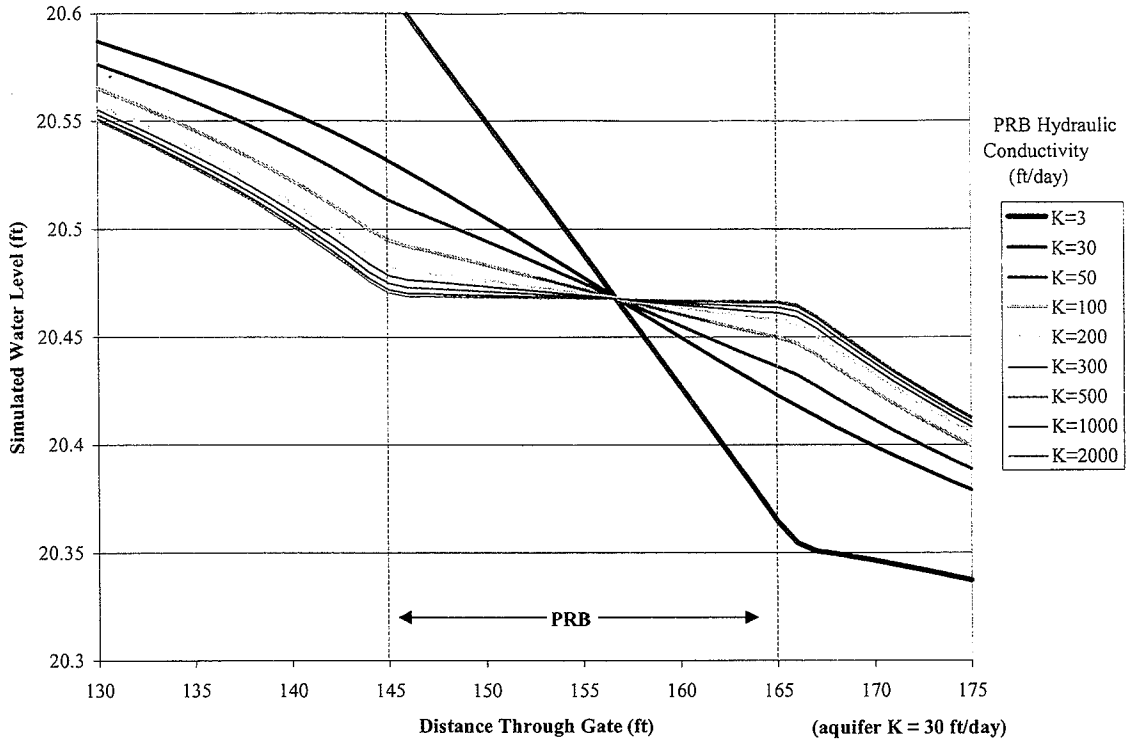

Figure 6-17. Simulated Hydraulic Gradient Through a PRB for a Range of PRB Conductivity. As shown, the gradient in the PRB is very low with a high PRB hydraulic conductivity.

barrier in the hanging wall configuration is less likely to experience flow under or over the barrier as long as the PRB material is more conductive than the surrounding aquifer material. Consequently, continuous barriers are more appropriate for situations requiring a hanging wall.

6.2.4 Angled Flow into the PRB. One of the problems encountered at some PRB sites is that the orientation of the PRB is not perpendicular to the groundwater flow direction due to temporal variations, insufficient characterization, or poor design. This can lead to insufficient residence time or capture of the untargeted part of groundwater. At the interface of the PRB and aquifer, flow lines will be refracted due to the difference in hydraulic conductivity. The amount of refraction that occurs is expressed in the tangent law:

$$\frac{\tan \phi_1}{\tan \phi_2} = \frac{K_1}{K_2}$$

Φ_1 = angle of groundwater flow to PRB
Φ_2 = angle of refraction in PRB,
K_1 = hydraulic conductivity of aquifer, and
K_2 = hydraulic conductivity of PRB.

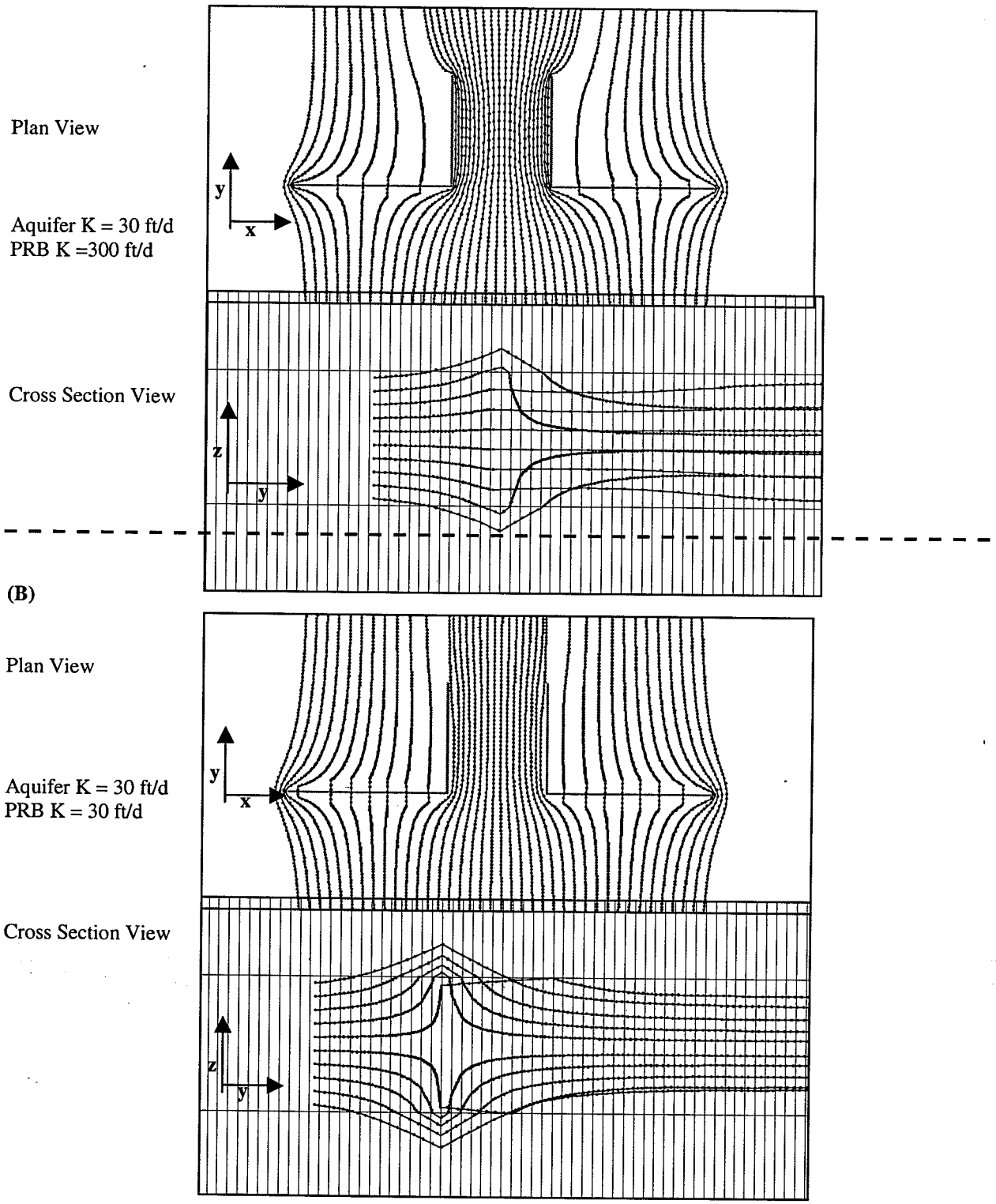

Figure 6-18. Particle Tracking Through a Hanging Wall PRB Configuration. With PRB K set at 300 ft/day (A) only a small portion of groundwater flows under/over the wall, but with PRB K set at 30 ft/day (B) a large proportion of groundwater flows under/over the wall.

This formula demonstrates how the flow direction will be changed when water flows into the reactive barrier at an angle. Figure 6-19 shows a graph of the amount of refraction that will occur for different angles of groundwater flow to the PRB and for hydraulic conductivity differences. When the barrier is properly installed, the angle of groundwater flow to the barrier is 90°, and the hydraulic conductivity of the barrier is equal or greater than the aquifer, no refraction will occur and the flow direction will stay the same as in the aquifer. If groundwater is flowing at an angle to the barrier, and the barrier is much more permeable than the aquifer; then groundwater will be refracted in the barrier. For example, groundwater flowing at an angle of 30° to a barrier that is ten times more permeable than the aquifer would result in flow refracted nearly 80° in the barrier. This suggests that while flow is at an angle in the aquifer, it will flow nearly straight along the width of the barrier resulting in longer residence times.

Aquifer gradients may vary in direction with precipitation events, pumping, and various other processes. An example of the effect of the change in flow direction on plume capture is shown in Figure 6-20. One strategy to ensure that a PRB will capture the desired contamination plume is to incorporate a safety factor into the design of the system, based on seasonal variations in gradient direction (Figure 6-21). The following safety factor accounts for seasonal variations in gradient direction when designing or evaluating a PRB system:

$$(\mathrm{TAN}\ (45° + \alpha/2))$$

where,

α = seasonal fluctuation in gradient direction (°).

The correction factor may be used to modify the width of the PRB. For example, an aquifer where the gradient varies by 5° seasonally would require only a 9% increase in width (Tan(45+(5°/2) = 1.09), while an aquifer where the gradient varies by 15° seasonally would require a 30% increase in width (Tan(45+(15°/2) = 1.30). The safety factor may be applied to either continuous reactive barriers (CRBs) or funnel-and-gate systems. With a CRB, the overall width may be adjusted. With a funnel-and-gate PRB, the entire width of the system may need to be adjusted or the barrier wings may be lengthened to increase the capture zone width. However, once the barrier wings become much wider than the gate portion of the PRB, the efficiency of the system is reduced so this should be considered when increasing the width of the PRB.

Another option to rectify an exiting PRB that has angled flow into the barrier is to conduct engineering modifications. To investigate the effect of different arrangements on a barrier that is not capturing the desired part of the plume, several scenarios (Table 6-8) were modeled. In the model, the aquifer was assigned a conductivity of 15 ft/d, an 8 ft by 2 ft barrier was assigned a conductivity of 1,000 ft/d, and a gradient of 0.01 was assigned at a 30° angle to the barrier. In this setup, it is assumed that barrier is not capturing the desired part of the plume because it was improperly installed or the groundwater flow direction changed. Figure 6-22 shows forward particle tracking through gate for the base scenario. Some of the plume is captured by the barrier due to the conductivity contrast, but over half of the plume flows around the barrier.

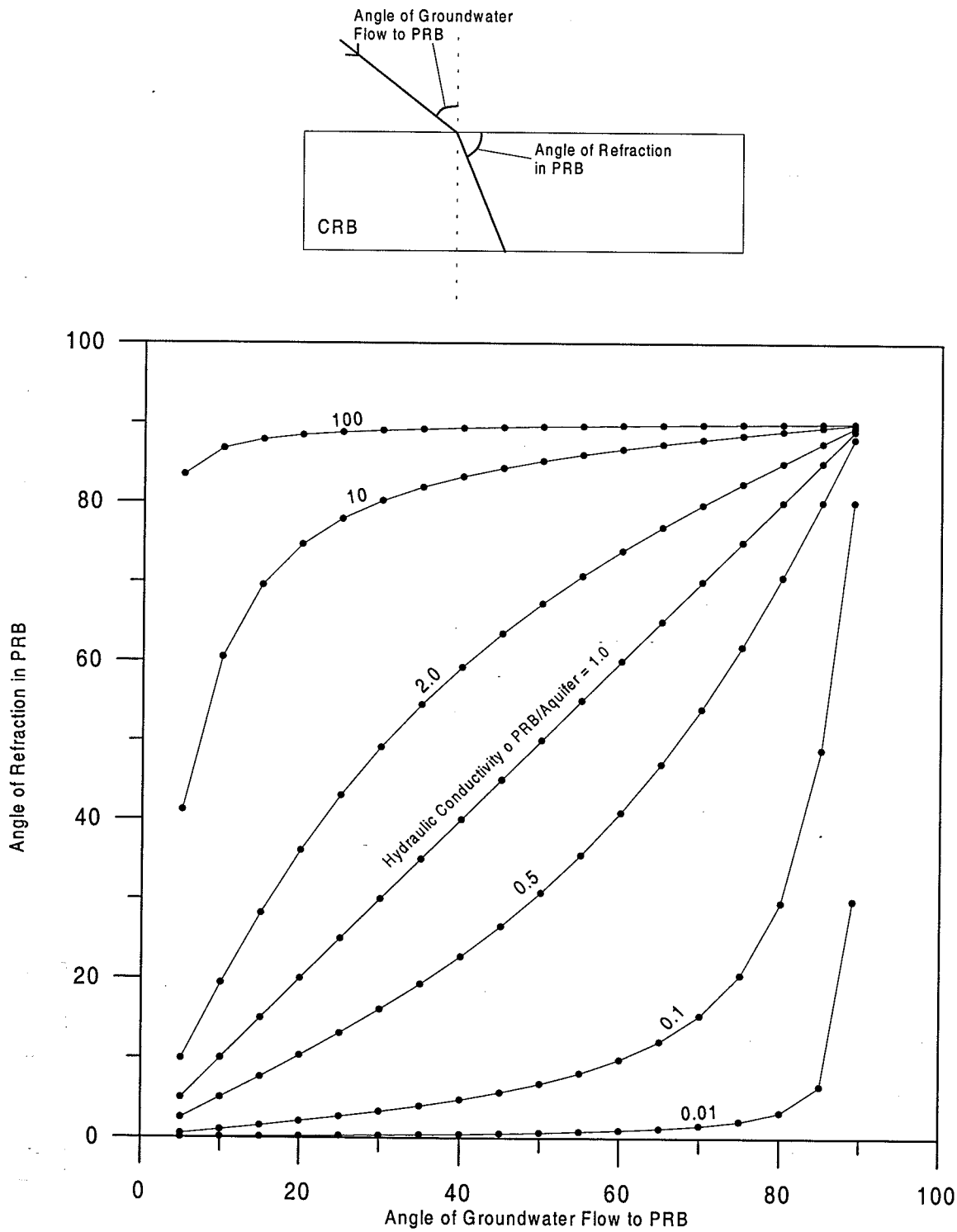

Figure 6-19. Graph of the Angle of Groundwater Flow to the PRB Versus the Angle of Refraction in a PRB for Various Ratios of Hydraulic Conductivity in the PRB and Aquifer

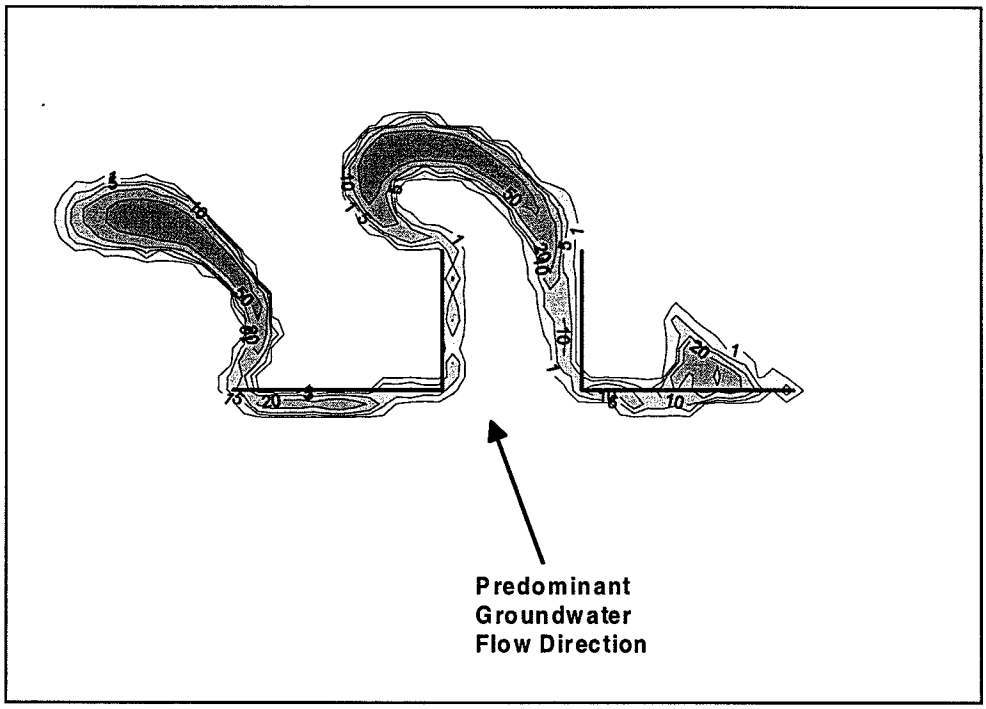

Figure 6-20. Transport Modeling of Plume Migration for a PRB Oriented at 70° to the Predominant Direction of Groundwater Flow Illustrating How Contamination is Diverted Around Portions of the PRB

Table 6-8. Summary of Modeling to Increase Capture for Groundwater Flow at an Angle to the PRB

Scenario	Figure	Plume Capture (approximate)	Comments
Base scenario	6-22	40%	Plume flows at an angle past the PRB.
Flanking trenches	6-23	30%	Plume captured by trenches rather than PRB.
Upgradient trench	6-24	100%	Some of the plume initially flows around the PRB.
Downgradient drain	6-25	95%	Removal of groundwater from drain required.
Flanking sheet-pile barrier	6-26	95%	Groundwater flow concentrated through a small portion of the PRB.
Additional reactive barrier	6-27	100%	New PRB positioned perpendicular to groundwater flow direction.

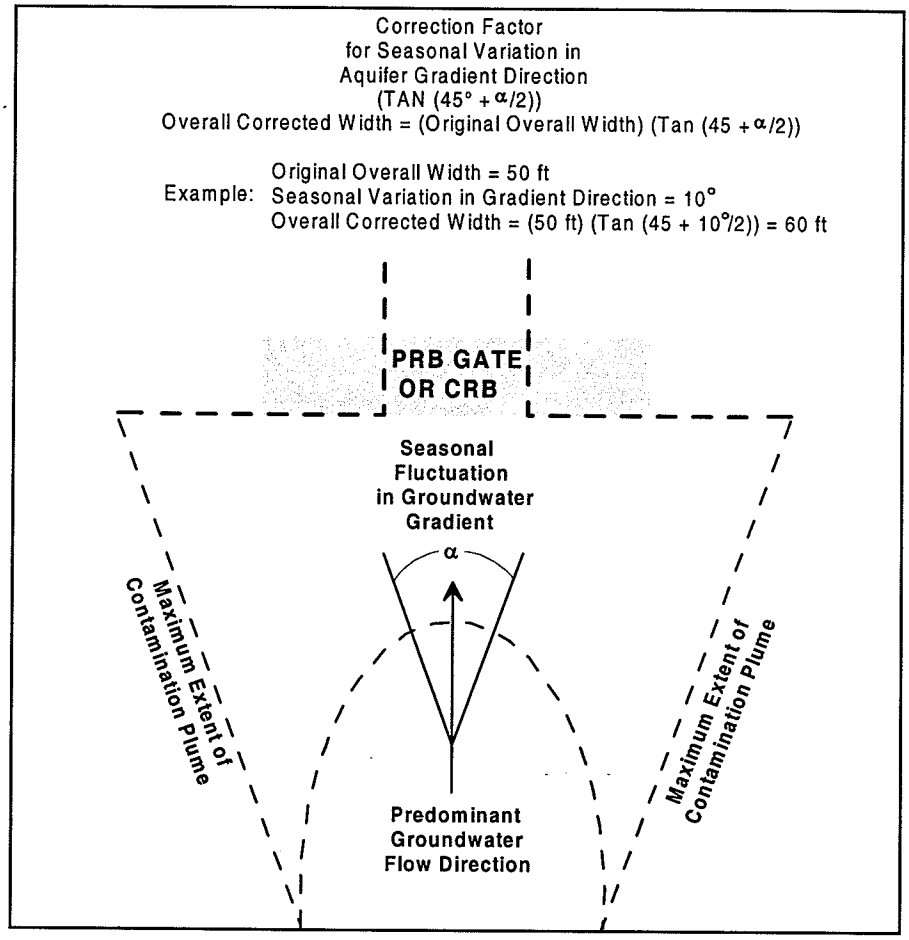

Figure 6-21. Diagram Illustrating Correction Factor for Seasonal Fluctuations in the Direction of Gradient

To resolve this situation, several remedies were considered. Adding high permeability trenches on either side of the barrier did not increase capture, as flow moved to the high permeability trench area rather than the gate (Figure 6-23). However, installing a drain immediately downgradient of the barrier captured most of the plume (Figure 6-24). The problem with this scenario is that it may entail active removal of the water from the drain. Installing a cutoff sheetpile barrier at the upgradient area of the barrier was also modeled (Figure 6-25). This solution redirects the plume through the barrier, but flow is concentrated in a small portion of the barrier. However, this scenario is fairly cost effective, as installing a sheet pile is relatively low cost compared to many of the other remedies, such as modifying the reactive cell dimensions. Adding a high conductivity trench upgradient of the barrier increased the capture zone dramatically (Figure 6-26). This setup also appears to direct groundwater throughout the reactive barrier as well, but may not capture some of the plume initially. A final scenario examined was installing another reactive barrier section perpendicular to the direction of groundwater flow (Figure 6-27). As would be expected, this scenario captures the plume. However, it effectively doubles the price of the barrier.

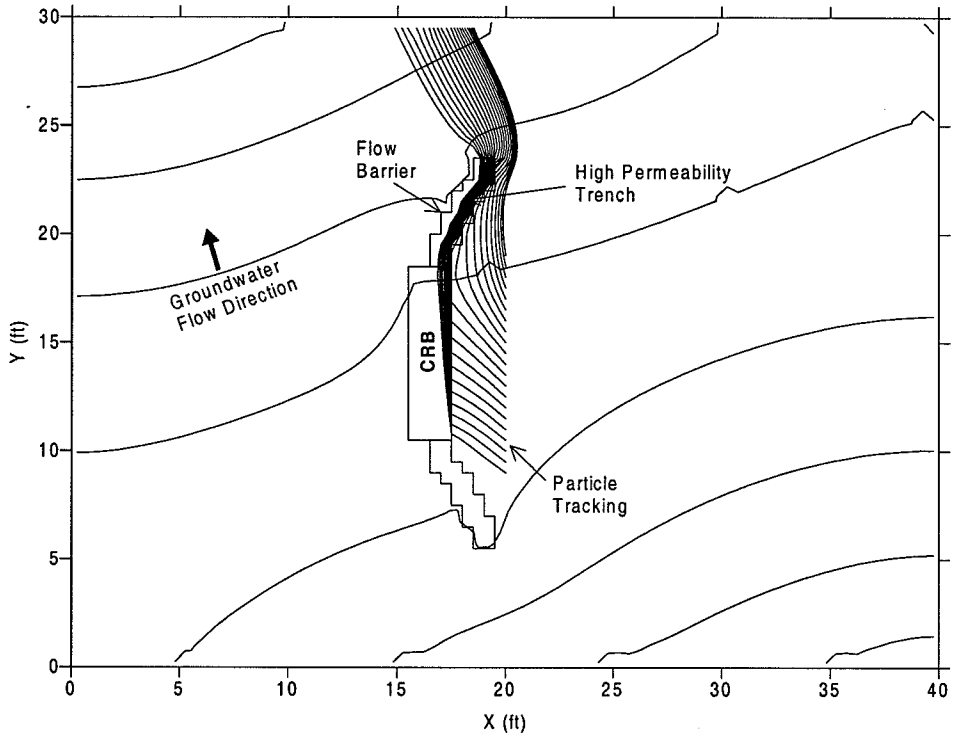

Figure 6-22. Base Case Model and Groundwater Flow at an Angle to the CRB

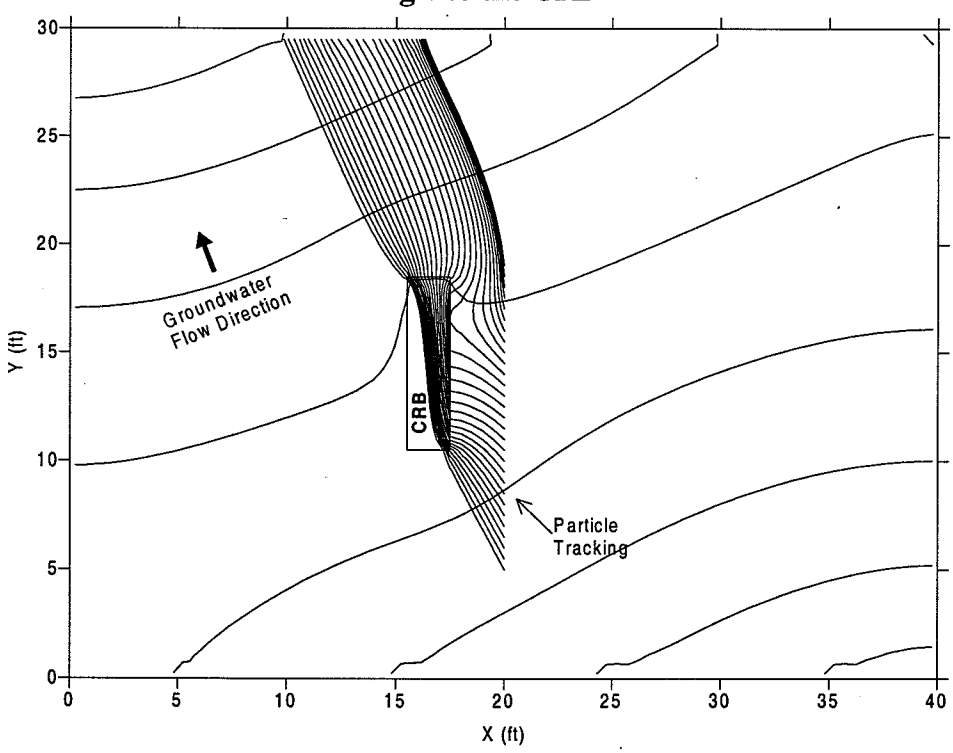

Figure 6-23. Model with Trench and Groundwater Flow at an Angle to the CRB

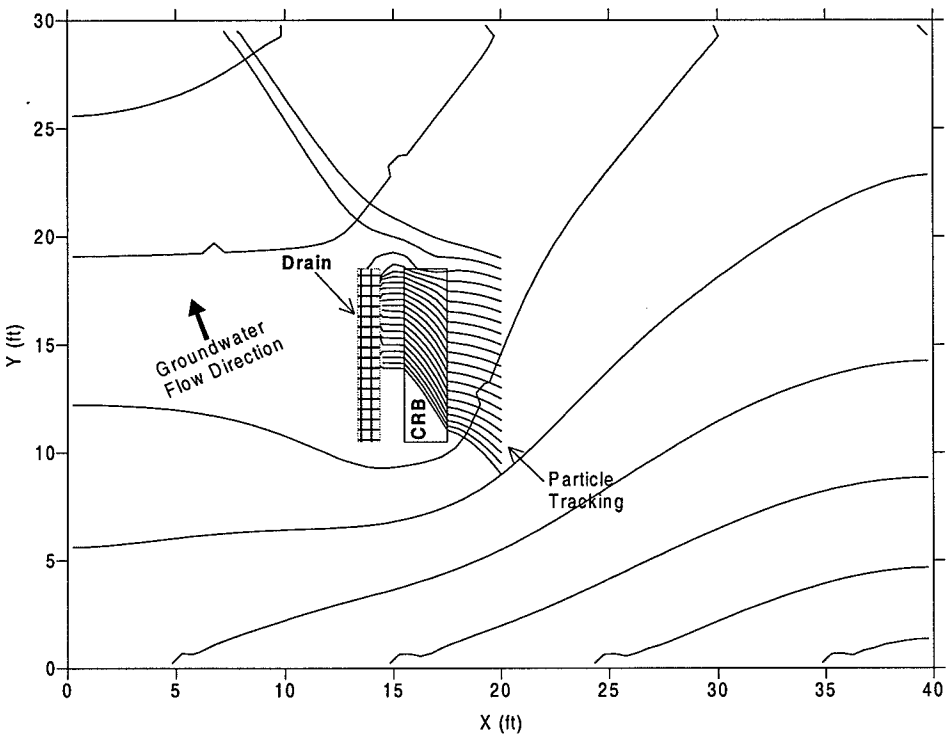

Figure 6-24. Model With Downgradient Drain and Groundwater Flow at an Angle to the CRB

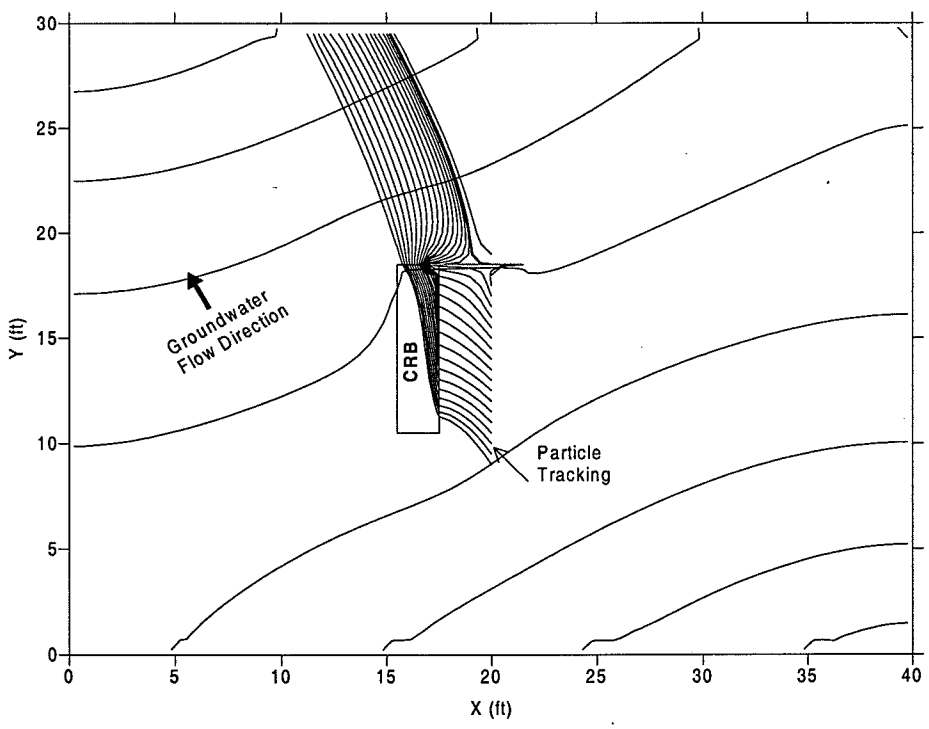

Figure 6-25. Model With Downgradient Barrier and Groundwater Flow at an Angle to the CRB

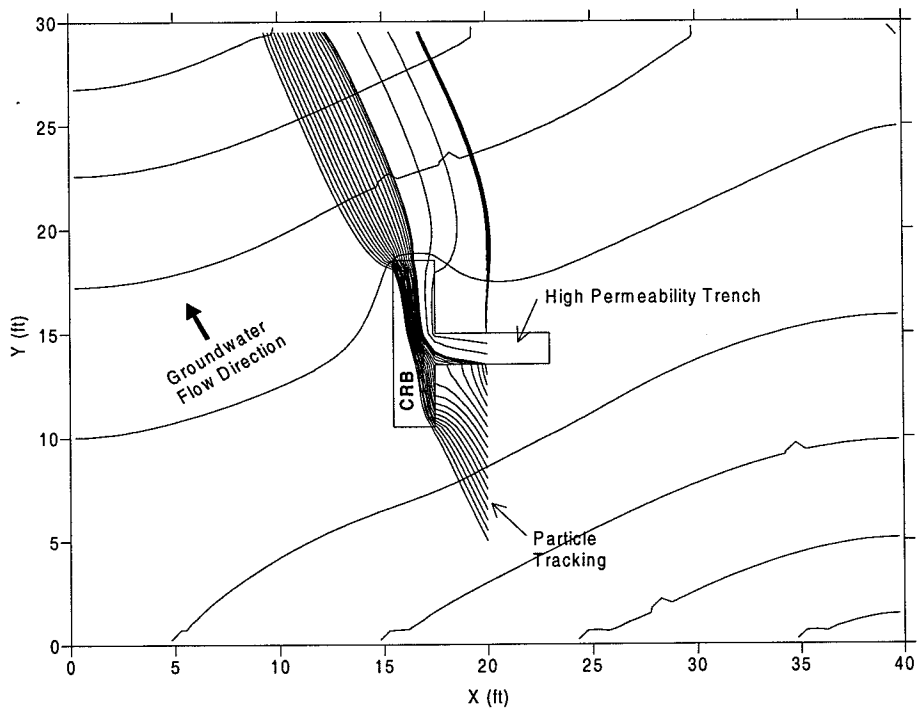

Figure 6-26. Model with Upgradient Trench and Groundwater Flow at Angle to the CRB

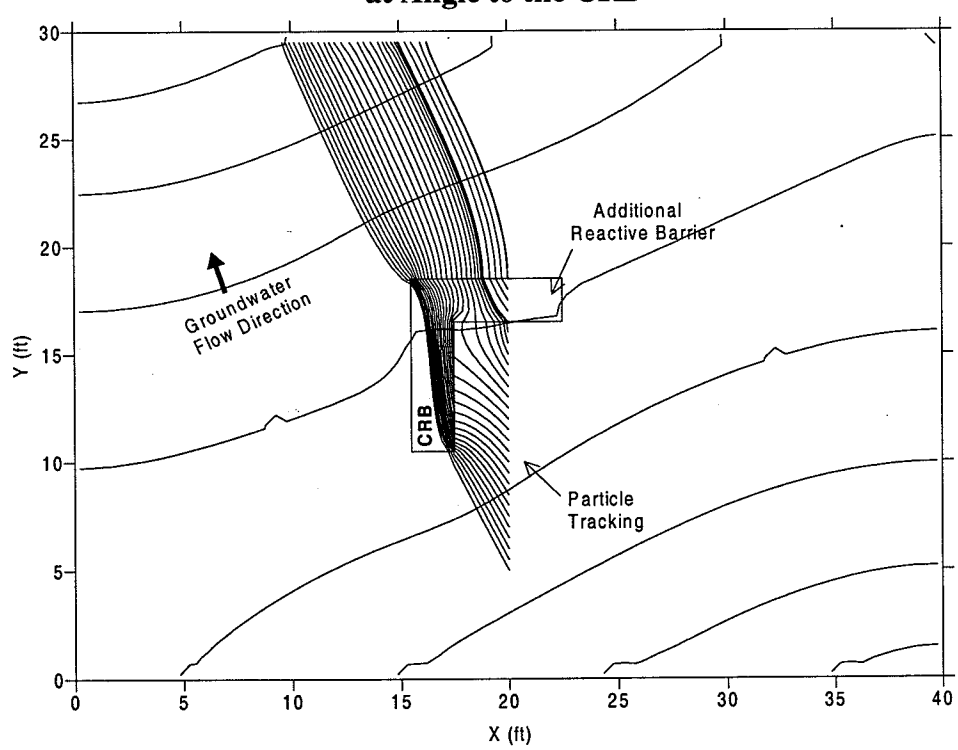

Figure 6-27. Model with Additional Reactive Barrier and Groundwater Flow at an Angle to the CRB

Table 6-8 summarizes the different scenarios designed to provide capture due to change in groundwater flow direction. Overall, it appears that installing a high conductivity upgradient trench leading to the barrier or a sheet pile barrier at the downgradient end of the barrier are most effective in directing flow into the barrier. Of these two options, the upgradient trench results in better flow throughout the barrier. A final option would be to add an additional reactive barrier along the downgradient end of the preexisting reactive barrier.

6.3 Implications for Hydraulic Performance

The ability of granular zero-valent iron to abiotically degrade dissolved chlorinated solvents to meet target treatment levels (generally MCLs) in the *reactive cell effluent*, when given sufficient residence time, has been adequately proven and documented at several PRB sites as well as in the laboratory. At sites where target treatment levels were exceeded in the reactive cell effluent or *downgradient aquifer*, the cause has been traced primarily to hydraulic performance concerns, such as inadequate residence time and unanticipated plume concentrations (e.g., Alameda), or due to flow bypass (e.g., Denver Federal Center). Accurate determination of upgradient flow divides and capture zones has proved difficult in the field due to the limitations of the available monitoring tools and uncertainties in the measurement parameters. Seasonal fluctuations in groundwater gradients and flow directions, and therefore in capture zone, have introduced additional complexity. Hydraulic performance is therefore the primary short-term concern at PRB sites. This is a concern that would benefit from a closer investigation of existing PRBs under varying site conditions. The general conclusions and recommendations based on the monitoring and assessment work conducted under the current project are described below:

6.3.1 Interpreting Groundwater Flow Patterns and Capture Zones. Interpretation of groundwater flow patterns over short distances is challenging. In smaller pilot-scale systems and even in the large full-scale systems, water level differences tend to be small over the shorter distances involved. If the site has a low hydraulic gradient to begin with, the problem of measuring small water level differences is exacerbated.

Although water-level measurements are helpful in understanding the overall flow patterns and monitoring barrier performance, even at larger barriers and sites with relatively high hydraulic gradients, the uncertainty in measurements makes it difficult to reach unambiguous conclusions. At most sites, the deflection in water level contours due to influence of PRBs is expected to take place only a foot or few feet away from the PRB. Over such short distances the uncertainty in water level measurements, combined with formation heterogeneity, can result in at least half an order of magnitude range for flow velocities. This is further complicated within the high-conductivity reactive cell zones, where the water levels become almost flat. In these conditions, it is difficult to determine if the water is flowing through the barrier at a very flat gradient or it is simply stagnating.

Finally, in thin continuous reactive barriers, such as the Seneca Army Depot, flow patterns within the reactive cell cannot be delineated. However, water levels within and outside the reactive cell can be used for flow pattern delineation and long-term monitoring.

Despite these uncertainties, periodic water level measurements provide a low-cost means to monitor the PRB sites for short and long-term variations from baseline flow conditions and timely detection of any performance issues. The use of water levels maps however requires careful and uniform screen interval selection, precise surveying, and consistent water level measurement at routine intervals. Of all the DoD Sites evaluated in the current project former NAS Moffett Field and former Lowry AFB provided the best water-level maps. At NAS Moffett field, groundwater flow is constrained by silty-clay deposits on both sides of the sand channel through which most of the flow occurs. At Lowry AFB, the hydraulic gradient is relatively sharp, and led to discernible water-level trends.

6.3.2 Evaluating Plume Bypass. It has been difficult to evaluate the potential for plume bypass around, under, or over the PRBs in pilot-scale barrier systems. Most of the pilot-scale barriers in this study were designed to capture only a part of the plume for demonstration of the technology. In addition, most of them were placed in the middle of the plume to demonstrate their performance with higher contaminant concentrations. Full-scale barriers that are located at the leading edge of the plume and target the entire plume would be more suitable for evaluating flow bypass because, initially, there is likely to be clean water around the wings of the barrier and on the downgradient side. Breakthrough can generally be verified by sampling the most downgradient well(s) within the reactive cell; this sample represents the effluent from the reactive cell just before it leaves the cell. However, many full-scale PRBs also are located within the plumes (e.g., Seneca Army Depot), because the PRBs location decisions are often driven by factors such as property boundaries and availability of above ground space for construction. In such cases, evaluating plume by-pass can become even more difficult.

6.3.3 Direct Measurement of Velocity. There is difficulty in directly measuring groundwater flow directions and velocities at most PRB locations. In situ probes manufactured by HydroTechnics™ have been used at some PRB sites (Dover AFB, NAS Alameda, and Cape Canaveral Air Station) to measure groundwater velocity. These probes have shown little success, especially when installed within the low gradient setting inside the PRBs. When installed outside the PRBs in the surrounding aquifers, the results typically have not matched those obtained from water level measurements. Downhole heat-sensors, such as the KV-meters, have also been used at some sites (Moffett Field, Lowry AFB, and Kansas City Plant) to measure groundwater velocity.

Generally, velocity and direction measurements are more reliable when the groundwater velocity is 0.5 ft/d or higher. Colloidal borescopes are an emerging tool for direct observation of flow in monitoring wells. These can be used in two-inch completed wells with sand packs to delineate the flow patterns across the monitoring network. An evaluation of these probes was conducted at Lowry AFB and Dover AFB. Preliminary results show that the probes work only in wells that have a stable colloidal flow pattern. Generally, long screen wells screened across the entire depth of the aquifer are desired because the probe can be used to locate zones with stable colloidal flow. However, they may work accurately only in the high flow zones within the aquifer. Currently, these probes should be considered experimental. If proven successful, this may be a relatively economical option for mapping groundwater flow patterns at highly

heterogeneous sites. Note that long-screen wells suitable for downhole probes may not be suitable for plume characterization, for which the need is for shorter screen wells.

6.3.4 Tracer Tests. Although, tracer tests are cumbersome and expensive to conduct, they provide a direct means of observing flow patterns and velocity through the barriers to confirm whether water is flowing through the PRBs. The use of tracer tests is not very common and therefore, insufficient data exists on their success as a performance assessment tools. No tracer tests were performed as part of the current project. A detailed tracer test at Former NAS Moffett Field PRB (Battelle, 1998) showed the movement of tracer from upgradient pea gravel to downgradient pea gravel. However, the tracer was not observed in the downgradient aquifer. Therefore, it was not clear from the tracer test whether the water was flowing through clear through the PRB or just stagnating within the reactive cell. A second tracer test at the same site with injection in the upgradient aquifer showed tracer in the well located directly upgradient of the reactive cell. However, it was not possible to detect it within the reactive barrier. Tracer tests are more complex and resource intensive than other monitoring tools, but may provide reliable information under most flow conditions.

6.3.5 Residence Time and Flow Volume. The estimation of flow volume and residence times through the reactive barriers can be calculated using the Darcy's Law with the water levels/hydraulic gradients along with estimates of porosity, permeability. The monitoring tools such as the velocity probes and tracer tests may also be applied. However, all of these methods provide a range of possible residence times or flow velocities at best. In most cases the measurements inside the reactive cells have been inconclusive due to conflicting flow direction data and low gradients. As a result, there is still no conclusive verification that the water is actually flowing through the barriers and determining accurate residence time is extremely challenging. The traditional methods, especially the water level measurements and the use of Darcy's law still provide useful information and these should be continued. In addition, carefully planned and extensively monitored tracer tests may be performed at selected site(s) to verify flow through the barrier and better understand flow patterns associated with the PRBs.

6.3.6 Role of Groundwater Models - Hydrogeologic modeling that incorporates the full range of hydraulic parameters, rather than average values, can be used to design optimum configuration, orientation, and dimensions for a PRB application. Modeling and field monitoring conducted at former NAS Moffett Field, Lowry AFB, and Dover AFB indicate that the design models are moderately good predictors of actual flow and residence time conditions, as long as certain conditions are satisfied:

- The local heterogeneities in the immediate vicinity of the PRB are well characterized and incorporated into the model. At Moffett Field the main heterogeneity consisted of a sand channel that was carrying the bulk of the flow.

- Effects of extraneous factors have been considered. At Lowry AFB, an adjacent stream tends to draw part of the groundwater flow away from the PRB. At a DOE

site that was surveyed for this study, the effects of a nearby pump-and-treat system on the plume caused actual flow conditions to deviate from the modeled flow.

- The modeling takes into account the effects of seasonal variations and characterization uncertainties. For example, at Dover AFB PRB, a range of flow directions and aquifer hydraulic conductivity values were modeled to determine an optimum orientation and width of the PRB.

Some general recommendations based on the findings of hydraulic assessments include:

- During the site screening and characterization stage, it is important to evaluate all existing information on site geology (lithologic characters including spatial variations), hydrogeologic parameters (permeability, porosity, soil bulk density), water levels including seasonal variations and long-term fluctuations, and presence of natural and man-made features, such as drains, streams, ponds, dams etc., that may influence flow. It is also important to understand the contaminant plume distribution and attempt to anticipate its long-term behavior. New data must be collected where needed. The additional site characterization expense at this early stage can reduce the probability of potentially expensive adjustments to the PRB in the future.

- It must be realized that uncertainty is inherent in all aspects of subsurface geology. This uncertainty is further enhanced by the measurement error ranges of the tools used for characterization and performance assessments. For example, despite most carefully conducted hydraulic conductivity measurements, it would be difficult to estimate this parameter with accuracy better than about half an order of magnitude. Similarly, water level measurements in low hydraulic gradient sites can be difficult to interpret over short distances. The PRBs design must take this uncertainty into account through modeling of flow scenarios that encompass the full range of variability in the field parameters.

- The design of the PRBs should carefully consider the ranges of uncertainties in the parameters used in the design. Computer simulations may be used to evaluate the impact of parameter ranges on future flow patterns. Similarly, the effect of groundwater flow direction changes or the effect of changes in plume behavior can be evaluated with groundwater flow modeling. Stochastic simulations may also be used to determine the probability ranges. The modeling studies can be used to determine the level of safety in the design and to evaluate trade-offs between increased safety factors versus future corrective actions.

- The use of safety factors in the design should be carefully considered and communicated to the site stakeholders. The underlying issue in design safety factors is related to economics, i.e., determining whether to over-design the PRB

and spend extra money during the initial construction of the PRB or to risk the need for potentially expensive future adjustments to the PRB construction. For example, it may be possible to account for extreme changes in groundwater flow directions by doubling the length of the barrier. However, if the site is large enough for adding additional PRB segments if needed, the extra investment could be delayed or avoided. A proper communication of such options to the stakeholders will avoid future problems for technology acceptance. In general, the amount of safety factor incorporated into a PRB design should be based on the measured variability in site characteristics, as well as the professionally judged uncertainty in the hydraulic and plume distribution estimates.

- There has been very little work on monitoring of the downgradient contaminant plume evolution. This is partly due to the fact that many PRBs are placed within the plume, rather than at its leading edge, delaying the emergence of a clean front. A carefully planned study of the downgradient contaminant distribution over time should be performed to verify the presence of a clean front of the plume in the water exiting the PRB. This is one of the most reliable means of verifying that the water is actually flowing through the PRBs rather than stagnating within the reactive cell.

In summary it can be said that the challenge in validating the hydraulic performance pf PRBs is not that any of the monitoring shows that the PRBs are not working as desired, but that it is difficult to conclusively show how well the hydraulic objectives of the PRB, capture zone and residence time, are being achieved. The main reason for this is the lack of monitoring tools that can override the uncertainties in geologic media and provide high resolution over short distances at a reasonable cost.

7.0 Update on PRB Construction and Costs

7.1 Advances in PRB Construction Methods

Several construction techniques are available for the installation of PRBs. The most appropriate method for a given project will depend on the site lithology, the proposed depth of installation, health and safety factors, construction costs, and other considerations. This review is based on the analysis of information contained in a database of 94 PRB projects and the lessons learned regarding PRB installations garnered from both literature and remediation site profiles. The information in this review should help remedial project managers understand the advantages and limitations associated with each PRB construction method and ultimately aid in the selection of a PRB installation approach appropriate to the particular conditions at their site.

The majority of PRB projects completed to date (as shown in Figure 7-1) have been installed using trenching techniques. Backhoe trenching, along with the use of sheet piling or trench boxes for excavation shoring, is the most cost-effective PRB construction method at sites with an installation depth of less than 30 ft bgs. Other trenching or geotechnical techniques should be considered at greater depths (Day et al., 1999). As shown in Figure 7-2, the majority of PRBs (~ 68%) have been installed at depths ranging from 20 to 50 ft bgs, however, two recent installations have reached a depth of 120 ft bgs.

As the number of PRB field applications has grown, so too has the sophistication, reliability, and number of commercially available construction techniques adapted to PRB installation. Several advances in construction techniques have allowed for more cost-effective and/or deeper PRBs including improvements in trenching techniques (e.g., biodegradable slurry trenching) and the use of geotechnical techniques (e.g., hydraulic fracturing).

7.1.1 PRB Configurations. The following are some of the PRB configurations that have been used or proposed so far:

- **Continuous Reactive Barrier** - A continuous reactive barrier is a continuous zone of reactive medium (e.g., iron or iron/sand mix) that extends across the entire width of the plume. The wall can be hanging or keyed into the aquitard. The continuous reactive barrier is the most common PRB configuration and has been used at approximately 35 sites in the United States, Canada, and Europe. Based on a database of PRB projects with complete construction information, the widths of continuous reactive barrier remediation projects range from 4 to 915 ft and installation depths range from 10 to 120 ft bgs.

- **Funnel-and-gate** - The funnel is a channel with impermeable walls consisting of slurry cut-off walls or sealable sheet pile cut-off walls. The funnel is designed with an adequate span to achieve plume capture and directs groundwater, increasing the velocity, through the gate, which consists of a permeable zone of iron or iron/sand mix. The funnel-and-gate system is keyed into a low

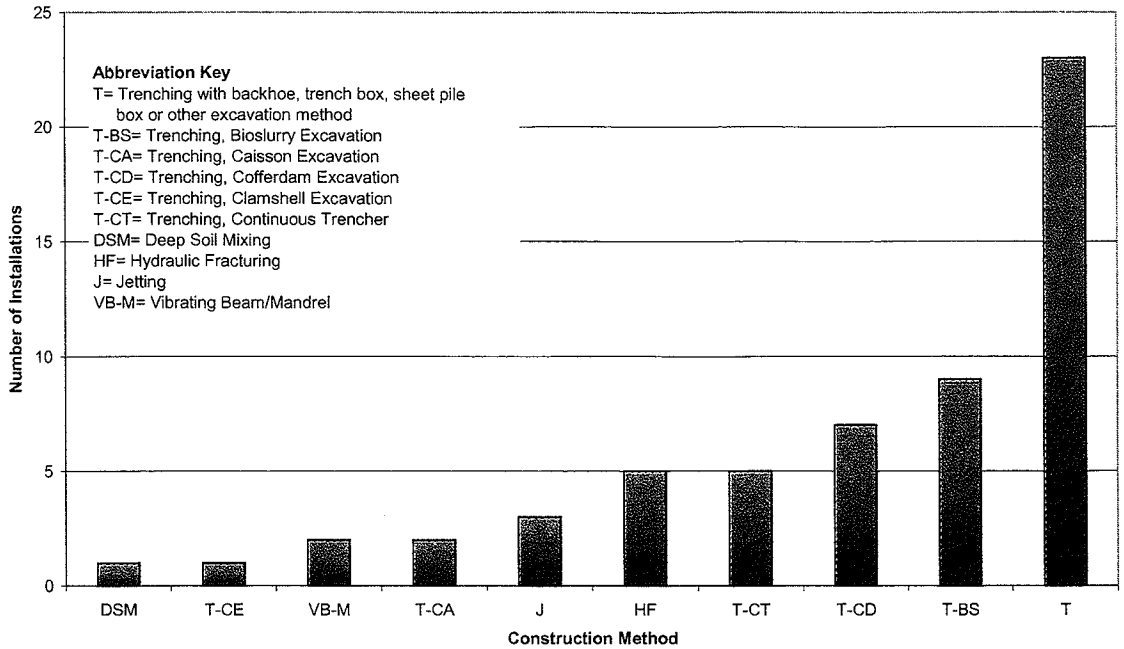

Note: Based on data from 58 pilot-scale and full-scale CRB or funnel-and-gate projects with complete construction method information.

Figure 7-1. Summary of PRB Construction Methods

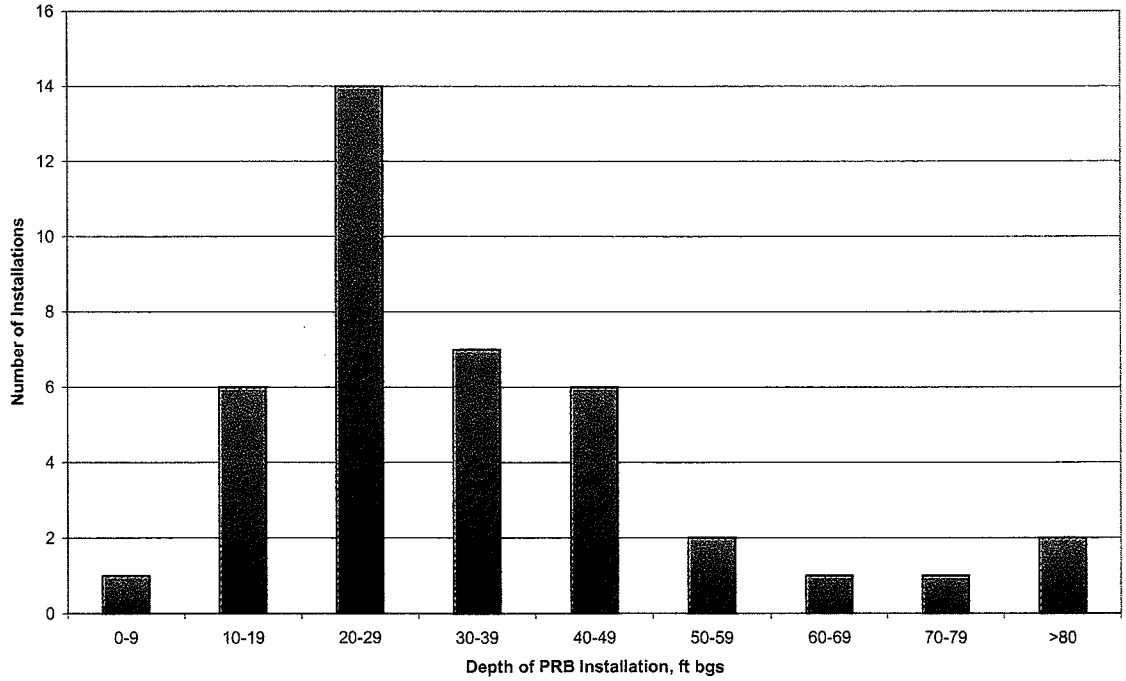

Figure 7-2. Depth of PRB Installations for all Construction Methods

permeability zone or aquiclude to prevent flow beneath the system. This PRB configuration has been used at approximately 21 sites in the United States, Canada, and Europe. Based on a database of PRB projects with complete construction information, funnel widths range from 15 to 1,040 ft, gate widths from 6 to 160 ft, and installation depths from 12 to 45 ft bgs (funnel-and-gate installation depths are typically shallower than continuous reactive barrier installations because of the practical depth limitations associated with driving sealable sheet pile to form cut-off walls).

- **Geosiphon™**- The Geosiphon™ is a passive remediation system which relies upon the natural hydraulic head difference (between the target treatment zone and a down-gradient discharge point) to produce flow through reactive media. The reactive media can be installed in situ as a filter pack around a groundwater extraction well or the reactive media can be housed in aboveground treatment units. This system was first used at the Savannah River site in South Carolina and consisted of an in situ granular iron treatment cell with dimensions of 20 ft deep x 8 ft in diameter. The groundwater extraction well, through which the siphon was applied, consisted of a 12 in diameter casing and screen. Approximately 2.7 gallons per minute (gpm) were removed through this system. An adaptation of this technology has also been used at the Lawrence Livermore National Laboratory to initiate passive groundwater flow (up to 8 gpm) to four aboveground drums filled with iron filings (WPI, 2001).

- **Reaction Vessels**- Several innovative PRB configurations involve the use of a passive groundwater collection system (e.g., gravel trench/high-density polyethylene [HDPE] piping or horizontal well) that directs groundwater to in situ or ex situ reactive media treatment vessels. These innovative configurations are often applied at sites with radioactive contamination due to the need to remove exhausted reactive material. At the Rocky Flats Environmental Technology site in Golden, Colorado, a system has been installed which consists of a 1,100 ft groundwater collection trench with HDPE piping routed to below grade, concrete-lined, treatment cells filled with sawdust and iron (RTDF, 2001). A system has been constructed at Bodo Canyon, Colorado that involves a collection drain for seep water from a uranium tailings disposal cell. The seep water is diverted to a holding tank and then distributed to four PRBs (RTDF, 2001). Two PRBs are constructed in a manner similar to septic leach fields and contain steel wool and copper, while two were constructed in steel tanks with baffles and contain iron foam plates and steel wool. At the Portsmouth Gaseous Diffusion Plant in Ohio, a pilot test involved the installation of a 500-ft horizontal well, used to collect and route contaminated groundwater through a series of iron-filled canisters (RTDF, 2001).

- **Other Passive Configurations**- Recent pilot studies conducted by the University of Waterloo at Borden and Killarney, Canada have involved the installation of

horizontal beds of compost material placed beneath septic system infiltration beds to reduce nitrate loading to groundwater.

- **Semi-Passive Configurations**- Although, PRBs were developed as an alternative to pump-and-treat and the passive nature of the systems are a major advantage, recent research has focused on the development of semi-passive remediation systems. One example is a pilot-scale nutrient injection wall installed at the Borden Aquifer site. Nutrient and injection wells were installed within a 13 ft long by 3 ft wide by 20 ft deep permeable wall containing filter sand. The goal is to cycle the injection and flushing of substrates through the wall to stimulate biodegradation of the contaminants, while operating the system passively 99% of the time. The injected nutrients will spread downgradient through diffusion and dispersion, which will lead to a zone of enhanced contaminant biodegradation (Devlin and Einarson et al., 1999).

Each of the PRB configurations described above can be installed through the use of a variety of construction techniques. As Figure 7-3 illustrates, the majority of PRBs installed to date are continuous barriers, followed by funnel-and-gate, and then Geosiphon™ and other configurations.

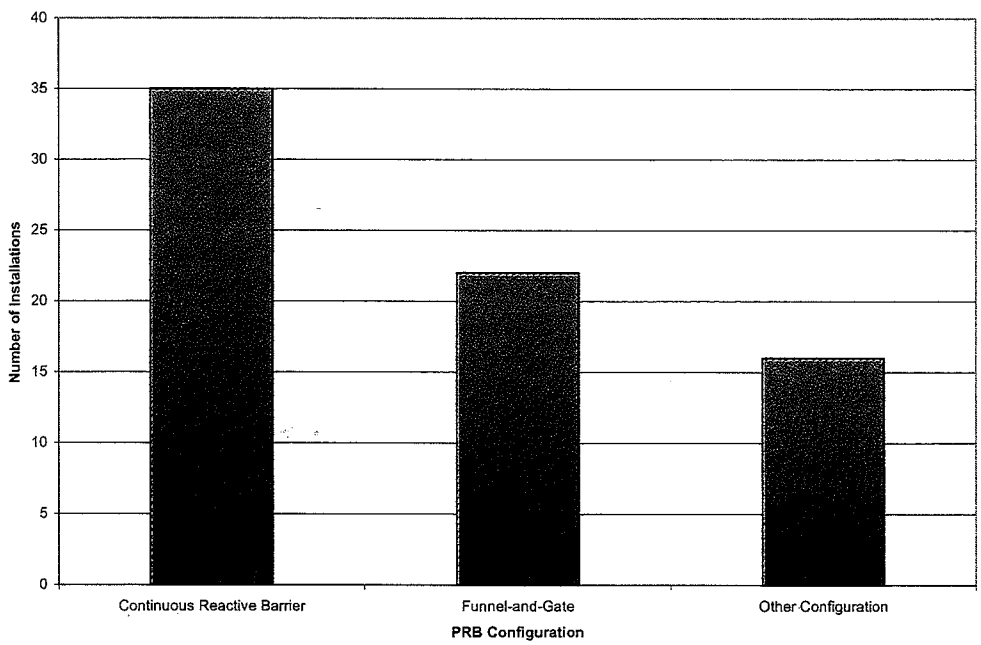

Note: Based on data from 73 full-scale and pilot-scale PRB projects with complete configuration information

Figure 7-3. Summary of PRB Configurations

7.1.2 PRB Construction Techniques. Several factors (including costs and depth of installation) will impact the selection of the appropriate PRB construction method. Other important factors include the site lithology, the required PRB dimensions, site access, waste generation, and worker health and safety. Table 7-1 shows the maximum and average installation depth based on field applications for each construction method. Although, improvements in construction techniques continue, PRB installations have generally not approached the maximum installation depths deemed to be feasible by technology vendors for jetting, vibrated beam, and deep soil mixing techniques. The advantages and limitations associated with each construction technique used in the installation of PRBs are described below.

Table 7-1. Summary of Reactive Barrier Construction Techniques

Construction Technique	Maximum Depth of Field Applications (ft)	Average Depth of Field Applications (ft)
Backhoe Trenching	80	30
Clamshell Trenching	N/A	N/A
Caisson Excavation	45	43
Continuous Trenching	25	23
Biopolymer Trenching	65	34
Jetting	50	47
Hydraulic Fracturing	120	91
Vibrated Beam	26	26
Mandrel	43	43
Deep Soil Mixing	40	40

(a) 30 ft for conventional backhoe, 80 ft for modified backhoe.
N/A = not available

7.1.2.1 Backhoe and Clamshell Trenching Methods. Backhoes are the most common type of equipment used for conventional trench excavation and are the cheapest and fastest method available for shallow trenches (<30 ft bgs). The digging apparatus is staged on a crawler-mounted vehicle and consists of a boom, a dipper stick with a mounted bucket, and either mechanical cables or hydraulic cylinders to control motion. Bucket widths generally range in size up to 5.6 ft. At recent PRB installation sites, modified backhoes that can reach depths down to 80 ft bgs have been successfully used. The trench will have to be stabilized as it is excavated and a cofferdam or box formed from interlocking sheet pile is commonly used. A trench box (a pre-fabricated metal box) can also be used to stabilize the excavation. The trench box is advanced as each new section is excavated and backfilled with reactive media. Another option for excavation equipment is the use of a crane-operated grabbing tool called the clamshell, which can be used to excavate to approximately 200 ft bgs. The excavation is accomplished through repeated lifting and lowering of the clamshell bucket under the influence of gravity. More information on the use of backhoes and clamshells for excavation can be found

in the design guidance (Gavaskar et al., 2000). The advantages associated with conventional backhoe excavation are:

- Conventional technology.
- Dimensions and continuity of the PRB are easily established.

The limitations of backhoe excavation are:

- Practical depth limitations to backhoe excavation.
- High spoils generation.
- Dewatering and treatment of extracted groundwater may be needed.
- Worker health and safety issues due to confined space entry.
- Clamshell excavation has a relatively low production rate compared to backhoe excavation.
- Abandonment/removal of utilities may be necessary.

7.1.2.2 ***Caisson Excavation Method.*** Caissons are load-bearing enclosures that are used to protect an excavation and are a relatively inexpensive way of installing PRBs at depths inaccessible with a standard backhoe. Caissons may have any shape in cross-section and are built from common structural materials. The caissons can be pre-fabricated and transported to the site or built in sections at the site. More information on the use of caissons for excavation can be found in the design guidance (Gavaskar et al., 2000). The advantages associated with caisson excavation techniques based on recent PRB field projects are as follows:

- Dimensions of PRB easily maintained.
- Requires no internal bracing and can be completed without personnel entry.
- Installed without significant de-watering and associated treatment of contaminated groundwater.

The limitations of caisson excavation are as follows:

- Practical depth limitations.
- High spoils generation.
- Cobbles/boulders can result in off-vertical installation or refusal.
- Caisson removal may be difficult.
- Subsidence of granular iron may occur due to both vibrations and/or entry into the thin annular space left by caisson removal.

- Smearing or densification may reduce the overall permeability of the barrier, even though the reactive medium inside remains permeable.
- Abandonment/removal of utilities may be necessary.

The caisson technique was used to install the Geosiphon™ at the Savannah River site which involved driving an 8 ft diameter cylinder to 20 ft bgs, excavation of the native soil, followed by backfilling with granular iron (WPI, 2001). The caisson excavation method was also used at Dover AFB. A vibratory hammer, mounted on a crane, was used to both install and pull out the caisson, which consisted of an 8 ft diameter cylinder driven to approximately 45 ft bgs. Some difficulty was experienced in removing the caisson as the steel material of the caisson started to fail or tear as it was being removed. In addition, some subsidence or settling of the iron reactive media was experienced due the application of the vibratory hammer and the entry of the reactive media into the annular space left by caisson removal (Battelle, 1999).

7.1.2.3 ***Continuous Trenching Method.*** The use of a continuous trencher is possible for barriers installed from 25 to 30 ft bgs. The continuous trencher is capable of simultaneously excavating a narrow, 12- to 24-inch wide trench and immediately refilling it with either a reactive medium and/or a continuous sheet of impermeable, high-density HDPE liner. The trencher operates by cutting through soil using a chain-saw type apparatus. The boom is equipped with a trench box, which stabilizes the trench walls as a reactive medium is fed from an attached, overhead hopper. More information on the use of continuous trenching can be found in the design guidance (Gavaskar et al., 2000). The advantages associated with continuous trenching techniques based on recent PRB field projects are as follows:

- Dimensions of PRB easily maintained.
- Amount of spoils minimized by vertical orientation of cut.
- Installed without significant de-watering and associated treatment of contaminated groundwater.

The limitations of continuous trenching are as follows:

- Practical depth limitations.
- Wet, very unconsolidated materials can be difficult to excavate.
- Obstructions such as large cobbles/boulders disrupt sawing process.
- Abandonment/removal of utilities may be necessary.

The continuous trenching technique was used to install a funnel-and-gate system at a maintenance facility in Oregon. This technique was chosen because it was relatively inexpensive, less disruptive, and minimized spoils generation compared to other trenching techniques. The dimensions of the slurry wall funnel were 650 ft long, 6 in wide, and up to 30 ft deep. The slurry wall was installed in a two-week time frame. Some equipment difficulties were experienced and replacement parts were frequently required. The initial gate design called for a

14 in thick reaction zone, but this was modified in the field to consist of two parallel 9 in walls connected with sheet piling. A cobble zone disrupted the placement of the second gate and the wall had to be completed with traditional excavation techniques (Romer, 1998).

7.1.2.4 ***Biodegradable Slurry (Biopolymer) Trenching Method.*** The use of biodegradable slurry or bioslurry to shore up excavations is a relatively recent advance in trenching techniques and was first employed for the installation of a PRB by GeoCon at the Bear Creek Valley site in 1997. The technique involves the use of a bioslurry, typically made of powdered guar bean, to exert hydraulic pressure and prevent the collapse of the trench as it is excavated. The bioslurry consists of water with a 0.7% guar gum mixture by weight, which increases the viscosity of the liquid to a jello-like consistency. Other additives to the bioslurry include soda ash (for pH adjustment) and a biostat or preservative (e.g., sulfur compounds). Both the pH adjustment and the preservative act to impede the breakdown of the slurry by microbes during trench installation. After the trench is excavated and bioslurry is added, granular iron is introduced into the trench through a tremie tube or displaced over a gradually sloping side-wall. Once the excavation and iron placement are complete, the guar gum slurry is broken down by adding a liquid enzyme breaker, leaving the iron or other reactive media in place in the trench. After the bioslurry has been successfully degraded, initial reports indicate that the reactivity and permeability of the soils or reactive media are not significantly affected. The advantages associated with biodegradable slurry trenching techniques based on recent PRB field projects are:

- Dimensions of PRB easily maintained.
- Relatively quick installation (no cofferdams or caissons to place/remove).
- Flexible design.
- Installed without de-watering and associated treatment of contaminated groundwater.
- Minimizes spoils generation compared to other trenching techniques.
- Health and safety enhanced as workers do not enter trench.
- Biodegradable slurry suppresses vapors.

The limitations of the bioslurry method are:

- Practical depth limitations associated with trenching.
- Difficulty may be encountered in controlling optimal behavior of the biodegradable slurry (e.g., instability of slurry may cause slump or sidewall failure or delayed breakdown of slurry may require excessive water flushing and treatment costs).
- There may be some regulatory concern over the addition of a biocide into the groundwater

- Although spoils generation lower than other trenching techniques, management of wet and muddy spoils makes segregation/disposal of less contaminated soil difficult.
- Preferential sorting in iron/sand mixture may occur during placement in trench.
- Slurry build-up on iron may occur if iron/sand mixture not pre-wetted to fill voids.
- Vertical installation of monitoring wells difficult in biodegradable slurry.
- Abandonment/removal of utilities may be necessary.

Two recent PRB projects that involved the use of bioslurry excavation methods at DoD facilities are Pease AFB and the Lake City Army Ammunition Plant (LCAAP).

The project at Pease AFB involved the construction of a 150-ft continuous reactive barrier with a 30 in thick reactive zone and an installation depth of 36 ft bgs. The original plan was to key into the bedrock layer, but this approach was not feasible due to the mechanical limitations of the Caterpillar® 375L excavator and the fact that the bedrock was less fractured and weathered than anticipated. In addition, the bedrock was hit at a much shallower depth than anticipated, so the trench was not installed as deep as initially planned. This lead, however, to an opportunity to extend the trench length without increasing installation costs. The reactive media was tremie grouted into the excavation and samples were collected to ensure that no preferential sorting had occurred. No preferential sorting was noted and the backfill was well-mixed with the percent iron by weight values comparable to the design target. Although a plan had been devised to segregate the most contaminated spoils during excavation, this could not be accomplished due to the wet and muddy state of the spoils. Also, because of a delay in the breakdown of the slurry, excessive water was generated during flushing of the system, which increased waste treatment costs. The continuous reactive barrier installation occurred over a one-month time period (Cange, 2000).

The bioslurry excavation method was also used at LCAAP to install a 380 ft long and 2 ft thick continuous reactive barrier that was keyed into the bedrock at 65 ft bgs. Slump or sidewall failure was experienced during installation at certain locations along this barrier. This might suggest that 65 ft bgs is approaching the practical installation depth limitation for successful bioslurry excavations or that the bioslurry mix was not optimized.

Both projects experienced some difficulty with management of the bioslurry. It is important that the pH, total dissolved solids, and total hardness of the water used in preparing the bioslurry meet appropriate guidelines. Also, the viscosity and pH of the slurry should be monitored to ensure that the gel strength of the slurry is maintained at a high level so that adequate hydrostatic pressure is exerted on the trench walls (GeoCon, 2001).

7.1.2.5 ***Jetting Method.*** Jet grouting involves the injection of grout or slurry at high pressures into the ground. The high velocity erodes the soil and replaces some or all of it

with grout or slurry. The delivery mechanism used for PRB installation is a triple-rod injection system, which delivers a granular iron/guar gum slurry mixture, air, and water into the subsurface. If the injection rod is rotated as it is brought up, a column of the injected media is created. Using this approach, a continuous barrier can be created by installing a row, or multiple rows of overlapping columns. Alternately, a thin panel of media can be installed by not rotating the rod and creating a row of overlapping panels. More information on the use of jetting can be found in the design guidance (Gavaskar et al., 2000). The advantages associated with jetting techniques based on recent PRB field projects are:

- Practical depth of installation much deeper than trenching techniques.
- Installation around subsurface obstructions and boulders possible, so abandonment/removal of utilities not necessary.
- Equipment has small footprint, therefore, method good for small sites with relatively limited access.
- Health and safety enhanced by minimizing worker exposure to contaminated soils.
- Jetting of columns may result in more uniform dimensions.

The limitations of jetting include:

- Exact dimensions of barrier difficult to control with thin panel emplacement.
- Need sophisticated tools to monitor and confirm dimensions and integrity of barrier.
- Health and safety issues may be encountered if uncontrolled fine dust is generated from jetting.

A continuous reactive barrier was installed with the jetting technique at Travis AFB. The barrier is a thin panel emplacement installed at a depth of 50 ft bgs with an 80 ft width and a reactive zone thickness of 4 to 5 ft. Approximately, 300 tons of iron filings mixed with aquifer materials was used. Jetting was also used to install a PRB at a DuPont plant in North Carolina. The jetting technique was selected because the number of subsurface utilities and obstructions limited the practicality of excavation. The PRB is 375 ft long and installed at a depth of 15 ft bgs. Both columnar and thin panel emplacement techniques were used at this site (Shultz and Landis, 1998).

7.1.2.6 ***Hydraulic Fracturing Method.*** Hydraulic fracturing involves the installation of a series of wells along the length of the proposed barrier and propagation of a controlled vertical fracture through each well. The fracture is initiated through the use of a specially designed, downhole tool or frac tool, which cuts a vertical notch in the subsurface. The fracture is then propagated and filled with granular iron suspended in a hydrated guar-based slurry. The emplaced material in one frac well coalesces with the emplaced material in the

adjacent frac well, thus forming a continuous vertical wall. The advantages associated with hydraulic fracturing techniques based on recent PRB field projects are:

- Practical depth of installation much deeper than trenching techniques.
- Installation around subsurface obstructions and boulders possible, so abandonment/removal of utilities not necessary.
- Equipment has small footprint, therefore, method good for small sites with relatively limited access.
- Health and safety enhanced by minimizing worker exposure to contaminated soils.

The limitations of the hydraulic fracturing method are:

- Challenge to consistently inject panels of uniform depth and thickness.
- May require multiple barriers to obtain sufficient reactive media thickness.
- Need sophisticated tools to monitor and confirm dimensions and integrity of barrier.
- Difficulty may be encountered in controlling optimal behavior of the biodegradable slurry (e.g., delayed breakdown of slurry may result in more time needed to establish groundwater flow through wall).

A DoD site that employed the hydraulic fracturing technique is Maxwell AFB, AL. At Maxwell AFB, boreholes were advanced to 75 to 80 ft bgs, followed by installation and grouting of PVC casing. Next, a high pressure jet cutting tool was used to cut slots through the PVC casing to produce panels aligned in either a V or Y configuration. The PRB was installed from 55 ft bgs (the top of the wall) to 75 ft bgs (the bottom of the wall). Approximately, 40 tons or iron filings, humates, enzymes, and guar gum were used. The radio-wave imaging method (RIM) was used to monitor the location and thickness of the wall panels. Full-scale application at this site is not likely due the difficulty in consistently injecting treatment panels of uniform length and thickness.

The other site is a private site. At the Caldwell Trucking Site, New Jersey, both hydraulic fracturing and permeation infilling were used to install two PRBs. Both PRBs were 50 ft deep with a 3 in reactive zone, while the first wall was 150 ft in length and the second wall was 90 ft in length. The construction of the PRBs consisted of the propagation of fractures in wells spaced at 15 ft intervals followed by the pumping of a gel containing iron down into the unconsolidated sand and fractured bedrock. During construction some difficulty was experienced with the behavior of the guar gum gel. The low temperature and high pH of the mixture delayed breakdown of the gel, so a pH buffer and additional enzyme were needed to complete the degradation process (RTDF, 2001).

7.1.2.7 ***Vibrated Beam/Mandrel Methods.*** This construction technique involves driving an H-beam or mandrel with a sacrificial shoe at the bottom into the ground with a vibratory hammer to create a void space. As the beam is raised, the grout or slurry is injected into the void space through special nozzles at the bottom of the beam. An impermeable barrier is thus installed by driving in overlapping panels. The advantages associated with vibrated beam/mandrel techniques based on recent PRB field projects are:

- Dimensions of PRB easily maintained.
- Amount of spoils minimized (e.g., no excavation required).
- Installed without de-watering and associated treatment of contaminated groundwater.
- Possible to install barrier using up to a 45-degree angle to avoid subsurface or aboveground structures.
- Health and safety enhanced by minimizing worker exposure to contaminated soils.

The limitations with vibrated beam or mandrel methods are:

- Practical depth limitations.
- Beam dimensions limit barrier thickness to a few inches in many cases.
- Noise and vibration from equipment may be unacceptable to nearby receptors.

The vibrated beam method was used to construct a 425 ft slurry cut-off wall at a site in Tifton, GA. The slurry wall was installed 20 ft down-gradient of a groundwater collection trench that was filled with gravel and contained an HDPE drainage pipe (Andromalos et al., 1999).

A pilot study at Cape Canaveral Air Station in Florida tested the use of the mandrel construction method. The mandrel barrier is 52 ft long, 4 in thick, and was installed at a depth of 45 ft bgs. Approximately, 98 tons of iron were used in the installation. Some difficulty was experienced in maintaining the integrity of the wall. Because of the short thickness of the reactive zone, small deviations from the vertical resulted in discontinuities. This problem can be avoided by overlapping adjacent sections of the barrier. The vibrations from driving the mandrel also caused disturbance to nearby buildings and personnel (Battelle, 1999).

7.1.2.8 ***Deep Soil Mixing Methods.*** For deep soil mixing, two or three special augers equipped with mixing paddles are lined up in series. These augers penetrate the ground and mix fine iron and soil together. The iron can be mixed with biodegradable slurry and pumped to the mixing augers while they are advanced slowly through the soil. An alternate method includes, the installation of iron-filled casings in the subsurface with a vibratory hammer followed by deep soil mixing. The advantages associated with deep soil mixing techniques based on recent PRB field projects are summarized as follows:

- Dimensions of PRB easily maintained.
- Health and safety enhanced by minimizing worker exposure to contaminated soils.
- Amount of spoils minimized (e.g., no excavation required).
- Installed without de-watering and associated treatment of contaminated groundwater.

The limitations of deep soil mixing are:

- Amount of reactive medium installed is limited without significant soil removal.
- Several passes with mixing are needed to increase homogeneity of the soil, gravel, iron mixture.
- Casing installation to place iron in the subsurface can meet resistance and slow down installation.
- Augers for casings available only in 3 to 8 ft diameters.

The first application of deep soil mixing for the construction of a PRB was carried out at the Cape Canaveral Air Station in Florida in 1998. The project involved both deep soil mixing and vibro-installation techniques to install the iron filings. First, 6-inch diameter casings were driven into the target treatment zone to a depth of 40 ft bgs using a vibratory hammer. Next, iron filings were backfilled into the casings. The casings were subsequently removed which left columns of iron filings in place in the subsurface. The final step was to use the deep soil mixing equipment (with a 5 ft diameter auger) to mix the iron with the surrounding soil.

The continuous reactive barrier at Cape Canaveral consisted of 11 of these overlapping mixed columns with a total length of approximately 44 ft, a reaction zone thickness of 4 ft, and a depth of 40 ft bgs. The wall contained approximately 16% iron by weight. The continuous reactive barrier was keyed into an underlying clay layer. In addition, a "mixing zone" was established ahead of the barrier that consisted simply of native soils that were subject to deep soil mixing to increase their permeability. Lessons learned from the project include the fact that three or more mixing passes may be necessary to improve the PRB construction and achieve a more uniform mixture of iron, native soil, and gravel. Percent iron values by weight ranged from 13.5% to 20.9% and were close to the 16% design target. Installation of the casings for granular iron introduction was somewhat problematic and could have been improved by pre-mixing the soils prior to installation (Reinhart, 2000).

7.2 Update on New and Existing PRBs and Cost of PRB Applications

Tables 7-2 and 7-3 summarize much of the information that is available on the PRBs installed in the United States. The information in these tables includes the site characteristics, PRB features, and PRB costs at various sites. As seen in these tables, the costs of PRBs vary widely depending on a variety of site and PRB characteristics. In general, the depth and the length of a PRB

continue to drive the costs of a PRB application. The deeper the aquifer and the longer the PRB, the greater is the cost. The Remedial Action Cost Engineering and Requirements System (RACER) model developed by the DoD is a good way of obtaining preliminary cost estimates of a PRB application during the preliminary site assessment or conceptual model stage, when the detailed design of the PRB has not yet been developed. Site owners can then take advantage of RACER's database of costs for various activities, such as trenching or drilling, for which RACER provides costs based on the state in which the PRB will be installed. However, once the detailed design of a PRB has been completed, site specific costs based on actual bids from suppliers and contractors should be obtained.

Another way of looking at the cost of a PRB is as a life cycle cost or present value for long-term application. The present value of a PRB can then be compared to the present value of an equivalent pump-and-treat system for economic analysis of the technology choice at a site. Present value is a method of discounting future costs to the present, a method that is widely used for estimating costs of long-term projects. The design guidance (Gavaskar et al., 2000) contains a detailed description of the present value method as applied to PRBs. Present value estimates have been calculated during previous projects (Battelle, 1998; Battelle, 2000a) for two of the PRB sites in the current project – former NAS Moffett Field and Dover AFB. Table 7-4 summarizes the present value estimates at these two sites. These present values were reviewed in the light of longevity expectations from the PRBs at these sites, based on the longevity evaluation in the current project.

The accelerated long-term column tests described in Section 5.2 provide some measure of the longevity of the granular iron PRBs. The issue of longevity of the PRB translates into an issue of economics. Will the PRB retain it reactivity and hydraulic performance long enough for the capital invested in the PRB to be worthwhile? For the Dover AFB site, for example, in Table 7-4, the present value of a PRB is calculated for different life expectancies of a PRB (5 years, 10 years, or 15 years). If the PRB loses its reactivity and/or hydraulic performance in 5 years, and has to be regenerated or replaced in some fashion (with the associated extraordinary maintenance costs), then the present value over 30 years of operation is higher for a PRB than it is for an equivalent pump-and-treat system (see Appendix D for details). An equivalent pump-and-treat system would be one that captures and treats the same amount of water flowing through the PRB. If the PRB can function without needing regeneration or replacement for 10 years or more, the present value of the PRB becomes less than that of an equivalent pump-and-treat system. In other words, the savings realized from the lower operating costs of a PRB more than offset the higher capital investment required; at many sites, PRBs need a higher capital investment than a pump-and-treat system. The bar may be set higher at sites that already have a functioning pump-and-treat system, perhaps installed as an interim remedy; in this case, capital invested in the pump-and-treat system is treated as a sunk cost and is not included in the present value analysis. The reduction in operating costs resulting from a PRB would have to be sufficiently high to offset the entire capital invested in the PRB.

Although the breakeven point (year in which the present value of a PRB becomes lower than the present value of the pump-and-treat system) may vary from site to site, depending on various site

and PRB characteristics, the range of breakeven points is probably between 7 to 15 years (see Appendix D). The accelerated column tests show that even at sites with relatively high levels of dissolved solids (e.g., Lowry AFB) the PRB is likely to continue performing acceptably beyond the breakeven point (7 to 15 years after installation). One caveat is that the thickness of the reactive cell has to incorporate enough of a safety factor to handle a possible decline in reactivity of about 3 to 4 times its original value over this time period. A greater thickness would mean higher materials (iron) and construction (trenching) costs; however, the cost of a PRB is not particularly sensitive to its thickness, as it is to the depth and length of a PRB. Once the construction equipment has been mobilized to the site, a PRB with 6-foot thickness is not likely to cost proportionately more than a PRB with 3-foot thickness. However, the tradeoff between a higher safety factor (and the concomitantly higher capital investment) now versus the risk of future potentially expensive contingency measures (see Section 8.1.2), in case of PRB failure, has to be weighed carefully at each site.

It is difficult to narrow down the life expectancy of PRBs beyond this type of scenario development, based on the longevity evaluation in Section 5. It would be difficult to say, for example, that the PRB at former NAS Moffett Field is likely to last for 'x' number of years or that the PRB at Lowry AFB is likely to last for 'y' number of years, based on the accelerated column tests. One reason for the difficulty in translating the accelerated column test results to field PRB performance is the uncertainty in the groundwater velocity estimate at the site. At most sites, hydraulic conductivity estimates and, consequently, the groundwater velocity estimates vary in a range that is half or one order of magnitude wide. This variability itself causes a factor-of-5 or -10 uncertainty in the number of pore volumes passing through the PRB. In addition, potential smearing across the face of the PRB and/or preferential pathways in the reactive medium, as well as seasonal fluctuations in flow velocity and direction, make it difficult to judge the number of pore volumes of groundwater flowing through the PRB every year. The uncertainty in the number of pore volumes of groundwater that a PRB is exposed to each year is a primary logistical reason why it is difficult to estimate its effective life.

Therefore, the economic scenarios discussed above – comparing present values of PRBs and pump-and-treat systems at different life expectancies of a PRB – are probably the best approach. Given the short history of the PRB technology, the accelerated column tests provide some comfort that the rate of loss of reactivity observed in the columns makes it possible for PRBs to be worthwhile at sites where the breakeven point for the PRB is less than 25 or 30 years, a not too difficult target to meet at most sites. At the same time, it is recognized that the life of the PRB is finite, that at some point in the future the contingency measures described in Section 8.1.2 may be required, assuming that the contaminant plume will outlive the PRB.

Table 7-2. Update on Design, Construction, and Cost of PRBs

PRB Site	PRB Type	Depth to Aquitard (ft bgs)	Reactive Cell Thickness (ft)	Amount of Reactive Medium (tons)	Gate or CRB Width (ft)	Funnel Width (ft)	Gate or CRB Construction Method	Funnel Construction Method	PRB Cost
Elizabeth City, NJ	CRB	25[a]	2	450	150		Continuous trenching		$500,000 total
DOE facility, Kansas City, MO	CRB	30	6	666	130		Cofferdam		$1,300,000 total installation
Watervliet Arsenal, NY	CRB with 2 trenches	7-25	2.5	166	Trench A 205; Trench B 83		Trench box		$113,000 design, $278,000 installation
Former manufacturing site, NJ	CRB	15-23	5	720	127		Cofferdam		$725,000 installation
Seneca Army depot activity, NY	CRB	8 to 10	1	203	650		Trench		$100,000 design, $350,000 installation
Industrial site, SC	CRB		1	400	325		Continuous trenching		$350,000 installation
Caldwell Trucking, NJ	CRB with 2 trenches		0.25	250	150 and 90		Hydraulic Fracturing		$670,000 for 90 ft and $450,000 for 150 ft
Private electronics firm, Mountain view, CA	CRB			90					$80,000-$100,000 total
Dry cleaning site, Germany	CRB			69 iron 85 iron sponge	74 (33 granular iron & 41 iron sponge)		Overlapping boreholes		$93,000 total
Massachusetts Military Reservation, MA	CRB		0.28	44	48		Hydraulic Fracturing		$160,000 installation

Table 7-2. Update on Design, Construction, and Cost of PRBs (Continued)

PRB Site	PRB Type	Depth to Aquitard (ft bgs)	Reactive Cell Thickness (ft)	Amount of Reactive Medium (tons)	Gate or CRB Width (ft)	Funnel Width (ft)	Gate or CRB Construction Method	Funnel Construction Method	PRB Cost
Belfast, Northern Ireland	Funnel-and-gate					80 to 100	In situ reaction vessel	Bentonite cement slurry walls	$20,000 iron $350,000 construction
Industrial facility, NY	Funnel-and-gate	20	3.5	45	12	15	Cofferdam	Sheet piling	$30,000 iron $250,000 construction
Industrial facility, NY	CRB (2 walls)	18	1	742	Trench A = 120 ft; trench B = 370 ft		Continuous trenching		$797,000 installation
Intersil, Sunnyvale, CA	Funnel-and-gate	20	4	220	36	535 (300 and 235 gates	Cofferdam	Cement-bentonite slurry wall	$170,000 iron $720,000 construction
Canadian Forces Base, Borden, Canada	CRB	20	5	61	5		Clamshell excavation, sheet pile box for shoring		$25,000- $30,000 total
Denver Federal Center	Funnel-and-gate (with 4 gates)	23-30	2 to 6		160 (40 ft × 4)	1,040	Cofferdam	Sealable-joint sheet piling	$1,000,000 total
Former NAS Moffett Field	Funnel-and-gate	25	6	75	10	40 (20 × 2)	Backhoe excavation, sheet pile box for shoring	Sealable-joint sheet piling	$323,000 installation
Somersworth Sanitary Landfill Superfund Site	Funnel-and-gate	40	4			30	Caisson	Bentonite slurry walls	$175,000 total construction
Somersworth Sanitary Landfill Superfund Site	CRB	40	2.3	100	21		Bioslurry trench		$175,000 construction

Table 7-2. Update on Design, Construction, and Cost of PRBs (Continued)

PRB Site	PRB Type	Depth to Aquitard (ft bgs)	Reactive Cell Thickness (ft)	Amount of Reactive Medium (tons)	Gate or CRB Width (ft)	Funnel Width (ft)	Gate or CRB Construction Method	Funnel Construction Method	PRB Cost
Somersworth Sanitary Landfill Superfund Site	CRB	40	2.5		915 (24 panels 30-50 ft long)		Bioslurry trench		$200,000 design, $2,000,000 installation
Former Lowry AFB, CO	Funnel-and-gate with angled funnel	17	5		10	28 (14 × 2)	Cofferdam	Sealable-joint sheet piling	$530,000 installation
Portsmouth gaseous diffusion plant, OH	Above ground	32							$4,000,000 total
ORNL, TN	Funnel-and-gate						Concrete treatment canisters		$1,000,000 for both barriers
ORNL, TN	CRB	22-30	2	80	26	225	Bioslurry trench		$1,000,000 for both barriers
East Garrington gas plant, Canada	Trench with 2 gates				6	290 (145 × 2)	Vertical culverts	Trench sealed with liner	$67,200 construction
Fry Canyon site, UT	Funnel-and-gate with 3 barriers		3		7				$140,000 installation $30,000 design
Private site, Tifton, GA	Funnel-and-gate					400		Vibrating beam	$520,000 construction and reactive media
Former NAS Alameda, CA	Funnel-and-gate; compound gate with 2 reactive cells in series	20	10		15	20 (10 × 2)	Trench with concrete pad on bottom	Waterloo Barrier™ Sealable Sheet Piles	$400,000 construction
Public school, Ontario, Canada	Funnel-and-gate		6		6	32 (16 × 2)		Sealable sheet pilings	$5,000 construction

Table 7-2. Update on Design, Construction, and Cost of PRBs (Continued)

PRB Site	PRB Type	Depth to Aquitard (ft bgs)	Reactive Cell Thickness (ft)	Amount of Reactive Medium (tons)	Gate or CRB Width (ft)	Funnel Width (ft)	Gate or CRB Construction Method	Funnel Construction Method	PRB Cost
Tonolli Superfund Site, PA	Groundwater trench		3		1,100		Trench constructed using a trackhoe and trench boxes.		
Aircraft maintenance facility, OR	Funnel-and-gate with 2 gates	24	1.5' gate 1 and 3' gate 2		Gate 1, 50 ft and gate 2, 50 ft	650	Continuous trencher and trackhoe and drag box	Soil-bentonite slurry	$600,000 construction
Industrial site, KS	Funnel-and-gate	30	3	70	20	980 (490 × 2)	Cofferdam	Soil bentonite slurry	$400,000 installation
Cape Canaveral Air Station, FL	CRB (2 walls)	43	1 ft (mandrel)	98 (mandrel) 107 JAG	70	100.5 (51.5 and 49 barriers)	Mandrel and JAG emplacement		$279,000 mandrel system $238,000 JAG system
Cape Canaveral Air Station, FL	CRB	40	4		40 (11 columns)		Deep soil mixing		$220,000 total
Dover AFB, DE	Funnel-and-gate with 2 gates	40-45	4	54 iron 5 pyrite	8 (2 gates, 4 ft each)	60	Caissons	Sealable sheet piles	$22,000 iron $25,000 pyrite $327,000 construction
Rocky Flats, Mound Site Golden, CO	Reaction Vessels			(300 ft^3)		230	Gravity-fed reaction vessel with collection trenches		$590,000 total
Rocky Flats, East Trenches Plume Golden, CO	Reaction Vessels	26	6.5		(12 x 13 each vessel)	1,200	Gravity-fed reaction vessel with collection trenches		$1,300,000 total
Rocky Flats, Solar Ponds Plume Golden, CO	Reaction Vessels		10		(32 x 17 first vessel, 11 x 17 second vessel)	1,100	Gravity-fed reaction vessel with collection trenches		$1,300,000 total

Table 7-2. Update on Design, Construction, and Cost of PRBs (Continued)

PRB Site	PRB Type	Depth to Aquitard (ft bgs)	Reactive Cell Thickness (ft)	Amount of Reactive Medium (tons)	Gate or CRB Width (ft)	Funnel Width (ft)	Gate or CRB Construction Method	Funnel Construction Method	PRB Cost
Wood-treating facility, NH	Funnel-and-gate				30	650		Sealable sheet piles	
100D Area, Hanford site, WA	In situ redox manipulation	85	50		150		Injecting sodium dithionite into existing wells		$480,000 construction
Savannah River site, Aiken, SC	Geosiphon cell								$26,400 iron $119,115 total costs
Industrial facility, LA	CRB	23	1	616.5	720		Continuous trenching		$260,000 total
DoD facility, Warren, AFB	CRB	28-38	4	1680	565		Trench box		$2,400,000 installation, design $217,000
DoD facility, Pease AFB, NH	CRB	33	2.5		150		Bioslurry trench		$300,000 total
Industrial facility, MA	CRB	17	2.5		180		Sheet pile box		$420,000 total
Industrial facility, OH	CRB	20	1	72	200		Open trench excavation		$70,000 total
DoD facility, Travis AFB, CA	CRB	50	4-5	300	80		Jetting		$360,000 construction
NASA facility, LA	Granular iron placed around leaking manhole			22.5			Sheet pile box		
Maxwell AFB, AL	CRB	75	0.08-0.3	40			Hydraulic Fracturing		

Table 7-2. Update on Design, Construction, and Cost of PRBs (Continued)

PRB Site	PRB Type	Depth to Aquitard (ft bgs)	Reactive Cell Thickness (ft)	Amount of Reactive Medium (tons)	Gate or CRB Width (ft)	Funnel Width (ft)	Gate or CRB Construction Method	Funnel Construction Method	PRB Cost
Former Mill Site, UT	Funnel-and-gate		2-4		100		Excavation using sheet pile box	Soil-bentonite slurry wall	$800,000 installation
Bodo Canyon, CO	Leach Field (PRB A/B); Reaction vessels (PRB C/D/E)		1 (PRB A/B) 6 (PRB C/D/E)	(70 ft^3) PRB C/D/E	20 (PRB A/B) Vessel is 6 x 3 x 4.2 ft (PRB C/D/E)		PRB A/B constructed similar to septic leach fields. Retention pond runoff routed thru reaction vessels or steel tanks with baffles (PRB C/D/E).		$255,000 installation, $125,000 design
Chalk River Laboratories, Canada	Wall and Curtain	31.2-39.4	6.6	(153.4 yd^3)	36.1	98.4 (cut off wall width)	Excavation	Steel cut-off wall	$300,000 total
DuPont, NC	CRB		0.17-0.33	100	375		Jetting		$200,000 total
DuPont, Ca	CRB	120	0.5		110		Hydraulic Fracturing		$150,000 design, $1,000,000 installation
Vapokon Petrochemical Works, Denmark	Funnel-and-gate	42	2	(105 yd^3)	50	400	Excavation using sheet piles		$240,000 design, $700,000 installation
Former Manufacturing Site, WA	Funnel-and-gate	32	3	180	45 (each of 2 gates)		Bioslurry trench	Cement bentonite (CB) cut-off wall	$50,000 design, $350,000 installation

Table 7-2. Update on Design, Construction, and Cost of PRBs (Continued)

PRB Site	PRB Type	Depth to Aquitard (ft bgs)	Reactive Cell Thickness (ft)	Amount of Reactive Medium (tons)	Gate or CRB Width (ft)	Funnel Width (ft)	Gate or CRB Construction Method	Funnel Construction Method	PRB Cost
Lake City Army Ammunition Plant	CRB	60	2		380		Bioslurry trench		ROD estimated present worth cost of $3,494,000
DoD facility, Vandenberg AFB, CA	Biobarrier		1-2 ft bioactive zone		15 ft x 1.5 ft x 12 ft (LxWxD)		Trench/excavation		
Industrial Site, Australia	CRB		5-6.6		16.4		Sheet pile trench box		
DOE West Valley Demonstration Project, NY	CRB	28	6		30		Excavation with type 48-sheet piling		$1,000,000 installation
Cedar Crest, Albuquerque, NM	CRB (air stripping + biodegradation)				30		Trench excavated using a backhoe		Total Installation Costs $4,788
Newbury Park, CA	RSF (reactant sand-fracking)	fractured bedrock aquifer		3900 lb of iron foam proppant			Hydraulic Fracturing		$ 200,000
Naval Weapons Industrial Reserve Plant, TX	CRB	25	2.5		1,375		Continuous Trenching		Cost savings over pump-and-treat $2,000,000

(a) PRB is not keyed in to aquitard.
CRB = Continuous reactive barrier.
JAG = Jet-assisted grouting.

Table 7-3. Update on PRB Site Characteristics and Monitoring

PRB Site (Installation Date)	Scale of PRB	Target Contaminants	Reactive Medium	Target Cleanup Levels	Groundwater Velocity in Aquifer (ft/day)	Monitoring Update and Remarks
Elizabeth City, NC (June 1996)	Full[a]	Cr^{+6} (3,430 μg/L) TCE (4,320 μg/L) *cis*-DCE (12 mg/L) VC (0.1 mg/L)	Granular iron	MCLs: Cr (50 μg/L) TCE (5 μg/L)	Extremely variable with depth, with a highly conductive layer at roughly 4.5 to 6.5 m bgs.	MCLs met in reactive cell; plume migration below hanging PRB possible.[a]
DOE facility, Kansas City, MO (April 1998)	Full	*cis*-DCE (1,500 μg/L) VC (291 μg/L)	Granular iron	MCLs: *cis*-DCE (70 μg/L) VC (2 μg/L)	0.025 in clay zone; 1.13 in gravel zone	Possible plume bypass around south end of PRB. MCLs met in reactive cell.
Watervliet Arsenal, NY (October 1998)	Full	PCE (1,100 μg/L) TCE (1,500 μg/L) *cis*-DCE (4,200 μg/L) *trans*-DCE (11 μg/L) VC (1,700 μg/L)	Granular iron and sand mixture	PCE, TCE, *cis*-DCE, *trans*-DCE (5 μg/L) VC (2 μg/L)	0.15	
Former manufacturing site, NJ (September 1998)	Full	1,1,1-TCA (1,200 ppb) PCE (19 ppb) TCE (110 ppb)	Granular iron and sand mixture	PCE, TCE (1 μg/L) 1,1,1-TCA (30 μg/L) VC (5 μg/L)	0.6	
Seneca Army depot activity, NY (December 1998)	Full	TCE (51,000 μg/L) DCE (130,000 μg/L)	Granular iron and sand mixture	TCE, *cis*-DCE (5 μg/L) VC (2 μg/L)	0.17	Samples taken after 4 quarters of monitoring indicated 100% removal of TCE. Removal of DCE was less than expected and will require more iron.
Industrial site, SC (November 1997)	Full	TCE (25 mg/L) *cis*-DCE (3.5 mg/L) VC (0.9 mg/L)	Granular iron and sand mixture	MCLs: TCE (5 μg/L) *cis*-DCE (70 μg/L) VC (2 μg/L)	0.14	
Caldwell Trucking, NJ (April 1998)	Full	TCE (6,000-8,000 μg/L)	Granular iron	50 μg/L TCE	1.1	

Table 7-3. Update on PRB Site Characteristics and Monitoring (Continued)

PRB Site (Installation Date)	Scale of PRB	Target Contaminants	Reactive Medium	Target Cleanup Levels	Groundwater Velocity in Aquifer (ft/day)	Monitoring Update and Remarks
Private electronics firm, Mountainview, CA	Pilot	*cis*-DCE (5-10 mg/L) TCE (1 mg/L) VC (5-50 mg/L)	Granular iron			
Massachusetts military reservation (June 1998)	Pilot	TCE (15 μg/L) PCE (300 μg/L)	Granular iron suspended in a guar gum slurry	MCLs: PCE, TCE (5 μg/L)	1	
Industrial facility, NY (May 1995)	Pilot	TCE (300 μg/L) *cis*-DCE (500 μg/L) VC (80 μg/L)	Granular iron	MCLs: TCE (5 μg/L) *cis*-DCE (70 μg/L) VC (2 μg/L)	1	MCLs met within 1.5 ft of travel through the reactive media. The precipitates did not appear to significantly affect system performance. Consistent VOC degradation over a 2-year monitoring period.
Industrial facility, NY (December 1997)	Full	TCE (200-1,280 μg/L) *cis*-DCE (300-1,800 μg/L) VC (26-53 μg/L)	Granular iron	MCLs: TCE, DCE (5 μg/L) VC (2 μg/L)	0.6	Wall constructed over top of pilot system. MCLs met in iron zone. Relic VOCs in down-gradient aquifer wells.
Intersil, Sunnyvale, CA (February 1995)	Full	TCE (50-200 μg/L) *cis*-DCE (450-1,000 μg/L) VC (500 μg/L) Freon® 113 (60 μg/L)	Granular iron	TCE (5 μg/L) *cis*-DCE (6 μg/L) VC (0.5 μg/L) Freon® (1,200 μg/L)	1	MCLs being met after 5 years of operation.

Table 7-3. Update on PRB Site Characteristics and Monitoring (Continued)

PRB Site (Installation Date)	Scale of PRB	Target Contaminants	Reactive Medium	Target Cleanup Levels	Groundwater Velocity in Aquifer (ft/day)	Monitoring Update and Remarks
Denver Federal Center (October 1996)	Full	TCE (600 μg/L) 1,1,1-TCA (200 μg/L) *cis*-1,2-DCE (470 μg/L) 1,1-DCE (230 μg/L) VC (15 μg/L)	Granular iron	TCA (200 μg/L) TCE (5 μg/L) *cis*-DCE (70 μg/L) 1,1-DCE (7 μg/L) VC (2 μg/L) 1,1-DCA (5 μg/L)	0.5	Cleanup targets met in iron, except 1,1-DCA (8 μg/L) in gate effluent. Upgradient mounding may be causing plume bypass over or around the PRB. CVOC concentrations increasing in the groundwater flowing around the south end of barrier. Also, plume potentially may be moving under the barrier.
Former NAS Moffett Field (April 1996)	Pilot[a]	TCE (1,300 μg/L) *cis*-DCE (230 μg/L)	Granular iron	MCLs: TCE (5 μg/L) *cis*-DCE (70 μg/L)	0.2-0.5	MCLs met in reactive cell. Plume underflow possible through intentional gap between thin aquitard and base of PRB.[u]

Table 7-3. Update on PRB Site Characteristics and Monitoring (Continued)

PRB Site (Installation Date)	Scale of PRB	Target Contaminants	Reactive Medium	Target Cleanup Levels	Groundwater Velocity in Aquifer (ft/day)	Monitoring Update and Remarks
Somersworth Sanitary Landfill Superfund Site (November 1996)	Pilot	TCE, *cis*-DCE, VC (<300 μg/L)	Granular iron and sand mixture	MCLs: TCE (5 μg/L) *cis*-DCE (70 μg/L) VC (2 μg/L)	0.5 to 2.0	Constructability test using bioslurry trench completed in October 1999, prior to full-scale application.
Somersworth Sanitary Landfill Superfund Site (2000)	Full	PCE (410 μg/L) TCE (370 μg/L) *cis*-DCE (530 μg/L) VC (1,900 μg/L)	Granular iron and sand mixture	MCLs: PCE (5 μg/L) TCE (5 μg/L) *cis*-DCE (70 μg/L) VC (2 μg/L)	0.5 to 2.0	
Former Lowry AFB, CO (December 1995)	Pilot	TCE (1,400 μg/L)	Granular iron	MCLs: TCE (5 μg/L) *cis*-DCE (70 μg/L)	1	MCLs met
Portsmouth gaseous diffusion plant, OH	Pilot	TCE (70-150 μg/L)	Granular iron in canisters	MCL (5 μg/L)		MCLs met
ORNL, TN	Full	HNO_3, uranium, technetium	Granular iron			
Fry Canyon Site, UT	Full	Uranium (20,700 μg/L)	Bone char phosphate, foamed zero-valent iron, and amorphous ferric oxide		1.5	
Private Site, Tifton, GA	Full	Pesticides and VOCs	Activated carbon			

Table 7-3. Update on PRB Site Characteristics and Monitoring (Continued)

PRB Site (Installation Date)	Scale of PRB	Target Contaminants	Reactive Medium	Target Cleanup Levels	Groundwater Velocity in Aquifer (ft/day)	Monitoring Update and Remarks
Former NAS Alameda, CA (December 1996)	Pilot	*cis*-DCE (250 mg/L) VC (65 mg/L) Toluene (8 mg/L) TCE; 1-1 DCE; tDCE<1000 µg/L each	Granular iron in first reactive cell; biosparging in following cell		0.42-1.25	Breakthrough of CVOCs due to higher-than-expected CVOC concentrations in gate influent. Residence time in iron reactive cell inadequate.
Tonolli Superfund Site, PA	Full	Pb (328 ppb) Cd (77 ppb) As (313 ppb) Zn (1,130 ppb) Cu (140 ppb)	Limestone			
Aircraft maintenance facility, OR (March 1998)	Full	VOCs (500 µg/L)	Granular iron		3.0	MCLs met in iron zone.
Industrial Site, KS (January 1996)	Full	TCE (400 µg/L) 1,1,1-TCA (100 µg/L)	Granular iron		0.2	Two additional gates and 3,200 ft of slurry wall were added to system in November 1999.
Cape Canaveral Air Station, FL (November 1997)	Pilot	TCE (90 mg/L) DCE (170 mg/L) VC (7 mg/L)	Granular iron		0.1 to 0.5	

Table 7-3. Update on PRB Site Characteristics and Monitoring (Continued)

PRB Site (Installation Date)	Scale of PRB	Target Contaminants	Reactive Medium	Target Cleanup Levels	Groundwater Velocity in Aquifer (ft/day)	Monitoring Update and Remarks
Cape Canaveral Air Station (1999)	Pilot	TCE (29 mg/L) cis-DCE (44 mg/L) trans-DCE (0.8 mg/L)	Granular iron			TCE and its daughter products are at non-detect with the PRB, with exception of VC.
Dover AFB, DE (January 1998)	Pilot	PCE (5,617μg/L) TCE (549 μg/L) *Cis-DCE* (529 μg/L)	Granular iron (pretreatment zones containing iron-sand or iron-pyrite mixtures)	MCLs: PCE, TCE (5 μg/L) *cis-DCE* (70 μg/L) VC (2 μg/L)	0.06-0.3	MCLs met.
Rocky Flats Mound Site, Golden, CO (1998)	Full	PCE (130 μg/L) TCE (160 μg/L) CCl_4 (130 μg/L) CCl_3 (26 μg/L) *cis*-DCE (62 μg/L) *trans*-DCE (12 μg/L) U (9.5 pCi/L)	Granular iron	MCLs: PCE, TCE (5 μg/L) *cis*-DCE (70 μg/L) *trans*-DCE (7 μg/L) CCl_4 (5 μg/L) CCl_3 (100 μg/L) U (10 pCi/L)	(0.1 to 2 gpm in reaction vessel)	VOCs are routinely non-detect in effluent samples and U are below stream standards. Direct discharge allowed.
Rocky Flats, East Trenches Plume, CO (1999)	Full	TCE (4,500 μg/L) PCE (490 μg/L) CCl_4 (240 μg/L) CCl_3 (100 μg/L) *cis*-DCE (70 μg/L) MeCl (470 μg/L)	Granular iron and pea gravel	MCLs: PCE, TCE (5 μg/L) *cis*-DCE (70 μg/L) trans-DCE (7 μg/L) CCl_4 (5 μg/L) CCl_3 (100 μg/L) MeCl (5 μg/L)		With the exception of methylene chloride, VOCs are routinely non-detectable.
Rocky Flats, Solar Ponds Plume (1999)	Full	nitrate (170 mg/L) U (28 pCi/L)	Granular iron and sawdust and leaf mold.	Surface water standards nitrate (100 mg/L) U (10 pCi/L)		Water exiting the treatment cell typically contains < 5 mg/L nitrate and < 1 pCi/L of U.
Wood-treating facility, NH	Pilot	Nonaqueous-phase liquid				

Table 7-3. Update on PRB Site Characteristics and Monitoring (Continued)

PRB Site (Installation Date)	Scale of PRB	Target Contaminants	Reactive Medium	Target Cleanup Levels	Groundwater Velocity in Aquifer (ft/day)	Monitoring Update and Remarks
100D Area, Hanford site, WA	Full	Chromate (2 mg/L)	Chemical reducing agent			
Savannah River site, Aiken, SC (July 1997)	Pilot	TCE (200-250 μg/L) *cis*-DCE (20-50 μg/L) NO_3 (10-70 mg/L)	Granular iron	MCLs: PCE, TCE (5 μg/L) *cis*-1,2-DCE (70μg/L) VC (2 μg/L)	Controlled flowrate	MCLs met in iron zone of Geosiphon.
DoD facility, Shaw AFB, SC (November 1998)	Full	1,1,1-TCE (6,000 μg/L) 1,1-DCA (10,000 μg/L) *cis*-DCE (1,400 μg/L) 1,1-DCE (450 μg/L) VC (240 μg/L)	Granular iron	MCLs: 1,1,1-TCE (200μg/L) 1,1-DCE (7 μg/L) *cis*-DCE (70 μg/L) VC (2 μg/L)	1.5	Thin iron zones, desorption of VOCs from aquifer strongly influenced results. Design should include consideration of production of daughter products in specifying width and retention time of PRB.
Industrial facility, LA (November 1998)	Full	TCE (10,000 μg/L) PCE (260,000 μg/L) *cis*-DCE (66,000 μg/L) VC (32,000 μg/L) TCE (5,000 μg/L)	Granular iron	PCE (25μg/L) TCE (210 μg/L) *cis*-DCE (116,000 μg/L) VC (358 μg/L)	0.0003	Very low flow velocity.
DoD facility, WY (August 1999)	Full	TCE (21,000) *cis*-DCE (5,600) VC (120)	One segment granular iron; two segments granular iron sand mixture	MCLs: TCE (5 μg/L) *cis*-DCE (70 μg/L) VC (2 μg/L)	1.33	
DoD facility, NH (August 1999)	Full	TCE (4,700 μg/L) *cis*-DCE (10,000 μg/L) VC (1,700 μg/L)	Granular iron and sand mixture	MCLs: TCE (5 μg/L) *cis*-DCE (70 μg/L) VC (2 μg/L)	0.03	

Table 7-3. Update on PRB Site Characteristics and Monitoring (Continued)

PRB Site (Installation Date)	Scale of PRB	Target Contaminants	Reactive Medium	Target Cleanup Levels	Groundwater Velocity in Aquifer (ft/day)	Monitoring Update and Remarks
Industrial facility, MA (August, 1999)	Full	PCE (17,000 μg/L) TCE (100 μg/L) *cis*-DCE (100 μg/L) VC (20 μg/L)	Granular iron	MCLs: TCE (5 μg/L) *cis*-DCE (70 μg/L) VC (2 μg/L)		
Industrial facility, OH (November, 1999)	Full	TCE (8,000 μg/L) *cis*-DCE (50 μg/L) *trans*-DCE (50 μg/L) VC (30 μg/L)	Granular iron and sand mixture	MCLs: TCE, PCE (5 μg/L) *cis*-DCE (70 μg/L) VC (2 μg/L) 1,1-DCE (7 μg/L)	0.01	
DoD facility, Travis AFB, CA (July 1999)	Pilot	TCE (10,000 μg/L) *cis*-DCE (300 μg/L) 1,1-DCE (700 μg/L) *cis*-DCE (23,200 μg/L)	Fine grained granular iron mixed with aquifer material	MCLs: TCE, PCE (5 μg/L) *cis*-DCE (70 μg/L) VC (2 μg/L) 1,1-DCE (7 μg/L)	0.2	
NASA Facility, LA (August 1999)	Pilot	TCE (22,500 μg/L) VC (6,810 μg/L) *cis*-DCE (23,200 μg/L)	Granular iron	TCE (2,600 μg/L) VC (4,500 μg/L) *cis*-DCE (70,300 μg/L)		
Maxwell AFB, AL (July 1998)	Pilot	TCE (720 μg/L) PCE (<1 μg/L)	Granular iron suspended in a guar gum slurry		0.07-0.2	
Former Mill Site, UT (1999)	Full	U (700 μg/L) Se (40 μg/L) V (400 μg/L) As (10 μg/L)	Granular iron (13% by volume) with gravel		2.4 to 18 (within the PRB)	PRB has reduced concentrations of As, Se, U, and V to non-detect within the barrier. Iron concentrations exiting wall are lower than expected.

Table 7-3. Update on PRB Site Characteristics and Monitoring (Continued)

PRB Site (Installation Date)	Scale of PRB	Target Contaminants	Reactive Medium	Target Cleanup Levels	Groundwater Velocity in Aquifer (ft/day)	Monitoring Update and Remarks
Bodo Canyon (1995)	Pilot	As (186 μg/L) Mo (1180 μg/L) Se (337 μg/L) U (5540 μg/L) V (8800 μg/L Zn (1600 μg/L)	PRB A/D steel wool PRB B steel wool/ copper wool PRB C Fine-grained iron with aluminosilicate PRB E Granular iron		(Flowrate from holding tank 0.3 to 2 gpm)	Effluent concentrations in PRB C were: As 2.2 μg/L, Mo 359 μg/L, Se 5.9 μg/L, U 1.2 μg/L, V <6 μg/L, and <4 μg/L for Zn. After 3 years, flow ceased in PRB C due to plugging.
Dupont, NC (1999)	Full	TCE (10-300 μg/L)	Granular cast iron, plus clay/iron slurry jetted into source zone	North Carolina Groundwater Standard of 2.8 μg/L TCE.	0.05 to 0.1	The source treatment reduced the TCE mass by 95%. Negotiating with state to turn-off downgradient Pump-and-Treat System.
Dupont, CA (No Date)	Full	CCl_4 (20-40 ppm) $CHCl_3$ (1-3 ppm) Freon 11 (10 ppm) Freon 113 (3 ppm)	Granular cast iron			
Haardkrom Site (1999)	Full	TCE (40-1,400 μg/L) Hexavalent Cr (8-110 μg/L)	Granular iron			Design does not effectively control for uneven distribution of contaminants along PRB.
Former Manufacturing Site, WA (1999)	Full	PCE (50 mg/L) TCE (23 mg/L) cis-DCE (8 mg/L) VC (0.8 mg/L)	Iron filings	Protection of surface water quality: PCE (4.2 μg/L) TCE (56 μg/L) cis-DCE (80 μg/L) VC (2.9 μg/L)		Six months after installation, the measured treatment efficiencies ranged from 65 to 99% for chlorinated compounds. Natural attenuation allowed cleanup goals to be met prior to surface water discharge.

Table 7-3. Update on PRB Site Characteristics and Monitoring (Continued)

PRB Site (Installation Date)	Scale of PRB	Target Contaminants	Reactive Medium	Target Cleanup Levels	Groundwater Velocity in Aquifer (ft/day)	Monitoring Update and Remarks
Lake City Army Ammunition Plant (2000)	Full	TCE (0.005 mg/L) *cis*-DCE (0.007 mg/L) VC (0.002 mg/L)	Granular iron	MCLs		CVOCs downgradient still elevated above MCLs. Groundwater mounding ahead of PRB.
DoD facility Vandenberg AFB	Pilot	MTBE	oxygen	MTBE 5 μg/L	1-2 (sandy units)	System has been operating for 3 years. Upgradient MTBE concentrations are at 300 μg/L compared to downgradient levels of <5 μg/L.
DOE West Valley Demonstration Project, NY	Pilot	Sr-90	Clinoptilolite (zeolite)			Radioactive half-life of Sr-90 is 28 years. Wall is designed to last 20 to 25 years. During first 14-months of operation, effective removal of Sr-90 was observed.
Cedar Crest, Albuquerque, NM	Pilot	MTBE (40 µg/L)	crushed gravel	MTBE ND two years after construction	2	The performance of the barrier was monitored monthly over a period of 5 months.
Newbury Park, CA	Pilot	TCE (83 mg/L) Cr VI (8,4 mg/L)	iron foam proppants	TCE 52 mg/L after 5 days of pumping Cr VI n.d after 5 days		Pumps may be damaged by biofouling due to polysaccharide contained in fracking fluids.
Naval Weapons Industrial Reserve Plant, TX	Pilot	Perchlorate (4 to 91,000 ppb)	Gravel/compost amended with vegetable/cottonseed oil to assist in biodegradation	Perchlorate 66 ppb		Reduced average perchlorate concentrations in the trench from 20,000 μg/L to ND within two weeks of installation.

(a) PRB is not keyed in to aquitard.
MTBE = methyl-*tert*-butyl ether.

Table 7-4. Present Value Estimates for PRBs Versus Pump-and-Treat Systems at Dover AFB and Former NAS Moffett Field

Cost/Longevity Scenario	Dover AFB[a]	Former NAS Moffett Field[b]
Pump-and-Treat System		
Capital investment	$502,000	$ 1,412,000
Annual O&M cost[c]	$214,000	$ 695,000
Present value for 30 years of operation (discount rate is 2.9%)	**$4,857,000**	**17,081,000**
PRB		
Capital Investment	$947,000	$ 4,911,000
Annual O&M Cost	$148,000	$72,000
Present value over 30 years, if the PRB life is 5 years	$5,463,000	$ 23,653,000
Present value over 30 years, if the PRB life is 10 years	**$4,618,000**	**$14,382,000**
Present value over 30 years, if the PRB life is 15 years	$4,338,000	$11,313,000
Present value over 30 years, if the PRB life is 20 years	$4,123,000	$9,119,000
Present value over 30 years, if the PRB life is 30 years	$4,064,000	$8,429,000

(a) Costs based on Battelle, 2000a.
(b) Costs based on Battelle, 1998.
(c) In addition to the recurring annual O&M cost, a periodic maintenance cost that allows various components of the pump-and-treat system to be replaced at regular intervals is included in the present value calculation.

8.0 Regulatory Issues

In the current project, the approach taken by several State regulatory agencies in reviewing new PRB applications was studied. This section was developed based on a survey and feedback obtained from several member States in the ITRC's Permeable Reactive Barriers Team; the New Jersey Department of Environmental Protection facilitated this survey (Turner, 2001). Members of the Permeable Barriers Team who provided valuable feedback include:

- Louisiana Department of Environmental Quality (Stafford and Dave, 2001; Bradford and Dave, 2001)
- Massachusetts Department of Environmental Protection (Marra, 2001)
- New Hampshire Department of Environmental Services (Hewitt, 2001)
- Oregon Department of Environmental Quality (Dana, 2001).

Although this survey was initiated as a means of obtaining generic information about the number and types of PRBs and their monitoring systems, it provided valuable insights into valid regulatory concerns, the type of monitoring that would be required to address these concerns, and the types of contingency measures envisioned by the regulators and site owners. An encouraging theme in the survey was the amount of thought that had gone into reviewing PRB applications and the amount of attention paid by regulators to the economic impacts of their recommendations on site owners. The results of this survey are provided in Section 8.1.

8.1 Regulatory Issues with Permeable Barriers

The following information was compiled from a survey of state regulatory agencies and provides valuable guidance to site owners considering PRB applications for groundwater remediation.

8.1.1 Applications Received for Installation of New PRBs. Some State regulatory agencies were directly involved in the approval process for new applications for PRBs; others left it to the site owners and their representatives to evaluate and select their own remedies, but provided input to the decision. In reviewing the information in these applications, the following regulatory concerns appeared to have been inadequately addressed by some site owners or their representatives:

- Inadequate site characterization at the proposed location of the PRB. Insufficient information was provided on plume size, location, orientation, and groundwater/plume movement.
- Possibility of flow under, over, or around the PRB
- Possibility of reduced permeability of the PRB over time
- Possibility of groundwater mounding

- Inadequate reactive cell thickness
- Constructability of the PRB with respect to deep installations, earth support, etc.
- Inadequate consideration of the effects of biocides, breaker enzymes, and their byproducts (obviously a reference to site owners implementing the bioslurry method of installation).

This indicates the necessity of for site owners to conduct sufficient local characterization in the immediate vicinity of the proposed PRB, model different flow scenarios that incorporate the uncertainties in the site characterization, incorporate appropriate safety factors in the design, and developing a suitable monitoring scheme. These issues can be addressed appropriately during the site characterization and design stage. The PRB design guidance report (Gavaskar et al., 2000) provides a methodology for preliminary assessment of a site for the feasibility of PRB (developing a conceptual model of the site and proposed PRB), site characterization, and design.

8.1.2 Contingency Plans in Case of PRB Failure. State regulators often require that one or more of these contingency measures be incorporated in a PRB application, to prevent contaminant migration in case of PRB failure:

- Ability to operate a pump-and-treat system, if monitoring shows contaminant breakthrough or bypass for the PRB.
- Ability to pump the PRB as an interceptor trench, a variation of the pump-and-treat measure.
- Extension of the PRB to capture more of the plume, if monitoring shows that the capture zone is inadequate.
- Blocking the end(s) of the PRB with an impermeable barrier (slurry wall or sheet piling).
- Ability to install a second PRB downgradient from or adjacent to the first one.

Regulators noted that the actual contingency measure adopted would depend on the mechanism of failure – that is, whether failure would occur because of loss of reactivity, inadequate residence time, inadequate groundwater capture, etc. Means of measuring hydraulic performance and identifying appropriate contingency measures to deal with any future loss of hydraulic performance were key issues that regulators thought would benefit from more research.

One challenge that is foreseen, based on the results of the current project, is that determination of the functioning/malfunctioning of the PRB would take time. Many PRBs are built inside a plume, a decision often driven by the relative spacing of the plume boundary and property

boundary, presence of aboveground features, etc. At these sites, it may take many years to see a clean groundwater front emerging on the downgradient side of the PRB. In the meantime, it would be difficult to determine whether any observed downgradient contamination is due to diffusion of contaminants persisting in fine-grained layers in the downgradient aquifer or due to flow bypass or breakthrough. Breakthrough can often be addressed by monitoring the groundwater immediately inside the downgradient edge of the reactive cell in the PRB. On the other hand, flow bypass could be more challenging to identify. The monitoring strategies in Section 8.1.3 often were recommended by regulators in an effort to obtain early warning of any impending failures, and are probably the best approach possible, given the limitations described above.

One contingency approach that has not been considered so far, probably because of lack of sufficient research on the subject, is regeneration of the reactive medium. Although some regeneration techniques, such as ultrasound and pressure pulsing, have been proposed, the field application of these techniques and the cost of their application needs further study.

8.1.3 Monitoring of a PRB after Installation. Some variation of the following monitoring strategies were recommended by regulators when reviewing PRB applications:

- Monitoring inside the reactive cell for potential breakthrough
- Monitoring for bypass at the two ends of the PRB
- Monitoring in the downgradient aquifer for breakthrough and verification that cleanup targets are met at the compliance boundary
- A monitoring well located close to the PRB in a potential bypass route
- Upgradient piezometers to detect short-term and/or long-term plugging of the PRB
- Monitoring of the permeable zone beneath the aquitard to verify absence of downward migration.

Although the combination of monitoring locations selected tended to vary among sites, the overall strategy inherent in these requirements focuses on potential routes of failure and has three features:

- Verify that the PRB is able to meet applicable cleanup targets at a downgradient compliance boundary. Interestingly, although the hope often was that the effluent from the PRB would be below MCLs or state-mandated cleanup levels or, in some cases, below detection, the overall goal was to meet cleanup targets at a compliance boundary that could be some distance downgradient. The cleanup targets were often MCLs, but were sometimes risk based.

- Desire to distinguish between possible failure due to breakthrough (reduced reactivity or reduced residence time) versus due to bypass (inadequate hydraulic capture). Implicit in this strategy was the desire to choose an appropriate contingency measure, that is, a contingency measure that would address the mode of failure. As an example, it would be futile to extend the ends of the PRB, if downgradient contamination was occurring due to breakthrough from the reactive medium.

- Desire for an early warning of impending failure. In the long term, the monitoring strategy seeks to identify potential loss of reactivity or potential loss of permeability before the downgradient water quality deteriorates significantly.

This is a well thought out monitoring strategy, but may be subject to the limitations of the monitoring tools available. As discussed in Section 8.1.2, for a new PRB installed inside the plume, it could be years before the cause of persistent downgradient contamination is determined. The longevity evaluation in the current project indicates that simple indicators, such as pH and ORP, may not be useful as early warning indicators; the reactivity of the iron in the long-term column tests continued to decline, even as the pH and ORP distribution in the column remained the same. Water level changes over the short distances involved when tracking flow through or around the PRB are often within the margin of error for the measurements, and therefore difficult to interpret. Direct flow measurements using sensors provide point estimates of flow velocity and direction; the point flow may not always match the bulk flow in the aquifer.

The regulatory agencies have taken some of the limitations of the monitoring tools into account. For example, the recommendation that monitoring wells evaluating potential flow bypass be placed as close to the PRB as possible, takes into account modeling results that show that the PRB's impact on the flow regime in the aquifer extends only a few feet from PRB. At the same time, regulators have refrained from making effective, but expensive, tools, such as tracer tests, mandatory, out of consideration for the economic impact on site owners. The ITRC also leaves it to the site owners and the local regulators to decide, on a site-specific basis, the types and frequency of various monitoring events (e.g., quarterly monitoring of target contaminants, but less frequent monitoring of geochemical parameters). The best approach is probably some combination of tools that, on a site-specific basis and with proper implementation (such as proper spacing of wells based on the hydraulic gradient at the site), provide the most information.

8.2 Future Regulatory Direction on PRBs

The main vehicle for future regulatory guidance on the PRB technology is the ITRC' Permeable Reactive Barrier Team. Although, the ITRC's guidance is not binding on the member or non-member States, the documents produced by the ITRC have been useful to both the State regulatory agencies and site owners preparing applications for PRB implementation at their sites. The two guidance documents produced by the ITRC are available through their website at www.itrcweb.org, and include:

- Regulatory Guidance for Permeable Reactive Barriers Designed to Remediate Chlorinated Solvents, 2nd Edition (December 1999)

- Regulatory Guidance for Permeable Reactive Barriers Designed to Remediate Inorganic and Radionuclide Contamination (September 1999) Pages 1-10 Pages 11-53

The ITRC continues to convene through telephone conference calls and periodic meetings. The ITRC also provides document review guidance and feedback from a regulatory perspective for key PRB evaluation projects, such as the current project.

9.0 Technology Implementation

This section discusses at the technology need and plans for transferring the results of the current project to potential end users.

9.1 DoD Need

There are no reliable estimates of the number of DoD or other sites with groundwater contaminated with chlorinated solvents. Given the prevalence of chlorinated solvent usage at Air Force, Navy, and Army bases for activities such as aircraft de-painting, ship repair, dry cleaning, automotive maintenance, parts degreasing, fire training, etc., such sites probably number in the thousands. In addition, there are numerous DoD sites with other groundwater contaminants, such as chromium or perchlorate, which are amenable to treatment with PRBs.

The primary challenge facing these sites is the need to keep operating pump-and-treat systems for the next several decades or centuries, as long as the persistent plumes of these contaminants last. A passive alternative, namely, a PRB, offers obvious advantages in terms of reduced O&M costs and more potential uses of the affected property.

9.2 Transition

The following actions are planned to transition the results of the current project to various stakeholders (site owners and their representatives, regulators, citizens' groups, etc.):

- The final report on the current project will be posted on the ESTCP and ITRC Web sites.

- The DoD, DOE, and U.S. EPA have also decided to prepare a summary report (20 to 30 pages) that outlines the results and conclusions of their respective studies. In addition, some input to this report will be provided by the ITRC. This summary report from the three agencies will be available for posting on various websites, such as those maintained by ESTCP, ITRC, and the U.S. EPA's Technology Innovation Office (TIO).

- The main project participants of the DoD project (Navy, Army, and Air Force) will distribute the final report to the Remedial Program Managers (RPMs) in their respective field divisions.

- The project team will seek to present the results of the current project in prominent public forums, such as the SERDP annual symposium in Washington, D.C., DOE's Containment Conference in Orlando, and the Third International Conference on Remediation of Chlorinated and Other Recalcitrant Compounds.

10.0 Summary of Results and Lessons Learned

The results and lessons learned from the evaluation of PRBs at several DoD sites are summarized in this section.

10.1 Longevity Evaluation

Longevity refers to the period over which a PRB continues to retain an acceptable level of reactivity and hydraulic performance. In the current project, longevity was evaluated primarily at two sites – former NAS Moffett Field and former Lowry AFB, which have groundwater containing moderate and high levels of dissolved solids, respectively. Dissolved solids, especially inorganic geochemical constituents of the groundwater, such as calcium and carbonates, can precipitate out under the strongly reducing conditions created by the iron medium. These precipitates can potentially coat the reactive surfaces of the iron and reduce its reactivity. In addition, water itself can be reduced by iron to form hydrous iron oxides, which potentially cause passivation of the iron. Both PRBs were installed five or more years ago and have been exposed to groundwater flow over this period. The following monitoring tools were used to evaluate longevity at these two sites:

- Sampling and analysis of groundwater influent to and effluent from the PRB to evaluate loss of geochemical groundwater constituents.

- Sampling and analysis of iron cores from the two PRBs. In addition, silt was collected from the silt traps in monitoring wells in the iron to analyze the deposits that were either formed in the vicinity of these wells or had been transported by advective flow from the upgradient direction.

- Accelerated long-term column tests to establish a direct link between period of exposure of the iron to groundwater and the reactivity of the iron. The same iron and groundwater used at the former NAS Moffett Field and former Lowry AFB were used in the columns.

- Geochemical modeling to evaluate possible reactions and products contributing to the loss of reactivity of the iron

The results of the longevity evaluation indicate that the reactivity of the iron deteriorates progressively over time with exposure to groundwater. The results of the longevity evaluation can be summarized as follows:

- At former NAS Moffett Field, TCE, PCE, and cis-1,2 DCE in the effluent from the reactive cell iron continues to be below their respective MCLs and below detection. Most of the treatment occurred in the upgradient half of the iron. A noticeable clean groundwater front is not clearly identifiable in the downgradient aquifer, although there are some preliminary signs that it could occur in the

future. After five years of PRB operation in the sand channel enclosed by silty clay sides, it was expected that introduction of CVOC-free groundwater effluent would lead to a noticeable improvement in downgradient groundwater quality, despite some contrary site conditions. One or more of the site conditions that could be acting to delay or prevent an improvement in downgradient groundwater quality are:

- Less groundwater flowing through reactive cell or gate than is predicted, or some water that may be flowing around or below the PRB. A best guess of the amount of water that has flowed through the PRB in the five years since installation is 200 pore volumes (based on a representative residence time estimate of 9 days in the iron). In some wells screened at shallower depths, a proportionate relative decline in CVOC and inorganic constituents (e.g., calcium) is noticeable over time, which would support this scenario. CVOC levels have declined somewhat over time in the upgradient aquifer too, making the determination more difficult.
- Recontamination of cleaner groundwater effluent from the PRB with contaminated groundwater flowing under the PRB (the pilot-scale PRB intentionally was not keyed into the clay layer for fearing of breaching a thin aquitard) or from the lower aquifer zone. The downgradient monitoring wells that are screened at a depth near the base of the PRB continue to be the most contaminated, indicating that there is underflow. However, vertical gradients that were upward in the vicinity of the PRB before PRB installation have consistently turned downward after the installation; this would tend to reduce the mixing of groundwater flowing under and through the PRB.
- Contaminated groundwater flowing around the funnel walls of the pilot-scale PRB that was designed to capture only a small part of a regional plume. This is less likely because the sand channel, which probably accounts for most of the groundwater flow in the local region of the PRB, directs flow mostly through the gate. The funnel walls encounter minimal additional groundwater flowing through the silty-clay deposits around the channel.
- Diffusion of CVOCs trapped in the silty clay layers surrounding the sand channel. This type of contaminant persistence has been observed at other sites, even with pump-and-treat systems. However, diffusion is a slow process and water quality improvement immediately downgradient of the PRB would still be expected.

- At former Lowry AFB, TCE, cis-1,2 DCE, and trans-1,2 DCE were treated to below MCLs and below detection in the upgradient half of the reactive cell iron. This indicates that, given sufficient residence time, not only the primary contaminants, but also the reduction byproducts can be treated by iron to below detection. At this site too, a noticeable clean groundwater front was not visible on

the downgradient side of the PRB, after four years of operation. Possible reasons include:

- Mixing of the PRB effluent with contaminated groundwater flowing around the pilot-scale PRB installed inside the plume to capture only part of the plume.
- Less groundwater flowing through the more conductive reactive cell or gate than predicted or than may be flowing around the PRB.

- Most of the dissolved calcium, iron, magnesium, sulfate, nitrate, and silica in the groundwater flowing through the PRB at former NAS Moffett Field were removed. Levels of alkalinity and total dissolved solids were considerable reduced. These constituents are likely to have precipitated out in the PRB. The groundwater pH rose from 7.0 to 10.9 and the ORP dropped from 134 to –821 mV in the iron. These trends are consistent with previous monitoring events conducted after the PRB was installed. There is no sign that the pH or ORP conditions in the reactive cell are being carried over into the downgradient aquifer. However, some of the shallower downgradient wells located just two feet from the downgradient edge of the PRB are showing some signs of decline in levels of inorganic constituents, such as calcium and alkalinity, indicating the effects of treated groundwater emerging from the reactive cell.

- At former Lowry AFB, most of the dissolved calcium, iron, magnesium, manganese, nitrate, and dissolved silica were removed from the groundwater flowing through the reactive cell. Levels of alkalinity, sulfate, and dissolved solids were considerably reduced. The groundwater pH rose from 6.9 to 11.5 and ORP dropped from –13 to –725 mV in the iron. These trends are consistent with trends seen in previous monitoring events. There were no signs that any of the geochemical changes in the reactive cell were being transmitted to the downgradient aquifer; a downgradient well, about 5 ft away from the PRB, had the same geochemical constitution as the upgradient groundwater, indicating that any contribution of the treated water emerging from the PRB was overwhelmed by groundwater flowing around the PRB.

- At former NAS Moffett Field, geochemical analysis of iron cores from the PRB showed the following:

  - Calcium, silicon, and small amounts of sulfur were the elements identified on the iron particles.
  - Aragonite, calcite (both forms of calcium carbonate), and iron carbonate hydroxide (similar to siderite) were the mineral species identified on the iron particles.

- Most of these minerals were concentrated in the iron samples collected from the upgradient edge of the reactive cell, indicating that the rest of the iron had not encountered much precipitation. A best guess estimate of 200 pore volumes of groundwater may have flowed through the iron at this site; as indicated by the accelerated column tests, at this age the iron still has not encountered any noticeable effects from precipitation.

- Calcite, iron oxyhydroxide (FeOOH) or goethite, ettringite (calcium-aluminum sulfate), and katoite (calcium-aluminum silicate) were the mineral species identified in the silt from the silt traps in the monitoring wells in the PRB at former NAS Moffett Field. The elements iron and magnesium were identified in the silt, but could not be associated with any particular mineral species. Some mineral species (such as feldspar, muscovite, mica and clay minerals) that probably originated from the pea gravel (granite) were also identified. The presence of minerals in the silt traps that are traceable to the groundwater indicates that not all the precipitates formed deposit on the iron medium. Finer, colloidal particles can be transported by the flow to other locations within the PRB, some of which become trapped in the monitoring wells.

- Iron oxyhydroxide (goethite) and silica were the main minerals traceable to the groundwater that were found on the iron cores from the upgradient edge of the reactive cell at former Lowry AFB. Surprisingly, no calcium or carbonate was detected on the iron core samples analyzed. This finding is in marked contrast to the results of the column test simulation using Lowry site groundwater and Master Builder iron, where two forms of calcium carbonate were detected throughout most of the column. The disparity in these results could be due to extremely slow groundwater movement in the Lowry field barrier, which would have caused any little precipitation that may have occurred to take place in the most upgradient portion of the iron that may not have been adequately represented in any of the cores samples taken. A best guess of the amount of water flowing through the Lowry AFB site is 60 pore volumes in the four years from installation to this sampling event (based on a representative residence time estimate of 25 days in the iron). Therefore, although the groundwater at Lowry AFB has higher dissolved solids levels, the amount of groundwater that the iron has been exposed to probably is relatively low.

- In terms of mass and vertical thickness of deposits in the wells, less silt was found in the monitoring wells at former Lowry AFB than at former NAS Moffett Field, even though the silt traps at Moffett Field had been flushed periodically. A minor amount of rankinite (calcium silicate), though tentatively identified, was the only mineral traceable to a precipitation reaction within the barrier . The groundwater at Lowry AFB is particularly high in dissolved solids, especially sulfate, alkalinity, and calcium. It is surprising that no signs of precipitates associated with these constituents were found on the iron medium or in the monitoring well

silt. Once again, the column test results differed from the field measurements in that sulfur was detected on the iron medium used in the column test. Similarly, one possible explanation for this is that the groundwater flow through the PRB is much less than predicted.

- Microbiology results, based on PLFA profiles, from the Moffett Field reactive cell and adjacent aquifer showed a predominance of Gram-negative bacteria, indicating that highly adaptable bacterial communities were present. These results also showed that the aquifer soil downgradient of the Moffett Field PRB had a less diverse microbiological community than the soil upgradient of the PRB. Furthermore, the upgradient soil contained a high proportion of biomarkers indicative of metal-reducing bacteria, whereas no such markers were detected in the downgradient soil. Total cell mass was highest in the upgradient soil and lowest in the downgradient soil; the cell mass in the iron cell was between these extremes. PLFA analysis of the iron samples indicates that different bacteria contributed to the anaerobic Gram-negative populations in these samples. The iron samples contained proportionally five times less the amount of a biomarker for sulfate reducing bacteria than the upgradient soil. Altogether, these results may be indicating that the microbial community is still becoming acclimated to conditions inside the PRB. No significant buildup of microbial populations was visible on the iron itself.

- Samples of iron from the Lowry PRB too contained a highly diverse microbial communities composed primarily of Gram-negative bacteria. However, some iron samples were composed mainly of eukaryote PLFA or had equal distributions of eukaryotes and normal saturated PLFA. The Gram-negative communities were in a stationary phase of growth and did not show signs of environmental stress.

- Geochemical modeling was used to predict a likely sequence of mineral precipitation events, based on groundwater responses to changes in pH and ORP in the presence of zero-valent iron. Four separate scenarios were run with the following possible phases common to each run: calcite, magnesite, brucite, ferrous hydroxide, and tobermorite. In each of the four scenarios, one or more of the following minerals were allowed to form: siderite, mackinawite; marcasite, and magnetite. All four scenarios predicted changes in pH and ORP that were similar to those observed in the field or laboratory column tests. Also, all four scenarios predicted declines in inorganic species in the groundwater, but at somewhat different proportions. When iron corrosion rate data from available literature were used to predict precipitation rates, the model predictions matched the trends in groundwater chemistry in the Moffett Field barrier for all major species except dissolved silica. The reason for failing to predict silica loss in the barrier was that the likely silica-controlling phase is not known, although thermodynamic data for such a phase may not be available anyway. However, the

published iron corrosion rate data are much too slow to model the changes occurring during short residence times inside the columns. Despite providing ample indication of the types and quantities of precipitates formed in the PRB, groundwater monitoring, iron core analysis, and geochemical modeling provided no links between time and reactivity of the iron, as it was unclear how these precipitates affected the reactivity of the iron in the long-term. To establish some preliminary links between period of exposure to groundwater and potential loss of reactivity of the iron, long-term accelerated column tests were conducted with the same groundwater and iron as from the field PRBs at former NAS Moffett Field and former Lowry AFB.

- The two columns were adjusted to a flow rate whereby pH and ORP reached a plateau (indicating that majority of the reactions between the iron and groundwater had occurred in the column), but was fast enough that many pore volumes of groundwater could be passed through the column (or many years of PRB operation could be simulated). After some trial-and-error, a flow rate of 12.5 ft/day was eventually established as optimum for the column test. At this flow rate, all the precipitates generated stayed in the column (at higher flow rates, there was a tendency for finer precipitates to be transported out with the flow. If a representative normal flow rate of 0.5 ft/day is assumed at both sites, than the flow in the columns is accelerated 25 times. The 1,300 pore volumes of groundwater passed through each column and the 1.5 years of column testing represented approximately 25 to 30 years of operation in the field PRBs. A related test conducted with the same columns showed that the TCE half-life was independent of the flow rate over a wide range of flow rates.

- The column tests show that over the 1,300 pore volumes of flow that the iron was exposed to, the half-life of TCE increased approximately by a factor of 2 in the Moffett Field column and by a factor of 4 in the Lowry AFB column. While some effects of aging may be intrinsic to the iron, itself, or to the manufacturing process, other differences may be due to the inorganic content of the water and the subsequent precipitation of dissolved solids. Former NAS Moffett Field has groundwater with a moderate level of dissolved solids and former Lowry AFB has groundwater with relatively high levels of dissolved solids; consequently, Lowry AFB showed a greater decline in reactivity over the same period of exposure to groundwater as the Moffett Field column.

- The mechanism for the loss of TCE reactivity is not known with certainty. However, it does appear from the column testing that iron in both column tests lost reactivity fairly uniformly, rather than developing a front of inactivated iron that progressively migrates along the length of the column. One reason for the uniform change in reactivity may be deposition of non-electrically conductive coatings on the iron grains, such as calcium carbonate, amorphous silicates, sulfide and sulfate minerals, and ferrous hydroxide. Because of the accelerated

flow rate in the columns, these precipitates were distributed along a longer distance than would normally occur in a field barrier. However, it is important to note that ferrous hydroxide can form by reaction of water with iron, even if the water has no ionic content. So, for example, if a barrier is very thick or if water moves through very slowly, most of the ionic content of the water will be scrubbed out near the influent end, leaving water with low ionic content in a downgradient portion of the barrier. In this downgradient portion of the barrier, corrosion by hydrogenolysis may still occur at a fixed rate and the iron may become coated by ferrous hydroxide.

- An explanation for the decrease in reaction rate of iron is that non-conductive coatings inhibit the beta-elimination pathway, where TCE is converted to ethene and ethane following a transition state that involves creation of an acetylene-based molecule. Due to the complexity of the process and number of electrons that must be involved, the probability of forming the acetylene transition state may decline as the coating thickness increases. However, since the pH and ORP do not seem to be much affected by aging of the iron, it seems that reduction of water continues as it did prior to aging. This could indicate that TCE and other chlorinated ethenes could continue to be reduced by a simpler mechanism, such as the hydrogenolysis pathway, which is known to occur, but which is also a slower and less efficient reaction than beta-elimination. In addition to a reduced rate of TCE degradation, one consequence of the hydrogenolysis pathway replacing beta-elimination as the dominant degradation mechanism is that byproducts such as DCE and VC would be produced in greater quantity. If this supposition is correct, then TCE half-lives would not become infinitely long as predicted by the exponential decline in reaction rate described in the column test results. Rather, TCE half-lives would migrate from a predominantly beta-elimination process to one that is predominantly driven by hydrogenolysis.

- One practical consequence of declining degradation rate while hydrogenolysis is still occurring is that measurement of pH and ORP may not be indicative of declining performance. Thus, these simple measurements may not be useful tools for predicting the long-term decline of a barrier.

- The pH and ORP distribution in the two columns remained relatively constant once the test flow rate of 12.5 ft/day was established in the columns, even though the reactivity of the iron declined. This indicates the following:

    - The geochemical constituents of the groundwater *do* affect the reactivity of the iron upon long-term exposure to groundwater.
    - The rate of decline in iron reactivity over time is dependent on the native level of dissolved solids in the groundwater.

- The PRB is likely to be passivated before the entire mass of zero-valent iron is used up, unless some way of regenerating or replacing the reactive medium is developed and implemented.

- The porosity and permeability of the iron (and hence the residence time) was not considerably affected over the duration of the test, as indicated by a tracer test conducted in the column after 1,300 pore volumes of flow. Therefore, the reactive performance of the iron is likely to decline much faster than any potential decline in long-term hydraulic performance.

- The progressive decline in iron reactivity over time indicates that the residence time required to meet groundwater cleanup targets also will be progressively higher in the long term. One way of ensuring that sufficient residence time is available in the future is to incorporate a higher safety factor in the currently designed flow-through thickness of the reactive medium in the PRB. Therefore, there is a tradeoff between current cost and future PRB performance.

10.2 Hydraulic Performance Evaluation

The hydraulic performance of a PRB is related to its achievement of the desired groundwater capture zone and residence time in the reactive medium. In the current project, hydraulic performance was evaluated in detail at four sites:

- Former NAS Moffett Field
- Former Lowry AFB
- Seneca Army Depot
- Dover AFB.

In addition, the progress of a separate evaluation project at former NAS Alameda was tracked for related features of interest. The following tools were used to evaluate hydraulic performance:

- Water level measurements
- HydroTechnics™ in-situ flow sensors
- Colloidal borescope

In addition, the use of tracer tests and down-hole flow sensors at former NAS Moffett Field in a separate project was tracked for related features of interest. The results of the performance evaluation indicated the following:

- At former NAS Moffett Field, water level measurements indicated that the PRB continues to capture groundwater from an approximately 30 ft-wide zone that extends about halfway across each funnel wall. The estimated groundwater velocity range at the site is 0.0017 to 19.0 ft/day, with 0.7 ft/day being a representative velocity based on the most common value. A representative residence time in the 6-foot thick reactive cell is probably 9 days, which is similar

to the time taken by a tracer to traverse the thickness of the iron during a previous project. The wide range of hydraulic conductivities and, consequently, the wide range of possible groundwater velocities at this site increase the uncertainty of the residence time estimates. The wide range reflects the layered setting at the site with most of the flow occurring through the sand channel (higher conductivity and higher velocity) and some flow occurring through the silty clay deposits (lower conductivity and lower velocity). The upgradient pea gravel homogenizes the flow to a great extent before it enters the iron. There is no clear evidence of a clean front emerging in the downgradient aquifer, but contaminant and geochemical groundwater data do show signs of treated water effluent from the PRB. A representative residence time of 9 days would indicate that approximately 40 pore volumes of groundwater per year (approximately 200 pore volumes over 5 years) have flowed through the PRB and mixed with groundwater flowing around and under the PRB. Of all the sites examined in the current project, flow conditions could most definitively be identified at this site, probably because of the constrained flow through the sand channel.

- At former Lowry AFB, water level measurements indicated that the PRB continues to capture groundwater from an approximately 20 ft-wide zone that is upgradient of the gate and extends across the western funnel wall. Most of the flow upgradient of the eastern funnel wall moves to the stream flowing on the east. Therefore, the PRB is probably capturing the desired numerical volume of groundwater, but not the targeted volume. The estimated groundwater velocity range at the site is 0.013 to 0.36 ft/day, with 0.2 ft/day being a representative velocity based on the most common value. A representative residence time in the 5-foot thick reactive cell is probably 25 days, although a range of residence times from 14 to 385 days is possible. The wide range of hydraulic conductivities and, consequently, the wide range of possible groundwater velocities at this site increase the uncertainty of the residence time estimates. A representative residence time of 25 days would indicate that approximately 15 pore volumes of water per year (or 60 pore volumes over the four years since installation) had flowed through the PRB, at the time of sampling in 1999. Two HydroTechnics™ in-situ flow sensors and the colloidal borescope (down-hole instrument) were tested at Lowry AFB, but the flow velocity and direction indicated by these probes did not always match the flow predicted by water level measurements. The differences between the two types of measurements may be the difference between bulk flow (water levels), on the one hand, and localized (HydroTechnics™ sensor) or preferential (colloidal borescope) flow on the other.

- At Seneca Army Depot, a flow divide was not clearly discernible at the northern end of the PRB (the only end of the long PRB that was adequately monitored). Water level maps indicate that the flow divide (or capture zone limit) is somewhere close to the end of the continuous reactive barrier. The estimated groundwater velocity range at the site is 0.011 to 7.0 ft/day, with 0.8 ft/day being

a representative velocity based on the most common value. A representative residence time in the 1-foot thick reactive cell is probably 1 day, which is similar to the time taken by a tracer to traverse the thickness of the iron during a previous project. The wide range of hydraulic conductivities and, consequently, the wide range of possible groundwater velocities at this site increase the uncertainty of the residence time estimates. A representative residence time of 1 day would indicate that approximately 365 pore volumes of water per year are flowing through the PRB.

- At Dover AFB, the challenge in evaluating flow was the extremely low gradient. Some capture of groundwater was discernible during certain water level measurement events, but during many events, water levels were relatively flat throughout the area of interest. HydroTechnics™ and colloidal borescope measurements were not always in agreement with water level measurements in indicating flow. Again, the difference may lie in the difference between bulk flow and localized or preferential flow. Groundwater velocity and residence time estimates vary over a wide range.

- At former NAS Alameda, a separate project showed that a previously undiscovered highly concentrated sliver of the plume was causing unexpectedly high CVOC concentrations to appear in the effluent from the iron portion of the PRB (residence time in the iron was not sufficient to handle the higher concentration). This sliver remained undiscovered until an original comprehensive characterization with longer-screen wells was supplemented by an intensive matrix of depth-discrete monitoring points. This indicates that even with relatively comprehensive characterization, plume or geologic uncertainties could affect the adequacy of the installed PRB, and future modifications or contingencies may be necessary. Some of this uncertainty can be minimized by obtaining good horizontal and vertical spatial coverage during characterization of the geology and plume.

- In general, at none of the DoD sites monitored during the current project, was there any evidence of any gross hydraulic failures. There was no persistent mounding of water levels that would be indicative of PRB plugging, a major initial concern with PRBs. Some flow problems such as flow bypass around the eastern funnel wall at Lowry AFB caused by an adjacent stream and inadequate residence time at former NAS Alameda were identified with available monitoring tools and could be avoided at future PRB sites with proper characterization and flow modeling. At many DoD sites though, the challenge was in using available tools to show more conclusively that flow was progressing as designed. Factors that created this challenge include:

    - Inability to discern flow based on water levels that were relatively flat over the area of interest

- Propensity of direct measurement tools (flow sensors) to measure localized or preferential flow, rather than bulk flow
- Sometimes conflicting results from different flow measurement tools (e.g., water levels and flow sensors)
- Absence so far of a clearly noticeable clean groundwater front emerging from PRBs that had been installed inside the plume at DoD sites.
- Highly variable hydraulic conductivity distribution at many sites, even ones recognized as being relatively sandy and homogeneous, and the consequent uncertainty in groundwater velocity and residence time estimates.
- Seasonal variations in flow velocity and direction.

10.3 Summary of Recommendations

- The geochemical composition of the groundwater at a prospective PRB site should be determined during site characterization. When designing the flow through thickness of the reactive cell, an appropriate safety factor should be applied to increase the thickness of the reactive cell to account for future decline in reactivity of the medium. The magnitude of the safety factor is a matter of professional judgment and should be determined on the basis of:
  - The dissolved solids level in the groundwater. In general, groundwater may be classified as containing low- (<500 mg/L), moderate- (500 to 1,000 mg/L), and high- (>1,000 mg/L) dissolved solids levels. A higher dissolved solids level would merit a higher safety factor.
  - The best understanding of groundwater flow velocity and residence time that the PRB is expected to achieve. The age (longevity) of the reactive medium may be better expressed in terms of the number of pore volumes of groundwater that the PRB is likely to be exposed to than absolute time (number of years).
  - The tradeoff between increased capital investment (in a thicker PRB) versus shorter useful life. The present value method can be used to determine breakeven points under different longevity scenarios. At many sites, unless the PRB is particularly long, adding extra thickness to a PRB may involve a less-than-proportionate increase in cost, because mobilization and demobilization of the construction equipment and operators generally is the major (fixed) cost of construction.
- Once the PRB has been installed, the frequency of monitoring to verify longevity should be determined on the basis of the best understanding of groundwater velocity. For groundwater velocities of 1 ft/day or less, which would include most sites, the rate of change in reactivity observed in the accelerated column

tests makes it unlikely that a monitoring frequency of less than one year would be necessary for early indication of declining reactivity.

- Adequate characterization of a prospective site for PRB application would involve the following elements:

  - Determination of the horizontal and vertical spatial distribution of geologic media and contaminants in the immediate vicinity of the proposed PRB.
  - Determination of the spatial distribution of hydraulic conductivity and gradients in the immediate vicinity of the proposed PRB.
  - Determination of seasonal variations (at least four quarters) in hydraulic gradients and, consequently, flow velocity and direction.

- When defining groundwater flow in the vicinity of the proposed PRB, a monitoring network consisting of wells screened at uniform depths should be used, as much as practically possible. Water level measurements, when properly conducted, still are the best indicators of bulk flow through the aquifer.

- The selective use of flow sensors to obtain direct groundwater flow velocity and direction measurements may be considered to define localized or preferential flow at particularly heterogeneous sites, in order to supplement water level data, if desired. Tracer tests, when successful can provide the most definitive estimate of flow at most sites; however, tacter tests are more resource intensive and may be feasible only for demonstration projects.

- Hydrogeologic modeling of the flow regime before and after installation of the PRB to simulate the known variability in hydraulic conditions at the site and any judged uncertainties. The variability and uncertainty can be incorporated in the design with appropriate safety factors, while considering the tradeoff between increased PRB dimensions and the risk of sub-optimal hydraulic performance of the PRB. A suitable orientation, configuration, and dimensions of the PRB can be determined with these considerations.

- The hydraulic effects of neighboring features, such as flowing streams, irrigation, or pump-and-treat systems should be monitored. If the effects of these features cannot be directly measured, they sometimes can be simulated through modeling.

- Most of the above recommendations relate to pre-construction efforts. A PRB is a relatively fixed installation and once installed, changes could be costly. Also, because of the limitations of various monitoring tools, sub-optimal performance of the PRB and its causes may not be discovered for many years. Therefore, most of the precautions need to be taken in the design stage. Monitoring of the PRB after construction provides verification of performance (and compliance) and may

be more useful as a tool to develop appropriate modifications or contingency measures, if required, to restore the reactivity or hydraulic performance in the future.

- Although, pH and ORP are useful short-term indicators of reactive medium effectiveness and flow stability, they may not be useful as early-warning indicators of declining reactivity.

- A time series of measurements of C/C_0, the ratio of contaminant concentrations at two fixed points, one in the upgradient aquifer (C_0) and one in the reactive cell (C), may provide a better indication of a significant decline in reactivity, after taking into account seasonal variations in influent plume concentrations.

- With most PRBs likely to be located inside the plume boundary, at many sites, it may be several years before a noticeable decline in contaminant concentrations is observed at a downgradient compliance point, as indicated by the difficulty in discerning a clean front emerging from various existing PRBs. However, if all other indicators of performance are acceptable, it may be important to persevere until signs of improvement in downgradient groundwater quality are observed. This may be true not just of PRBs, but other containment type measures, such as low-extraction rate pump-and-treat systems, also. It may be important to determine, through monitoring and understanding of the site, possible causes of persistent downgradient contamination, in order to allay regulatory concerns.

- Continued use of water level measurements probably is the best way to verify flow through the PRB, in terms of capture zone and residence time. Selective use of direct flow measurement sensors could be considered to obtain further definition of flow, if necessary.

- Although the technology has come quite far in a relatively short time, further research may be desirable in the following areas:

    - Better understanding of the rate and mechanisms of loss of reactivity of the reactive medium (in many cases, iron)
    - Development of methods for in-situ regeneration of the reactive medium.
    - Better monitoring tools or better use of existing tools to adequately define the hydraulic flow regime over the short distances involved in PRB applications
    - Better definition of the use of safety factors and the tradeoffs between future performance and current cost of PRB applications.

11.0 References

Andromalos, K.B., B.H. Jasperse, and R.M. Schindler. 1999. *Current State of the Art Installation Techniques for In-Situ Reactive Wall Groundwater Treatment Systems.* GeoCon Publication #99-423.

Arnold, W.A., and A.L. Roberts. 2000. "Inter- and Intraspecies Competitive Effects in Reactions of Chlorinated Ethylenes with Zero-Valent Iron in Column Reactors." *Environ. Eng. Sci., 17*: 291-302.

Ballard, S. 1996. "The In-Situ Permeable Flow Sensor: A Ground-Water Flow Velocity Meter." *Groundwater, 34*(2): 231-240.

Battelle. 1995. *Solute Transport Code Verification Report for RWLK3D.* Internal Draft.

Battelle. 1997. *Design/Test Plan: Permeable Barrier Demonstration at Area 5, Dover AFB.* Prepared for Air Force Research Laboratory, Tyndall AFB, FL. November 14.

Battelle. 1998. *Performance Evaluation of a Pilot-Scale Permeable Reactive Barrier at Former Naval Air Station Moffett Field, Mountain View, California.* Prepared for NFESC, Port Hueneme, CA. November 20.

Battelle. 1999. *Permeable Reactive Barriers Survey Report.* Prepared for NFESC, Port Hueneme, CA. November 19.

Battelle. 2000a. *Design, Construction, and Monitoring of the Permeable Reactive Barrier in Area 5 at Dover Air Force Base.* Final. Prepared for Air Force Research Laboratory, Tyndall AFB, FL. March 31.

Battelle. 2000b. *Annual 1999 Progress Report.* Prepared for NFESC, Port Hueneme, CA. January.

Battelle. 2000c. *Recommendations for Modeling the Geochemical and Hydraulic Performance of a Permeable Reactive Barrier.* Prepared for NFESC, Port Hueneme, CA.

Battelle. 2000d. *Monitoring Plan for the Evaluation of Permeable Reactive Barriers at Multiple Department of Defense Sites.* Prepared for NFESC, Port Hueneme, CA; project funded by ESTCP and SERDP. June 19.

Bouwer, H. 1989. "The Bouwer and Rice Slug Test—an Update." *Ground Water, 27*(3): 304-309.

Bouwer, H., and R.C. Rice. 1976. "A Slug Test for Determining Hydraulic Conductivity of Unconfined Aquifers with Completely or Partially Penetrating Wells." *Water Resources Research, 12*(3): 423-428.

Bradford, D., and N. Dave. 2001. Personal communication to Battelle from Douglas Bradford and Narendra Dave. April 30.

Cange, J. 2000. *Installation of a Permeable Reactive Wall at Pease Air Force Base Using the Biopolymer Slurry Technique.* Summary of the Remediation Technologies Development Forum Permeable Reactive Barriers Action Teem Meeting in Melbourne, FL. February 16-17, 2000.

Dana, W. 2001. Personal communication to Battelle from William Dana, Oregon Department of Environmental Quality. April 30.

Day, S.R., S.F. O'Hannesion, and L. Marsden. 1999. "Geotechnical Techniques for the Construction of Reactive Barriers." *Journal of Hazardous Materials, 67*(3): 285-297.

Devlin, J.F., and J.F. Einarson et al.,. 1999. "Field Demonstration of Permeable Wall Flushing for Biostimulation of a Shallow Sandy Aquifer." *Ground Water Monitoring and Remediation, 19*(1): 75-83.

Einarson, M.D., R.L. Langdon, and J.F. Einarson et al.,. 2000. *Hydraulic Performance of a Funnel-and-Gate Treatment System in a Shallow Tidally-Affected Aquifer.* Prepared for NFESC, Port Hueneme, CA. January.

Fort, J.R. 2000. "Physical Performance of Granular Iron Reactive Barriers under Aerobic and Anoxic Conditions." M.S. Thesis, University of Wisconsin, Madison, WI.

Gavaskar, A.R., N. Gupta, B. Sass, R. Janosy, and J. Hicks. 2000. *Design Guidance for Application of Permeable Reactive Barriers for Groundwater Remediation.* Prepared for the Air Force Research Laboratory, Tyndall AFB, FL. March 31.

Génin, J.-M.R., A.A. Olowe, P. Refait, L. Simon. 1996. TITLE. *Corr. Sci., 38*: 1751-1762.

GeoCon. 2001. *Technical Specification Bio-Polymer Slurry Drainage Trench Construction.* GeoCon Publication #ENG/TECHSPBP2.

Gupta, N., and T. Fox. 1999. "Hydrogeologic Modeling for Permeable Reactive Barriers." *Journal of Hazardous Materials, 68*: 19-39.

Hewitt, J. 2001. Personal communication to Battelle from James Hewitt, New Hampshire Department of Environmental Services. May 7.

Hsieh, P.H., and J.R. Freckelton. 1993. *Documentation of a Computer Program to Simulate Horizontal-Flow Barriers Using the U.S. Geological Survey's Modular Three-Dimensional Finite-Difference Ground-Water Flow Model.* U.S. Geological Survey Open File Report 92-477. 30 pp.

Johnson, T.L., M.M. Scherer, and P.G. Tratnyek. 1996. "Kinetics of Halogenated Organic Compound Degradation by Iron Metal." *Environ. Sci. & Technol., 30*: 2634-2640.

Kearl, P.M., N.E. Korte, and T.A. Cronk. 1992. "Suggested Modifications to Ground Water Sampling Procedures Based on Observations with the Colloidal Borescope." *Ground Water Monitoring and Remediation (Spring)*: PAGES.

Kearl, P.M. 1997. "Observations of Particle Movement in a Monitoring Well Using the Colloidal Borescope." *Journal of Hydrology (200)*: 323-344.

Mackenzie, P.D., D.P. Horney, and T.M. Sivavec. 1999. "Mineral Precipitation and Porosity Losses in Granular Iron Columns." *Journal of Hazardous Materials, 68*: 1-17.

Marra, K. 2001. Personal communication from Kenneth Marra, Massachusetts Department of Environmental Protection. April 30.

McDonald, M.G., and A.W. Harbaugh. 1988. *A Modular Three-Dimensional Finite Difference Ground Water Flow Model.* Techniques of Water Resources Investigations 06-A1, U.S. Geological Survey Open-File Report 83-875. 576 pp.

Odziemkowski, M.S., T.T. Schuhmacher, R.W. Gillham, and E.J. Reardon. 1998. "Mechanism of Oxide Film Formation on Iron in simulating Groundwater Solutions: Raman Spectroscopic Studies." *Corr. Sci., 40*: 371-389.

O'Hannesin, S.F. 1993. A Field Demonstration of a Permeable Reaction Wall for the In Situ Abiotic Degradation of Halogenated Aliphatic Organic Compounds. Unpublished M.S. thesis, University of Waterloo, Ontario, Canada.

Parkhurst, D.L., and C.A.J. Appelo. 1999. *User's Guide To PHREEQC (Version 2) - A Computer Program For Speciation, Batch-Reaction, One-Dimensional Transport, and Inverse Geochemical Calculations.* U.S. Geological Survey, Water-Resources Investigations Report 99-4259.

Parsons Engineering Science, Inc. 2000. *Draft Feasibility Memorandum for Groundwater Remediation Alternatives Using Zero Valent Iron Reactive Wall at the Ash Landfill, Seneca Army Depot Activity Romulus, New York.* Prepared for Army Corps of Engineers, Huntsville, AL.

Pollack, D.W. 1989. *Documentation of Computer Programs to Complete and Display Pathlines Using Results from the U.S. Geological Survey Modular Three-Dimensional Finite-Difference Groundwater Model.* USGS Open File Report 89-381. 81 pp.

PRC, see PRC Environmental Management, Inc.

PRC Environmental Management, Inc. 1996. *Naval Air Station Moffett Field, California, Iron Curtain Area Groundwater Flow Model.* June.

Puls, R.W., R.M. Powell, and C.J. Paul. 1995. "In Situ Remediation of Ground Water Contaminated with Chromate and Chlorinated Solvents Using Zero-Valent Iron: A Field Study." *Extended Abstracts from the 209th ACS National Meeting Anaheim, CA, 35*(1): 788-791. Anaheim, CA. Div. of Environ. Chem., Am. Chem. Soc., Washington, DC.

Reardon, E.J. 1995. "Anaerobic Corrosion of Granular Iron: Measurement and Interpretation of Hydrogen Evolution Rates." *Environ. Sci. Technol., 29:* 2936-2945.

Refait, P., and J.-M.R. Génin. 1994. TITLE. *Corr. Sci., 36:* 55-65.

Reinhart, D. 2000. *NASA PRB Installation Using Deep-Soil Mixing: Lessons Learned.* Summary of the Remediation Technologies Development Forum Permeable Reactive Barriers Action Teem Meeting in Melbourne, FL. February 16-17, 2000.

Remediation Technologies Development Forum. 2001. *Permeable Reactive Barrier Installation Profiles.* Available at http://www.rtdf.org/public/permbarr/prbsumms. Updated August 1.

Romer, J. 1998. *Installation of a Reactive Iron Permeable Barrier Using Continuous Trenching.* Summary of the Remediation Technologies Development Forum Permeable Reactive Barriers Action Teem Meeting in Beaverton, OR. April 15-16, 1998.

Sass, B., A. Gavaskar, W-S. Yoon, N. Gupta, E. Drescher, and C. Reeter. 2001. "Geochemical Investigation of Three Permeable Reactive Barriers to Assess Impact of Precipitation on Performance and Longevity." Proceedings of the International Containment & Remediation Technology Conference and Exhibition, Orlando, FL. June 12.

Scherer, M, B.A. Balko, and P.G. Tratnyek. 1999. "The Role of Oxides in Reduction Reactions at the Metal-Water Interface." In D.L. Sparks and T.J. Grundl (Eds.), *ACS Symposium Series 71g.*

Schikorr, G. 1929. TITLE. *Z. Elektrochim., 35:* 62-65.

Scherer, M.M., B.A. Balko, and P.G. Tratnyek. 1998. "The Role of Oxides in Reduction Reactions at the Metal-Water Interface." In D.L. Sparks and T.J. Gundl (Eds.), *ACS Symposium Series 715*. pp. 301-322.

Shultz, D.S., and R.C. Landis. 1998. "Design and Cost Estimation of Permeable Reactive Barriers." *Remediation, 9*(1): 57-57.

Sivavec, T. 2000. Personal communication with B. Sass, Battelle, by T. Sivavec, General Electric.

Stafford, T., and N. Dave. 2001. Personal communication to Battelle from Thomas Stafford and Narendra Dave, Louisiana Department of Environmental Quality. April 30.

Totten, L.A., U. Jans, and A.L. Roberts. 2001. "Alkyl Bromides as Mechanistic Probes of Reductive Dehalogenation: Reactions of Vicinal Dibromide Stereoisomers with Zero-Valent Metals." *Env. Sci. & Technol., 35*: 2268-2274.

Turner, M. 2001. Personal communication to Battelle from Matt Turner, New Jersey Department of Environmental Protection. April 10.

Versar, Inc. 1997. *Final Evaluation of Long-Term Performance Reactive Wall Demonstration Project. Prepared for Air Force Center for Environmental Excellence (AFCEE/ERB) Base Closure Restoration Division.* Prepared for Brooks AFB, TX. December.

WPI, See Worldwide Performance and Innovation.

Worldwide Performance and Innovation. 2001. "Geosiphon™ Goes With the Flow." *Initiatives Online, 8 (Spring).* WEB ADDRESS.

Yabusaki, S., K. Cantrell, B. Sass, and C. Steefel. 2001. "Multicomponent Reactive Transport in an In Situ Zero-Valent Iron Cell." *Environ. Sci. & Technol., 35*: 1493-1503.

Zapico, M.M., S. Vales, and J.A. Cherry. 1987. "A Wireline Piston Core Barrel for Sampling Cohesionless Sand and Gravel Below the Water Table." *Ground Water Monitoring Review*: 74-82.

Zheng, C. 1990. *MT3D: A Modular Three-Dimensional Transport Model for Simulation of Advection, Dispersion, and Chemical Reactions of Contaminants in Groundwater Systems.* S.S. Papadopulus and Associates.

Appendix A

Points of Contact

Appendix A
Points of Contact

Lead Agency Contact:	Charles Reeter Naval Facilities Engineering Service Center (NFESC) 1100 23rd Avenue, Code 411 Port Hueneme, CA 93043 Tel: (805) 982-4991; Fax: (-4304) E-mail: reetercv@nfesc.navy.mil
Battelle Project Manager:	Arun Gavaskar Battelle 505 King Avenue Columbus, OH 43201 Tel: (614) 424-3403; Fax: (-3667) E-mail: gavaskar@battelle.org
AFRL Project Manager:	Tim McHale Air Force Research Laboratory (AFRL) 139 Barnes Drive Tyndall AFB, FL 32403 Tel: (904) 283-6239; Fax: (-6064)
USACE:	Steve White U.S. Army Corps of Engineers (USACE) 12565 West Center Road Omaha, NE 68144 Tel: (402) 697-2660; Fax (-2673)
AFCEE Representative:	Robert Edwards Waste Policy Institute 100 N.E. Loop 410, Suite 1200 San Antonio, TX 78216
SERDP/ESTCP:	Andrea Leeson SERDP Program Office 901 North Stuart Street, Suite 303 Arlington, VA 22203 Tel: (703) 696-2118 E-mail: vogelc@acq.osd.mil
ITRC:	Matthew Turner New Jersey Department of Environmental Protection 401 E. State Street, CN028 Trenton, NJ 08625 Tel: (609) 633-0719; Fax: (-1454)

Appendix B

Data Archiving and Demonstration Plan

Appendix B
Data Archiving and Demonstration Plan

The data collected during this project and the demonstration plan (Battelle, 2000d) are archived with NFESC and Battelle. These data and documents can be obtained from the following:

Charles Reeter
NFESC
1100 23rd Avenue, Code 411
Port Hueneme, CA 93043
Tel: (805) 982-4991; Fax: (-4304)
E-mail: reetercv@nfesc.navy.mil

Arun Gavaskar
Battelle
505 King Avenue
Columbus, OH 43201
Tel: (614) 424-3403; Fax: (-3667)
E-mail: gavaskar@battelle.org

Appendix C

Geochemical Data

Appendix C-1

Moffett Microbial Report

microbial insights

2340 Stock Creek Blvd.
Rockford TN 37853-3044
Phone (865) 573-8188
Fax: (865) 573-8133
Email: microbe@microbe.com

Microbial Analysis Report

Client: Sam Yoon
Battelle
505 King Ave
Columbus, OH 43201

Phone: 614-424-4569

Fax: 614-458-4509

MI Identifier: 6bat **Date Rec.:** 5/17/01 **Report Date:** 6/14/01

Analysis Requested: PLFA

Project: Moffett

Comments:

NOTICE: This report is intended only for the addressee shown above and may contain confidential or privileged information. If the recipient of this material is not the intended recipient or if you have received this in error, please notify Microbial Insights, Inc. immediately. Thank you for your cooperation.

microbial insights

2340 Stock Creek Blvd.
Rockford TN 37853-3044
Phone (865) 573-8188
Fax: (865) 573-8133
Email: microbe@microbe.com

Microbial Analysis Report

Executive Summary

The microbial communities from 4 samples (Soil #1, Soil #2, IC-1, and IC-5) were characterized by phospholipid fatty acid content (PLFA Analysis). Results from this analysis revealed the following:

- Biomass content (as determined by the total concentration of PLFA) was similar in samples Soil # 1 and IC-1, whereas Soil # 2 had a much lower amount of biomass (by more than one order of magnitude).
- There were notable differences in community structure among all four samples. Soil # 2 differed the most from the other sample, due to a less diverse community structure.
- Evidence of anaerobic metal reducing bacteria were detected in Soil #1, IC-1 and IC-5 with the proportions of specific biomarkers suggesting marked differences in their bacterial makeup between Soil #1 and the iron samples.
- Biomarker ratios indicative of growth rates and environmental stress showed that the Gram-negative bacterial populations in the soil samples and IC samples differed in their responses to their environmental conditions.

Overview of Approach:

Phospholipid Fatty Acid (PLFA) Analysis

The analysis of microbial membrane lipids, specifically phospholipid fatty acids (PLFA), is an effective tool for monitoring microbial responses to their environment. Lipids are essential cellular components of the membrane of all cells and play a role as storage materials. The PLFA profiles simultaneously contain general information about the phylogenetic identity and physiological status of microbes. The microbial membrane reflects the nature of both the intracellular components and the extracellular environmental conditions. Thus, PLFA analysis tells us what types of microbes are present in a system and how they are reacting to environmental factors (e.g., pollution or disturbance). PLFA analysis is based on the extraction and separation of lipid classes, followed by quantitative analysis using gas chromatography/mass spectrometry (GC/MS). The individual fatty acids differ in chemical composition depending on the organism and environmental conditions. PLFA analysis provides quantitative insight into three important attributes of microbial communities: viable biomass, community structure, and metabolic activity.

Procedures:

PLFA analysis

Lipids were recovered using the modified Bligh and Dyer method [1]. Extractions were performed using one-phase chloroform-methanol-buffer extractant. Lipids were recovered, dissolved in chloroform, and fractionated on disposable silicic acid columns into neutral-, glyco-, and polar-lipid fractions. The polar lipid fraction was transesterified with mild alkali to recover the PLFA as methyl esters in hexane. PLFA were analyzed by gas chromatography with peak confirmation performed by electron impact mass spectrometry (GC/MS). PLFA nomenclature follows the pattern of A:BωC. The "A" position identifies the total number of carbon atoms in the fatty acid. Position B is the number of double bonds from the aliphatic (ω) end of the molecule. Position "C" designates the carbon atom from the aliphatic end before the double bond. This is followed by a "c" for *cis* or a "t" for *trans* configuration. The prefix "i" and "a" stand for *iso* and *anteiso* branching. Mid-chain branching is noted by "me," and cyclopropyl fatty acids are designated as "cy" (3). Example: 18:1ω7c is 18 carbons long with one double bond occurring at the 7th carbon atom from the ω end, and the hydrogen molecules attached to the doubly bonded carbon molecules are in the cis conformation.

Results and Discussion:

Biomass Content

Phospholipid fatty acids are found in the membranes of all living cells but decompose quickly upon cell death because cellular enzymes hydrolyze the phosphate group within minutes to hours of cell death (1). Thus, measuring the total amount of PLFA content provides a quantitative measure of the viable microbial biomass present.

For these samples, biomass content was similar between Soil #1 and IC-1 (~10^6 cells/g) all of which was essentially bacterial. Sample IC-5 had approximately 1/3 the amount of biomass detected in Soil #1 and IC-1. Biomass content in Soil #2 was very low, differing by more than an order of magnitude from Soil #1 (Figure 1, Table 2).

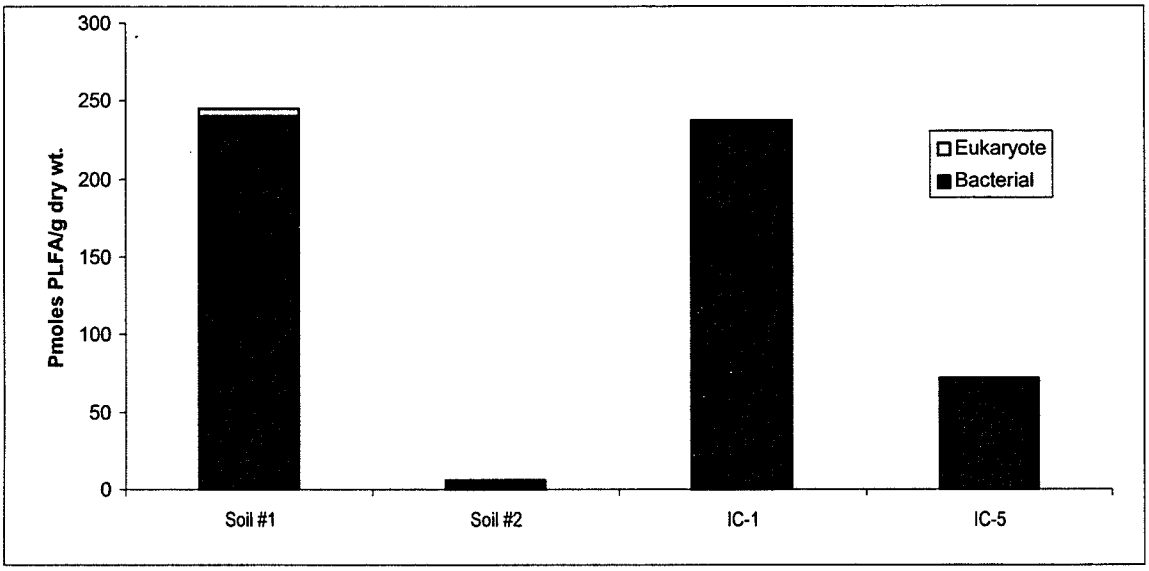

Figure1. Biomass content is presented as the total amount of phospholipid fatty acids (PLFA) present in a given sample. Bacterial biomass is calculated based upon PLFA attributed specifically to bacteria, whereas eukaryotic biomass is based on PLFA associated with higher organisms.

Community Structure

The PLFA patterns derived from environmental samples provide a quantitative profile of the microbial population, which accurately mirrors differences in community composition. Specific groups of microbes contain different fatty acid profiles, making it possible to distinguish between them (3-5). Table 1 describes the six major structural groups employed.

Table1. Description of PLFA Structural Groups.

PLFA Structural Group	General classification
Monoenoic (Monos)	Found in Gram-negative bacteria, which can be fast growing, utilize many carbon sources, and adapt quickly to a variety of environments.
Terminally Branched Saturated (TerBrSats)	Representative of Gram-positive bacteria, but also are found in the cell membranes of some Gram-negative bacteria.
Branched Monoenoic (BrMonos)	Commonly found in the cell membranes of obligate anaerobes, such as sulfate- or iron-reducing bacteria
Mid-Chain Branched Saturated (MidBrSats)	Common in Actinomycete, sulfate-reducing bacteria, and certain Gram-positive bacteria.
Normal Saturated (Nsats)	Ubiquitous in both prokaryotic and eukaryotic organisms though dominant fatty acids within this group will vary among organisms.
Polyenoic	Found in organisms such as fungi, protozoa, algae, higher plants, and animals.

PLFA profiles showed a predominance of Gram-negative bacteria in all four samples (indicated by percentage of monoenoic PLFA). Comparison of the two soil samples showed a noticeable difference between their community structures with soil #1 having a more diverse community composition (as define by the variety of PLFA detected). The most notable difference between the soil samples was high proportions of biomarkers indicative of metal-reducing bacteria (Figure 2) in soil #1 (no such markers were detected in Soil #2).

Specifically, high proportions of the mid-chain branched biomarker 10me16:0, which is prominent in sulfate reducing bacteria *Desulfobacter,* was detected in soil #1. Compared to the iron samples (IC-1 and IC-5) , soil #1 had proportionally about five times the amount of 10me16:0.

Although, both soil samples were primarily composed of Gram-negative bacteria (monoenoic PLFA); the proportions of fatty acids contributing to this structural group differed greatly. Effectively all of the fatty acids for this group in Soil #2 were derived from 18-carbon fatty acids whereas the biomarkers for Gram-negative bacteria were more evenly distributed within Soil #1.

The most notable difference between the iron samples comes from the amount of i17:1w7c, which was very prominent in the IC-1 sample. IC-1 also had the highest proportion of i15:0, whereas IC-2 had the highest proportion of a17:0. Again, these differences indicate different bacteria contributed to the anaerobic Gram-negative populations in these samples.

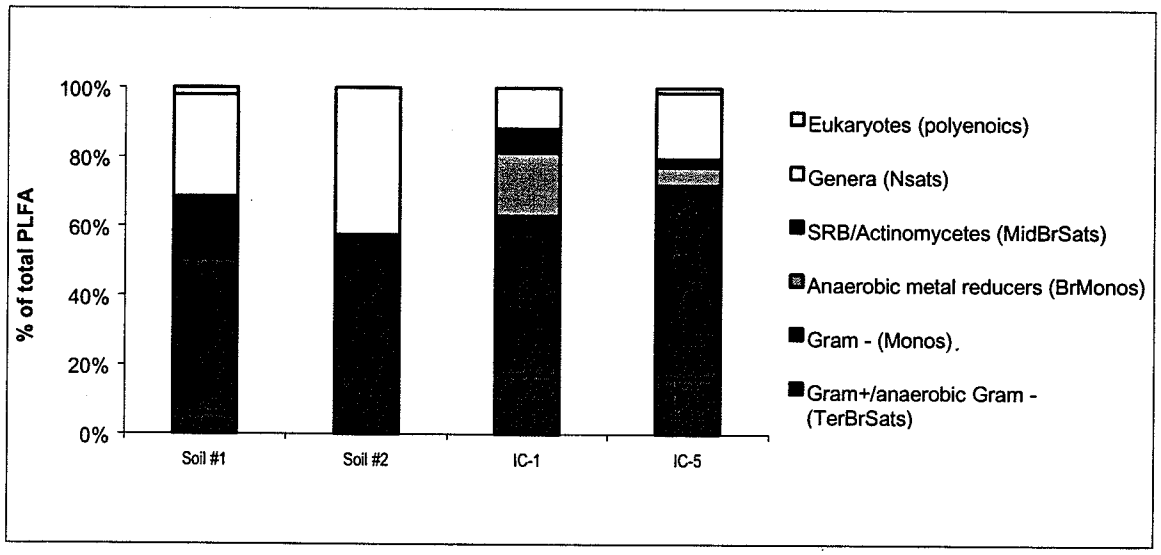

Figure 2. A comparison of the relative percentages of total PLFA structural groups in the samples analyzed. Structural groups are assigned according to PLFA chemical structure, which is related to fatty acid biosynthesis. See Table 1 for detailed descriptions of structural groups.

Profiles of individual fatty acids for each sample are available upon request.

Metabolic Activity

Lipid composition of microorganisms is a product of metabolic pathways and thus reflects phenotypic responses of the organisms to their environment. Knowledge of specific lipid biosynthetic pathways can provide insight into the metabolic activity of the microbial community because certain fatty acids provide indications of turnover rate and physiological responses to environmental conditions. Specifically, Gram-negative bacteria form cyclopropyl fatty acids (f.a.) (cy17:0 & cy19:0) preferentially over monoenoic f.a. (16:1w7c and 18:1w7c) as the turnover rate decreases.

Some Gram-negative bacteria preferentially synthesize 16-carbon f.a., while other preferentially synthesize 18-carbon fatty acids. These groups will be designated Group A and Group B, respectively. Although there is not always a difference in the way these bacterial groups respond to environmental conditions, they did respond differently in these samples. Group A organisms had much faster growth rates than the Group B bacteria in Soil #1 according to the f.a. ratios, in large part because of the very slow growth rates of the Group B organisms. Within soil #2 the Group B bacteria also showed slow growth, but still had faster rates than the same group in

Soil #1. Group A biomarkers were not even detected in Soil #2. The opposite trend was present in the iron samples (Figure 3), where the Group B bacteria had much faster growth rates than the Group A bacteria.

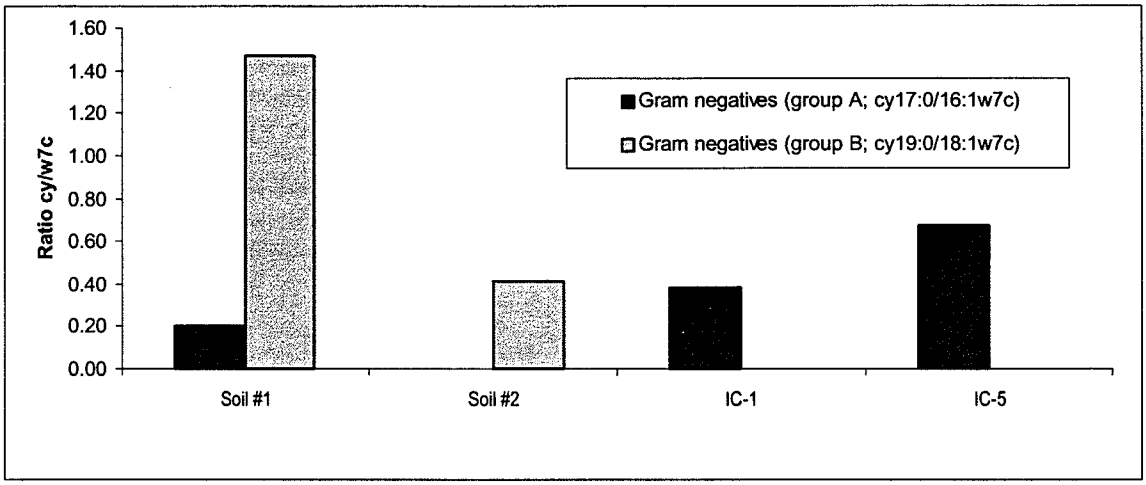

Figure 3. Growth rate of the Gram-negative community as assessed by the ratio of cyclopropyl f. a. to ω7c f. a. Specifically, 16:1ω7c and 18:1ω7c fatty acids are converted to cyclopropyl fatty acids (cy17:0 & cy19:0) as microbial growth slows (i.e., a high ratio indicates decreased turnover rate). Ratios greater than 0.15 indicate slowed growth rates, whereas ratios less than 0.05 indicate fast growth rates.

Gram-negative bacteria also generate *trans* fatty acids to minimize the permeability of their cellular membranes as an adaptation to less favorable environments (6). The ratios of these fatty acids support the different responses of the Group A and Group B bacteria in the iron samples indicated above. The Group A bacteria were more stressed than the Group B bacteria in the iron samples. Additionally, the Group A bacteria appeared to have been more stressed in the iron samples than in Soil #1 (there were no 16:1w7 biomarkers detected in Soil #2). The Group B bacteria did not have fatty acid ratios indicative of stress (no decreased membrane permeability) in any samples, though the IC-1 ratio was close. This observation is especially important for Soil #2 because only 18-carbon monoenoic f.a. were detected in that sample (Figure 4). It is also important for Soil #1 because the Group B bacteria had very slow growth rate ratios, despite the fact that the "stress" ratios do not indicate these bacteria were under environmental stress.

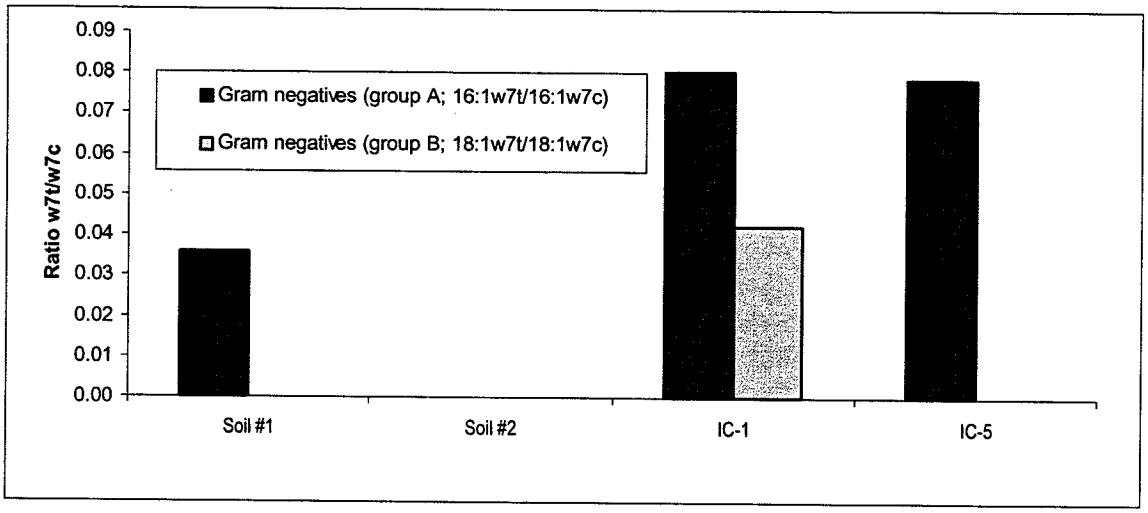

Figure4. Adaptation of the Gram-negative community to changes in the environment is determined by the ratio of ω7t/ω7c fatty acids. Ratios (16:1ω7t/16:1ω7c and 18:1ω7t/18:1ω7c) greater than 0.05 have been shown to indicate an adaptation to a toxic or stressful environment, resulting in decreased membrane permeability.

Table 2. Summary of PLFA results.

Sample Name	Biomass (pmoles PLFA/g dry wt.)					Community Structure (% of total PLFA)						Physiological status	
	Total Biomass	Cell equivalent value[1]	Bacterial biomass	Eukaryotic biomass	Rratio bacteria/ eukarya	Gram+/ anaerobic Gram - (TerBrSats)	Gram - (Monos)	Anaerobic metal reducers (BrMonos)	SRB/ Actinomycetes (MidBrSats)	Genera (Nsats)	Eukaryotes (polyenoics)	Growth Phase (cy/w7c)	Adaptation (w7t/w7c)
Soil #1	245	4.80E+06	240	5	48:1	5.7	44.7	0.5	17.7	29.3	2.1	1.67	0.04
Soil #2	6	1.19E+05	6	ND	NC	0.0	57.6	0.0	0.0	42.4	0.0	0.42	0.00
IC-1	238	4.75E+06	238	N D	NC	17.0	46.0	18.3	6.9	11.7	0.0	0.39	0.12
IC-5	71	1.41E+06	70	1	69:1	16.2	55.7	5.3	2.4	18.9	1.4	0.67	0.08

[1] The cell equivalent value is calculated from experiments with typical bacteria isolated from soil and water. This value is based on 2.0×10^{12} cells per gram dry weight of cells and 10^{8} picomoles of phospholipid/gram dry weight of cells. The number of cells/gram of dry weight may vary and is dependent on the environmental conditions from which the microorganisms were recovered.

Quality Assurance Section

Sample Arrival and Holding Times:

Four samples were received on 5/17/01, accompanied by a chain of custody form. All arrival conditions and required holding times were acceptable according to SOP #SREC.

Sample Analysis and QA/QC Parameters:

Samples were analyzed under the U.S. EPA Good Laboratory Practice Standards: Toxic Substances Control Act (40 CFR part 790). All samples were processed according to standard operating procedures.

Notes: No QC or analytical problems were encountered.

Calibrations and Solvent Checks:

All laboratory equipment and instruments used throughout the analyses were calibrated and operated within acceptable ranges. The instruments were calibrated according to Standard Operating Procedures (EQ4). All solvents used in these analyses were tested for purity.

Data Validation:

All data analyses were performed correctly. All calculations and transcriptions of raw and final data were verified.

References:

1. White, DC, WM Davis, JS Nickels, JD King and RJ Bobbie. 1979. Determination of the sedimentary microbial biomass by extractable lipid phosphate. *Oecologia* 40:51-62.
2. Balkwill, D L, FR Leach, JT Wilson, JF McNabb, and DC White. 1988. Equivalence of microbial biomass measures based on membrane lipid and cell wall components, adenosine triphosphate, and direct counts in subsurface sediments. *Microbial Ecology* 16:73-84
3. Pinkart, HC, DB Ringelberg, YM Piceno, SJ Macnaughton, and DC White. Biochemical approaches to biomass measurements and community structure analysis. *In*: Manual of Environmental Microbiology, 2nd Edition (DE Stahl, CH Hurst, GR Knudsen, M. J. McInerney, LD Stetzenbach, and MV Walter, eds.) American Society for Microbiology Press, Washington, DC. In press.
4. White, DC, JO Stair, and DB Ringelberg. 1996. Quantitative Comparisons of in situ Microbial Biodiversity by Signature Biomarker Analysis. *J. Indust. Microbiol.* 17:185-196
5. Dowling, NJE, F Widdel, and DC White. 1986. Phospholipid ester-linked fatty acid biomarkers of acetate-oxidizing sulfate reducers and other sulfide forming bacteria. *J. Gen. Microbiol.* 132: 1815-1825
6. Edlund, A, PD Nichols, R Roffey, and DC White. 1985. Extractable and lipopolysaccharide fatty acid and hydroxy acid profiles from *Desulfovibrio* species. *J. Lipid Res.* 26:982-988
7. White, DC and DB Ringelberg. 1995. Utility of signature lipid biomarker analysis in determining in situ viable biomass, community structure, and nutritional/ physiological status of the deep subsurface microbiota. *In:* The Microbiology of the Terrestrial Subsurface (Amy, PS and DL Halderman, eds.) CRC Press, Boca Raton, FL

Appendix C-2

TCE Half-Lives at Three Flowrates

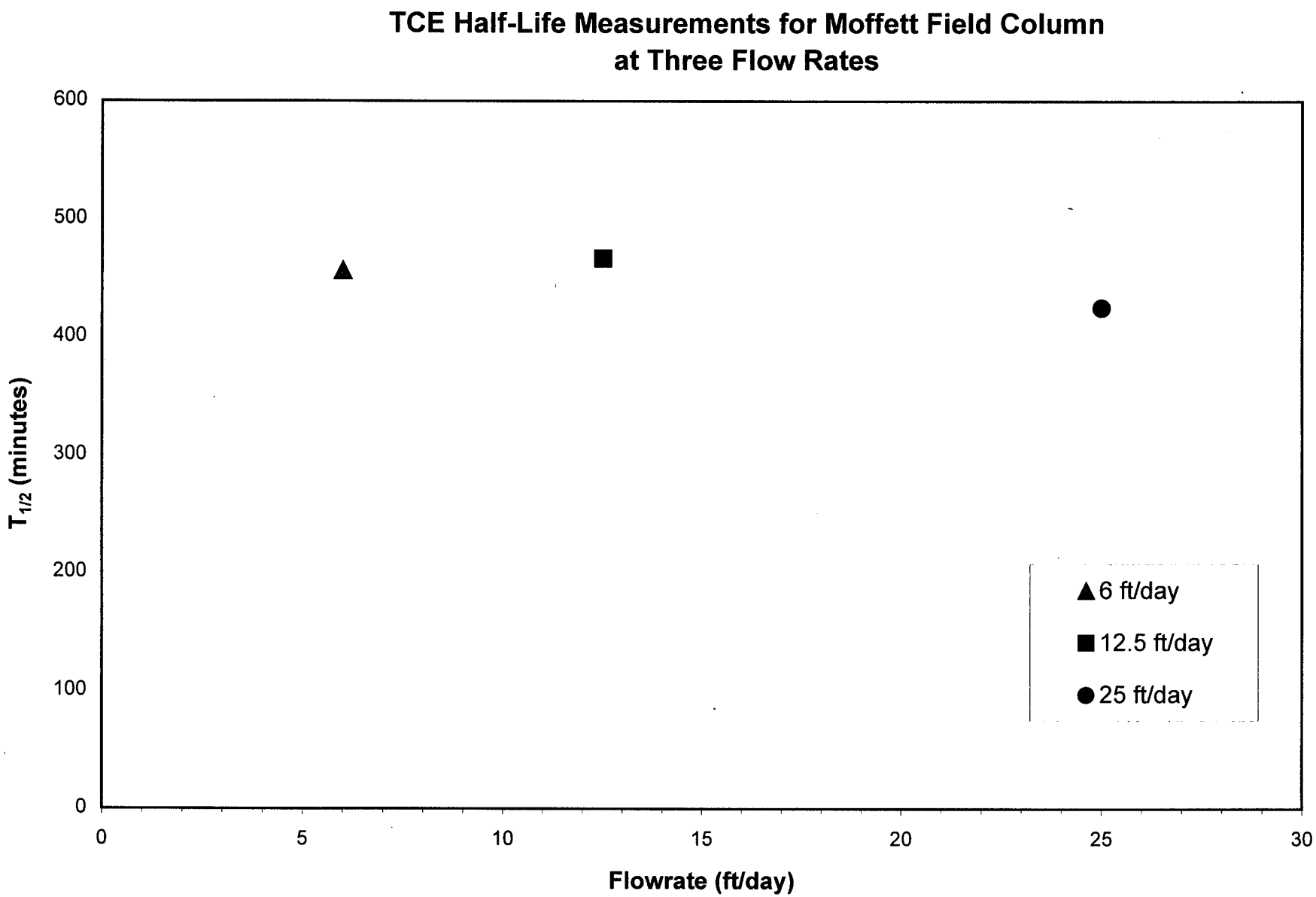
TCE Half-Life Measurements for Moffett Field Column
at Three Flow Rates
600
500
400
300
200
100
0
$T_{1/2}$ (minutes)
0
5
10
15
20
25
30
Flowrate (ft/day)
6 ft/day
12.5 ft/day
25 ft/day

Appendix C-3

Column Test Results

TCE Column Test Results for Moffett Field Simulation

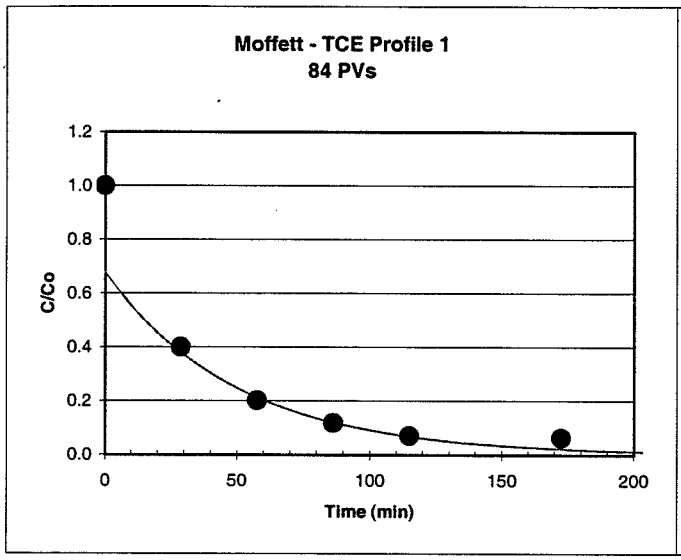

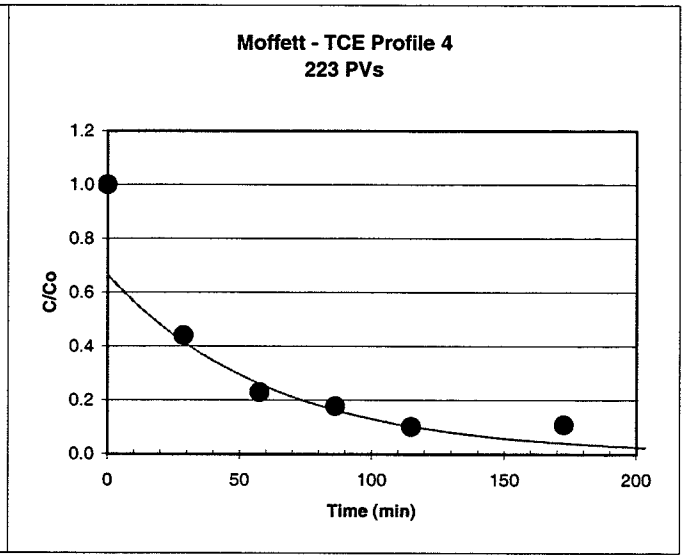

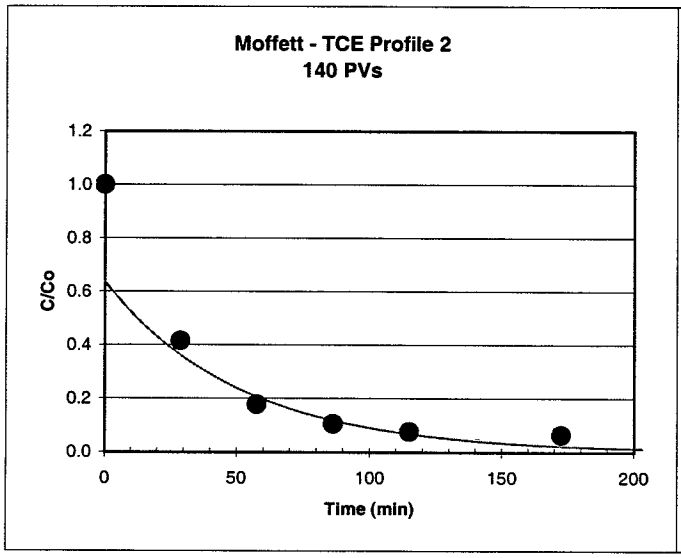

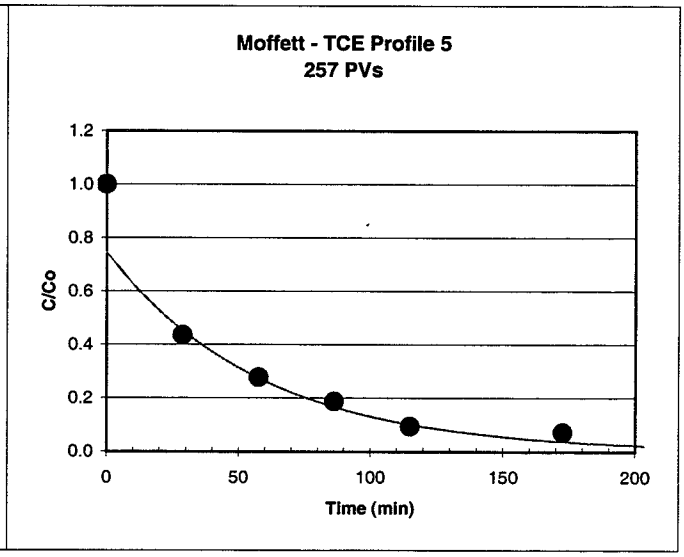

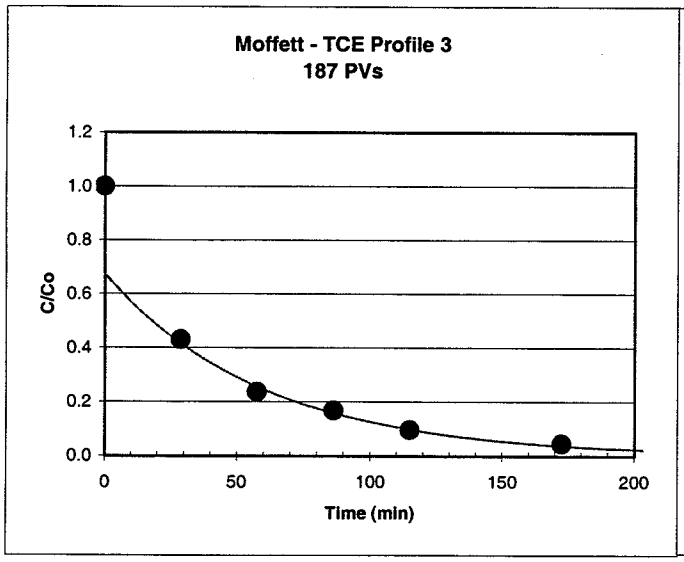

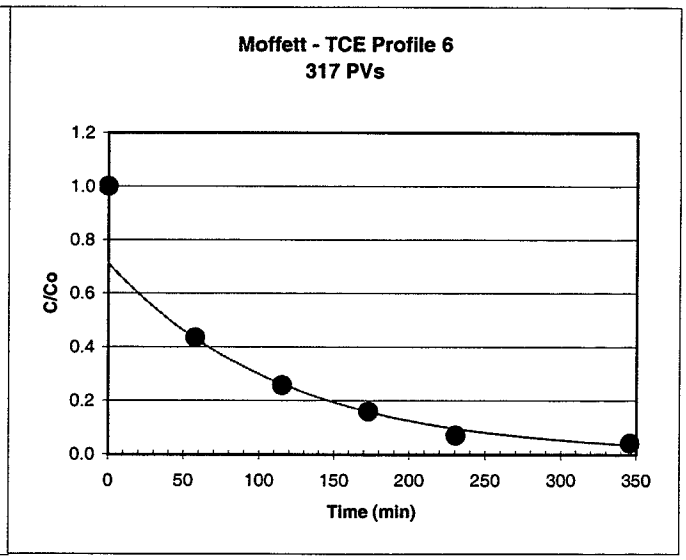

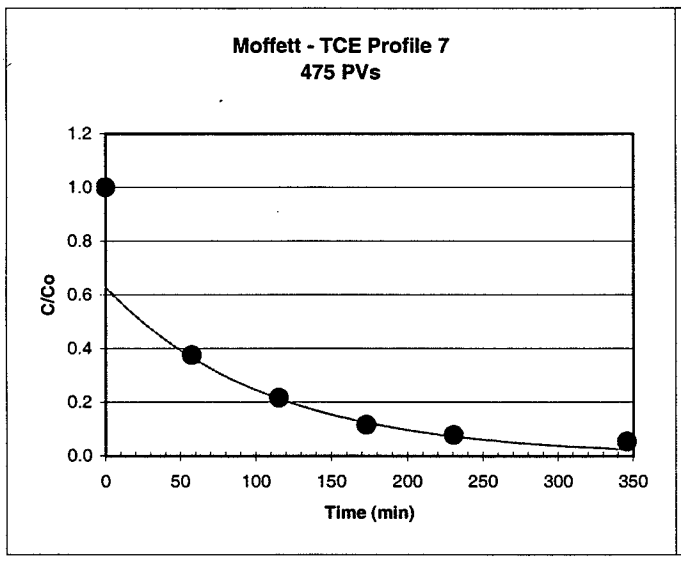
Moffett - TCE Profile 7
475 PVs
C/Co
1.2
1.0
0.8
0.6
0.4
0.2
0.0
0
50
100
150
200
250
300
350
Time (min)

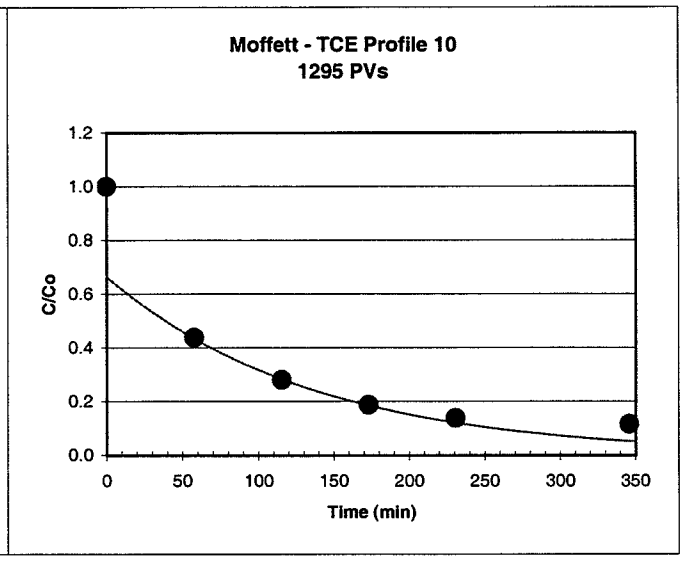
Moffett - TCE Profile 10
1295 PVs
C/Co
1.2
1.0
0.8
0.6
0.4
0.2
0.0
0
50
100
150
200
250
300
350
Time (min)

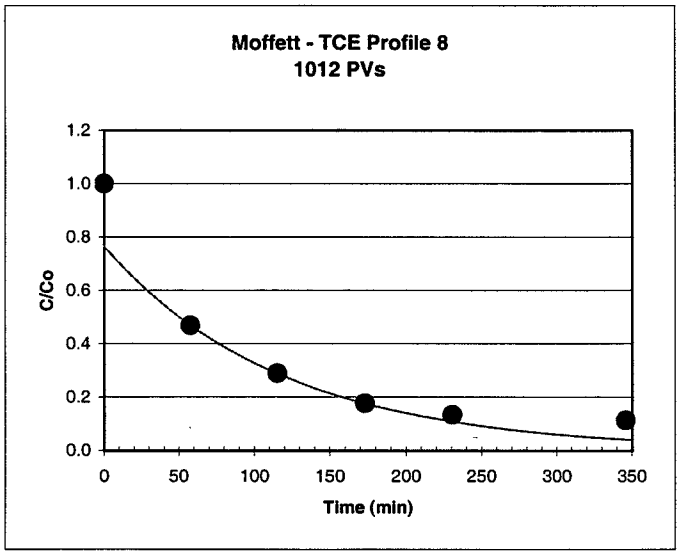
Moffett - TCE Profile 8
1012 PVs
C/Co
1.2
1.0
0.8
0.6
0.4
0.2
0.0
0
50
100
150
200
250
300
350
Time (min)

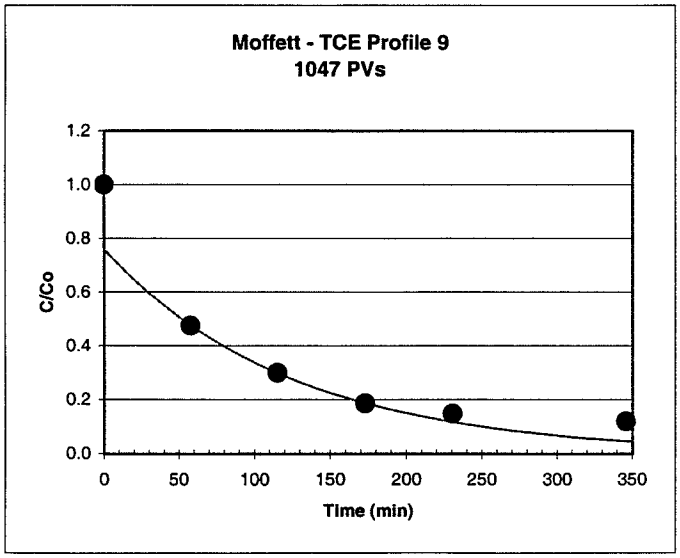
Moffett - TCE Profile 9
1047 PVs
C/Co
1.2
1.0
0.8
0.6
0.4
0.2
0.0
0
50
100
150
200
250
300
350
Time (min)

TCE Column Test Results for Lowry Simulation

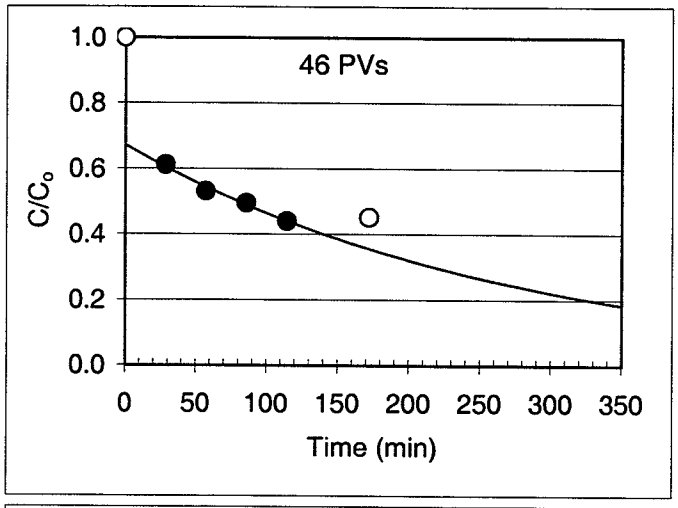

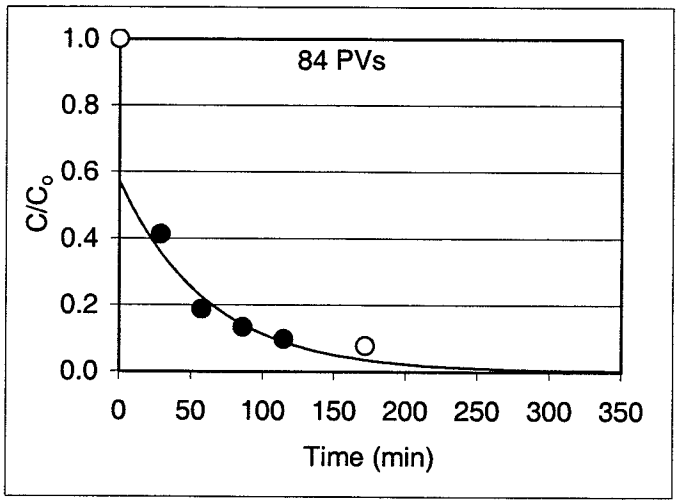

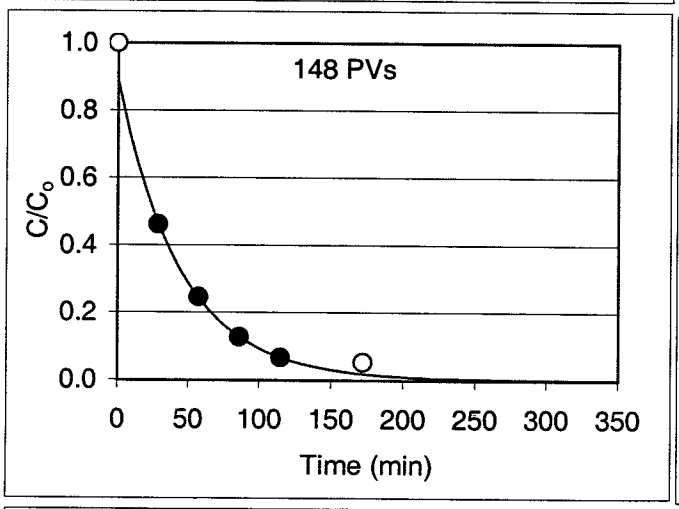

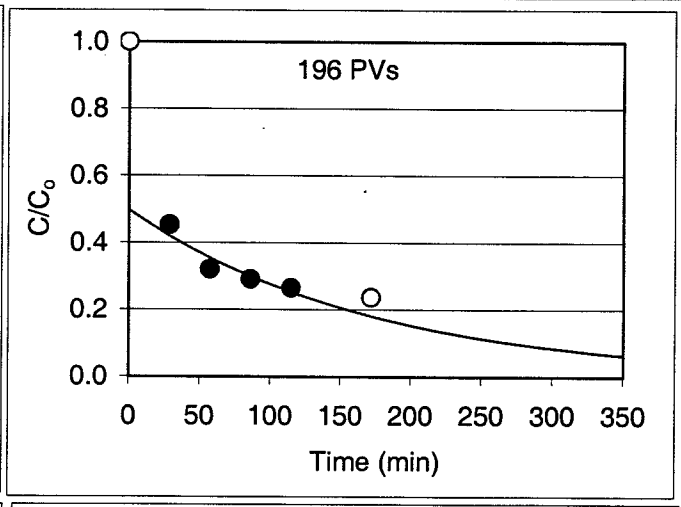

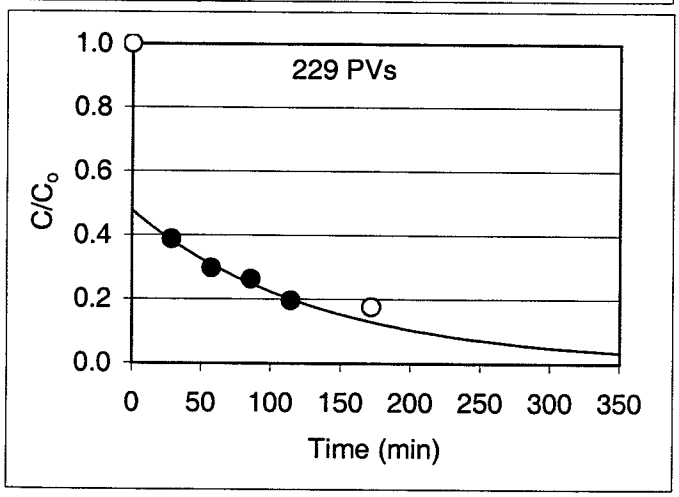

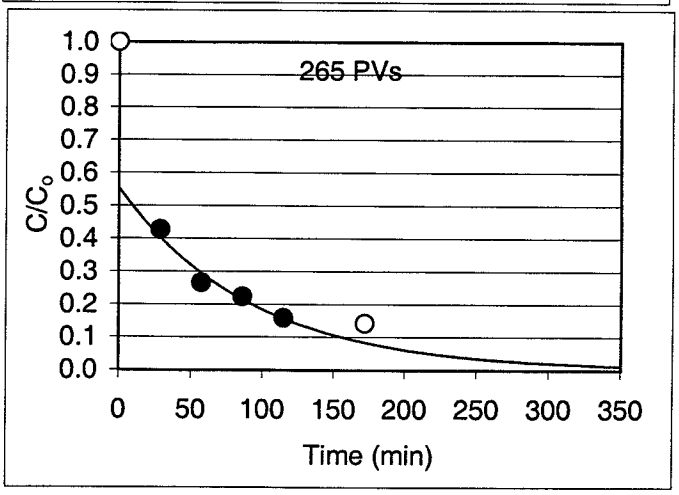

TCE Column Test Results for Lowry Simulation

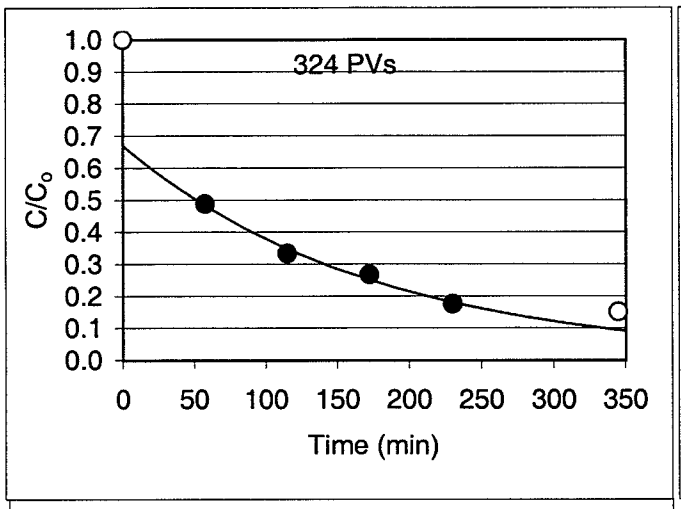

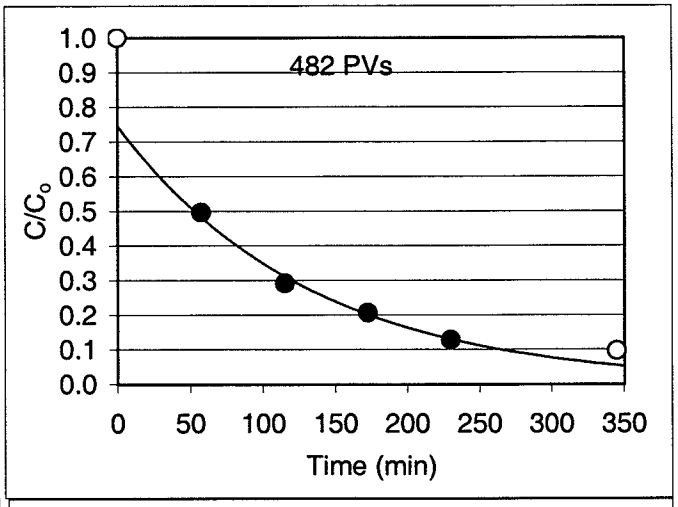

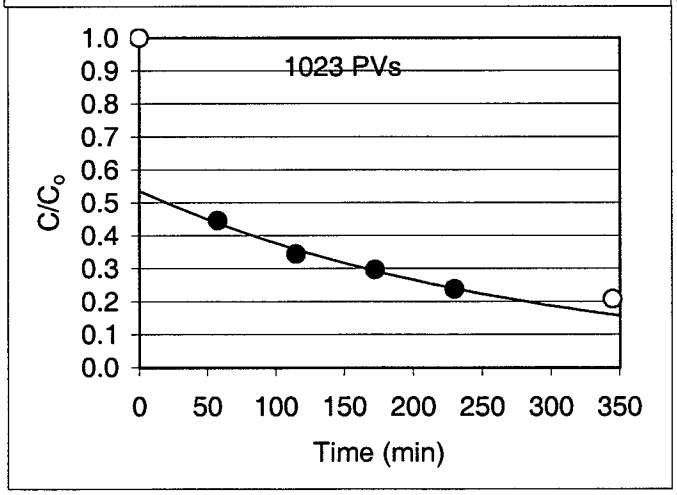

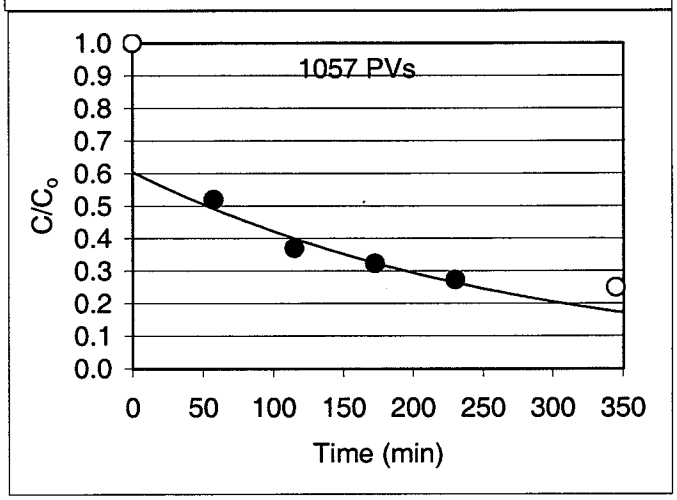

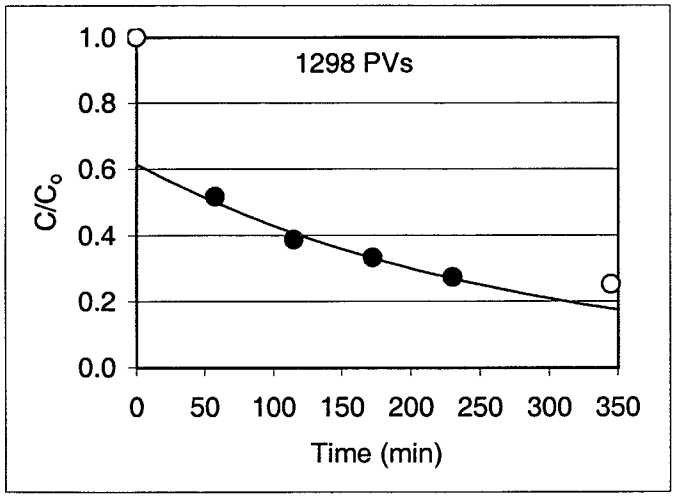

Moffett Column Tracer Test

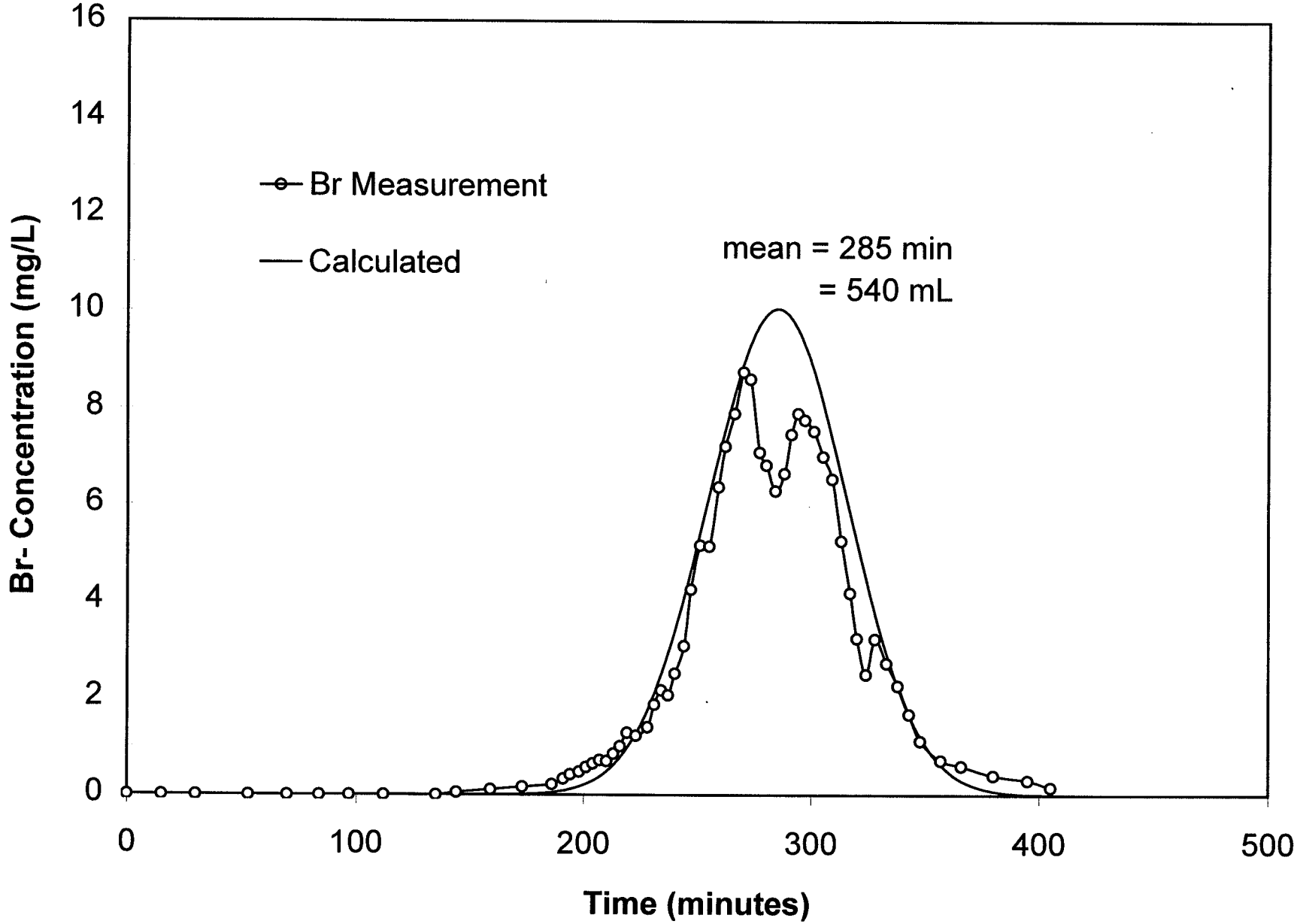

brtrace1-a.xls, TT#1-fit

Appendix C-4

Geochemical Models

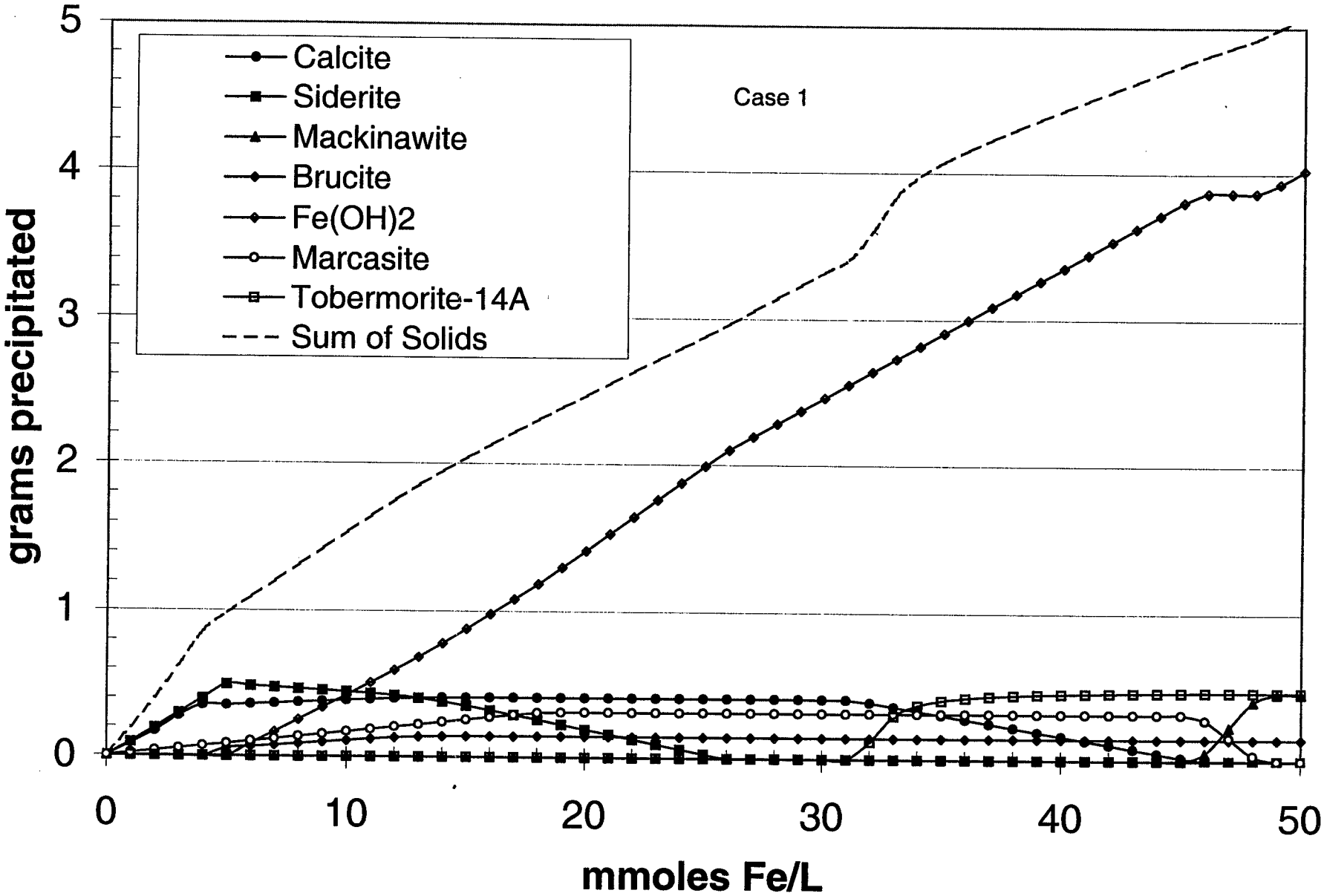

Column Test simulation.xls, Chart2-1a

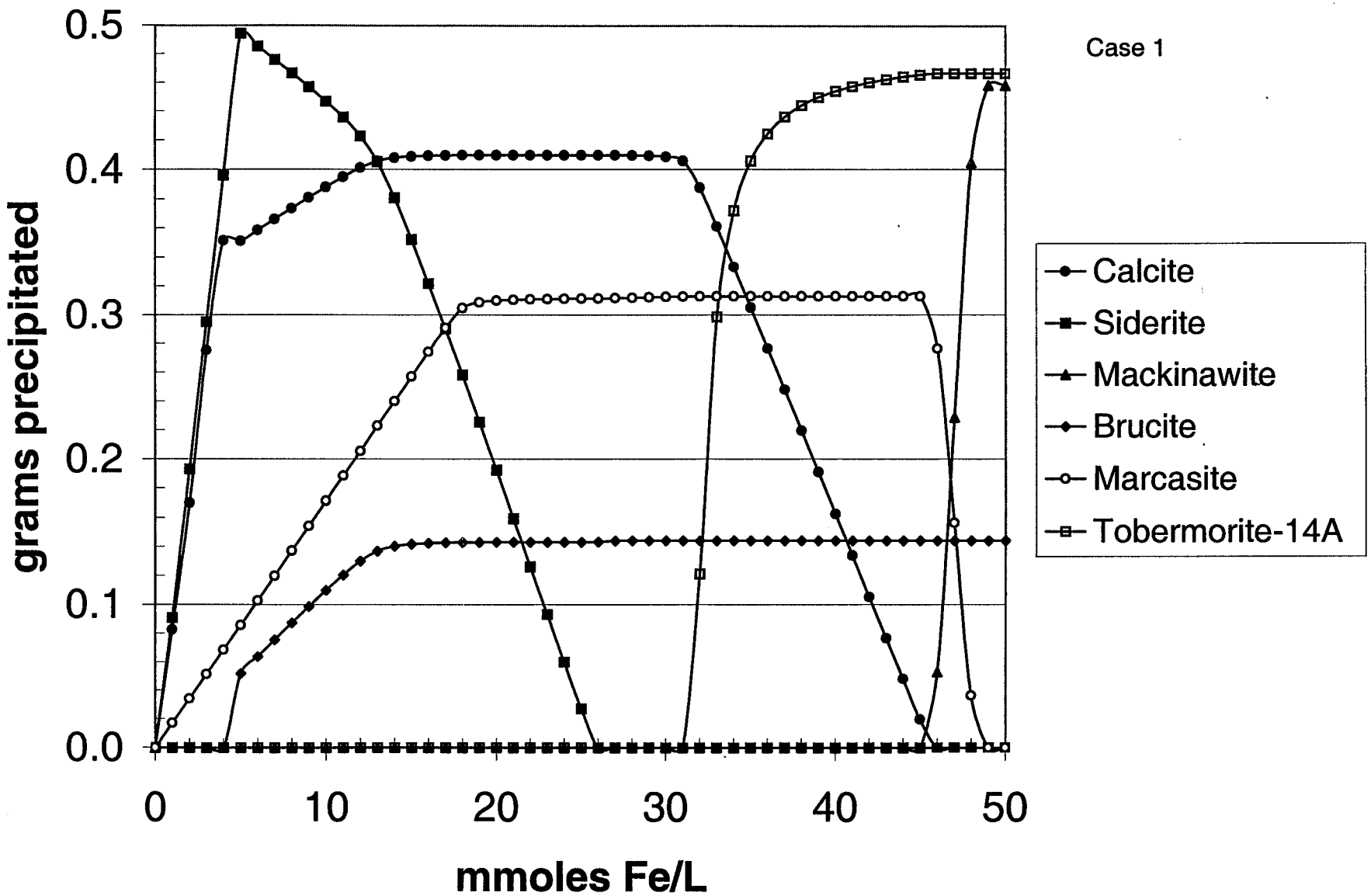

Column Test simulation.xls, Chart2-1b

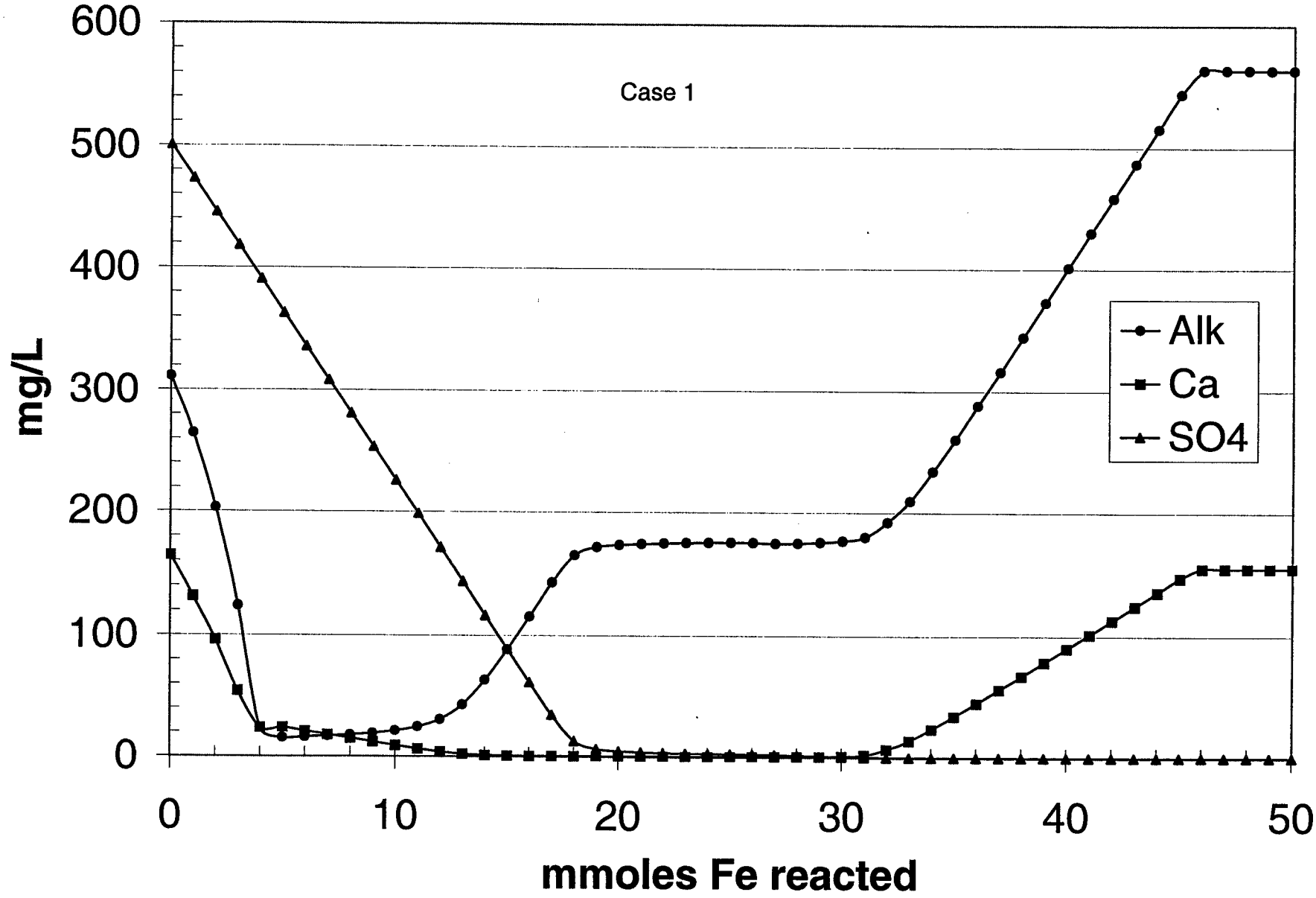

Column Test simulation.xls, Chart2-2a

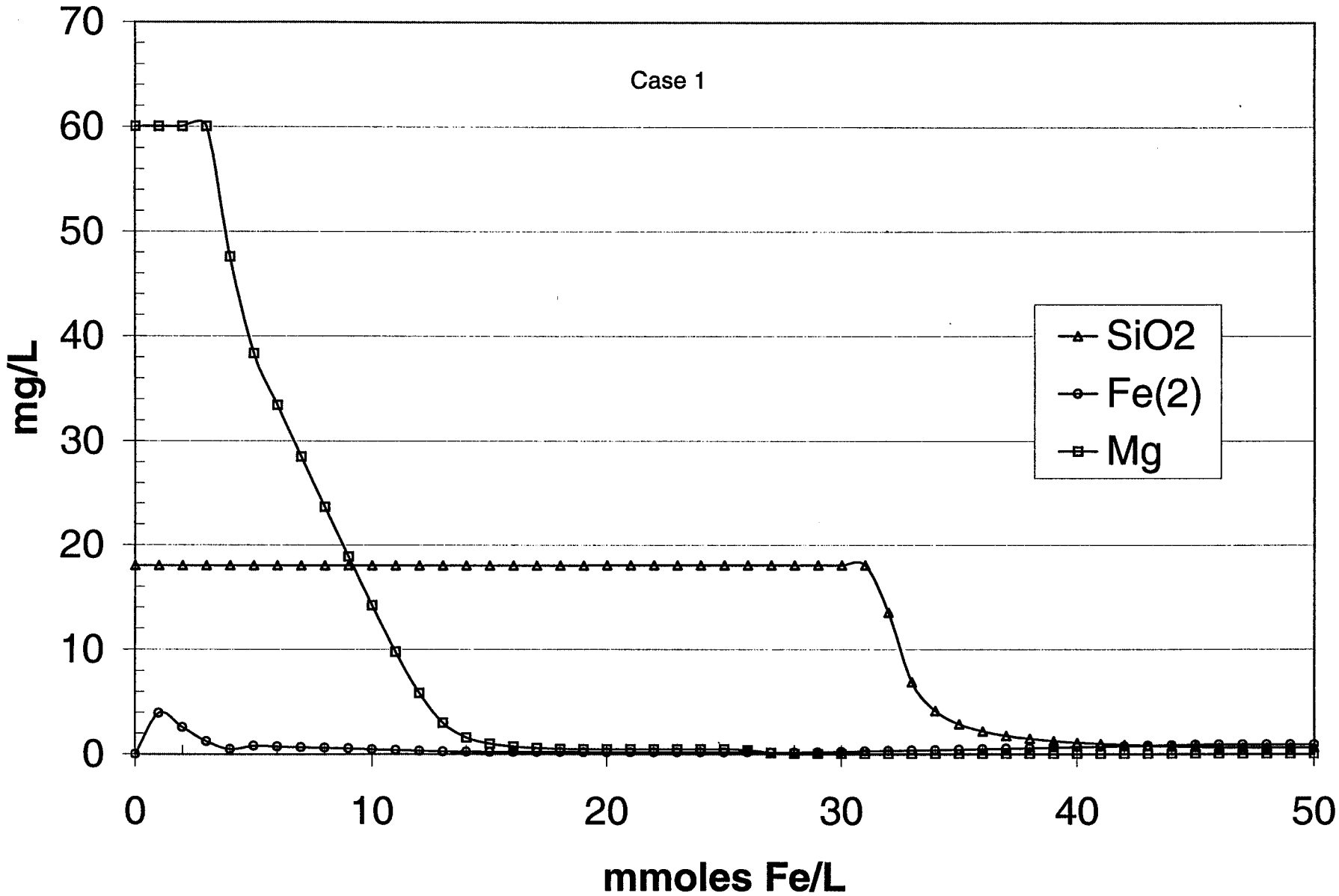

Column Test simulation.xls, Chart2-2b

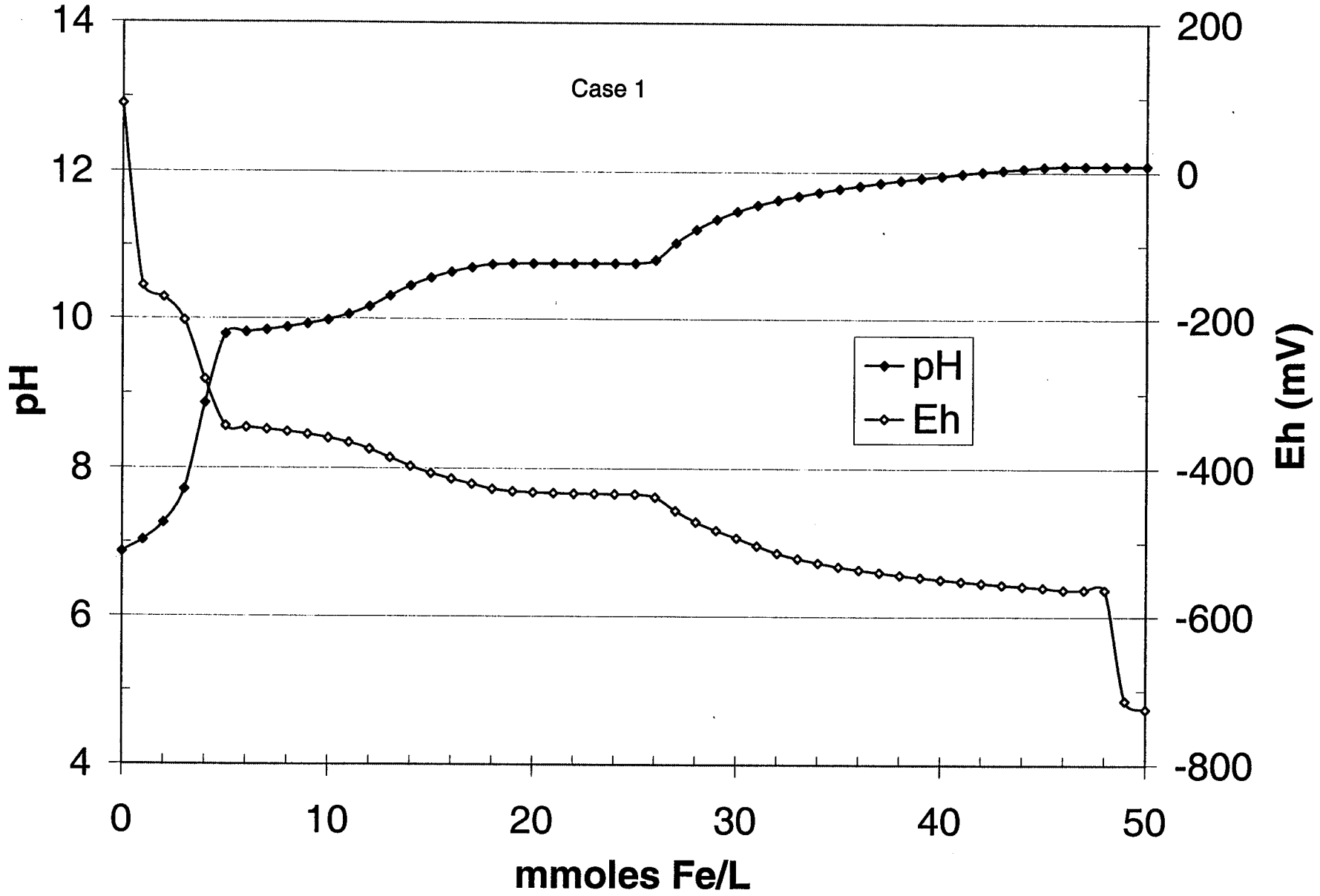

Column Test simulation.xls, Chart2-3

Mackinawite Marcasite precipitation allowed

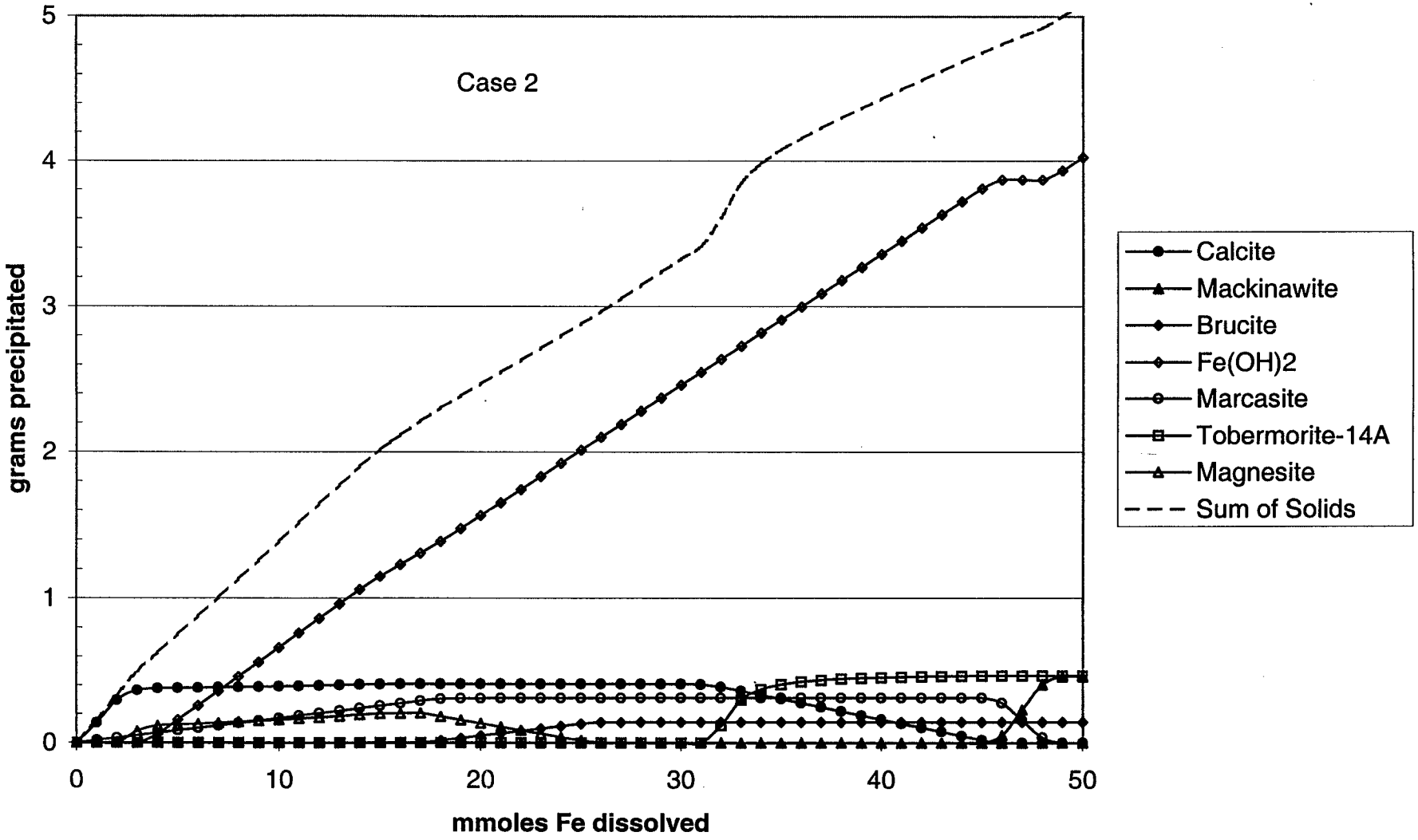

Column Test simulation.xls, Chart4-1a

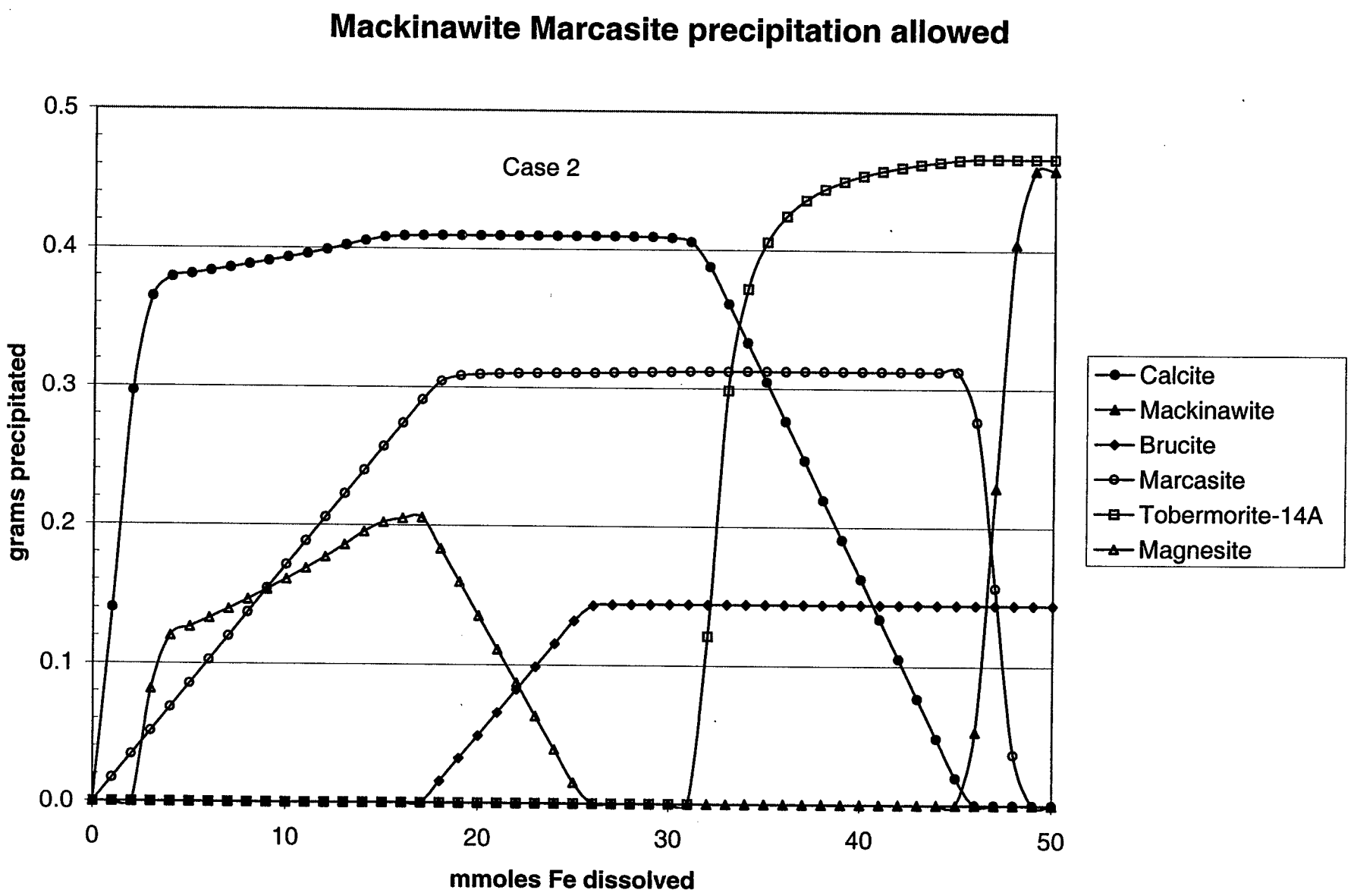

Column Test simulation.xls, Chart4-1b

Mackinawite Marcasite precipitation allowed

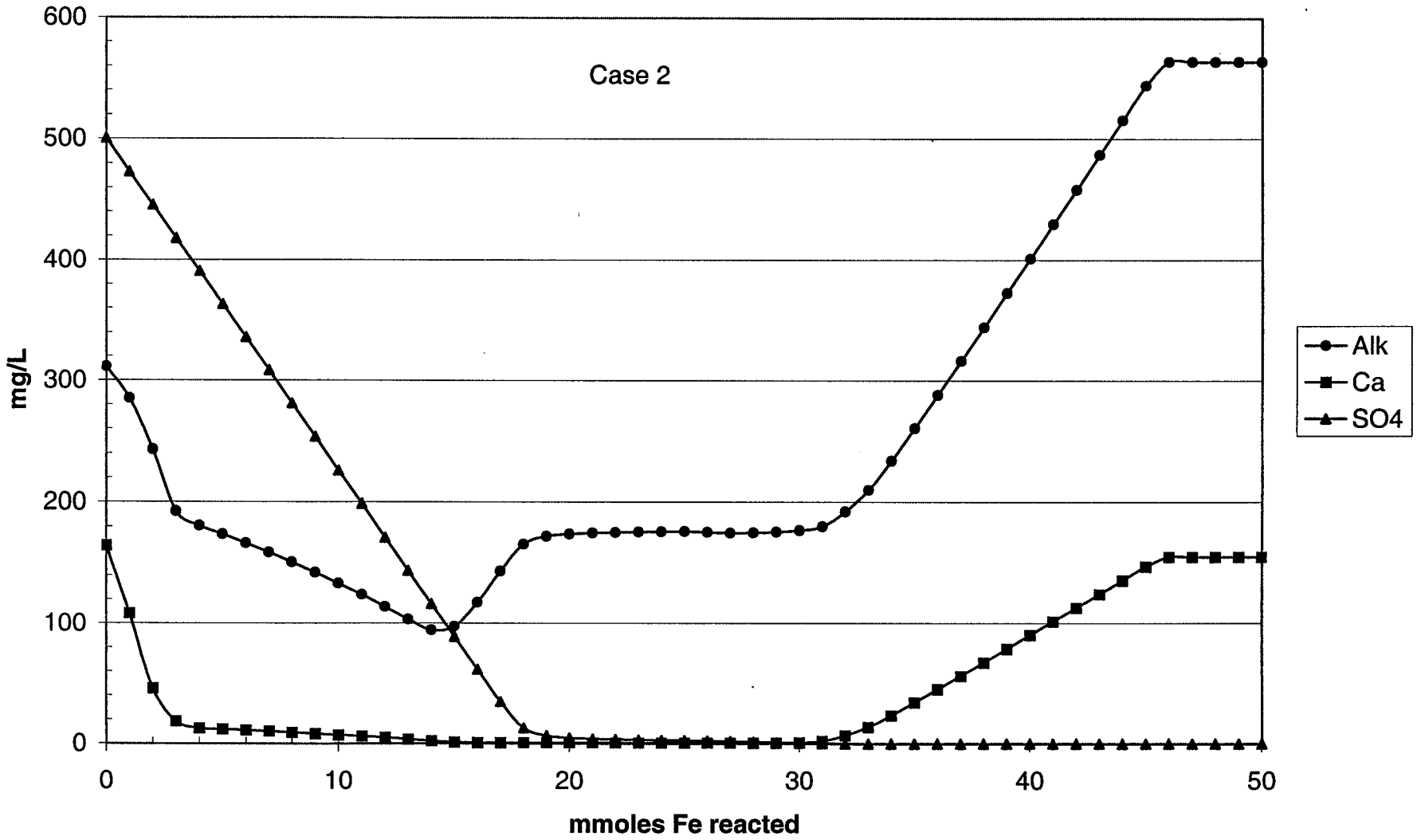

Column Test simulation.xls, Chart4-2a

Mackinawite Marcasite precipitation allowed

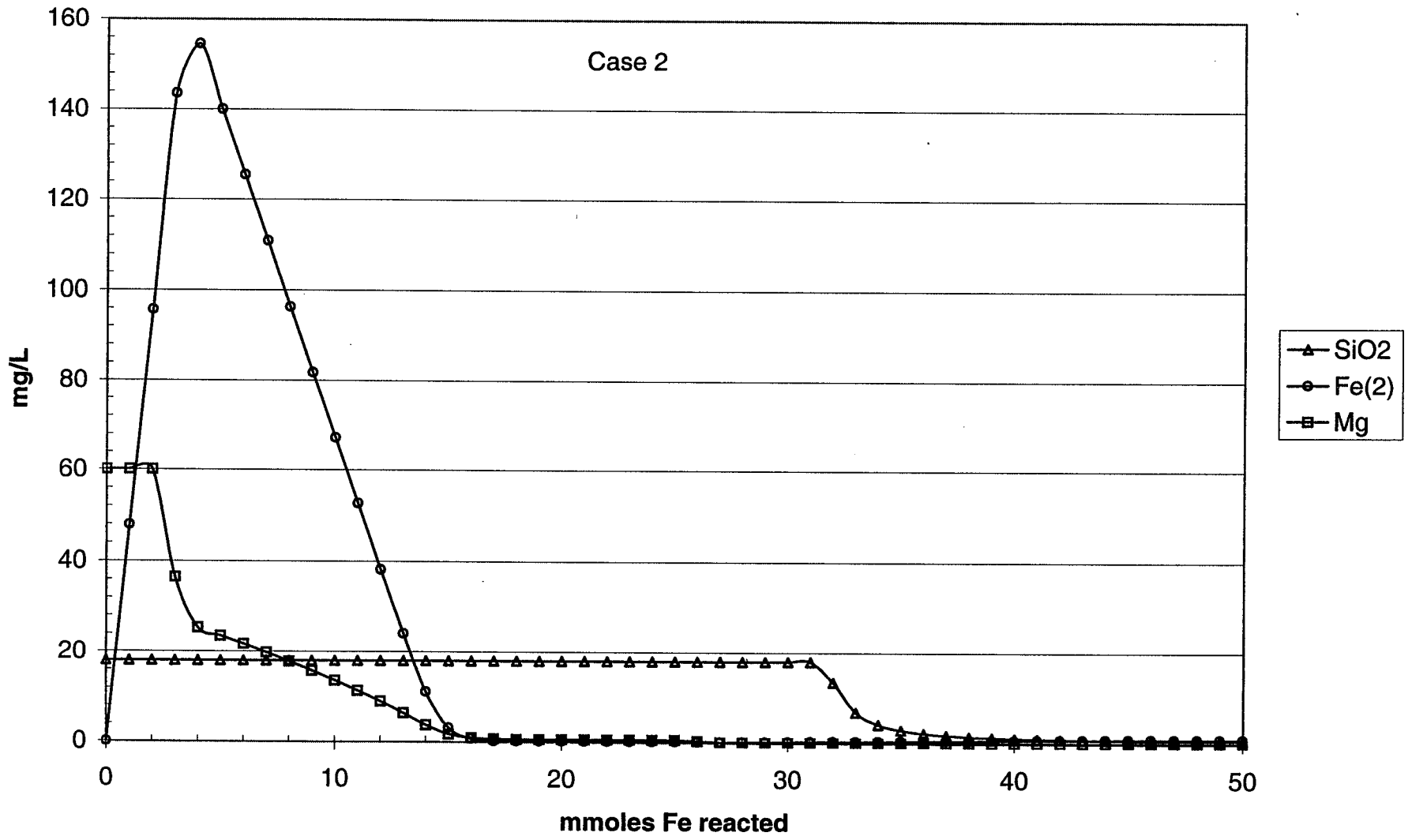

Column Test simulation.xls, Chart4-2b

Mackinawite Marcasite precipitation allowed

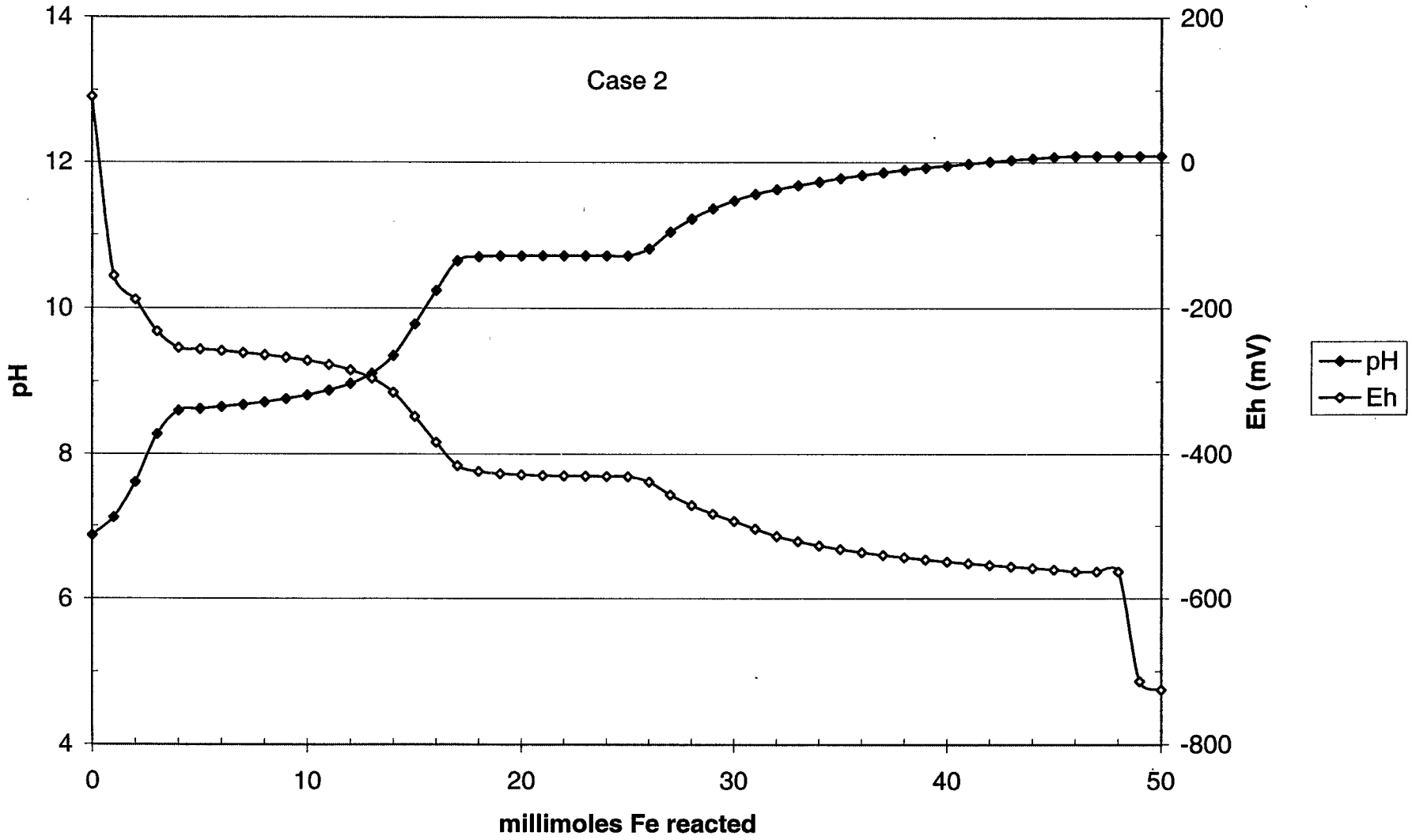

Column Test simulation.xls, Chart4-3

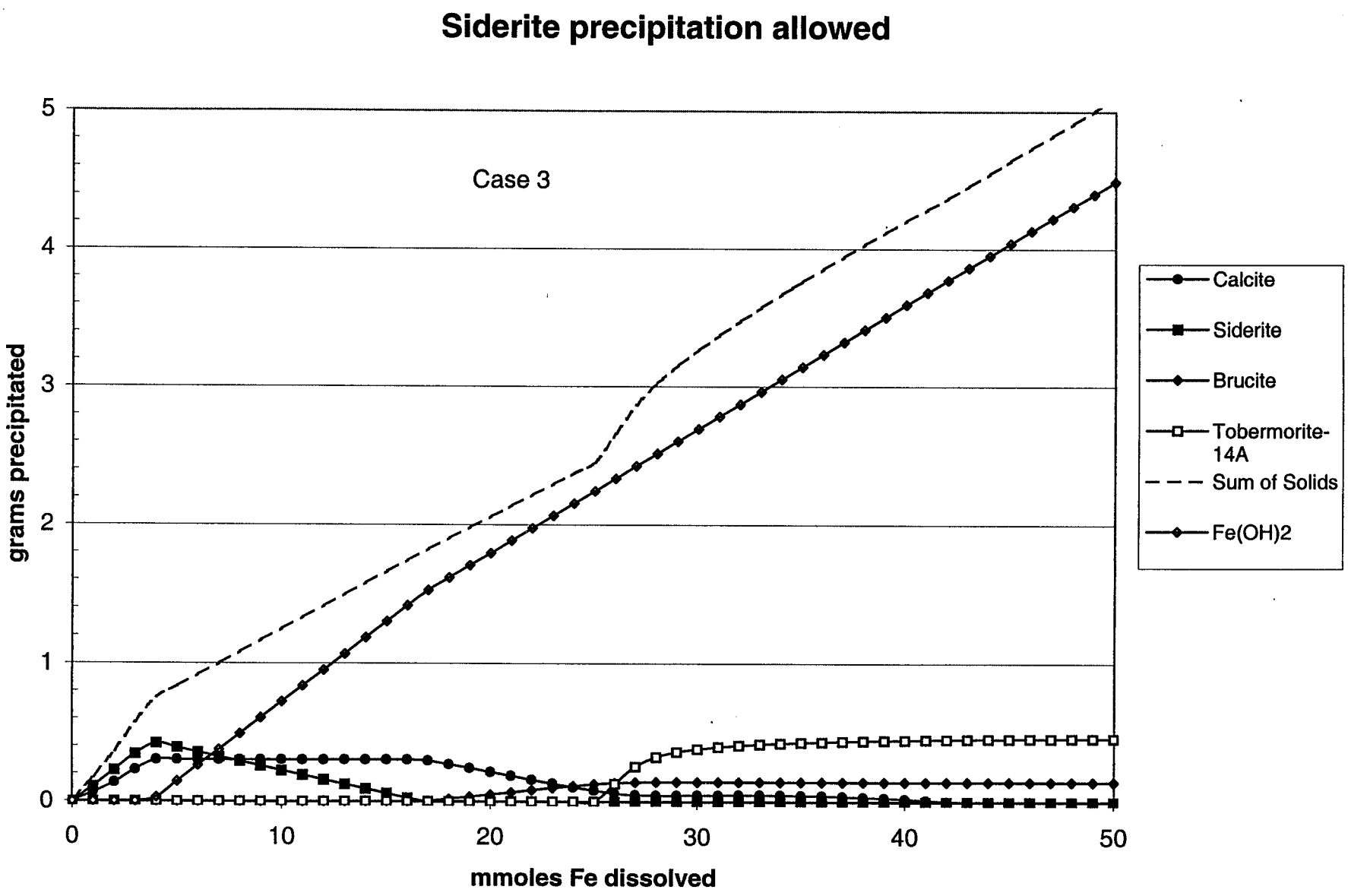

Column Test simulation.xls, Chart3-1a

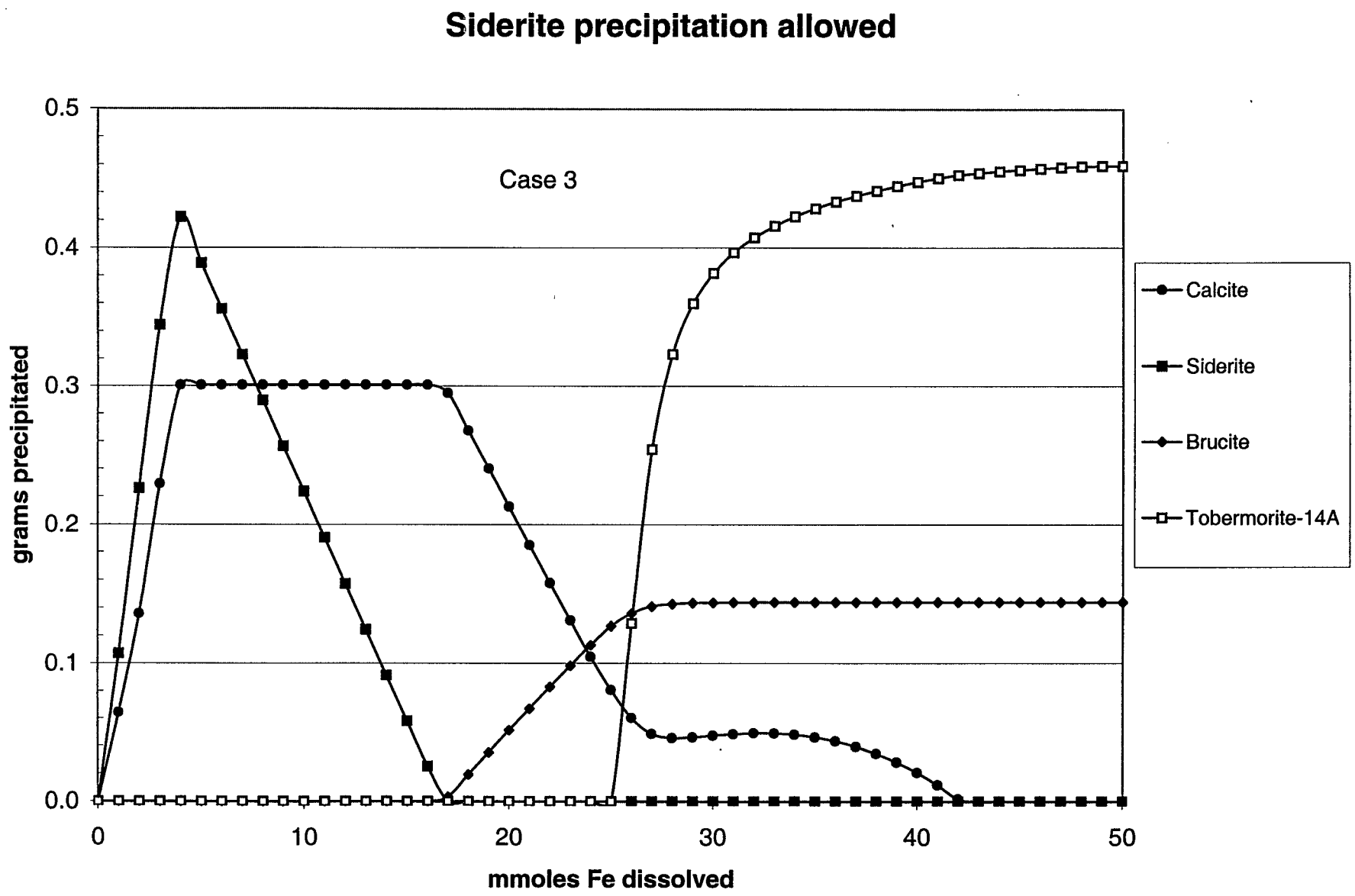

Column Test simulation.xls, Chart3-1b

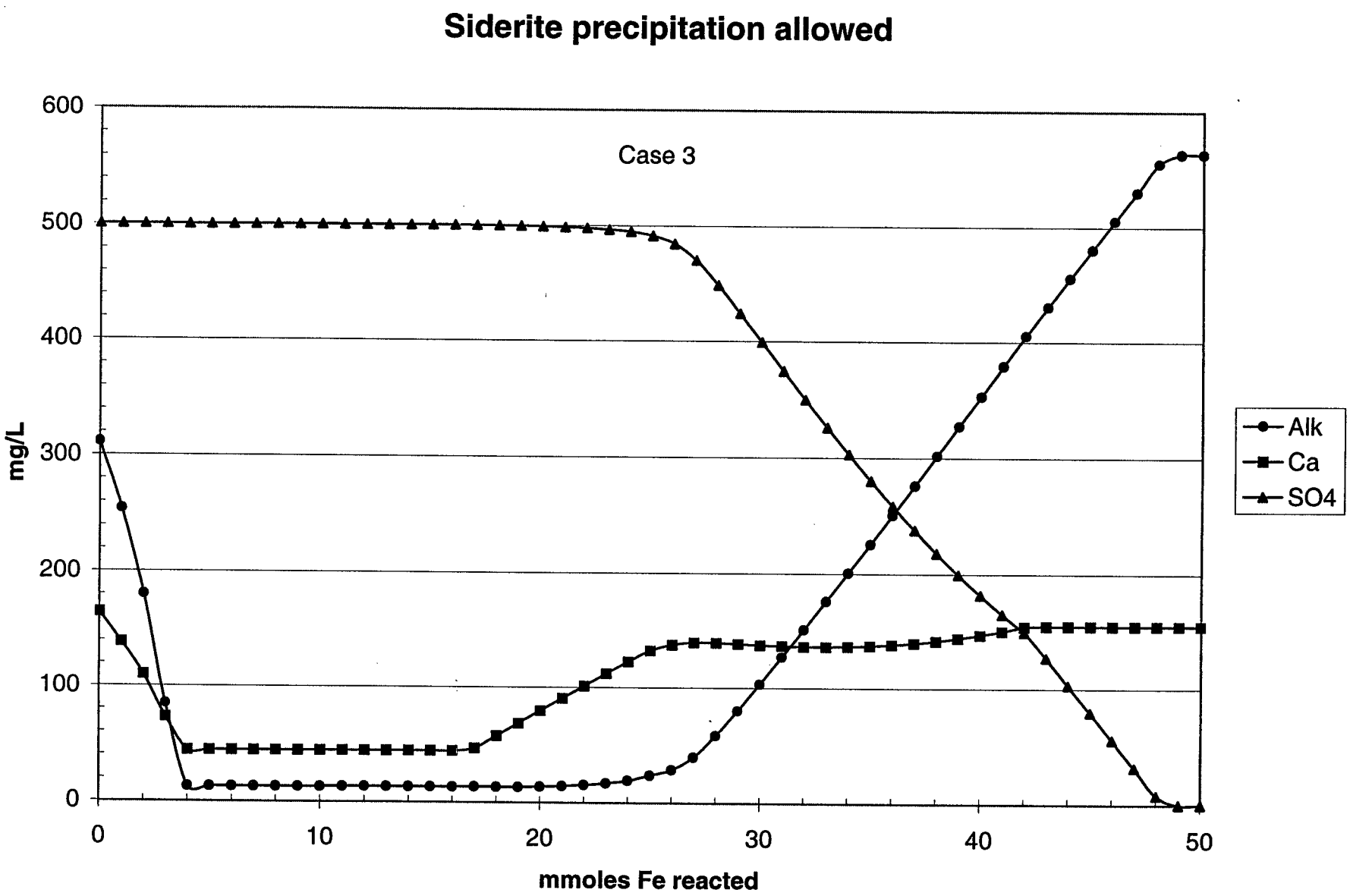

Column Test simulation.xls, Chart3-2a

Siderite precipitation allowed

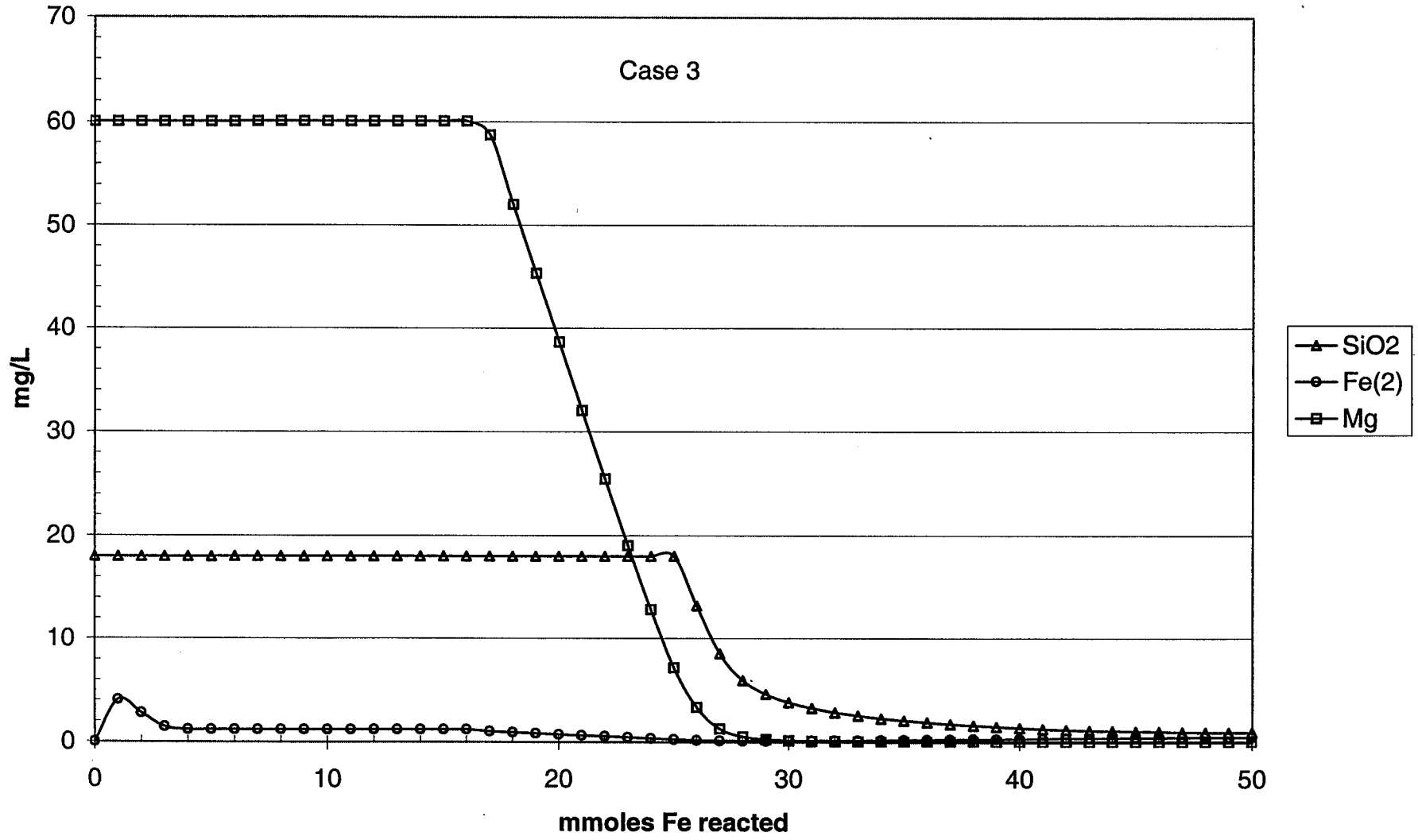

Column Test simulation.xls, Chart3-2b

Appendix C-5

Column Test Data

Results of Column Test for Moffett Field Simulation

Parameter (µg/L)	PVs 42	PVs 84	PVs 142	PVs 187	PVs 223	PVs 257	PVs 317	PVs 475	PVs 1012	PVs 1047	PVs 1295	PVs 1358	PVs 1450	PVs 1454	PVs 1470
Dichloroethane	<5	<5	<5	<5	<5	<5	<5	<5	<5	<5	<5	<5	<5	<5	<5
cis-1,2-Dichloroethene	31.6	28.5	29.3	34.5	36.7	34.9	35.4	38.6	35.5	33.9	38.7	42.5	40.8	49.7	37.6
trans-1,2-Dichloroethene	4.38	4.77	3.86	4.14	3.96	4.29	4.65	4.12	5.34	5.07	5.49	4.89	5.01	5.36	5.27
Trichloroethene	69.4	758.6	1263.4	476.5	522.7	459.7	483.5	796.8	643.1	523.1	575.4	616.3	578.5	583.2	571.4
Tetrachloroethene	<5	<5	<5	<5	<5	<5	<5	<5	<5	<5	<5	<5	<5	<5	<5
Vinyl Chloride	<2	<2	<2	<2	<2	<2	<2	<2	<2	<2	<2	<2	<2	<2	<2
Dichloroethane	<5	<5	<5	<5	<5	<5	<5	<5	<5	<5	<5	<5	<5	<5	<5
cis-1,2-Dichloroethene	34.5	32.1	34.5	39.7	32.5	34.5	37.8	36.3	39.2	37.1	39.6	41.4	35.8	36.9	40.5
trans-1,2-Dichloroethene	5.64	6.11	5.79	4.98	5.36	5.49	5.26	5.13	4.89	4.68	5.01	5.16	4.96	4.72	5.03
Trichloroethene	37.5	303.5	524.1	204.7	229.7	199.8	210.1	298.7	301.4	248.1	251.3	457.4	383.7	336.3	296.2
Tetrachloroethene	<5	<5	<5	<5	<5	<5	<5	<5	<5	<5	<5	<5	<5	<5	<5
Vinyl Chloride	<2	<2	<2	<2	<2	<2	<2	<2	<2	<2	<2	<2	<2	<2	<2
Dichloroethane	<5	<5	<5	<5	<5	<5	<5	<5	<5	<5	<5	<5	<5	<5	<5
cis-1,2-Dichloroethene	32.8	36.3	38.2	41.0	40.8	37.5	36.9	32.4	34.7	39.4	41.7	44.6	40.8	38.7	34.1
trans-1,2-Dichloroethene	5.09	5.46	5.83	5.56	5.29	5.69	5.19	5.86	5.50	5.84	5.92	6.13	5.75	5.80	5.73
Trichloroethene	34.1	152.3	224.2	112.3	119.7	127.0	123.7	171.4	185.4	156.4	161.4	278.9	274.2	258.7	265.2
Tetrachloroethene	<5	<5	<5	<5	<5	<5	<5	<5	<5	<5	<5	<5	<5	<5	<5
Vinyl Chloride	<2	<2	<2	<2	<2	<2	<2	<2	<2	<2	<2	<2	<2	<2	<2
Dichloroethane	<5	<5	<5	<5	<5	<5	<5	<5	<5	<5	<5	<5	<5	<5	<5
cis-1,2-Dichloroethene	35.8	39.6	41.2	43.8	37.6	40.9	39.1	37.5	41.2	41.0	43.7	44.0	44.9	41.7	47.3
trans-1,2-Dichloroethene	5.73	6.14	6.29	5.89	6.09	5.77	5.39	6.01	5.76	5.91	6.02	6.35	6.14	5.83	6.06
Trichloroethene	31.4	88.6	131.4	79.8	92.4	86.0	76.7	91.2	113.2	97.2	107.2	255.7	182.7	214.1	241.1
Tetrachloroethene	<5	<5	<5	<5	<5	<5	<5	<5	<5	<5	<5	<5	<5	<5	<5
Vinyl Chloride	<2	<2	<2	<2	<2	<2	<2	<2	<2	<2	<2	<2	<2	<2	<2
Dichloroethane	<5	<5	<5	<5	<5	<5	<5	<5	<5	<5	<5	<5	<5	<5	<5
cis-1,2-Dichloroethene	36.7	31.4	42.5	39.6	34.6	43.1	37.5	29.7	26.5	27.9	34.2	39.7	36.9	43.9	43.5
trans-1,2-Dichloroethene	5.49	4.98	5.93	5.29	5.30	5.64	5.71	4.88	4.15	4.60	4.91	5.12	5.64	5.96	5.23
Trichloroethene	31.9	53.1	95.3	45.7	52.3	43.1	33.8	61.0	85.6	76.9	79.2	201.4	117.3	185.6	213.2
Tetrachloroethene	<5	<5	<5	<5	<5	<5	<5	<5	<5	<5	<5	<5	<5	<5	<5
Vinyl Chloride	<2	<2	<2	<2	<2	<2	<2	<2	<2	<2	<2	<2	<2	<2	<2
Dichloroethane	<5	<5	<5	<5	<5	<5	<5	<5	<5	<5	<5	<5	<5	<5	<5
cis-1,2-Dichloroethene	36.1	41.2	43.5	37.6	44.1	39.7	38.4	34.3	37.5	39.0	40.1	42.5	47.6	39.8	42.1
trans-1,2-Dichloroethene	5.82	6.42	6.82	6.25	6.09	6.17	6.64	6.78	6.02	6.13	6.26	6.05	5.87	6.62	6.74
Trichloroethene	30.5	47.5	79.6	20.9	56.4	32.4	19.7	42.1	72.5	61.8	66.4	185.3	99.2	146.1	176.3
Tetrachloroethene	<5	<5	<5	<5	<5	<5	<5	<5	<5	<5	<5	<5	<5	<5	<5
Vinyl Chloride	<2	<2	<2	<2	<2	<2	<2	<2	<2	<2	<2	<2	<2	<2	<2

Results of Column Test for Moffett Field Simulation

Inorganic Measurements

Moffett - Filtered		249 PVs - 25 ft/day		317 PVs - 25 ft/day		327 PVs - 6 ft/day		1310 PVs - 12.5 ft/day		
Parameter	Units	Filtered Inlet Result	Filtered Outlet Result	Filtered Inlet Result	Filtered Outlet Result	Filtered Inlet Result	Filtered Outlet Result	Unfiltered Inlet Result	Unfiltered A Result	Unfiltered Outlet Result
pH	-	7.38	9.73	7.36	10.03	7.36	10.09	7.35	8.92	10.23
ORP	-	31.5	-686.9	10.5	-699.5	3.9	-693.4	22.3	-583.4	-699.1
Calcium	mg/L	90	69	200	85	200	65	250	238	139
Iron	ug/L	<30	<30	<30	240	<30	<30	160	8,700	13300
Magnesium	mg/L	64	65	59	59	60	49	63	62	75
Alkalinity	mg/L	395	375	400	160	390	32	330	310	258
Sulfate	mg/L	675	575	550	550	575	725	650	600	550
Dissolved silica	mg/L	NA	NA	17.0	8.4	16.45	3.25	18.00	18.00	15.5

Moffett - Unfiltered		148 PVs - 25 ft/day			249 PVs - 25 ft/day		317 PVs - 12.5 ft/day		327 PVs - 6 ft/day		1310 PVs - 12.5 ft/day	
Parameter	Units	Unfiltered Inlet Result	Unfiltered A Result	Unfiltered Outlet Result	Unfiltered Inlet Result	Unfiltered Outlet Result	Unfiltered Inlet Result	Unfiltered Outlet Result	Unfiltered Inlet Result	Unfiltered Outlet Result	Unfiltered Inlet Result	Unfiltered Outlet Result
Calcium	mg/L	305	308	325	89	52	195	82	195	58	165	212
Iron	ug/L	290	26500	32300	50	2180	<30	9100	<30	970	280	15700
Magnesium	mg/L	90	82	80	63	53	59	57	59	68	61	63
Alkalinity	mg/L	423	439	562	400	395	410	215	450	45	330	298
Sulfate	mg/L	1870	1850	1920	625	600	575	550	575	850	425	575
Dissolved silica	mg/L	21.3	21.2	16.5	NA	NA	18.25	10.25	16.25	4.44	18	15.5
Sodium	mg/L	845	903	882								
Potassium	mg/L	3.08	3.15	2.97								
Manganese	ug/L	1530	1510	1360								
TOC	mg/L	7.2	7.3	9.8								
Residue, Dissolved	mg/L	2600	2560	2710								
Chloride	mg/L	152	155	184								
Nitrate	mg/L	1.86	1.91	1.92								

Results of Column Test for Moffett Field Simulation

pH Data			Port					
Flowrate (ft/day)	Date	Time	I	A	B	C	D	O
25	6/14/00	0.729167	7.25	8.41	8.81	9.35	9.62	9.68
25	6/20/00	0.625	7.32	8.51	8.85	9.42	9.65	9.63
25	6/23/00	0.6875	7.29	8.48	8.88	9.46	9.69	9.72
25	6/30/00	0.638889	7.35	8.51	8.86	9.51	9.72	9.74
25	7/6/00	0.604167	7.31	8.55	8.91	9.58	9.77	9.81
25	7/13/00	0.645833	7.29	8.59	8.96	9.62	9.81	9.86
25	7/20/00	0.739583	7.38	8.53	8.89	9.53	9.74	9.73
25	7/28/00	0.666667	7.32	8.56	8.92	9.57	9.81	9.85
12.5	8/7/00	0.604167	7.36	8.73	9.01	9.62	9.96	10.03
6	8/12/00	0.666667	7.36	8.82	9.26	9.86	10.12	10.09
12.5	9/7/00	0.6875	7.29	8.79	9.21	9.79	10.06	10.09
12.5	10/10/00	0.479167	7.35	8.86	9.35	9.83	10.09	10.21
12.5	11/16/00	0.444444	7.41	8.91	9.42	9.74	10.01	10.16
12.5	12/19/00	0.708333	7.46	8.88	9.37	9.9	10.15	10.25
12.5	1/24/01	0.666667	7.39	8.72	9.32	9.7	10.19	10.27
12.5	2/12/01	0.770833	7.42	8.93	9.48	9.92	10.06	10.19
12.5	4/12/01	0.625	7.43	8.96	9.55	9.99	10.11	10.16
12.5	5/7/01	0.763889	7.38	8.91	9.5	9.91	10.13	10.18
12.5	6/27/01	0.666667	7.35	8.92	9.56	9.96	10.18	10.23

ORP Data			Port					
PVs	Date	Time	I	A	B	C	D	O
15	6/14/00	0.729167	35.8	-555.2	-615.7	-642.2	-672.5	-676.8
58	6/20/00	0.625	15.2	-549.5	-611.5	-638.5	-668.3	-669.5
84	6/23/00	0.6875	21.4	-564.8	-621.4	-647.8	-676.8	-679.5
134	6/30/00	0.638889	10.5	-568.5	-627.5	-653.2	-681.2	-683.5
153	7/6/00	0.604167	25.4	-561.5	-628.4	-651.4	-676	-676.9
203	7/13/00	0.645833	2.9	-559.6	-631.4	-657.3	-681.2	-683.4
249	7/20/00	0.739583	31.5	-563.8	-639.5	-660.5	-683.7	-686.9
283	7/28/00	0.666667	16.3	-567.9	-642.1	-669.2	-692.7	-693.6
317	8/7/00	0.604167	10.5	-572.3	-653.2	-676.9	-701.1	-699.5
327	8/12/00	0.666667	3.9	-581.6	-663.4	-685.4	-699.4	-693.4
408	9/7/00	0.6875	14.7	-577.6	-659.3	-683.7	-696.6	-695.4
499	10/10/00	0.479167	6.5	-582.4	-660.4	-690.4	-699.7	-702.4
592	11/16/00	0.444444	21.2	-586.4	-662	-685.4	-691.4	-693.4
739	12/19/00	0.708333	11.3	-572.6	-664.7	-686.9	-697.4	-693.4
816	1/24/01	0.666667	12.4	-581	-658.7	-679.4	-695.1	-695.1
923	2/12/01	0.770833	9.8	-583.2	-669.1	-683.6	-693.8	-694.2
1047	4/12/01	0.625	12.3	-586.2	-671.4	-685	-694.7	-698.3
1103	5/7/01	0.763889	19.4	-581.4	-666.7	-681	-690.1	-697.6
1310	6/27/01	0.666667	22.3	-583.4	-676.4	-686.9	-693.4	-699.1

Results of Column Test for Lowry Simulation

Parameter (µg/L)	PVs 46	PVs 84	PVs 148	PVs 196	PVs 229	PVs 265	PVs 324	PVs 482	PVs 1023	PVs 1057	PVs 1298
Dichloroethane	<5	<5	<5	<5	<5	<5	<5	<5	<5	<5	<5
cis-1,2-Dichloroethene	36.4	38.5	41.0	37.6	40.5	39.1	35.7	37.6	34.3	36.1	38.6
trans-1,2-Dichloroethene	7.53	6.73	6.98	6.88	6.79	6.93	7.24	7.11	6.86	6.54	7.25
Trichloroethene	77.8	569.2	4454.5	444.5	576.9	652.3	529.3	896.1	645.7	582.6	591.3
Tetrachloroethene	<5	<5	<5	<5	<5	<5	<5	<5	<5	<5	<5
Vinyl Chloride	<2	<2	<2	<2	<2	<2	<2	<2	<2	<2	<2
Dichloroethane	<5	<5	<5	<5	<5	<5	<5	<5	<5	<5	<5
cis-1,2-Dichloroethene	38.4	34.5	31.2	36.7	37.8	38.6	39.7	33.4	37.4	33.1	35.9
trans-1,2-Dichloroethene	7.89	7.24	7.35	7.14	7.07	7.23	7.06	6.98	6.56	6.74	6.19
Trichloroethene	47.6	234.5	2054.8	201.3	223.8	278.6	257.8	444.0	287.5	302.4	305.4
Tetrachloroethene	<5	<5	<5	<5	<5	<5	<5	<5	<5	<5	<5
Vinyl Chloride	<2	<2	<2	<2	<2	<2	<2	<2	<2	<2	<2
Dichloroethane	<5	<5	<5	<5	<5	<5	<5	<5	<5	<5	<5
cis-1,2-Dichloroethene	39.1	36.9	38.5	35.3	40.0	37.5	36.9	35.4	38.7	42.1	44.1
trans-1,2-Dichloroethene	8.09	7.35	7.59	7.49	7.63	8.14	7.94	7.64	7.12	6.39	7.01
Trichloroethene	41.3	106.8	1096.2	142.3	171.6	173.4	176.4	261.4	222.1	215.6	228.7
Tetrachloroethene	<5	<5	<5	<5	<5	<5	<5	<5	<5	<5	<5
Vinyl Chloride	<2	<2	<2	<2	<2	<2	<2	<2	<2	<2	<2
Dichloroethane	<5	<5	<5	<5	<5	<5	<5	<5	<5	<5	<5
cis-1,2-Dichloroethene	37.5	41.3	39.8	42.3	37.5	39.8	44.5	41.2	44.5	37.8	39.6
trans-1,2-Dichloroethene	7.19	7.23	7.05	6.98	7.24	6.86	7.08	6.87	6.97	6.49	6.90
Trichloroethene	38.5	75.6	564.8	129.3	151.3	145.7	141.2	184.7	191.7	188.3	196.4
Tetrachloroethene	<5	<5	<5	<5	<5	<5	<5	<5	<5	<5	<5
Vinyl Chloride	<2	<2	<2	<2	<2	<2	<2	<2	<2	<2	<2
Dichloroethane	<5	<5	<5	<5	<5	<5	<5	<5	<5	<5	<5
cis-1,2-Dichloroethene	41.2	43.4	40.9	39.7	36.9	41.9	42.5	40.2	37.8	36.1	37.8
trans-1,2-Dichloroethene	8.25	7.64	7.85	7.77	7.59	7.83	7.69	7.81	8.16	7.79	7.57
Trichloroethene	34.2	55.2	294.3	117.8	113.2	103.4	93.1	115.1	153.4	158.9	161.2
Tetrachloroethene	<5	<5	<5	<5	<5	<5	<5	<5	<5	<5	<5
Vinyl Chloride	<2	<2	<2	<2	<2	<2	<2	<2	<2	<2	<2
Dichloroethane	<5	<5	<5	<5	<5	<5	<5	<5	<5	<5	<5
cis-1,2-Dichloroethene	39.5	38.6	43.5	37.6	34.6	35.6	32.3	36.7	39.0	38.1	37.6
trans-1,2-Dichloroethene	8.11	7.98	7.68	7.52	7.69	7.03	7.27	7.61	7.71	7.09	7.64
Trichloroethene	35.1	43.6	232.1	105.0	101.2	92.3	79.6	86.4	134.2	145.4	148.6
Tetrachloroethene	<5	<5	<5	<5	<5	<5	<5	<5	<5	<5	<5
Vinyl Chloride	<2	<2	<2	<2	<2	<2	<2	<2	<2	<2	<2

Results of Column Test for Lowry Simulation

Inorganic Measurements

Lowry- Filtered		252 PVs - 25 ft/day		324 PVs - 12.5 ft/day		334 PVs - 6 ft/day		1316 PVs - 12.5 ft/day		
Parameter	Units	Filtered Inlet Result	Filtered Outlet Result	Filtered Inlet Result	Filtered Outlet Result	Filtered Inlet Result	Filtered Outlet Result	Filtered Inlet Result	Filtered A Result	Filtered Outlet Result
pH	-	7.41	9.83	7.45	9.91	7.39	10.06	7.45	8.9	10.16
ORP	-	43.9	-691.0	21.4	-690.4	28.3	-691.4	20.7	-596.3	-694.5
Calcium	mg/L	146	41.8	279	177	276	69	277	252	210
Iron	ug/L	40	<30	<30	<30	<30	<30	180	4,050	1760
Magnesium	mg/L	75	33.1	70	73	70	44.9	72	70	69
Alkalinity	mg/L	510	150	610	315	610	65	525	483	420
Sulfate	mg/L	1400	1425	1375	1350	1250	1100	1175	1,250	1300
Dissolved silica	mg/L	NA	NA	19.4	8.8	17.6	2	18.3	18.3	10.4

Lowry - Unfiltered		148 PVs - 25 ft/day			252 PVs - 25 ft/day		324 PVs - 12.5 ft/day		334 PVs - 6 ft/day		1316 PVs - 12.5 ft/day	
Parameter	Units	Unfiltered Inlet Result	Unfiltered A Result	Unfiltered Outlet Result	Unfiltered Inlet Result	Unfiltered Outlet Result	Unfiltered Inlet Result	Unfiltered Outlet Result	Unfiltered Inlet Result	Unfiltered Outlet Result	Unfiltered Inlet Result	Unfiltered Outlet Result
Calcium	mg/L	268	276	298	143	95	276	136	270	89	263	224
Iron	ug/L	300	38500	40100	50	2820	<30	2730	<30	610	190	21100
Magnesium	mg/L	65	70	72	75	66	69	64	69	79	71	72
Alkalinity	mg/L	329	359	453	575	415	590	278	580	95	453	443
Sulfate	mg/L	1880	1960	2020	1350	1175	1225	1375	1300	1275	1250	1275
Dissolved silica	mg/L	21.3	20.5	14.9	NA	NA	18.75	7.75	17.9	2.37	18.3	10.4
TOC	mg/L	7.3	7.6	10.2								
Residue, Dissolved	mg/L	2940	2960	3320								
Sodium, Total	mg/L	440	448	530								
Potassium, Total	mg/L	2.13	2.2	2.04								
Manganese, Total	ug/L	1360	1340	1170								
Chloride	mg/L	119	152	174								
Nitrate	mg/L	1.65	1.72	1.73								

Results of Column Test for Lowry Simulation

pH Data

Flowrate (ft/d)	Port	I	A	B	C	D	O	
25	6/12/00	0.583333	7.35	8.42	8.73	9.39	9.68	9.75
25	6/15/00	0.6875	7.32	8.46	8.76	9.46	9.72	9.72
25	6/20/00	0.604167	7.38	8.41	8.79	9.49	9.75	9.71
25	6/23/00	0.666667	7.36	8.49	8.81	9.47	9.77	9.76
25	6/30/00	0.625	7.31	8.59	8.95	9.56	9.9	9.92
25	7/6/00	0.604167	7.35	8.54	8.92	9.49	9.82	9.78
25	7/13/00	0.645833	7.36	8.61	8.95	9.64	9.92	9.86
25	7/20/00	0.739583	7.41	8.59	8.9	9.54	9.83	9.83
25	7/28/00	0.666667	7.34	8.54	8.83	9.48	9.79	9.76
12.5	8/7/00	0.604167	7.45	8.63	8.95	9.63	9.92	9.91
6	8/12/00	0.666667	7.39	8.72	9.01	9.72	10.03	10.06
12.5	9/7/00	0.6875	7.32	8.81	9.02	9.69	10.01	9.98
12.5	10/10/00	0.479167	7.41	8.78	9.05	9.67	9.97	10.03
12.5	11/16/00	0.444444	7.49	8.73	9.11	9.61	9.92	9.97
12.5	12/19/00	0.708333	7.38	8.81	9.07	9.73	10.01	10.12
12.5	1/24/01	0.666667	7.43	8.79	8.99	9.65	10.07	10.04
12.5	2/12/01	0.770833	7.4	8.86	9.1	9.63	9.93	9.99
12.5	4/12/01	0.625	7.48	8.91	9.16	9.72	9.95	10.09
12.5	5/7/01	0.763889	7.39	8.87	9.23	9.8	9.96	10.11
12.5	6/27/01	0.666667	7.45	8.9	9.29	9.86	9.99	10.16

ORP Data

PVs	Port	I	A	B	C	D	O	
15	36689	0.583333	35.6	-558.9	-615.4	-642.5	-678.2	-672.5
35	36692	0.6875	38.4	-571.4	-620.5	-640.1	-682.2	-680.5
55	36697	0.604167	25.2	-576.5	-624.5	-643.8	-685.9	-683.4
84	36700	0.666667	15.6	-572.3	-625.8	-642.5	-686.2	-690.4
137	36707	0.625	2.8	-582.3	-631.5	-648.4	-690.5	-693.2
155	36713	0.604167	15.9	-576.2	-634.5	-649.5	-686.2	-688.9
196	36720	0.645833	36.8	-582.3	-643.5	-653.9	-681.2	-685.3
252	36727	0.739583	43.9	-576.9	-649.8	-656.7	-689.4	-691
292	36735	0.666667	23.1	-572.3	-645.2	-651.8	-681.3	-684.7
324	36745	0.604167	21.4	-579.3	-654	-659.7	-691.3	-690.4
334	36750	0.666667	28.3	-586.7	-663.4	-669.7	-693.7	-691.4
412	36776	0.6875	22.5	-591.4	-665.9	-672.4	-692.5	-689.7
505	36809	0.479167	19.6	-583.7	-661.4	-671.4	-693.4	-694.8
612	36846	0.444444	17.4	-589.4	-667.2	-673.5	-694.7	-691.4
744	36879	0.708333	19.3	-591.3	-663.4	-677.4	-690.8	-693.2
844	36915	0.666667	22.5	-583.4	-663.8	-672	-691.5	-689.3
937	36934	0.770833	20.4	-585.1	-667.4	-672.9	-690.8	-693.6
1057	36993	0.625	12.8	-588.9	-671.4	-676.1	-695.3	-695.7
1113	37018	0.763889	15.4	-591.2	-669.8	-675	-691.2	-693.7
1316	37069	0.666667	20.7	-596.3	-672.4	-677.6	-693.2	-694.5

Appendix C-6

TCE and Inorganics in Downgradient Aquifer

Graphs Showning Absolute and Relative Amounts of TCE, Ca, and Alkalinity in the Downgradient Aquifer at Moffett Field – May 2001

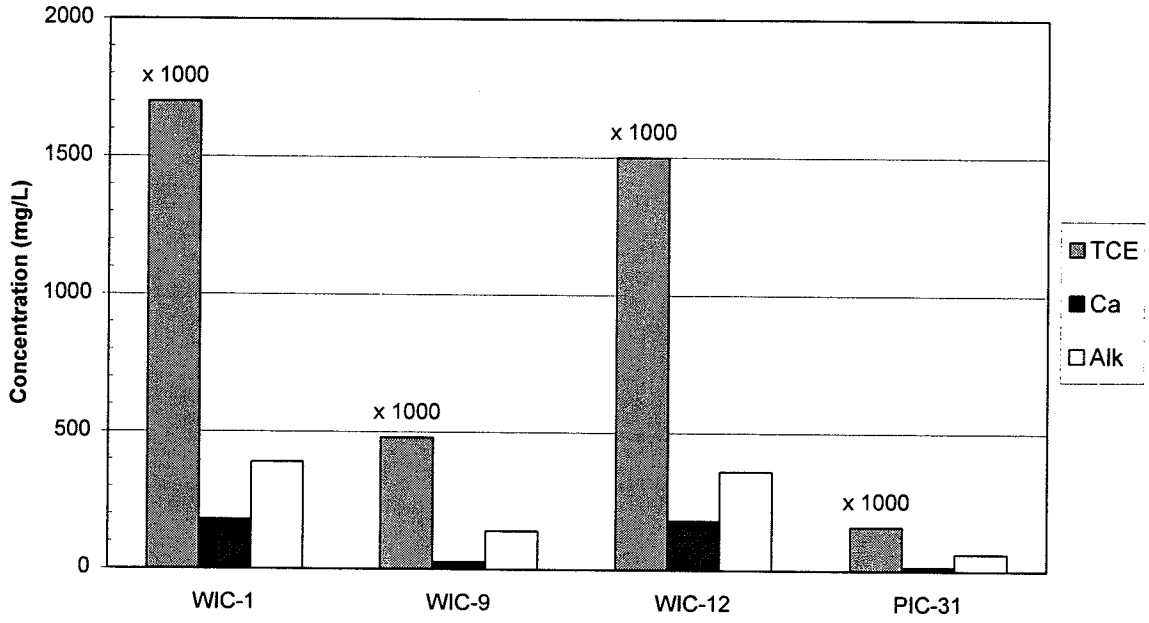

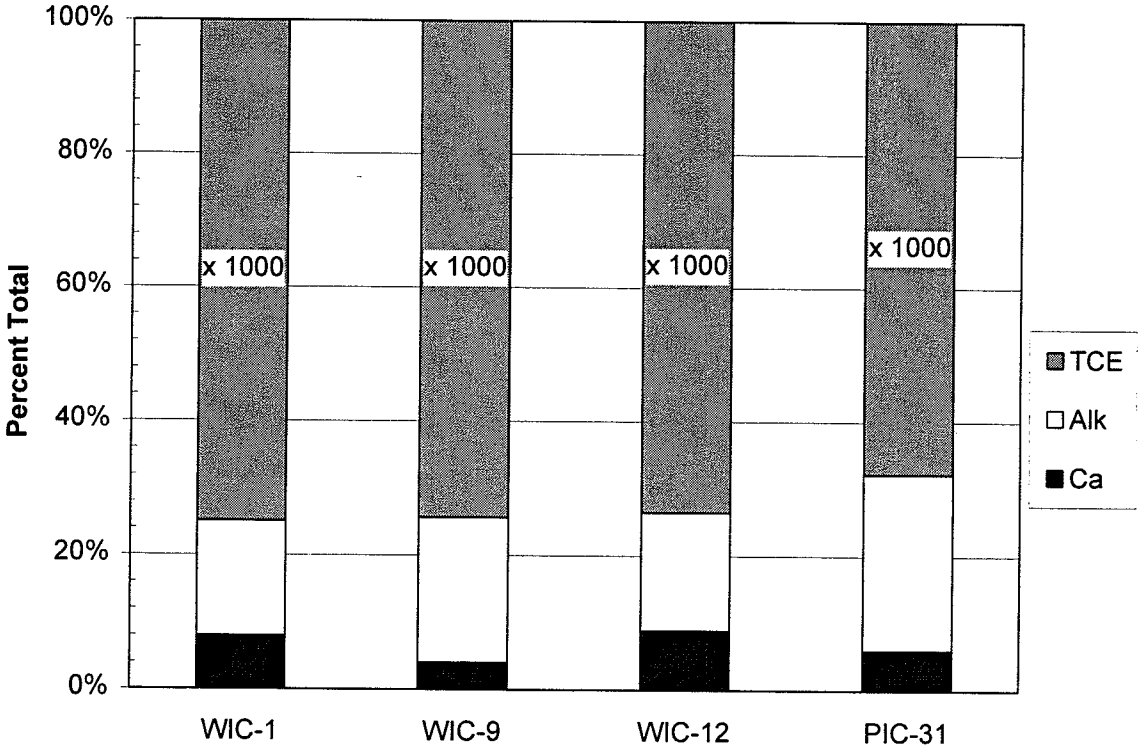

Appendix D

Supporting Information for Cost and Longevity Scenarios

Table D-1. Present value calculations for former NAS Moffett Field for PRB life expectancy of 5 years

Year	Discount factor (r=2.9%)	P&T Cost	PV(P&T)	PV(P&T) - cumulative	PRB Cost	PV(PRB)	PV(PRB) - cumulative
0	1	$1,412,086	$1,412,086	$1,412,086	$4,910,943	$4,910,943	$4,910,943
1	0.971817	$694,746	$675,166	$2,087,252	$72,278	$70,241	$4,981,184
2	0.944429	$694,746	$656,138	$2,743,390	$72,278	$68,261	$5,049,445
3	0.917812	$694,746	$637,646	$3,381,037	$72,278	$66,338	$5,115,783
4	0.891946	$694,746	$619,676	$4,000,713	$72,278	$64,468	$5,180,251
5	0.866808	**$1,194,746**	$1,035,616	$5,036,329	**$4,690,400**	$4,065,678	$9,245,929
6	0.842379	$694,746	$585,240	$5,621,568	$72,278	$60,886	$9,306,815
7	0.818639	$694,746	$568,746	$6,190,314	$72,278	$59,170	$9,365,984
8	0.795567	$694,746	$552,717	$6,743,032	$72,278	$57,502	$9,423,487
9	0.773146	$694,746	$537,140	$7,280,172	$72,278	$55,881	$9,479,368
10	0.751357	**$1,194,746**	$897,681	$8,177,852	**$4,690,400**	$3,524,164	$13,003,532
11	0.730182	$694,746	$507,291	$8,685,143	$72,278	$52,776	$13,056,308
12	0.709603	$694,746	$492,994	$9,178,137	$72,278	$51,289	$13,107,597
13	0.689605	$694,746	$479,100	$9,657,237	$72,278	$49,843	$13,157,440
14	0.67017	$694,746	$465,598	$10,122,835	$72,278	$48,439	$13,205,879
15	0.651282	**$1,194,746**	$778,117	$10,900,952	**$4,690,400**	$3,054,775	$16,260,654
16	0.632928	$694,746	$439,724	$11,340,676	$72,278	$45,747	$16,306,401
17	0.61509	$694,746	$427,331	$11,768,007	$72,278	$44,457	$16,350,858
18	0.597755	$694,746	$415,288	$12,183,295	$72,278	$43,205	$16,394,063
19	0.580909	$694,746	$403,584	$12,586,879	$72,278	$41,987	$16,436,050
20	0.564537	**$1,194,746**	$674,478	$13,261,357	**$4,690,400**	$2,647,905	$19,083,954
21	0.548627	$694,746	$381,156	$13,642,514	$72,278	$39,654	$19,123,608
22	0.533165	$694,746	$370,414	$14,012,928	$72,278	$38,536	$19,162,144
23	0.518139	$694,746	$359,975	$14,372,903	$72,278	$37,450	$19,199,594
24	0.503537	$694,746	$349,830	$14,722,733	$72,278	$36,395	$19,235,989
25	0.489346	**$1,194,746**	$584,644	$15,307,377	**$4,690,400**	$2,295,226	$21,531,215
26	0.475554	$694,746	$330,390	$15,637,766	$72,278	$34,372	$21,565,587
27	0.462152	$694,746	$321,078	$15,958,845	$72,278	$33,403	$21,598,991
28	0.449127	$694,746	$312,029	$16,270,874	$72,278	$32,462	$21,631,453
29	0.43647	$694,746	$303,236	$16,574,110	$72,278	$31,547	$21,663,000
30	0.424169	**$1,194,746**	$506,774	$17,080,884	**$4,690,400**	$1,989,522	$23,652,521

Table D-2. Present value calculations for former NAS Moffett Field for a PRB life expectancy

Year	Discount factor (r=2.9%)	P&T Cost	PV(P&T)	PV(P&T) - cumulative	PRB Cost	PV(PRB)	PV(PRB) - cumulative
0	1	$1,412,086	$1,412,086	$1,412,086	$4,910,943	$4,910,943	$4,910,943
1	0.971817	$694,746	$675,166	$2,087,252	$72,278	$70,241	$4,981,184
2	0.944429	$694,746	$656,138	$2,743,390	$72,278	$68,261	$5,049,445
3	0.917812	$694,746	$637,646	$3,381,037	$72,278	$66,338	$5,115,783
4	0.891946	$694,746	$619,676	$4,000,713	$72,278	$64,468	$5,180,251
5	0.866808	**$1,194,746**	$1,035,616	$5,036,329	$72,278	$62,651	$5,242,902
6	0.842379	$694,746	$585,240	**$5,621,568**	$72,278	$60,886	**$5,303,788**
7	0.818639	$694,746	$568,746	$6,190,314	$72,278	$59,170	$5,362,957
8	0.795567	$694,746	$552,717	$6,743,032	$72,278	$57,502	$5,420,459
9	0.773146	$694,746	$537,140	$7,280,172	$72,278	$55,881	$5,476,341
10	0.751357	**$1,194,746**	$897,681	**$8,177,852**	**$4,690,400**	$3,524,164	**$9,000,505**
11	0.730182	$694,746	$507,291	$8,685,143	$72,278	$52,776	$9,053,281
12	0.709603	$694,746	$492,994	**$9,178,137**	$72,278	$51,289	**$9,104,570**
13	0.689605	$694,746	$479,100	$9,657,237	$72,278	$49,843	$9,154,413
14	0.67017	$694,746	$465,598	$10,122,835	$72,278	$48,439	$9,202,852
15	0.651282	**$1,194,746**	$778,117	$10,900,952	$72,278	$47,073	$9,249,925
16	0.632928	$694,746	$439,724	$11,340,676	$72,278	$45,747	$9,295,672
17	0.61509	$694,746	$427,331	$11,768,007	$72,278	$44,457	$9,340,129
18	0.597755	$694,746	$415,288	$12,183,295	$72,278	$43,205	$9,383,334
19	0.580909	$694,746	$403,584	$12,586,879	$72,278	$41,987	$9,425,321
20	0.564537	**$1,194,746**	$674,478	$13,261,357	**$4,690,400**	$2,647,905	$12,073,226
21	0.548627	$694,746	$381,156	$13,642,514	$72,278	$39,654	$12,112,879
22	0.533165	$694,746	$370,414	$14,012,928	$72,278	$38,536	$12,151,415
23	0.518139	$694,746	$359,975	$14,372,903	$72,278	$37,450	$12,188,865
24	0.503537	$694,746	$349,830	$14,722,733	$72,278	$36,395	$12,225,260
25	0.489346	**$1,194,746**	$584,644	$15,307,377	$72,278	$35,369	$12,260,629
26	0.475554	$694,746	$330,390	$15,637,766	$72,278	$34,372	$12,295,001
27	0.462152	$694,746	$321,078	$15,958,845	$72,278	$33,403	$12,328,404
28	0.449127	$694,746	$312,029	$16,270,874	$72,278	$32,462	$12,360,867
29	0.43647	$694,746	$303,236	$16,574,110	$72,278	$31,547	$12,392,414
30	0.424169	**$1,194,746**	$506,774	$17,080,884	**$4,690,400**	$1,989,522	$14,381,935

Table D-3. Present value calculations for former NAS Moffett Field for a PRB life expectancy of 15 years

Year	Discount factor (r=2.9%)	P&T Cost	PV(P&T)	PV(P&T) - cumulative	PRB Cost	PV(PRB)	PV(PRB) - cumulative
0	1	$1,412,086	$1,412,086	$1,412,086	$4,910,943	$4,910,943	$4,910,943
1	0.971817	$694,746	$675,166	$2,087,252	$72,278	$70,241	$4,981,184
2	0.944429	$694,746	$656,138	$2,743,390	$72,278	$68,261	$5,049,445
3	0.917812	$694,746	$637,646	$3,381,037	$72,278	$66,338	$5,115,783
4	0.891946	$694,746	$619,676	$4,000,713	$72,278	$64,468	$5,180,251
5	0.866808	**$1,194,746**	$1,035,616	$5,036,329	$72,278	$62,651	$5,242,902
6	0.842379	$694,746	$585,240	**$5,621,568**	$72,278	$60,886	**$5,303,788**
7	0.818639	$694,746	$568,746	$6,190,314	$72,278	$59,170	$5,362,957
8	0.795567	$694,746	$552,717	$6,743,032	$72,278	$57,502	$5,420,459
9	0.773146	$694,746	$537,140	$7,280,172	$72,278	$55,881	$5,476,341
10	0.751357	**$1,194,746**	$897,681	$8,177,852	$72,278	$54,307	$5,530,647
11	0.730182	$694,746	$507,291	$8,685,143	$72,278	$52,776	$5,583,424
12	0.709603	$694,746	$492,994	$9,178,137	$72,278	$51,289	$5,634,712
13	0.689605	$694,746	$479,100	$9,657,237	$72,278	$49,843	$5,684,555
14	0.67017	$694,746	$465,598	$10,122,835	$72,278	$48,439	$5,732,994
15	0.651282	**$1,194,746**	$778,117	$10,900,952	**$4,690,400**	$3,054,775	$8,787,769
16	0.632928	$694,746	$439,724	$11,340,676	$72,278	$45,747	$8,833,516
17	0.61509	$694,746	$427,331	$11,768,007	$72,278	$44,457	$8,877,973
18	0.597755	$694,746	$415,288	$12,183,295	$72,278	$43,205	$8,921,178
19	0.580909	$694,746	$403,584	$12,586,879	$72,278	$41,987	$8,963,165
20	0.564537	**$1,194,746**	$674,478	$13,261,357	$72,278	$40,804	$9,003,968
21	0.548627	$694,746	$381,156	$13,642,514	$72,278	$39,654	$9,043,622
22	0.533165	$694,746	$370,414	$14,012,928	$72,278	$38,536	$9,082,158
23	0.518139	$694,746	$359,975	$14,372,903	$72,278	$37,450	$9,119,608
24	0.503537	$694,746	$349,830	$14,722,733	$72,278	$36,395	$9,156,003
25	0.489346	**$1,194,746**	$584,644	$15,307,377	$72,278	$35,369	$9,191,372
26	0.475554	$694,746	$330,390	$15,637,766	$72,278	$34,372	$9,225,744
27	0.462152	$694,746	$321,078	$15,958,845	$72,278	$33,403	$9,259,147
28	0.449127	$694,746	$312,029	$16,270,874	$72,278	$32,462	$9,291,609
29	0.43647	$694,746	$303,236	$16,574,110	$72,278	$31,547	$9,323,157
30	0.424169	**$1,194,746**	$506,774	$17,080,884	**$4,690,400**	$1,989,522	$11,312,678

Table D-4. Present value calculations for former NAS Moffett Field for a PRB life expectancy of 20 years

Year	Discount factor (r=2.9%)	P&T Cost	PV(P&T)	PV(P&T) - cumulative	PRB Cost	PV(PRB)	PV(PRB) - cumulative
0	1	$1,412,086	$1,412,086	$1,412,086	$4,910,943	$4,910,943	$4,910,943
1	0.971817	$694,746	$675,166	$2,087,252	$72,278	$70,241	$4,981,184
2	0.944429	$694,746	$656,138	$2,743,390	$72,278	$68,261	$5,049,445
3	0.917812	$694,746	$637,646	$3,381,037	$72,278	$66,338	$5,115,783
4	0.891946	$694,746	$619,676	$4,000,713	$72,278	$64,468	$5,180,251
5	0.866808	**$1,194,746**	$1,035,616	$5,036,329	$72,278	$62,651	$5,242,902
6	0.842379	$694,746	$585,240	**$5,621,568**	$72,278	$60,886	**$5,303,788**
7	0.818639	$694,746	$568,746	$6,190,314	$72,278	$59,170	$5,362,957
8	0.795567	$694,746	$552,717	$6,743,032	$72,278	$57,502	$5,420,459
9	0.773146	$694,746	$537,140	$7,280,172	$72,278	$55,881	$5,476,341
10	0.751357	**$1,194,746**	$897,681	$8,177,852	$72,278	$54,307	$5,530,647
11	0.730182	$694,746	$507,291	$8,685,143	$72,278	$52,776	$5,583,424
12	0.709603	$694,746	$492,994	$9,178,137	$72,278	$51,289	$5,634,712
13	0.689605	$694,746	$479,100	$9,657,237	$72,278	$49,843	$5,684,555
14	0.67017	$694,746	$465,598	$10,122,835	$72,278	$48,439	$5,732,994
15	0.651282	**$1,194,746**	$778,117	$10,900,952	$72,278	$47,073	$5,780,067
16	0.632928	$694,746	$439,724	$11,340,676	$72,278	$45,747	$5,825,814
17	0.61509	$694,746	$427,331	$11,768,007	$72,278	$44,457	$5,870,272
18	0.597755	$694,746	$415,288	$12,183,295	$72,278	$43,205	$5,913,476
19	0.580909	$694,746	$403,584	$12,586,879	$72,278	$41,987	$5,955,463
20	0.564537	**$1,194,746**	$674,478	$13,261,357	**$4,983,221**	$2,813,213	$8,768,676
21	0.548627	$694,746	$381,156	$13,642,514	$72,278	$39,654	$8,808,330
22	0.533165	$694,746	$370,414	$14,012,928	$72,278	$38,536	$8,846,866
23	0.518139	$694,746	$359,975	$14,372,903	$72,278	$37,450	$8,884,316
24	0.503537	$694,746	$349,830	$14,722,733	$72,278	$36,395	$8,920,711
25	0.489346	**$1,194,746**	$584,644	$15,307,377	$72,278	$35,369	$8,956,080
26	0.475554	$694,746	$330,390	$15,637,766	$72,278	$34,372	$8,990,452
27	0.462152	$694,746	$321,078	$15,958,845	$72,278	$33,403	$9,023,855
28	0.449127	$694,746	$312,029	$16,270,874	$72,278	$32,462	$9,056,317
29	0.43647	$694,746	$303,236	$16,574,110	$72,278	$31,547	$9,087,864
30	0.424169	**$1,194,746**	$506,774	$17,080,884	**$72,278**	$30,658	$9,118,522

Table D-5. Present value calculations for former NAS Moffett Field for a PRB life expectancy of 30 years

Year	Discount factor (r=2.9%)	P&T Cost	PV(P&T)	PV(P&T) - cumulative	PRB Cost	PV(PRB)	PV(PRB) - cumulative
0	1	$1,412,086	$1,412,086	$1,412,086	$4,910,943	$4,910,943	$4,910,943
1	0.971817	$694,746	$675,166	$2,087,252	$72,278	$70,241	$4,981,184
2	0.944429	$694,746	$656,138	$2,743,390	$72,278	$68,261	$5,049,445
3	0.917812	$694,746	$637,646	$3,381,037	$72,278	$66,338	$5,115,783
4	0.891946	$694,746	$619,676	$4,000,713	$72,278	$64,468	$5,180,251
5	0.866808	**$1,194,746**	$1,035,616	$5,036,329	$72,278	$62,651	$5,242,902
6	0.842379	$694,746	$585,240	**$5,621,568**	$72,278	$60,886	**$5,303,788**
7	0.818639	$694,746	$568,746	$6,190,314	$72,278	$59,170	$5,362,957
8	0.795567	$694,746	$552,717	$6,743,032	$72,278	$57,502	$5,420,459
9	0.773146	$694,746	$537,140	$7,280,172	$72,278	$55,881	$5,476,341
10	0.751357	**$1,194,746**	$897,681	$8,177,852	$72,278	$54,307	$5,530,647
11	0.730182	$694,746	$507,291	$8,685,143	$72,278	$52,776	$5,583,424
12	0.709603	$694,746	$492,994	$9,178,137	$72,278	$51,289	$5,634,712
13	0.689605	$694,746	$479,100	$9,657,237	$72,278	$49,843	$5,684,555
14	0.67017	$694,746	$465,598	$10,122,835	$72,278	$48,439	$5,732,994
15	0.651282	**$1,194,746**	$778,117	$10,900,952	$72,278	$47,073	$5,780,067
16	0.632928	$694,746	$439,724	$11,340,676	$72,278	$45,747	$5,825,814
17	0.61509	$694,746	$427,331	$11,768,007	$72,278	$44,457	$5,870,272
18	0.597755	$694,746	$415,288	$12,183,295	$72,278	$43,205	$5,913,476
19	0.580909	$694,746	$403,584	$12,586,879	$72,278	$41,987	$5,955,463
20	0.564537	**$1,194,746**	$674,478	$13,261,357	$72,278	$40,804	$5,996,267
21	0.548627	$694,746	$381,156	$13,642,514	$72,278	$39,654	$6,035,920
22	0.533165	$694,746	$370,414	$14,012,928	$72,278	$38,536	$6,074,456
23	0.518139	$694,746	$359,975	$14,372,903	$72,278	$37,450	$6,111,906
24	0.503537	$694,746	$349,830	$14,722,733	$72,278	$36,395	$6,148,301
25	0.489346	**$1,194,746**	$584,644	$15,307,377	$72,278	$35,369	$6,183,670
26	0.475554	$694,746	$330,390	$15,637,766	$72,278	$34,372	$6,218,042
27	0.462152	$694,746	$321,078	$15,958,845	$72,278	$33,403	$6,251,446
28	0.449127	$694,746	$312,029	$16,270,874	$72,278	$32,462	$6,283,908
29	0.43647	$694,746	$303,236	$16,574,110	$72,278	$31,547	$6,315,455
30	0.424169	**$1,194,746**	$506,774	$17,080,884	**$4,983,221**	$2,113,727	$8,429,182

Table D-6. PV Analysis of PRB and P&T systems for Area 5 assuming 5-year life of PRB at Dover AFB

	PRB			P&T System		
Year	Annual Cost	PV of Annual Cost	Cumulative PV of Annual Cost	Annual Cost	PV of Annual Cost	Cumulative PV of Annual Cost
0	$947,000	$947,000	$947,000	$502,000	$502,000	$502,000
1	$148,000	$143,829	$1,090,829	$214,000	$207,969	$709,969
2	$148,000	$139,775	$1,230,604	$214,000	$202,108	$912,077
3	$148,000	$135,836	$1,366,441	$214,000	$196,412	$1,108,489
4	$148,000	$132,008	$1,498,449	$214,000	$190,876	$1,299,365
5	**$569,000**	$493,214	$1,991,663	$235,000	$203,700	$1,503,065
6	$148,000	$124,672	$2,116,335	$214,000	$180,269	$1,683,334
7	$148,000	$121,159	$2,237,493	$214,000	$175,189	$1,858,523
8	$148,000	$117,744	$2,355,237	$214,000	$170,251	$2,028,774
9	$148,000	$114,426	$2,469,663	$214,000	$165,453	$2,194,228
10	**$569,000**	$427,522	$2,897,185	$242,000	$181,828	$2,376,056
11	$148,000	$108,067	$3,005,252	$214,000	$156,259	$2,532,315
12	$148,000	$105,021	$3,110,273	$214,000	$151,855	$2,684,170
13	$148,000	$102,061	$3,212,335	$214,000	$147,575	$2,831,745
14	$148,000	$99,185	$3,311,520	$214,000	$143,416	$2,975,162
15	**$569,000**	$370,580	$3,682,099	$235,000	$153,051	$3,128,213
16	$148,000	$93,673	$3,775,773	$214,000	$135,446	$3,263,659
17	$148,000	$91,033	$3,866,806	$214,000	$131,629	$3,395,289
18	$148,000	$88,468	$3,955,274	$214,000	$127,920	$3,523,208
19	$148,000	$85,974	$4,041,248	$214,000	$124,314	$3,647,523
20	**$569,000**	$321,222	$4,362,470	$242,000	$136,618	$3,784,141
21	$148,000	$81,197	$4,443,667	$242,000	$132,768	$3,916,908
22	$148,000	$78,908	$4,522,575	$214,000	$114,097	$4,031,006
23	$148,000	$76,685	$4,599,260	$214,000	$110,882	$4,141,887
24	$148,000	$74,523	$4,673,783	$214,000	$107,757	$4,249,644
25	**$569,000**	$278,438	$4,952,221	$235,000	$114,996	$4,364,641
26	$148,000	$70,382	$5,022,603	$214,000	$101,769	$4,466,409
27	$148,000	$68,399	$5,091,001	$214,000	$98,901	$4,565,310
28	$148,000	$66,471	$5,157,472	$214,000	$96,113	$4,661,423
29	$148,000	$64,598	$5,222,070	$214,000	$93,405	$4,754,827
30	**$569,000**	$241,352	$5,463,422	$242,000	$102,649	$4,857,476

Table D-7. PV Analysis of PRB and P&T systems for Area 5 assuming 10-year life of PRB at Dover AFB

	PRB			P&T System		
Year	Annual Cost	PV of Annual Cost	Cumulative PV of Annual Cost	Annual Cost	PV of Annual Cost	Cumulative PV of Annual Cost
0	$947,000	$947,000	$947,000	$502,000	$502,000	$502,000
1	$148,000	$143,829	$1,090,829	$214,000	$207,969	$709,969
2	$148,000	$139,775	$1,230,604	$214,000	$202,108	$912,077
3	$148,000	$135,836	$1,366,441	$214,000	$196,412	$1,108,489
4	$148,000	$132,008	$1,498,449	$214,000	$190,876	$1,299,365
5	$148,000	$128,288	$1,626,736	$235,000	$203,700	$1,503,065
6	$148,000	$124,672	$1,751,408	$214,000	$180,269	$1,683,334
7	$148,000	$121,159	$1,872,567	$214,000	$175,189	$1,858,523
8	$148,000	$117,744	$1,990,311	$214,000	$170,251	$2,028,774
9	$148,000	$114,426	$2,104,737	$214,000	$165,453	$2,194,228
10	**$569,000**	$427,522	$2,532,259	$242,000	$181,828	$2,376,056
11	$148,000	$108,067	$2,640,326	$214,000	$156,259	$2,532,315
12	$148,000	$105,021	$2,745,347	$214,000	$151,855	$2,684,170
13	$148,000	$102,061	$2,847,408	$214,000	$147,575	$2,831,745
14	$148,000	$99,185	$2,946,593	$214,000	$143,416	$2,975,162
15	$148,000	$96,390	$3,042,983	$235,000	$153,051	$3,128,213
16	$148,000	$93,673	$3,136,656	$214,000	$135,446	$3,263,659
17	$148,000	$91,033	$3,227,690	$214,000	$131,629	$3,395,289
18	$148,000	$88,468	$3,316,158	$214,000	$127,920	$3,523,208
19	$148,000	$85,974	$3,402,132	$214,000	$124,314	$3,647,523
20	**$569,000**	$321,222	$3,723,354	$242,000	$136,618	$3,784,141
21	$148,000	$81,197	$3,804,550	$242,000	$132,768	$3,916,908
22	$148,000	$78,908	$3,883,459	$214,000	$114,097	$4,031,006
23	$148,000	$76,685	$3,960,143	$214,000	$110,882	$4,141,887
24	$148,000	$74,523	$4,034,667	$214,000	$107,757	$4,249,644
25	$148,000	$72,423	$4,107,090	$235,000	$114,996	$4,364,641
26	$148,000	$70,382	$4,177,472	$214,000	$101,769	$4,466,409
27	$148,000	$68,399	$4,245,871	$214,000	$98,901	$4,565,310
28	$148,000	$66,471	$4,312,341	$214,000	$96,113	$4,661,423
29	$148,000	$64,598	$4,376,939	$214,000	$93,405	$4,754,827
30	**$569,000**	$241,352	$4,618,291	$242,000	$102,649	$4,857,476

Table D-8. PV Analysis of PRB and P&T systems for Area 5 assuming 30-year life of PRB at Dover AFB

	PRB			P&T System		
Year	Annual Cost	PV of Annual Cost	Cumulative PV of Annual Cost	Annual Cost	PV of Annual Cost	Cumulative PV of Annual Cost
0	$947,000	$947,000	$947,000	$502,000	$502,000	$502,000
1	$148,000	$143,829	$1,090,829	$214,000	$207,969	$709,969
2	$148,000	$139,775	$1,230,604	$214,000	$202,108	$912,077
3	$148,000	$135,836	$1,366,441	$214,000	$196,412	$1,108,489
4	$148,000	$132,008	$1,498,449	$214,000	$190,876	$1,299,365
5	$148,000	$128,288	$1,626,736	$235,000	$203,700	$1,503,065
6	$148,000	$124,672	$1,751,408	$214,000	$180,269	$1,683,334
7	$148,000	$121,159	$1,872,567	$214,000	$175,189	$1,858,523
8	$148,000	$117,744	**$1,990,311**	$214,000	$170,251	**$2,028,774**
9	$148,000	$114,426	$2,104,737	$214,000	$165,453	$2,194,228
10	$148,000	$111,201	$2,215,937	$242,000	$181,828	$2,376,056
11	$148,000	$108,067	$2,324,004	$214,000	$156,259	$2,532,315
12	$148,000	$105,021	$2,429,026	$214,000	$151,855	$2,684,170
13	$148,000	$102,061	$2,531,087	$214,000	$147,575	$2,831,745
14	$148,000	$99,185	$2,630,272	$214,000	$143,416	$2,975,162
15	**$569,000**	$370,580	$3,000,852	$235,000	$153,051	$3,128,213
16	$148,000	$93,673	$3,094,525	$214,000	$135,446	$3,263,659
17	$148,000	$91,033	$3,185,558	$214,000	$131,629	$3,395,289
18	$148,000	$88,468	$3,274,026	$214,000	$127,920	$3,523,208
19	$148,000	$85,974	$3,360,001	$214,000	$124,314	$3,647,523
20	$148,000	$83,551	$3,443,552	$242,000	$136,618	$3,784,141
21	$148,000	$81,197	$3,524,749	$242,000	$132,768	$3,916,908
22	$148,000	$78,908	$3,603,657	$214,000	$114,097	$4,031,006
23	$148,000	$76,685	$3,680,342	$214,000	$110,882	$4,141,887
24	$148,000	$74,523	$3,754,865	$214,000	$107,757	$4,249,644
25	$148,000	$72,423	$3,827,289	$235,000	$114,996	$4,364,641
26	$148,000	$70,382	$3,897,671	$214,000	$101,769	$4,466,409
27	$148,000	$68,399	$3,966,069	$214,000	$98,901	$4,565,310
28	$148,000	$66,471	$4,032,540	$214,000	$96,113	$4,661,423
29	$148,000	$64,598	$4,097,137	$214,000	$93,405	$4,754,827
30	**$569,000**	$241,352	$4,338,490	$242,000	$102,649	$4,857,476

Table D-9. PV Analysis of PRB and P&T systems for Area 5 assuming 20-year life of PRB at Dover AFB

	PRB			P&T System		
Year	Annual Cost	PV of Annual Cost	Cumulative PV of Annual Cost	Annual Cost	PV of Annual Cost	Cumulative PV of Annual Cost
0	$947,000	$947,000	$947,000	$502,000	$502,000	$502,000
1	$148,000	$143,829	$1,090,829	$214,000	$207,969	$709,969
2	$148,000	$139,775	$1,230,604	$214,000	$202,108	$912,077
3	$148,000	$135,836	$1,366,441	$214,000	$196,412	$1,108,489
4	$148,000	$132,008	$1,498,449	$214,000	$190,876	$1,299,365
5	$148,000	$128,288	$1,626,736	$235,000	$203,700	$1,503,065
6	$148,000	$124,672	$1,751,408	$214,000	$180,269	$1,683,334
7	$148,000	$121,159	$1,872,567	$214,000	$175,189	$1,858,523
8	$148,000	$117,744	$1,990,311	$214,000	$170,251	$2,028,774
9	$148,000	$114,426	$2,104,737	$214,000	$165,453	$2,194,228
10	$148,000	$111,201	$2,215,937	$242,000	$181,828	$2,376,056
11	$148,000	$108,067	$2,324,004	$214,000	$156,259	$2,532,315
12	$148,000	$105,021	$2,429,026	$214,000	$151,855	$2,684,170
13	$148,000	$102,061	$2,531,087	$214,000	$147,575	$2,831,745
14	$148,000	$99,185	$2,630,272	$214,000	$143,416	$2,975,162
15	$148,000	$96,390	$2,726,662	$235,000	$153,051	$3,128,213
16	$148,000	$93,673	$2,820,335	$214,000	$135,446	$3,263,659
17	$148,000	$91,033	$2,911,369	$214,000	$131,629	$3,395,289
18	$148,000	$88,468	$2,999,836	$214,000	$127,920	$3,523,208
19	$148,000	$85,974	$3,085,811	$214,000	$124,314	$3,647,523
20	**$569,000**	$321,222	$3,407,032	$242,000	$136,618	$3,784,141
21	$148,000	$81,197	$3,488,229	$242,000	$132,768	$3,916,908
22	$148,000	$78,908	$3,567,138	$214,000	$114,097	$4,031,006
23	$148,000	$76,685	$3,643,822	$214,000	$110,882	$4,141,887
24	$148,000	$74,523	$3,718,346	$214,000	$107,757	$4,249,644
25	$148,000	$72,423	$3,790,769	$235,000	$114,996	$4,364,641
26	$148,000	$70,382	$3,861,151	$214,000	$101,769	$4,466,409
27	$148,000	$68,399	$3,929,549	$214,000	$98,901	$4,565,310
28	$148,000	$66,471	$3,996,020	$214,000	$96,113	$4,661,423
29	$148,000	$64,598	$4,060,618	$214,000	$93,405	$4,754,827
30	$148,000	$62,777	$4,123,395	$242,000	$102,649	$4,857,476

Table D-10. PV Analysis of PRB and P&T systems for Area 5 assuming 30-year life of PRB at Dover AFB

	PRB			P&T System		
Year	Annual Cost	PV of Annual Cost	Cumulative PV of Annual Cost	Annual Cost	PV of Annual Cost	Cumulative PV of Annual Cost
0	$947,000	$947,000	$947,000	$502,000	$502,000	$502,000
1	$148,000	$143,829	$1,090,829	$214,000	$207,969	$709,969
2	$148,000	$139,775	$1,230,604	$214,000	$202,108	$912,077
3	$148,000	$135,836	$1,366,441	$214,000	$196,412	$1,108,489
4	$148,000	$132,008	$1,498,449	$214,000	$190,876	$1,299,365
5	$148,000	$128,288	$1,626,736	$235,000	$203,700	$1,503,065
6	$148,000	$124,672	$1,751,408	$214,000	$180,269	$1,683,334
7	$148,000	$121,159	$1,872,567	$214,000	$175,189	$1,858,523
8	$148,000	$117,744	$1,990,311	$214,000	$170,251	$2,028,774
9	$148,000	$114,426	$2,104,737	$214,000	$165,453	$2,194,228
10	$148,000	$111,201	$2,215,937	$242,000	$181,828	$2,376,056
11	$148,000	$108,067	$2,324,004	$214,000	$156,259	$2,532,315
12	$148,000	$105,021	$2,429,026	$214,000	$151,855	$2,684,170
13	$148,000	$102,061	$2,531,087	$214,000	$147,575	$2,831,745
14	$148,000	$99,185	$2,630,272	$214,000	$143,416	$2,975,162
15	$148,000	$96,390	$2,726,662	$235,000	$153,051	$3,128,213
16	$148,000	$93,673	$2,820,335	$214,000	$135,446	$3,263,659
17	$148,000	$91,033	$2,911,369	$214,000	$131,629	$3,395,289
18	$148,000	$88,468	$2,999,836	$214,000	$127,920	$3,523,208
19	$148,000	$85,974	$3,085,811	$214,000	$124,314	$3,647,523
20	$148,000	$83,551	$3,169,362	$242,000	$136,618	$3,784,141
21	$148,000	$81,197	$3,250,559	$242,000	$132,768	$3,916,908
22	$148,000	$78,908	$3,329,468	$214,000	$114,097	$4,031,006
23	$148,000	$76,685	$3,406,152	$214,000	$110,882	$4,141,887
24	$148,000	$74,523	$3,480,676	$214,000	$107,757	$4,249,644
25	$148,000	$72,423	$3,553,099	$235,000	$114,996	$4,364,641
26	$148,000	$70,382	$3,623,481	$214,000	$101,769	$4,466,409
27	$148,000	$68,399	$3,691,879	$214,000	$98,901	$4,565,310
28	$148,000	$66,471	$3,758,350	$214,000	$96,113	$4,661,423
29	$148,000	$64,598	$3,822,948	$214,000	$93,405	$4,754,827
30	**$569,000**	$241,352	$4,064,300	$242,000	$102,649	$4,857,476

Appendix E

Supporting Information for the Hydraulic Performance Evaluation Results

Table 1. Hydraulic Parameters at Seneca Army Depot, New York.

Well	Northing (ft)	Easting (ft)	TOC (ft msl)	Total Depth (ft bgs)	Well Radius (in)	Screen Length (ft)	Slug Test Permeability (ft/day)	April 2001 Water Level (ft msl)	July 2001 Water Level (ft msl)
Bat-1	995205.7	419355.5	636.34	6.29	2	3	36.5	632.15	631.15
Bat-2	995201.0	419356.6	636.35	5.64	2	3	29.0	632.15	631.16
Bat-3	995207.7	419363.3	636.63	7.19	2	3	1.4	632.55	631.21
Bat-4	995203.2	419364.9	636.58	6.32	2	3	24.3	632.56	631.22
Bat-5	995198.0	419365.9	636.70	4.97	2	3	129.1[b]	632.55	631.21
Bat-6	995192.6	419366.9	636.68	NA	2	3	25.5	632.18	631.21
Bat-7	995200.6	419362.3	636.34	NA	1	3	NA	632.16	631.18
Bat-8	995195.9	419363.2	636.40	6.14	1	3	NA	632.16	631.19
Bat-9	995207.3	419369.7	636.94	5.39	2	3	1.5	632.57	631.22
Bat-10	995202.1	419370.9	636.92	5.66	2	3	1.9	632.55	631.22
Bat-11	995196.3	419372.4	636.91	6.19	2	3	67.6	632.57	631.22
Bat-12	995205.6	419375.6	636.85	5.84	2	3	1.4	632.56	631.20
Bat-13	995200.4	419376.2	636.70	6.30	2	3	1.1	632.58	631.20
Bat-14	995203.1	419386.1	637.19	5.63	2	3	12.3	632.55	631.23
MW-T10	995212.2	419359.5	636.07	7.08	2	5	38.2	632.33	631.28

(a) Based on early response.
(b) Poor response to slug due to shallow depth.
Shaded cells are within the CRB.

Table 2. Hydraulic Parameters at Dover AFB, Maryland.

Well	Northing	Easting	TOC	Total Depth (ft)	Well Radius (ft)	Screen Length (ft)	Test	Permeability (ft/day)	Static Water Level (ft bgs)
P1	411417.0	479577.5	27.08	22.20	2	5.0	a	307.65	15.65
P1	411417.0	479577.5	27.08	22.20	2	5.0	b	272.50	15.65
U6S	411394.9	479594.3	27.17	20.30	2	5.0	a	7.22	15.62
U6S	411394.9	479594.3	27.17	20.30	2	5.0	b	7.43	15.62
U15S	411400.8	479599.5	27.14	19.90	2	5.0	a	5.21	15.60
U15S	411400.8	479599.5	27.14	19.90	2	5.0	b	5.15	15.60
U5S	411390.0	479596.5	27.33	20.80	2	5.0	a	2.99	15.78
U5S	411390.0	479596.5	27.33	20.80	2	5.0	b	3.96	15.78
U14S	411395.4	479602.6	27.25	19.30	2	5.0	a	4.99	15.72
U14S	411395.4	479602.6	27.25	19.30	2	5.0	b	3.51	15.72
U4S	411385.1	479600.0	27.43	22.00	2	5.0	a	2.35	15.90
U4S	411385.1	479600.0	27.43	22.00	2	5.0	b	2.31	15.90
U13S	411390.7	479605.3	27.31	20.20	2	5.0	a	2.02	15.78
U13S	411390.7	479605.3	27.31	20.20	2	5.0	b	2.04	15.78
U3S	411379.0	479602.1	27.52	21.80	2	5.0	a	15.42	15.87
U3S	411379.0	479602.1	27.52	21.80	2	5.0	b	15.42	15.87
U12S	411385.1	479608.2	27.36	20.30	2	5.0	a	1.81	15.82
U12S	411385.1	479608.2	27.36	20.30	2	5.0	b	1.78	15.82
U2S	411374.4	479605.4	27.37	20.30	2	5.0	a	2.29	15.86
U2S	411374.4	479605.4	27.37	20.30	2	5.0	b	2.57	15.86
U11S	411380.1	479611.0	27.38	20.50	2	5.0	a	3.02	15.92
U11S	411380.1	479611.0	27.38	20.50	2	5.0	b	2.72	15.92
U1S	411368.8	479607.9	27.50	19.60	2	5.0	a	2.99	16.05
U1S	411368.8	479607.9	27.50	19.60	2	5.0	b	2.99	16.05
U10S	411375.1	479614.4	27.43	20.10	2	5.0	a	2.64	15.97
U10S	411375.1	479614.4	27.43	20.10	2	5.0	b	1.98	15.97
F14S	411380.9	479591.3	27.20	21.50	2	5.0	a	2478.49	15.75
F14S	411380.9	479591.3	27.20	21.50	2	5.0	b	2485.71	15.75
P7S	411415.8	479574.8	27.18	21.10	2	5.0	a	170.49	15.68
P7S	411415.8	479574.8	27.18	21.10	2	5.0	b	183.44	15.68
P14S	411414.7	479572.5	27.22	21.30	2	5.0	a	131.54	15.76
P14S	411414.7	479572.5	27.22	21.30	2	5.0	b	124.01	15.76
F1S	411383.8	479595.7	27.34	23.40	2	5.0	a	123.66	15.95
F1S	411383.8	479595.7	27.34	23.40	2	5.0	b	155.83	15.95
U4M	411385.3	479599.8	27.40	30.30	2	5.0	a	20.75	15.90
U4M	411385.3	479599.8	27.40	30.30	2	5.0	b	20.63	15.90

Table 2. Hydraulic Parameters at Dover AFB, Maryland (Continued)

Well	Northing	Easting	TOC	Total Depth (ft)	Well Radius (ft)	Screen Length (ft)	Test	Permeability (ft/day)	Static Water Level (ft bgs)
P10	411413.8	479574.0	27.10	35.90	2	5.0	a	468.94	15.62
P10	411413.8	479574.0	27.10	35.90	2	5.0	b	442.97	15.62
U7D	411413.4	479583.2	27.16	36.10	2	5.0	a	14.54	15.61
U7D	411413.4	479583.2	27.16	36.10	2	5.0	b	14.65	15.61
U7D	411413.4	479583.2	27.16	36.10	2	5.0	c	14.87	15.61
U8D	411418.9	479580.4	27.18	36.00	2	5.0	a	11.37	15.64
U8D	411418.9	479580.4	27.18	36.00	2	5.0	b	16.85	15.64
U8D	411418.9	479580.4	27.18	36.00	2	5.0	c	8.61	15.64
U4D	411385.1	479599.8	27.34	37.00	2	5.0	a	59.20	15.84
U4D	411385.1	479599.8	27.34	37.00	2	5.0	b	69.32	15.84
U5D	411390.1	479596.3	27.26	35.70	2	5.0	a	8.17	15.85
U5D	411390.1	479596.3	27.26	35.70	2	5.0	b	7.42	15.85
U3D	411379.0	479601.9	27.42	36.80	2	5.0	a	36.69	15.90
U3D	411379.0	479601.9	27.42	36.80	2	5.0	b	27.74	15.90
F10	411380.1	479592.3	27.33	36.50	2	5.0	a	1603.07	15.87
F10	411380.1	479592.3	27.33	36.50	2	5.0	b	1508.98	15.87
U9D	411423.5	479577.9	27.06	19.33	2	5.0	a	100.94	15.55
U9D	411423.5	479577.9	27.06	19.33	2	5.0	b	99.79	15.55
P7D	411416.0	479574.7	27.19	37.30	2	5.0	a	n/a	15.75

Table 3. Hydraulic Parameters at Lowry AFB, Colorado

Well ID	Northing	Easting	TOC (ft msl)	Total Depth (ft)	Well Radius (in)	Screen Length (ft)	Test	Permeability (ft/day)	Water Level (ft bgs)		
									10/13/99	3/22/00	3/2/01
N1	690255.51	2171732.2	5359.35	15	2	10	a	1.1	8.57	8.80	8.78
N1	690255.51	2171732.2	5359.35	15	2	10	b	1.1	8.57	8.80	8.78
N2	690250.81	2171737.9	5359.55	15	2	10	a	1.8	8.50	8.40	8.71
N2	690250.81	2171737.9	5359.55	15	2	10	b	2.3	8.50	8.40	8.71
N3	690256.05	2171743.2	5359.01	15	2	10	a	1.8	7.96	8.10	8.12
N3	690256.05	2171743.2	5359.01	15	2	10	b	1.6	7.96	8.10	8.12
N4	690275.94	2171734.2	5358.68	15	2	10	a	1.8	8.35	8.30	8.48
N4	690275.94	2171734.2	5358.68	15	2	10	b	2.0	8.35	8.30	8.48
N5	690275.73	2171737.9	5358.40	15	2	10	a	1.2	8.12	8.05	8.27
N5	690275.73	2171737.9	5358.40	15	2	10	b	1.3	8.12	8.05	8.27
N6	690276.41	2171740.4	5358.29	15	2	10	a	1.2	8.09	8.00	8.23
N6	690276.41	2171740.4	5358.29	15	2	10	b	1.7	8.09	8.00	8.23
N7	690252.96	2171764.4	5357.61	15	2	10	na	na	6.92	6.90	7.10
N9	690246.26	2171759.7	5358.35	15	2	10	a	2.0	7.41	7.40	7.51
N9	690246.26	2171759.7	5358.35	15	2	10	b	2.3	7.41	7.40	7.51
U1	690230.06	2171728.6	5359.86	15	2	10	a	1.8	8.68	8.70	8.86
U1	690230.06	2171728.6	5359.86	15	2	10	b	1.6	8.68	8.70	8.86
U2	690229.75	2171748.7	5359.98	15	2	10	na	na	8.81	8.80	8.01
U3	690240.08	2171721.2	5360.96	15	2	10	na	na	9.89	9.85	NA
U4	690239.58	2171738.1	5359.87	15	2	10	a	1.4	8.77	8.75	8.97
U4	690239.58	2171738.1	5359.87	15	2	10	b	2.8	8.77	8.75	8.97
U5	690238.76	2171757.9	5358.93	15	2	10	na	na	7.87	7.90	8.07
U6	690245.58	2171727.7	5359.69	15	2	10	na	na	8.65		8.83
U7	690246.06	2171747.6	5359.1	15	2	10	a	1.2	8.05	8.02	8.23
U7	690246.06	2171747.6	5359.1	15	2	10	b	1.1	8.05	8.02	8.23
U8	690248.2	2171713.6	5363.71	15	2	10	na	na	12.75	12.70	12.92
U9	690251.77	2171747.8	5359.45	15	2	10	na	na	8.39	8.40	8.58
U10	690252.92	2171752.9	5359.08	15	2	10	a	3.1	8.09	8.05	8.29
U10	690252.92	2171752.9	5359.08	15	2	10	b	2.9	8.09	8.05	8.29
F1	690262	2171734	5359.19	15	2	10	na	na	8.18	8.15	8.40
F2A	690262.36	2171738	5359.06	15	2	10	na	na	8.06	8.02	8.26
F3	690262.33	2171741.3	5359.33	15	2	10	na	na	8.32	8.31	8.53
R1	690263.92	2171734.6	5359.25	15	1	10	na	na	NM	8.25	8.49
R2A	690264.39	2171737.9	5359.28	15	1	10	na	na	8.24	8.21	8.45
R2B	690263.88	2171737.9	5359.26	15	1	10	na	na	8.24	8.24	8.45
R3	690264.31	2171741.2	5359.32	15	1	10	na	na	8.29	8.28	8.51
R4	690264.91	2171734.5	5359.28	15	1	10	na	na	8.23	8.20	8.41
R5A	690265.34	2171737.8	5359.32	15	1	10	na	na	8.26	8.20	8.41

Table 3. Hydraulic Parameters at Lowry AFB, Colorado (Continued)

Well ID	Northing	Easting	TOC (ft msl)	Total Depth (ft)	Well Radius (in)	Screen Length (ft)	Test	Permeability (ft/day)	Water Level (ft bgs)		
									10/13/99	3/22/00	3/2/01
R5B	690264.87	2171737.8	5359.32	15	1	10	na	na	8.27	8.27	8.42
R6	690265.3	2171741.1	5359.35	15	1	10	na	na	8.28	8.27	8.49
R7	690266.4	2171734.4	5359.32	15	1	10	na	na	8.26	8.23	8.47
R8A	690266.91	2171737.7	5359.27	15	1	10	na	na	8.24	8.19	8.46
R8B	690266.38	2171737.7	5359.28	15	1	10	na	na	8.25	8.24	8.46
R9	690266.83	2171741	5359.34	15	1	10	na	na	8.31	8.30	8.49
F4	690268.89	2171734.2	5359.27	15	2	10	na	na	8.25	8.24	8.46
F5A	690269.31	2171737.6	5359.3	15	2	10	na	na	8.26	8.23	8.44
F5B	690268.89	2171737.6	5359.32	15	2	10	na	na	8.27	8.25	8.51
F6	690269.29	2171740.9	5359.62	15	2	10	na	na	8.34	8.32	8.55

Table 4. Hydraulic Parameters at Former NAS Moffett Field, California

Well ID	Coordinates		Ground ft msl	TOC ft msl	Screen Depth (ft bgs)			Casing Diameter in.
	Easting	Northing			Top	Mid	Bottom	
Upgradient A1 Aquifer Zone Wells								
WIC-1	1548686.00	335786.00	18.5	18.23	19.00	21.50	24.00	2
WIC-5	1548689.50	335789.60	18.3	18.07	11.00	11.50	12.00	2
WIC-6	1548690.40	335789.40	18.3	18.04	15.00	15.50	16.00	2
WIC-7	1548690.00	335790.40	18.3	17.87	20.50	21.00	21.50	2
WIC-8	1548689.10	335790.60	18.2	18.07	24.00	24.50	25.00	2
PIC-6	1548754.00	335761.40	18.0	17.81	15.00	16.25	17.50	0.75
PIC-7	1548730.00	335768.70	17.9	17.71	15.00	16.25	17.50	0.75
PIC-8	1548699.00	335758.50	18.6	18.08	15.00	16.25	17.50	0.75
PIC-9	1548663.74	335761.82	18.9	18.51	15.00	16.25	17.50	0.75
PIC-10	1548635.00	335762.70	19.0	18.77	15.00	16.25	17.50	0.75
PIC-11	1548759.00	335726.40	18.1	17.91	15.00	16.25	17.50	0.75
PIC-12	1548705.00	335721.40	18.9	18.54	15.00	16.25	17.50	0.75
PIC-13	1548682.00	335711.40	19.1	18.70	15.00	16.25	17.50	0.75
PIC-14	1548649.00	335707.20	19.2	19.01	15.00	16.25	17.50	0.75
PIC-15	1548616.00	335701.90	19.4	19.16	15.00	16.25	17.50	0.75
PIC-24	1548713.00	335786.30	18.0	17.81	15.00	16.25	17.50	2
PIC-25	1548704.20	335786.80	18.2	18.00	15.00	16.25	17.50	2
PIC-26	1548677.20	335788.90	18.5	18.23	15.00	16.25	17.50	2
PIC-27	1548668.60	335789.50	18.5	18.31	15.00	16.25	17.50	2
PIC-28	1548708.10	335781.40	18.2	18.00	15.00	16.25	17.50	2
PIC-29	1548699.30	335781.50	18.3	18.17	15.00	16.25	17.50	2
PIC-30	1548672.00	335783.80	18.6	18.36	15.00	16.25	17.50	2
Upgradient A2 Aquifer Zone Wells								
WIC-2	1548690.64	335782.45	18.4	18.19	30.50	33.00	35.50	2
PIC-17	1548666.00	335759.60	18.8	18.56	31.50	32.75	34.00	0.75
PIC-19	1548701.97	335749.80	18.6	18.28	31.50	32.75	34.00	0.75
Upgradient Pea Gravel Wells								
WW-2	1548689.00	335792.50	18.3	17.98	10.58	15.67	20.75	2
WW-7A	1548690.59	335792.26	18.4	18.00	8.08	8.58	9.08	1
WW-7B	1548690.29	335792.18	18.4	17.99	11.00	11.58	12.17	1
WW-7C	1548690.56	335792.46	18.4	18.02	16.00	16.50	17.00	1
WW-7D	1548690.31	335792.51	18.4	17.98	20.67	21.00	21.33	1
WW-11	1548693.00	335792.30	18.3	17.93	10.00	15.00	20.00	2
WW-16A	1548694.79	335792.02	18.3	17.95	7.75	8.33	8.92	1
WW-16B	1548695.09	335792.09	18.3	17.94	10.75	11.17	11.58	1
WW-16C	1548694.98	335792.33	18.3	17.93	15.58	16.08	16.58	1
WW-16D	1548694.73	335792.25	18.3	17.93	20.25	20.83	21.42	1

Table 4. Hydraulic Parameters at Former NAS Moffett Field, California (Continued)

Well ID	Coordinates		Ground ft msl	TOC ft msl	Screen Depth (ft bgs)			Casing Diameter in.
	Easting	Northing			Top	Mid	Bottom	
Reactive Cell Wells								
WW-1A	1548687.34	335798.17	18.3	17.96	8.17	8.67	9.17	1
WW-1B	1548687.41	335797.98	18.3	17.96	11.00	11.58	12.17	1
WW-1C	1548687.67	335798.31	18.3	17.98	15.67	16.17	16.67	1
WW-1D	1548687.73	335798.04	18.3	17.97	20.33	19.50	18.67	1
WW-3	1548689.00	335793.90	18.3	17.95	10.50	15.50	20.50	2
WW-4A	1548689.16	335794.94	18.4	17.96	7.00	7.50	8.00	1
WW-4B	1548688.77	335794.97	18.4	17.98	10.00	10.50	11.00	1
WW-4C	1548688.90	335794.72	18.4	18.01	15.75	16.25	16.75	1
WW-4D	1548688.98	335795.11	18.4	17.97	20.50	21.00	21.50	1
WW-5	1548689.00	335797.20	18.3	18.01	10.00	15.00	20.00	2
WW-8A	1548690.18	335793.33	18.4	17.98	8.25	8.83	9.42	1
WW-8B	1548690.17	335793.63	18.4	17.95	11.08	11.58	12.08	1
WW-8C	1548690.37	335793.29	18.4	17.97	15.92	16.33	16.75	1
WW-8D	1548690.44	335793.60	18.4	17.98	20.50	21.00	21.50	1
WW-9A	1548690.48	335796.83	18.3	17.95	8.17	8.83	9.50	1
WW-9B	1548690.66	335797.16	18.3	17.94	11.00	11.42	11.83	1
WW-9C	1548690.72	335796.91	18.3	17.93	15.92	16.42	16.92	1
WW-9D	1548690.42	335797.20	18.3	17.94	20.50	21.00	21.50	1
WW-12	1548693.00	335793.80	18.2	17.91	10.00	15.00	20.00	2
WW-13A	1548692.58	335795.91	18.3	17.89	8.17	8.50	8.83	1
WW-13B	1548692.70	335795.65	18.3	17.90	11.00	11.50	12.00	1
WW-13C	1548692.41	335795.48	18.3	17.93	16.00	16.50	17.00	1
WW-13D	1548692.27	335795.82	18.3	17.97	20.58	21.00	21.42	1
WW-14	1548694.00	335796.80	18.2	17.86	10.75	15.25	19.75	2
WW-17A	1548694.91	335794.13	18.3	17.91	8.08	8.58	9.08	1
WW-17B	1548695.24	335794.35	18.3	17.91	11.00	11.50	12.00	1
WW-17C	1548695.23	335794.14	18.3	17.91	15.67	16.17	16.67	1
WW-17D	1548695.04	335794.51	18.3	17.92	20.33	20.83	21.33	1
Downgradient Pea Gravel Wells								
WW-6	1548689.00	335799.50	18.2	17.79	10.00	15.00	20.00	2
WW-10A	1548691.14	335799.80	18.3	17.88	7.83	8.33	8.83	1
WW-10B	1548691.16	335799.58	18.3	17.85	10.75	11.25	11.75	1
WW-10C	1548691.33	335799.51	18.3	17.84	15.67	16.08	16.50	1
WW-10D	1548691.50	335799.70	18.3	17.89	20.67	21.00	21.33	1
WW-15	1548693.00	335799.70	18.2	17.77	10.50	15.00	19.50	2
WW-18A	1548695.50	335799.41	18.2	17.81	7.83	8.33	8.83	1
WW-18B	1548695.80	335799.46	18.2	17.81	10.83	11.33	11.83	1
WW-18C	1548695.53	335799.66	18.2	17.84	15.67	16.17	16.67	1
WW-18D	1548695.74	335799.65	18.2	17.85	20.67	21.17	21.67	1

Table 4. Hydraulic Parameters at Former NAS Moffett Field, California (Continued)

Well ID	Coordinates		Ground ft msl	TOC ft msl	Screen Depth (ft bgs)			Casing Diameter in.
	Easting	Northing			Top	Mid	Bottom	
Downgradient A1 Aquifer Zone Wells								
PIC-1	1548754.00	335852.40	18.3	18.11	15.00	16.25	17.50	0.75
PIC-2	1548724.00	335823.80	17.8	17.64	15.00	16.25	17.50	0.75
PIC-3	1548687.00	335820.90	18.0	17.66	15.00	16.25	17.50	0.75
PIC-4	1548663.00	335822.10	18.2	17.83	15.00	16.25	17.50	0.75
PIC-5	1548635.00	335817.40	18.3	18.10	15.00	16.25	17.50	0.75
PIC-20	1548689.00	335828.80	17.8	17.43	15.00	16.25	17.50	0.75
PIC-21	1548691.00	335829.60	17.8	17.49	15.00	16.25	17.50	0.75
PIC-22	1548691.00	335828.60	17.9	17.48	15.00	16.25	17.50	0.75
PIC-23	1548692.00	335829.60	17.9	17.56	15.00	16.25	17.50	0.75
PIC-31	1548693.80	335801.50	18.1	17.90	10.00	15.00	20.00	2
PIC-32	1548695.40	335801.60	18.1	17.89	10.00	15.00	20.00	2
PZ9.8-2	1548702.33	335863.68	17.6	17.31	14.80	19.80	24.80	2
PZ9.8-4	1548662.33	335849.64	18.0	17.74	9.50	14.50	19.50	2
PZ9.8-6	1548665.00	335905.00	17.4	17.17	9.50	14.50	19.50	2
W9-35	1548691.75	335856.58	17.7	17.32	14.00	19.00	24.00	4
WIC-3	1548691.00	335816.00	18.0	17.94	19.00	21.50	24.00	2
WIC-9	1548691.30	335802.60	18.2	17.89	11.00	11.50	12.00	2
WIC-10	1548692.30	335802.40	18.2	17.94	16.00	16.50	17.00	2
WIC-11	1548691.70	335801.60	18.2	17.84	20.50	21.00	21.50	2
WIC-12	1548690.80	335801.80	18.2	17.95	25.00	25.50	26.00	2
Downgradient A2 Aquifer Zone Wells								
WIC-4	1548697.66	335816.34	18.0	17.70	29.50	32.00	34.50	2
W9-20	1548690.12	335861.66	17.6	16.97	30.00	37.50	45.00	4
PIC-16	1548665.00	335825.20	18.1	17.90	31.50	32.75	34.00	0.75
PIC-18	1548725.00	335824.80	17.8	17.62	31.50	32.75	34.00	0.75

TOC: Top of Casing.